

**Non-Proprietary**

**Steam Generator Inspection Program  
Return to Power Report  
San Onofre Nuclear Generating Station  
Unit 1  
September, 1982  
Southern California Edison Company**

**Volume I**

**REGULATORY DOCKET FILE COPY**

8209230372 820921  
PDR ADOCK 05000206  
Q PDR

Table of Contents

Volume I

Sections

- I. Introduction
- II. Sleeving Repair Program Inspection
  - A. General
  - B. Primary to Secondary Bundle Integrity Test
  - C. Secondary Side Leakage Test
  - D. Sleeved Tube Inspection
  - E. Leader - Follower Program
  - F. Non-Sleeved Tube Inspection
  - G. Conclusions
- III. Technical Specification Inspection
  - A. General
  - B. General Inspection
  - C. AVB Inspection
  - D. Denting Inspection
  - E. Conclusions
- IV. Foreign Materials Inspection
  - A. General
  - B. Scope
  - C. Inspection Techniques
  - D. Findings
  - E. Evaluation
  - F. Corrective Actions
  - G. Conclusions

REGULATORY DOCKET FILE COPY

## V. Summary and Conclusions

- A. Summary of Results
- B. Return to Power Conditions
- C. Future Inspections

## VI. References

### Appendices

- A. Sleeving Repair Inspection Tables and Figures
- B. Technical Specification Inspection
  - B.1 Tables and Figures
  - B.2 Flow Slot Maps and Photographs
  - B.3 Eddy Current Results at TSP Intersections
  - B.4 Dynamic Analysis of Tubes Assuming Partial Support
- C. Responses to NRC Requests for Additional Information
  - C.1 Reference Joint Design and Fabrication
  - C.2 Dissolution
    - C.3.1 Flow Induced Vibration Analysis
    - C.3.2 Steam Line Break Analysis Summary
    - C.3.3 Repair Report Addendum
  - C.4 NDE Capabilities of Reference Joint/ Safety Assessment
- D. Foreign Materials Inspection Tables and Figures

VOLUME II

Appendices (Continued)

- E. Investigation of Wrapper Supports
  - I. Introduction
  - II. Background
  - III. Visual Inspection
  - IV. Eddy Current Inspection of Peripheral Tubes
  - V. Plugging History of Peripheral Tubes
  - VI. Evaluation of Inspection Findings
  - VII. Metallurgical Analysis of Wrapper Support Bars
  - VIII. Flow Tests
  - IX. Visual Inspection of Alternate Wrapper Supports
  - X. Structural Analysis of Alternate Wrapper Supports and Steam Generator Internals
    - A. Preliminary SLB and SSE Evaluation
    - B. Structural Analysis under SLB
    - C. Structural Analysis under SSE
- F. Summary of Steam Generator Repairs

REGULATORY DOCKET FILE COPY

## Section I

### Introduction

On February 26, 1982, following 4.3 effective full power months of operation from the start of Cycle 8 operation, San Onofre Unit 1 was shut down as scheduled in order to perform required tests, plant modifications and steam generator inspections on an integrated outage basis. The purpose of this report is to describe the program of steam generator inspections performed during the outage, including individual inspection scope, findings, corrective actions, and conclusions; plans for return to power; and future inspection plans. In addition, this report documents SCE responses to NRC requests for additional information in Reference 1; these responses were also presented to NRC staff at the May 12, 1982 meeting in Bethesda, MD concerning San Onofre Unit 1 steam generators.

The steam generator inspection program described herein consists of: (a) inspections developed and implemented pursuant to San Onofre Unit 1 Provisional Operating License (POL) DPR-13 Condition 3.E and Technical Specification 4.16, and (b) secondary side foreign materials and loose parts inspections.

License Condition 3.E was instated by issuance on June 8, 1981 of Amendment No. 55 to the San Onofre Unit 1 POL. As such, the steam generator inspection required by Condition 3.E is in direct consequence of the program of steam generator diagnostics and repairs performed at San Onofre Unit 1 during the 1980-81 outage and reported in References 2, 3 and 4. Accordingly, the Condition 3.E inspections performed during the current (1982) outage focused on sleeved tubes over their sleeved lengths and on the region at or near the top of the tube sheet on the inlet side for non-sleeved tubes. This inspection is hereinafter referred to as the Sleeving Repair Inspection.

Consistent with Technical Specification 4.16 provisions on frequency of inspections, an inspection was performed this outage addressing Specification requirements on general surveillance of tube bundles and on special surveillance of anti-vibration bar (AVB) area wear, progression of denting and other previously detected tube degradation. The last such inspection was completed in July 1980. This inspection is hereinafter referred to as the Technical Specification Inspection.

Recent industry experience has underscored the potential for and consequences of foreign materials and loose parts being introduced into steam generators. Largely in view of this experience, a secondary side foreign materials and loose parts inspection was initiated during the current steam generator inspection outage. A similar such inspection focusing on the primary side coolant loops was performed in conjunction with steam generator repairs made during the 1980-81 San Onofre Unit 1 sleeving repair project. The current outage steam generator secondary side inspection is hereinafter referred to as the Foreign Materials Inspection.

Section II of the report contains the Sleeving Repair Inspection program description, findings, corrective actions and conclusions. This section also contains information in response to Enclosure 1, Part B (Staff Evaluation of the Proposed Inspection Program) of Reference 1. Associated tables and figures are contained in Appendix A.

Section III and Appendix B of the report contain the Technical Specification Inspection program description, findings, corrective actions, conclusions and associated tables, figures and photographs.

Appendix C documents information presented to the NRC during the May 12, 1982 meeting in Bethesda, MD pursuant to the NRC request for additional information in Reference 1 and provides additional information requested by the NRC at that meeting.

Section IV and Appendices D and E contain the Foreign Materials Inspection program description, findings, corrective actions, conclusions and associated tables, and figures.

Section V summarizes overall conclusions derived from the inspection program and responses to NRC concerns, and presents San Onofre Unit 1 plans for return to power and for future inspections. Appendix F contains summaries of the repair status of the steam generators including plugging repairs made this outage.

## Section II

### Sleeving Repair Inspection

#### A. General

The Sleeving Repair Inspection performed pursuant to POL Condition 3.E was designed to monitor the effectiveness of the 1980-81 steam generator sleeving repair program. A detailed description of the proposed inspection and consequent repair program was submitted to the NRC in advance of the outage in Reference 5 dated January 15, 1982. In response to subsequent NRC concerns and to improvements in inspection techniques identified in the course of the inspection, changes were made to the proposed program of Reference 5. The resultant program implemented during this outage is fully described below. In summary, the inspection program consisted of the following elements:

- Tube bundle pressure and leak tests to demonstrate margin to normal operating conditions and to identify leaking tubes.
- Eddy current testing by conventional, multi-frequency, bobbin coil techniques of approximately 10% of the sleeved tubes in each steam generator to assess the integrity of sleeve-tube assemblies.
- Eddy current and ultrasonic testing of leader-follower sleeve-tube assemblies, pre-selected during the 1980-81 repair outage, to assess the susceptibility to corrosive degradation of brazed joints.
- Eddy current testing of approximately 30% of the tubes outside the sleeving repair boundary on the inlet side of each steam generator utilizing multi-frequency, surface riding coil techniques to assess the extent to which IGA is occurring at the top of the tube sheet.



Each of these program elements, including findings, evaluations, resultant corrective actions, and conclusions is further discussed below. For reference, Figures A.1, A.2, and A.3 are provided showing the sleeving repair boundaries, types of sleeve joints, and plugging status of steam generators A, B and C, respectively, prior to the current outage.

#### B. Primary to Secondary Tube Bundle Integrity Test

During the course of unit shutdown, with the unit in a hot shutdown condition, a differential pressure of 1900 psid was established from the primary to secondary sides of the steam generators similar to the procedure employed during the 1980-81 repair outage. This differential pressure approaches that which might be expected following a main steamline or feedline break and serves to indicate overall tube bundle structural integrity and demonstrate gross margin to normal operating conditions for sleeved and non-sleeved tubes.

No problems were encountered in maintaining differential pressure and the test was satisfactorily concluded.

#### C. Cold Secondary Side Leakage Test

Following the primary to secondary side differential pressure test, with the unit in cold shutdown, a secondary to primary side pressure test at 800 psid was performed to identify any leaking tubes.

As a result, three sleeved tubes exhibited minor leakage (one to two drops per minute) on the inlet side of steam generator C. The tubes were R11-C43, R12-C35, and R34-C65; Figure A-4 of Appendix A shows the location of these tubes in relation to the 1980-81 repair boundary. Details on each tube are given below.

### R11 - C43

During pre-sleeving eddy current testing at the beginning of the 1980-81 outage, R11-C43 was reported as having a 99% through wall indication by conventional bobbin coil and a 97% indication by rotating pancake coil (RPC), both indications being observed at the top of the tube sheet and attributed to IGA. During sleeving, a 30-inch mechanical sleeve was installed in R11-C43. Subsequently, during the baseline ECT of sleeved tubes, a possible indication was reported in the tube at the top of the tube sheet near the lower transition of the mechanical sleeve expansion zone.

### R34 - C65

No indications were reported in 1980 prior to sleeving for R34-C65. A mechanical sleeve with a full length expansion was installed in R34-C65 during sleeving. No indication of tube or sleeve penetration was noted during the post-sleeving baseline ECT.

### R12 - C35

During pre-sleeving ECT in 1980, R12-C35 was reported as having a 98% through wall indication by bobbin coil and a 95% indication by RPC. During sleeving, a 30-inch brazed sleeve was installed and subsequently converted to a leak limiter by application of a lower mechanical joint. No UT of the brazed joint was performed on this sleeve. The post-sleeving ECT baseline, in 1981, disclosed a possible indication in the tube at the top of the tube sheet near the lower transition of the conversion expansion zone.

Each of the above sleeve-tube assemblies is a leak limiting sleeve as described in Reference 3. The minor amount of leakage observed is assessed to be bounded by the allowable leakage for such sleeves. The source of leakage can be attributed to pre-existing IGA in the tubes for R11-C43 and R12-C35 while no determination is made for R34-C65. It is noted that the amount of primary to secondary leakage observed during operation prior to the current outage was quite low, and in the range of the threshold of detectability for such leakage. As a conservative corrective measure, all three tubes have been plugged.

#### D. Sleeved Tube Eddy Current Inspection

##### 1. Description

The inspection plan consisted of inspecting approximately 10% of the sleeved tubes within the sleeving repair boundary of each steam generator from the inlet side through the first support plate. Tubes were selected for inspection in a pattern of every third row and column adjusted, as necessary, to ensure that a representative number of all types of sleeve joints were inspected. The inspection was performed using a magnetically biased conventional bobbin probe with multi-frequency techniques, consistent with the 1981 post-sleeving baseline inspection. Additional information on inspection techniques and capabilities is contained in Appendix C.4.

In the inspection, eddy current signatures obtained were compared to corresponding signatures from the 1981 baseline inspection. Sleeves exhibiting deviations from baseline data were subject to further evaluation on a case-by-case basis. Expansion of the basic inspection pattern to other sleeved tubes depended on the nature and extent of deviations identified. The plugging criteria of Technical Specification 4.16 were applied.

## 2. Findings

The completed inspection patterns using the conventional, multi-frequency bobbin coil are shown in Figures A.5, A.6, and A.7 for SG's A, B and C, respectively. Table A.1 summarizes quantities of sleeve types inspected in comparison to corresponding quantities installed.

With the exception discussed below, in all cases the signatures obtained this outage appeared unchanged from those obtained during the 1981 baseline inspection.

In each of the sleeves inspected, a new eddy current signal was observed in the upper transition region(s) of the sleeve joint(s). The characteristics of this signal were common to each sleeve inspected. Laboratory investigations were conducted and confirmed the suspicion that these signals resulted from the presence of magnetite in the annular gaps between the sleeve and tube at and above the upper transitions of the sleeve expansion zones. It is suspected that magnetite grit was deposited on tube walls, above the sleeves, as a result of the channel head decontamination process during sleeving, and collected in the gaps during subsequent plant operations. Additional information on the investigation of these magnetite eddy current signals is contained in Appendix C.4.

In addition to the conventional probe inspection, a crosswound eddy current coil was field tested in sleeved tubes. Based on laboratory work, significant improvement in sensitivity over the conventional bobbin coil is achievable in regions of the sleeve-tube assembly. However, due to probe production problems, the field test did not yield the expected results. Additional information is contained in Appendix C.4.

### 3. Evaluation

No deviations in eddy current signal characteristics at the sleeve joints and transition regions were observed. In the sleeve lengths outside the joint regions, no indications of degradation were observed. Were aggressive corrosive attack of the sleeve-tube assemblies occurring, some manifestation by eddy current would be expected given the inspection scope and given the operating interval since the previous inspection. In light of the results, such aggressive attack is evaluated as not occurring.

### 4. Corrective Action

No repairs to sleeved tubes were required as a result of the eddy current inspection findings.

## E. Leader-Follower Program

### 1. Description

The program as originally proposed during the 1980-81 sleeving repair outage is discussed in References 2 and 4. In summary, the program is designed to monitor in-situ leak tight braze joints for the formation of potential leak paths across the circumferential band of bonded braze material due to corrosive degradation when exposed to secondary side environmental conditions. The basis for such monitoring is that, unlike tube or sleeve wall degradation, small leak paths which may be developing across the braze region during operation are not necessarily detectable by eddy current techniques alone. Supplementary inspection by UT and continued monitoring of brazed joints preferentially exposed to potentially corrosive conditions will give early warning of susceptibility to leak path formation.

During the 1980-81 outage, tubes to be repaired with brazed sleeves were selected and deliberately penetrated through wall in the region to be spanned by the sleeves, thereby ensuring exposure of the brazed joint to secondary side conditions upon resumption of operation. These tubes were designated "leader" tubes. Neighboring tubes which were fitted with leak tight brazed sleeves and known to have no through wall tube penetrations were designated control or "follower" tubes. Both leader and follower tubes were inspected by ECT and UT during the 1981 baseline and those exhibiting normal eddy current and UT signatures for leak tight joints became the final leader-follower tubes.

The program calls for re-inspection of leader-follower tubes by ECT and UT during subsequent outages and comparison of data with baseline data to determine whether significant changes have occurred. If significant degradation is suspected in a leader or follower in the brazed region, then the tube is removed for metallurgical examination. Appropriate additional evaluations and corrective measures are then identified.

The leader-follower tubes were selected from steam generator A and Figure A-8 shows their locations.

## 2. Findings

For each leader and follower tube, both the eddy current and UT data showed no changes in comparison to data obtained during the 1981 baseline inspection.

## 3. Evaluation

During the cumulative 4.3 EFPM of operation since the baseline inspection, a number of cycles of unit start-up and shutdown occurred

which should have established representative secondary side conditions in the tube-sleeve annuli of leader tubes. Absence of any indication of change in the braze region during the current inspection suggests that no aggressive attack is occurring due to exposure to secondary side conditions. This is consistent with laboratory findings reported in Reference 2.

#### 4. Corrective Action

No corrective actions were required as a result of the leader-follower tube inspection program.

### F. Non-Sleeved Tube Inspection

#### 1. Description

This inspection was performed to monitor peripheral, non-sleeved tubes on the inlet side of each steam generator for IGA at the top of the tube sheet. The basic inspection pattern for each steam generator consisted of all non-sleeved tubes which lie within either two rows or columns of the sleeving repair boundary plus every fourth row and column in the remainder of the periphery. In addition, areas in the periphery where previous eddy current data indicate the potential for IGA activity were also inspected. The primary inspection technique consisted of a screening inspection through the first support plate using a multi-frequency, push-pull probe with surface riding coils, known as a "4x4" probe. The probe consists of upper and lower sets of four series-wound surface riding coils. Each set produces absolute signals which are then differentially analyzed. This inspection was supplemented by multi-frequency bobbin coil inspection of each tube to assist in the interpretation of 4x4 data.

Tubes with suspected IGA indications at the top of the tube sheet by 4x4 probe were then inspected using the RPC probe, as employed during the 1980-81 outage, to confirm whether IGA indications are present. Expansion to tubes surrounding those with IGA indications was done using the 4x4 probe until tubes with IGA indications were bounded by tubes having no IGA indications. The criteria for plugging non-sleeved tubes were (a) any tube with RPC-detectable indications at the top of the tube sheet, (b) any tube immediately adjacent to an RPC indication greater than or equal to 50% and (c) tubes within a broad boundary formed by tubes with IGA indications and tubes adjacent to tubes with IGA indications.

Details of the inspection plan, including results and proposed repairs, were discussed with NRC staff at a meeting in Forest Hills, PA on April 13, 1982.

## 2. Findings

The completed inspection patterns in steam generators A, B and C are shown in Figures A-9, A-10 and A-11, respectively. Inspection results are summarized as follows:

### SG-A

A total of 422 tubes were inspected from among the 1209 peripheral tubes for a percentage of 35%. Only one tube, R32-C73 which is located within the basic inspection pattern as shown in Figure A-9, had a possible IGA indication at the top of the tube sheet by the 4x4 probe; however, no RPC confirmatory inspection was performed due to ALARA considerations. The surrounding tubes had no indications of IGA by 4x4 probe.

### SG-B

A total of 396 tubes were inspected from among the 1357 peripheral tubes for a percentage of 29%. No indications of IGA at the top of the tube sheet were observed.



As a result of the supplementary bobbin coil inspection through the 1st support plate, additional data were collected in each steam generator on wastage type thinning known to have occurred above the top of the tubesheet. One tube in SG-B, R1-C52, had a wastage indication above the top of the tubesheet of 55%. Cumulative results from wastage data gathered during the peripheral tube inspection were factored into the evaluation of wastage in Section III.B of this report.

### SG-C

A total of 394 tubes were inspected from among the 1419 peripheral tubes for a percentage of 28%. A total of 7 tubes had possible IGA indications at the top of the tube sheet by the 4x4 probe and were then inspected using the RPC probe. From the RPC inspection, 6 of the tubes had indications recorded as less than 20% and one (R22-C20) as 40%. Each tube was in the basic inspection pattern within 2 rows or columns of the sleeving repair boundary as shown in Figure A-12.

### 3. Evaluation

As recorded in Table A-2, a total of 1212 tubes from among the total of 3985 peripheral, non-sleeved tubes in all three steam generators were inspected, for a combined percentage of 30%. Within the population of 1212 tubes inspected, there were 8 tubes, or less than 1%, having possible IGA indications not previously observed. Of these 8 tubes, the one in SG-A (R32C73) was evaluated from 4x4 data as marginal with respect to a possible IGA indication, and, as noted above, was not inspected by RPC. This tube is, however, located adjacent to the sleeving boundary in a region of possible IGA activity based on previous inspection results.

Of the remaining seven in SG-C, only one (R22C20), located adjacent to the sleeving boundary, had a quantifiable indication (40%). The other six, located adjacent to or, in one case, two tubes from the sleeving boundary, had very small indications which could not be discretely quantified and were evaluated as  $< 20\%$  indications.

The small number and largely indeterminate ( $< 20\%$ ) nature of indications do not lend themselves to a reliable, quantitative estimation of general rate of IGA in the periphery of the tube bundles. However, some qualitative, first order comparisons can be made to the situation as observed during the 1980-81 outage and as characterized in Reference 4.

In the 1980-81 outage, the rate of IGA progression in the so-called "active" region was conservatively estimated to be 15% per year of operation. For the purpose of establishing the return to power inspection interval, this corrosion rate was assumed to apply to peripheral tubes. Furthermore, based on 1980 RPC results and metallurgical evaluations of pulled tubes, peripheral tubes were assumed to have IGA of  $\leq 40\%$  present. On these bases, the inspection interval of six months would conservatively result in a general level of IGA in peripheral tubes of  $\leq 48\%$ . If these conditions were indeed occurring at large in the periphery, some correlation between the 1980 and 1982 IGA inspection statistics would be expected; in particular, a significant percentage of tubes having indications evaluated as  $< 20\%$  (i.e., actual degradation near the assumed threshold of detectability of IGA of 40%) would be expected in the 1982 results. As can be seen in Table A.2, such a correlation is not evident.

As stated in Reference 4, IGA is likely to have been occurring at San Onofre Unit 1 since 1973, suggesting an "actual" corrosion rate in the active region of less than the conservatively postulated 15% per operating year. With regard to the periphery, as reported in Reference 4, tubes pulled from near the periphery exhibited substantially less

IGA degradation than did tubes pulled from the central and so-called "active" regions. This would indicate an even lower "actual" corrosion rate in peripheral tubes. Moreover, the near absence of peripheral indications in both the 1980 and current inspections suggests that no significant rate of corrosion is occurring in the periphery.

It would appear, therefore, that IGA in the periphery is generally less than 40% and is progressing at a rate much less than 15% per year of operation.

In light of the above considerations, it is assessed that the conclusions of Reference 4 are conservative regarding degree of IGA penetration in peripheral tubes and its rate of progression. As such, the repair criteria invoked in both the 1980-81 and current outage continue to be regarded as adequately conservative.

#### 4. Corrective Actions

The repair criteria stated in F.1 above were applied to the inspection findings. As a result, one tube in SG-A was plugged; in SG-C, seven tubes were plugged due to IGA indications and an additional 13 adjacent tubes were plugged in response to the broad boundary plugging criterion. The resultant plugging locations for steam generators A and C are shown in Figures A.13 and A.14. In addition, one tube in SG-B was plugged due to a wastage type thinning indication above the top of the tube sheet as discussed in F.2 above.

#### G. Conclusions

The following conclusions are made regarding the sleeving repair

inspections:

1. Based on satisfactory completion of the 1900 psid primary-to-secondary differential pressure test, adequate margin to normal operating conditions for repaired and non-repaired tubes is demonstrated.
2. Leakage observed from tubes with leak limiting sleeves during the secondary side leakage test is consistent with low level primary to secondary leakage observed during plant operation prior to shutdown and with allowable leakage design margin for leak limiting sleeves.
3. Based on results of eddy current examination of sleeve-tube assemblies, no detectable structural changes are observed in sleeves or sleeve-to-tube joints.
4. Based on results of the leader-follower tube inspection program, no changes are observed in braze material due to exposure to secondary side environment.
5. NDE results for sleeve-tube assemblies and satisfactory completion of the 1900 psid primary-to-secondary differential pressure test indicate no detectable change to the primary pressure boundary formed by the sleeve-tube assemblies and the margin of safety for continued operation is thereby maintained consistent with that set forth in the SCE Sleeving Project Return to Power and Repair Reports.
6. Based on the results of the eddy current inspection in the periphery of the steam generators, the satisfactory completion of the primary-to-secondary differential pressure test, and the secondary side leakage

test, it is concluded that the extent and rate of progression of IGA in peripheral non-repaired tubes are conservatively bounded by the degradation assumptions for these tubes as set forth in the SCE 1981 Repair Report. As such, the basis for the repair boundary established in 1981 is adequately conservative.

## Section III

### Technical Specification Inspection

#### A. General

An inspection meeting the requirements of Technical Specification 4.16 was performed in addition to the Sleaving Repair Inspection discussed in Section II of this report. The previous Technical Specification Inspection was performed in all three steam generators beginning in April, 1980. The results of that inspection were transmitted to the NRC in Reference 6. Those and earlier inspection results indicate that the pattern of denting in SG's A and C is unchanged and that in all other respects the three steam generators are behaving in a like manner. Consistent with Technical Specifications provisions, one steam generator (SG-C) was selected for inspection this outage. The inspection and results for the general inspection and the special inspections of AVB wear and of denting are summarized below.

#### B. General Inspection

##### 1. Description

The program consisted of inspection from the hot leg through the U-bend to the 4th support plate on the cold leg of at least 3% of the total number of steam generator tubes plus inspection through the first support plate of tubes having previous wastage indications above the top of the tube sheet. Multi-frequency techniques with the conventional bobbin coil were employed. The resultant inspection pattern is shown in Figure B.1.

## 2. Findings

No imperfections were found in SG-C requiring supplementary inspections per T.S. 4.16, Paragraph B. However, as a result of the pluggable wastage indication in SG-B discussed in Section II.F.2 above, additional inspections were performed in SG-B of randomly selected tubes and tubes with previous indications of wastage. Wastage data obtained from SG-A hot leg during the supplemental bobbin coil inspection of non-sleeved tubes were also evaluated. Finally, to more fully characterize the extent of cold leg wastage occurring in the steam generators, an additional inspection was performed in SG-A cold leg. As a result of these additional inspections, no further pluggable indications and no significant changes to previous indications were found.

## 3. Evaluation

Wastage indications observed in each steam generator this outage were compared to corresponding indications from the previous inspection in 1980. The results are summarized in Table B.1 and indicate no significant change in the amount of wastage that is occurring.

## 4. Corrective Action

One tube, R-1-C52, in SG-B was plugged due to a 55% wastage indication.

## C. AVB Inspection

### 1. Description

Tubes having previous indications of AVB wear were inspected from either the hot leg or cold leg side depending on accessibility limitations due to restricted or sleeved tubes. Multi-frequency, conventional bobbin coil eddy current techniques were employed. The resultant inspection pattern is shown in Figure B.2.

## 2. Findings

No new indications of AVB wear were observed and no significant changes to previously identified indications were observed.

## 3. Evaluation

Table B.2 summarizes the results of comparisons of AVB wear indications this inspection with corresponding indications from the previous inspection. These results indicate that there is no apparent progression of AVB wear.

## 4. Correction Action

No corrective actions were required as a result of this inspection.

# D. Denting Inspection

## 1. Description

Tubes which were previously identified as being restricted in steam generator C hot leg were gauged through the fourth support plate using eddy current probes. Due to the presence of sleeves, access to support plate restrictions was from the cold leg for certain tubes. Any tube restricting passage of a .460 probe was plugged and the neighboring tubes gauged until no restrictions were noted in the surrounding tubes. Restriction sizes observed this outage were compared to previous inspection results to assess the progression of denting.

Photographic inspections of the upper support plate flow slots of SG-C and the lower support plate flow slots of SG-A and SG-C were also performed to assess the progression of flow slot hourglassing. In addition, photographs were taken of lower support plates in SG-B to verify the continuing absence of hourglassing in that generator. Upper support plate inspection of SG-C is accomplished through a 3 inch inspection port located above TSP #4 and aligned with the tube lane. Lower support plate inspections are accomplished through the secondary side hand holes above the tube sheet on either end of the tube lane.



## 2. Findings

Photographic inspection of upper support plate flow slots showed no evidence of flow slot hourglassing, sustaining the finding of previous inspections that hourglassing due to in-plane expansion of the tube support plates is confined to the lower support plates (TSP's 1 and 2) in SG-C. All available information indicates that this is the case in SG-A as well.

Photographic inspection of lower support plate flow slots in SG-A and -C showed no change in the extent of flow slot hourglassing and tube support plate cracking in comparison to previous inspection results. Continuing absence of flow slot hourglassing and support plate cracking was verified in SG-B. Enhanced photographic inspection techniques employed this outage did, however, disclose the possibility of cold leg restrictions in steam generators A and C which had not been previously identified. Copies of SG-A and -C photographs taken this outage and submitted to the NRC during the May 12, 1982 meeting are contained in Appendix B. These photographs are also accompanied by lower support plate maps showing the location of cracks as evidenced by the photographs. As a result of these photographic inspection findings, gauging programs were developed and implemented for the cold leg sides of SG's -A and -C in order to determine the location and size of restriction not previously identified. These programs were developed based on the gauging program at San Onofre Unit 1 as described in Reference 7. The resultant gauging programs and locations of restricted tubes are shown in Figures B.3 through B.8.

Table B.3 summarizes the restrictions observed on SG-C hot and cold legs and on SG-A cold leg.

## 3. Evaluation

Comparison of tube gauging data this outage with corresponding data from previous inspections indicates no pattern of increased restrictions

attributable to a significant progression of the denting process. In SG-C, for instance, 5 tubes were restricted to a probe size that previously passed, while 16 tubes passed a probe size that was previously restricted. These results are less indicative of progression of denting than they are of artifacts of the gauging process.

With respect to the cold leg gauging findings, as expected, restrictions are fewer in number and less severe than hot leg restrictions. Also, restrictions are associated with support plate "hard spot" locations, consistent with the pattern previously observed on SG's -A and -C hot legs and in other units with denting experience.

These gauging results coupled with the photographic inspection results of flow slots demonstrate that significant progression of denting is not occurring at San Onofre Unit 1.

The condition of the lower support plates in SG's -A and -C have raised questions concerning the possibility and consequences of tube degradation due to interaction between tubes and adjacent support plate ligaments or fragments. In response, postulated tube degradation mechanisms have been considered in light of available information and operating experience, both generic and specific to San Onofre Unit 1. The mechanisms considered include: (1) tube damage due to support plate fragments impacting tubing during accident conditions; (2) tube puncture due to shear loads imposed by broken support plate ligaments; (3) tube damage due to vibration during accident conditions; (4) tube damage due to excessive restriction; and (5) tube fretting and wear at support plate locations. Of these mechanisms, (1) through (4) have been addressed in previous submittals (Reference 7 and 8). Information concerning the potential for and consequences of fretting and wear is presented below.

Fretting, or "fretage", is largely mechanical metal removal which occurs relatively slowly and is associated with small relative motions of contacting surfaces. On alloys which have a passive film, such as Inconel 600, fretting in the presence of an otherwise noncorrosive aqueous medium can remove the film, resulting in a slight amount of metal dissolution, or corrosion, a process which is continually opposed by the relatively rapid repassivation kinetics. Nevertheless, over a great many cycles, significant amounts of metal can be removed by the combined processes of mechanical action and incremental corrosion. Fretting may therefore be considered as a form of corrosion-assisted wear.

A potentially more serious form of degradation of steam generator tubing is wear. Wear differs from fretting mechanistically in that the geometrical conditions causing wear require a relatively long distance of relative motion of the contacting surfaces, with little or no accumulation of detritus from the wear. Fretting typically occurs under both lower magnitudes and lower rates of relative movement than wear. Wear is not notably increased by the presence of an aqueous environment (which can sometimes even act as a lubricant), whereas fretting can be accelerated (by fretting corrosion) by the environment. A low wear rate, however, generally results in a higher amount of metal removal than a high fretting rate.

In Fe-Ni-Cr alloys which form a passive film and are normally in the passive condition in high-temperature water, corrosion typically occurs only due to changes in electrochemical potentials to non-passive values; these potential changes arise from chemical perturbation within

the localized aqueous environment. In the case of fretting, however, the disruption of the passive film is purely mechanical, not electrochemical. Hence, thermo-dynamically, the conditions favor repassivation, and experience indicates that the kinetics of repassivation are rapid. These considerations are consistent with experience in indicating that fretting, even at a high fretting rate, is a slower, less-damaging process than wear. Qualitatively, a low wear rate in Fe-Ni-Cr alloys, such as Inconel Alloy 600, is considered to represent a higher metal removal rate than is a high fretting rate.

Based on experience, neither wear nor fretting has been identified at support plate intersections in the San Onofre steam generators. The statistical data base for such good experience is formidable: A single steam generator of the Model 27 design at San Onofre contains approximately 30,000 tube-tube-support intersections. The 3 steam generators at San Onofre, in operation for 14 years, represent over one million intersection-years of satisfactory performance without identified fretting attack at support plate locations. To add to this experience base, a special eddy current inspection was done of a number of cold leg tube lengths in SG-C which are at or near cracked support plate locations as determined from photographs. The purpose of the inspection was to seek evidence of fretting at the first and second support plate intersections. The inspection was performed using the conventional bobbin coil in the multi-frequency mode (340/100 KHz differential, 340/100 KHz absolute). The results are presented in Table B-4. No fretting or wear indications were recorded at these support intersections. It is noted that for those intersections where tubes are dented, the dents would tend to mask indications of fretting. However, as discussed later, tube vibration leading to fretting or wear would not be expected to occur at dented intersections.

During the mid-1970's a fretting/wear type of degradation was identified in San Onofre steam generator tubing at the contact points of the large radius U-bends with the original-design, round, steel anti-vibration bars (AVB's). The degradation was arrested by the installation of new, flat-surfaced, Inconel 600 AVB's. The successful performance of the new AVB's over the last 5 years indicates that fretting or wear at U-bends does not appear to be an issue.

In certain steam generators of completely different design from those at San Onofre, as well as in feedwater heaters and condensers, flow-induced tube vibration leading to tube degradation at support plate intersections has sometimes been encountered. These processes are wear-related and rapid degradation has been reported. These wear processes are useful extreme examples in assessing consequence. Wear of the type recently encountered in the Westinghouse pre-heater steam generators at support plate intersections (in the "preheater" section of the generator) was rapid. However, leakage was the only consequence of such wear. In this event, the wear occurred axially over the full support plate thickness (3/4 in.) and over very nearly half the tube circumference (180°). The metal thinned to a minimum value of about 2 mils (from the original wall thickness of 43 mils), at which point penetration of the tube wall occurred locally. It should be emphasized that neither fretting (with the attendant incremental corrosion) nor wear produce or can produce metallurgical changes to an alloy such as Inconel 600 (although surface cold work may result from wear, particularly impact wear). Therefore, wear as a result of the tube support plate interaction will lead only to a localized penetration of the tube wall by the metallurgical process of a shear effect. The extent of a tear or break in this metallurgical process in a ductile material is always limited; it has never been observed to result in a severance or transverse break of a tube made of ductile material.

Two recently encountered extreme cases of wear at units other than San Onofre illustrate the characteristic behavior of limited break propagation in severely worn, ductile nuclear steam generator tubing. The first case involved a condition which occurred at the support (or baffle) plate intersections in a region of high cross flow. The lips of the "hole" leaking tube bore the microscopic appearance (from scanning electron microscopy fractography techniques) of shear. This observation substantiates that the severely thinned Inconel tube simply was unable to sustain the internal pressure stress and failed, in a locally highly confined manner, by the normal, ductile mechanism. Characteristic of such a mechanism, the tearing or shear was unable to propagate into thicker sections of the tube wall. The second example of ductile failure of severely worn steam generator tubing involved a fully pressurized ("active") nuclear steam generator tube which experienced axial wear; the wear scar was approximately 9 inches long and was located between the tubesheet and first support plate. After the wall thickness had been reduced to about 0.006 inches (from the original 0.050 inches), or after an almost 90% reduction in wall thickness, the tube experienced a purely ductile axial split. (The axial extent of the resultant burst was  $\sim 4$  inches.) Any fretting which could be postulated to occur at San Onofre steam generator support plate intersections would occur over a relatively much smaller axial extent than observed in the cases cited above and, if it were to remain undetected could be expected to result in a leak before break condition.

In the nuclear steam generators at San Onofre, the nearly 14 years of service (without any identified support plate fretting) have resulted in individually categorizable tube-support plate intersection types, each

of which may be qualitatively described in terms of hypothetical fretting events. These are enumerated and discussed below.

- a. A non-dented normal active tube undergoing hypothetical fretting, a slow process, would exhibit an easily detectable eddy current indication within the support plate zone if the fretting had proceeded to a depth in excess of 20% (0.011 inches) of the tube wall thickness. If continued fretting results in penetration in excess of the 50% plugging limit for Unit 1, then this condition would be identified during normally scheduled eddy current inspections and the effected tube would be removed from service by plugging. Plugging of such a tube should preclude the occurrence of primary-to-secondary leakage, although additional, mechanical-type degradation by further fretting could continue. Continued fretting of a plugged tube could eventually result in localized penetration of the tube wall, an event which would not be accompanied by any tube rupture phenomena (because of the absence of internal pressure)

Since fretting has not been identified as a degradation process in active tubes at San Onofre, it is unlikely that fretting is a degradation process for plugged tubes. If fretting degradation were to develop, the potential fretting, if severe, would be detectable on the active, unplugged tubes and not detectable on the plugged tubes. For undented previously plugged tubes, fretting could slowly result in the removal of metal over a fraction of the tube circumference. It is highly unlikely that undetected fretting within a support plate zone could result in tube severance. The potential for a severed tube to develop and subsequently be free to interact with and wear against neighboring tubes is therefore considered to be very low. This is supported by the absence of verified fretting on active tubes (indicating a low probability for fretting initiation).

- b. A "dented" tube, which by definition is a tube that is (a) tightly surrounded by support plate corrosion product in the tube to plate annulus and (b) constricted or reduced in diameter in the support plate zone, would not be free to fret unless support plate deterioration resulted in a loss in geometrical integrity of the intersection, a case which will be considered later. The probability of metal loss by fretting at a dented plate-tube intersection is therefore adjudged to be insignificant because of the hindrance of relative motion. In units more severely dented than San Onofre, instances of leakage at intact support plate intersections occurred by primary-side initiated intergranular cracking of the tubing associated with the severity of tube restriction. Tubes removed from such intact intersections did not exhibit O.D. surface indications of fretting. No such instances have been experienced at San Onofre Unit 1.
- c. A unique condition of dented tube-support plate intersections applies to the condition of cracked or broken support plate ligaments. In some cases adjacent to the tube lane flow slots the tube is not completely surrounded by the support plate due to broken ligaments and distortion that have occurred in the tube bundle. These conditions can conceivably increase the potential for tube vibration and fretting due to loss of tube support. The major consideration for this type of geometry is that the tube could become unsupported to the extent that lateral movement could develop into impact wear where the tube contacts the support. However, this type of geometry has existed in the lower support plate tube lane regions at San Onofre for a number of years, and no vibration-related tube degradation has been experienced. This



experience suggests that for tubes where only partial support exists at the first and/or second tube support plates, the associated tube vibration amplitudes are sufficiently low to preclude progressive fretting and eventual impact-type wear. A tube vibration analysis which assumes these support conditions were performed in order to analytically assess the vibration amplitude and consequent potential for fretting. These support conditions were analyzed for two cases -- with and without lateral preload at the tube to support plate intersections. The case with preload is considered to be most representative of actual tubing as evidenced by bowing of tubes along the flow lanes of SG's -A and -C at the lower support plate spans. Results of this analysis are contained in Appendix B.4 and show very small vibration amplitudes, particularly for the case of lateral pre-load. The experience at San Onofre Unit 1 is therefore supported by analysis and leads to the conclusion that fretting and eventual impact type wear would require the development of heretofore unexperienced conditions at San Onofre Unit 1. This experience and the Appendix B.4 analysis also strongly suggest that the actual support conditions in SG's -A and -C are, at worst, those of partial support described above.

- d. Consideration may also be given to a hypothetical situation in which a small section of tube support plate may have all connecting ligaments broken and become dislodged. Detachment of support plate ligaments into small fragments or fractions of fragments is a low-probability event since cracking of a ligament at one location tends to relieve stresses at surrounding locations which could otherwise lead to further cracking. In the unlikely event that a fragment is created, experience with foreign objects indicates that there is no

likelihood of a tube puncture process. Any residual freedom of motion of such a small object introduces no new considerations of fretting or wear.

In summary, fretting is a slow process, heretofore not experienced at support plate intersections in steam generators of the Series 27, San Onofre design. If the slow development of fretting proceeded to a depth in excess of 20% wall penetration at an undented intersection, it would be detectable by eddy current and subject to periodic monitoring by ECT. The metal removal in fretting or wear as a result of tube support plate interaction would be a localized process, both axially and circumferentially. Any complete wall penetration by a fretting or wear-related process would remain highly localized with limited propagation by tearing. Metallurgically, any tearing localized at the point of minimum wall would be exclusively ductile, consisting microscopically of shear. All experience and metallurgical considerations, including the absence of microstructural changes in the alloy by fretting or wear support the thesis that, in the worst case (wall penetration), a leak but not a break would develop from any fretting or wear at a tube-support plate intersection.

#### 4. Corrective Actions

One tube in SG-A and three tubes in SG-C, which were restricted to a .460 probe, were plugged.

#### E. Conclusions

Based on the results of the Technical Specifications Inspection, it is concluded that there are no significant active corrosion, fretting or wear processes occurring in the San Onofre Unit 1 steam generators. In particular, significant progression of denting and of AVB wear is not occurring, nor is there evidence of fretting occurring at tube and support plate intersections. Moreover, were fretting to occur at isolated intersections, leak-before-break would be the governing failure mechanism.

## Section IV

### Foreign Materials Inspection

#### A. General

Historical maintenance, inspection and repair activities at San Onofre Unit 1 have included application of a varying range of measures to control the introduction of foreign materials into the steam generators. Examples of such measures have included inventory control procedures for materials, tools, etc. entering and exiting steam generator channel heads, lanyards secured to tools and materials, installation of nozzle covers and other devices to capture debris or dropped objects, and inspections to locate and retrieve materials. During the 1980-81 sleeving project, a thorough foreign materials inspection was performed of the steam generator channel heads and associated primary coolant piping to assure removal of any materials introduced as a result of that extensive inspection and repair effort.

The above measures have typically been applied in association with a given steam generator inspection, maintenance, or repair activity. As such, a general foreign materials and loose parts inspection of the steam generator secondary sides, in particular, has not been performed to date. In the absence of such an inspection and in light of recent industry experience relating to interaction of secondary side foreign materials with steam generator tubing, a general inspection was initiated during the current outage to locate and retrieve any previously unidentified foreign materials and loose parts on the secondary side of each steam generator. An additional effort was also launched to locate and retrieve a self-reading dosimeter which was dropped into the upper internals

of SG-A while making modifications to the moisture separators during the current outage.

Preliminary findings from these inspections were communicated to the NRC. In particular, the NRC was apprised of the discovery of loose and missing wrapper support bars (WSB's) and of resultant adjustments made to the inspection program in order to disposition WSB findings.

In summary, the foreign materials inspection program, adjusted to reflect initial findings, consisted of the following elements:

1. Foreign Materials Inspection

- Full circumference visual inspection in each steam generator of the annular region between the tube bundle and shell at the top of the tube sheet in order to locate foreign materials.
- Visual inspections of the tube lanes of each steam generator to locate foreign materials.
- Secondary side visual inspection in SG-A to locate the dosimeter inadvertently dropped into the upper internals during current outage moisture separator modifications.
- Retrieval of foreign material.

2. Wrapper Support Investigation

- Full Circumference visual inspection in each steam generator of the tube bundle-wrapper-shell annular region above the top of the tube sheet to locate loose WSB's, locate and assess the condition of intact WSB's, and identify and examine locations where WSB's are missing.
- Retrieval of loose WSB's.
- Visual inspection of tubes in the neighborhood of loose WSB's in

order to detect gross indications of damage which may have occurred to tubes due to possible tube-WSB interaction.

- Eddy current inspection through the first support plate of the outermost active peripheral tubes in each steam generator for evidence of tube degradation due to possible foreign material or WSB interaction.
- Metallurgical analysis of removed WSB's to characterize failure mechanisms.
- Flow tests in a mock-up of the downcomer-wrapper-tube bundle region to assess the behavior of loose WSB's, including interaction with tubing, under simulated operating conditions.
- Visual inspection of alternate wrapper supports to verify support integrity.
- Structural analysis of wrapper supports and other steam generator internals to confirm steam generator tube integrity under SLB accident and SSE loading conditions.

The above program, including inspection scope, techniques, findings, evaluations, corrective actions and conclusions, is further discussed below, in Appendix D, and in Appendix E, Report on Steam Generator Wrapper Supports Investigation.

#### B. Scope

To establish the scope of the general inspection within each steam generator, consideration was given to several factors including pathways for introduction of foreign materials into the secondary side, regions of likely interaction between tubes and foreign materials, inspection history in given regions and the feasibility of available inspection techniques.

Figure D-1 shows the principal features of the Westinghouse Series 27 steam generators installed at San Onofre Unit 1. Primary pathways for the introduction of foreign materials into the secondary side are the secondary manway, the secondary handholes and, in SG-C only, the inspection port above the fourth support plate. Materials can also be introduced through the various process stream nozzles, particularly the feedwater nozzle.

Materials introduced through the secondary manway can migrate to the tube bundle either through (a) the swirl vanes or (b) down through the wrapper shell annulus after passing through openings in or around the downcomer flow resistance plate. In case (a), materials could either be confined to the top of the tube bundle region above the fourth tube support plate or drop to lower support plates or the tube sheet through the annular gap between the tube support plate and the wrapper and/or the support plate flow slots. In case (b), small objects passing by the flow resistance plate would drop to the top of the tube sheet where they could come in contact with tubing. This latter case also applies to small objects entering via the feeding openings.

Materials introduced through the secondary handholes would likely be confined to the top of the tube sheet in either the tube lane or in the annular region between the tube bundle and steam generator shell.

Materials introduced through the SG-C inspection port could drop through the wrapper-to-shell annulus to the top of the tube sheet or to the top of the fourth support plate if introduced through the wrapper opening as well. Since the inspection port is aligned with the tube lane, materials on the fourth support plate could conceivably drop to lower plates or the

tube sheet through the support plate flow slots, as well as through the tube support plate to wrapper gap. Past inspections through the inspection port have shown no evidence of foreign materials at the upper support plates.

Depending upon foreign material geometry, other migration paths may exist resulting in tube interactions. However, considering the various possibilities, it is judged that the most likely areas for materials to migrate into potentially damaging contact with tubing are the upper bundle region above the fourth support plate and the top of the tube sheet. Of these areas, the upper bundles of all steam generators were inspected for foreign materials in conjunction with the AVB modifications during the 1976-77 outage. As noted previously, a special upper bundle inspection was developed in SG-A this outage to locate and retrieve the dropped dosimeter. Moreover, hydraulic conditions which would promote interaction between steam generator tubing and foreign materials seem more likely to occur at the top of the tube sheet where downcomer flow is directed radially inward toward the tube bundle. Finally, personnel and equipment access and ALARA considerations weigh in decisions on the location and extent of regions within the steam generators to be inspected. Based on these considerations, the top of tube sheet regions in each steam generator were selected for performance of the general Foreign Materials Inspection this outage.

### C. Inspection Techniques

Inspection and retrieval techniques employed were governed by the steam generator internals geometry in the region above the top of the tube sheet. Figure D-2 depicts the internals arrangement and geometrical constraints in this region.



Visual inspections were accomplished using skid mounted TV cameras. For the annular inspection, geometrical constraints limited camera lighting and available view angle to the diagonal field of view associated with straight viewing. Right angle viewing was achievable for the tube lane inspection only.

Foreign objects were removed using either a magnet or a grappler. Small particles, loose sludge and magnetite deposits were removed using a vacuum system. Following retrieval and vacuuming efforts, a final visual inspection was performed to ensure that all foreign objects were identified and removed as required.

In the case of the dropped dosimeter in SG-A, a direct visual (no TV) inspection of the top of the tube bundle was performed through the swirl vane assembly. The dosimeter was located and was removed using a magnet.

#### D. Findings

Table D.1 of Appendix D is a tabulation of foreign materials and loose parts found in each steam generator. This table also summarizes the status of wrapper support bars identified as being intact in their original design locations, broken and lying atop the tube sheet near their original design locations, or missing.

As noted above, the findings relative to WSB's prompted a thorough investigation of wrapper supports to determine the cause of the conditions observed and the appropriate corrective actions. Details of this investigation are contained in Appendix E; the findings of this investigation are summarized below.

## FINDINGS OF THE WRAPPER SUPPORTS INVESTIGATION

1. The background investigation found that WSB's in Series 27 steam generators were observed to be subject to failure during the manufacturing process. This observation led to field modifications of Unit 1 steam generators to include alternate wrapper supports. No records of inspections and/or removal of WSB's prior to the current outage have been located.
2. Visual inspection of removed WSB's and original WSB locations showed similarity as to break locations at the threaded end and /or wrapper attachment piece.
3. Visual inspection of peripheral tubing in each steam generator, with particular attention to tubing adjacent to loose WSB's, showed no evidence of tube degradation.
4. Eddy current inspection of peripheral tubes showed no evidence of significant tube degradation which could be correlated with tube interaction with WSB's.
5. The plugging history of peripheral tubes showed no tube having been plugged due to indications of tube degradation between the tube sheet and first tube support plate.
6. Metallurgical analysis of removed WSB's indicated that fracture was due to a fatigue mechanism that occurred early in plant life. The fracture mechanism was common to all WSB's analyzed.
7. Flow tests at a Unit 1 steam generator mock-up utilizing a WSB removed from Unit 1 demonstrated that tube degradation due to WSB-tube interaction does not occur under simulated operating conditions.

8. Visual inspection of alternate wrapper supports showed that the supports and welds are intact. Abnormalities noted in certain support configurations were analyzed and found to be inconsequential relative to support structural integrity.
9. Structural analyses of the steam generator internals, including wrapper supports, demonstrated that the structural integrity of the internals and the tube bundle primary pressure boundary are maintained under the worst case SLB and SSE loading conditions.

## E. Evaluation

The collective findings of the foreign materials inspection and the wrapper supports investigation have been evaluated to determine what corrective actions, if any, are required beyond: a) removal of foreign material and loose WSB's and b) plugging of tubes with anomalous indications as discussed in Appendix E, Part IV of this report. Three items were identified for determination of possible corrective actions:

1. Disposition of intact WSB's in SG-A and -B.
2. Disposition of off-design configuration of alternate wrapper supports in SG-B and -C.
3. Suitability of foreign materials controls currently in place.

With respect to the intact WSB's, consideration was given to leaving them in their as-found conditions or to removing them from the steam generators. Removal of the WSB's cannot be accomplished without considerable difficulty in light of significant technical, equipment access, inspection, and personnel exposure issues which have been identified. Accordingly, WSB removal must be based on demonstrated need. Such need has not been demonstrated based on the findings of the wrapper supports investigation. The reasoning is as follows:

- The cumulative evidence from the wrapper supports investigation strongly suggests that the observed conditions of intact, loose and missing WSB's have been in existence since the beginning of plant operation.
- There is no evidence of prior tube plugging repairs or currently noted tube degradation in active tubes having occurred due to interaction between tubing and WSB's.
- The absence of tube degradation attributable to interaction between tubing and WSB's during normal operation is supported by the results of the flow tests.

- Insofar as WSB-tube interaction under accident conditions is concerned, the postulated tube degradation mechanisms would be impact damage or puncture during the short duration transient. These mechanisms have been explored in earlier work (see Reference 8) and are not a concern relative to tube integrity. Furthermore, since flow is directed radially outward from the tube bundle during the SLB accident, conditions which would promote interaction between WSB's and tubing are unlikely.
- Therefore, should intact WSB's become dislodged during operation, they would not be expected to significantly degrade adjacent tubing.
- Periodic secondary side inspections can be made in SG-A and B to observe the condition of WSB's and remove any which may have become dislodged.

With regard to the alternate wrapper supports, the structural analysis considering as-found conditions demonstrates that the supports are adequate to perform their required functions.

With regard to control of foreign materials, the measures implemented to date have been largely successful in excluding foreign objects from the steam generators in view of the significant inspection, maintenance and repair efforts which have been accomplished in the past. Notwithstanding this experience, an in-depth review of procedures and practices extending to steam generators and all other appropriate equipment is deemed warranted.

#### F. Corrective Actions

All identified foreign materials and loose WSB's were removed from the steam generator secondary sides. Intact WSB's in SG's-A and B were left in place. The alternate wrapper supports were accepted in their as-found conditions.

As a conservative measure, peripheral tubes with ID indications or restrictions in tube spans below the first support plate were plugged as follows: a) SG-A -- three tubes having ID indications, b) SG-B -- two tubes having ID indications, and, c) SG-C -- three tubes having restrictions.

An in-depth review of foreign material control measures will be undertaken and a formal program addressing foreign material exclusion and inventory control will be implemented prior to performing further major work in the Unit 1 steam generators.

At the next and subsequent refueling outages, the secondary sides of steam generators A and B will be visually inspected to determine the condition of intact wrapper support bars. Inspection results will dictate appropriate corrective actions at that time.

#### G. Conclusions

Based on the results of the foreign materials inspection and wrapper supports investigation it is concluded as follows:

- Significant tube degradation has not occurred due to the presence of foreign materials and loose WSB's.
- WSB's found to be intact in SG's-A and B can be left in place without effecting tube integrity.
- The steam generator internals configuration is structurally adequate under worst case faulted conditions (SLB and SSE) and is such that tube integrity is not adversely effected.

Summary and Conclusions

## A. Summary of Results

All elements of the Sleeving Repair Inspection were satisfactorily completed. The results provide evidence of tube bundle integrity, the effectiveness of the sleeving repair program and the conservatism of the repair criteria. Although eddy current inspection techniques employed are not without limitations, they are judged to be adequate for monitoring critical area of sleeved and non-sleeved tubes in light of the structural integrity considerations and safety assessment presented in Appendix C. Improvements in eddy current inspection techniques which are being developed within the industry are, nevertheless, being pursued and hold promise for application during future sleeving inspections.

In particular regard to IGA in the non-sleeved peripheral tubes, the collective results from the current and previous outage inspection programs and diagnostic studies indicate that the previously postulated extent and rate of progression of IGA and the associated repair criteria are conservative. The safety concerns for non-sleeved peripheral tubes are further mitigated considering the results of the structural integrity analysis in Appendix C of non-sleeved tubes with assumed extensive IGA degradation under postulated accident conditions. The analysis, in conjunction with laboratory studies and leaking tube history at San Onofre Unit I, supports the proposition that the probable failure mode for tubes with IGA at the top of the tube sheet is "leak before break". As such, tube rupture under accident conditions is not likely. Furthermore, the stringent allowable primary to secondary leakage limitations of the San Onofre Unit 1 Technical Specifications would mandate timely and orderly unit shutdown to remove any leaking tubes from service. Additionally, it is likely that, under the more realistic assessments

of extent and rate of progression of IGA in peripheral tubes, the eddy current inspections at normal inspection intervals will detect IGA tube degradation prior to penetrating through wall.

The results of the Technical Specification Inspection confirm the absence of continuing significant tube degradation processes related to tube wastage, AVB wear and denting and of fretting at tube-support plate intersections. Were fretting to occur undetected, leak-before-break would apply. Given the unlikelihood of fretting at support plate intersections and the probable failure mode, fretting at cracked support plate locations is not a safety concern at San Onofre Unit 1.

With regard to the foreign materials inspection, all loose materials were removed. The wrapper supports investigation demonstrates that no apparent tube degradation has occurred due to the presence of loose wrapper support bars on the secondary side over a number of years of operation. Flow tests verify this experience in demonstrating that damaging interactions between tubes and loose support bars do not occur under simulated operating conditions. The wrapper supports investigation further demonstrates the structural adequacy of the existing steam generator internals support configuration under worst case accident and seismic loading conditions.

#### B. Return to Power Conditions

At the conclusion of the previous outage, before return to power, revised secondary chemistry and steam generator soaking and flushing procedures were implemented. These procedures will continue to be implemented during unit start-up and subsequent operation following the current outage.

With regard to the reduced primary temperature conditions, which were also implemented last outage, insufficient data exist to reach definite conclusions as to their effectiveness in mitigating progression



of IGA at San Onofre Unit 1. Operation under these conditions is discretionary and it is intended to resume operation under these reduced conditions until otherwise warranted by prevailing circumstances.

All plugging repairs required as a result of this inspection have been completed. These repairs are summarized in Appendix F, Tables F.1 and F.2.

### C. Future Inspections

In consideration of the results of this inspection, the corrective actions taken, and the additional information contained herein, it is concluded that performance of steam generator eddy current inspections at the normal refueling outage interval (i.e., approximately 15 to 16 EFPM) is consistent with safe operation of the unit. However, prior to implementing this inspection interval, confirmatory inspection data will be obtained during an inspection at the next refueling outage in approximately 12 EFPM of operation following the current outage. At that time, a Technical Specification inspection incorporating sleeved and non-sleeved tube inspections will be performed. The inspection program will be similar to that performed during the current outage.

In addition, an in-depth review of measures relating to foreign material inventory, accountability and control will be undertaken. Prior to commencing further major work in the steam generators in subsequent outages, a formal Foreign Material Exclusion and Inventory Control Program will be implemented reflecting the results of the in-depth review and incorporating appropriate administrative and positive measures to control foreign materials. This program will be applied to other equipment, as appropriate, in addition to steam generators.

Lastly, at the next and subsequent refueling outages, the secondary sides of steam generators A and B will be visually inspected to determine the condition of intact wrapper support bars. Inspection results will dictate appropriate corrective actions at that time.

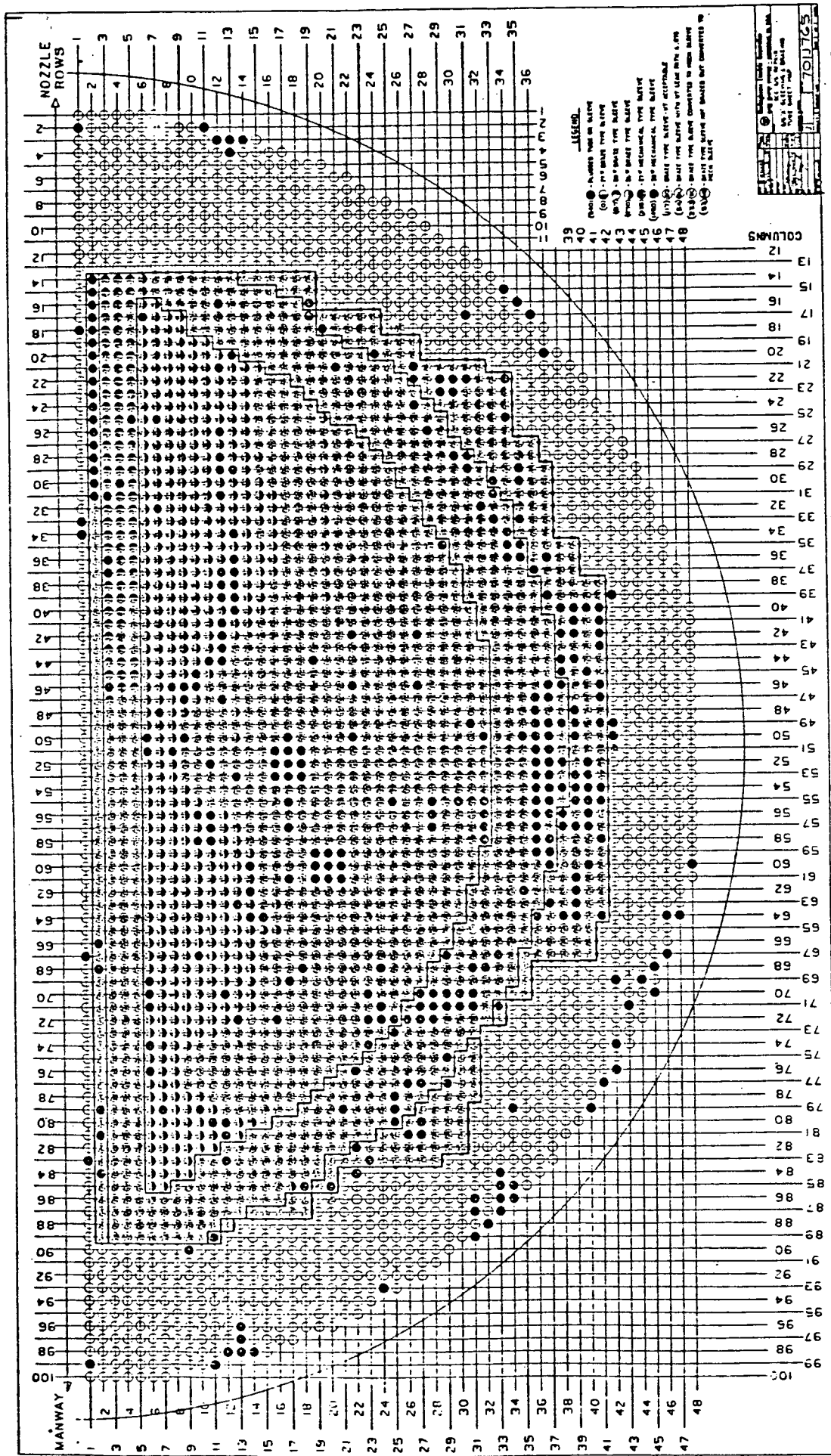
## References

1. NRC (D.M. Crutchfield) letter to SCE (R. Dietch) dated March 11, 1982, Subject: Proposed Steam Generator Inspection Program -- San Onofre Unit 1.
2. Steam Generator Repair Report, Revision 1, March 1981, San Onofre Unit 1.
3. SCE (K.P. Baskin) letter to NRC (D.M. Crutchfield) transmitting report entitled "Technical Evaluation Report of a Hybrid Joint," March 1981, San Onofre Unit 1.
4. Steam Generator Repair Program, Return to Power Report, April 1981, San Onofre Unit 1.
5. SCE (K.P. Baskin) letter to NRC (D.M. Crutchfield) dated January 22, 1982, Subject: Steam Generator Tube Inspections, San Onofre Unit 1.
6. SCE (K.P. Baskin) letter to NRC (D.M. Crutchfield), dated June 24, 1980, Subject: Steam Generator Inspections, San Onofre Unit 1.
7. SCE (K.P. Baskin) letter to NRC (D. Ziemann), dated April 17, 1978 and report entitled, "Steam Generator Denting Inspections", San Onofre Unit 1.
8. SCE (J.T. Head) letter to NRC (A. Schwencer), dated february 1, 1977 and report entitled, "Steam Generator Inspections, San Onofre Unit 1", dated January 30, 1977

APPENDIX A

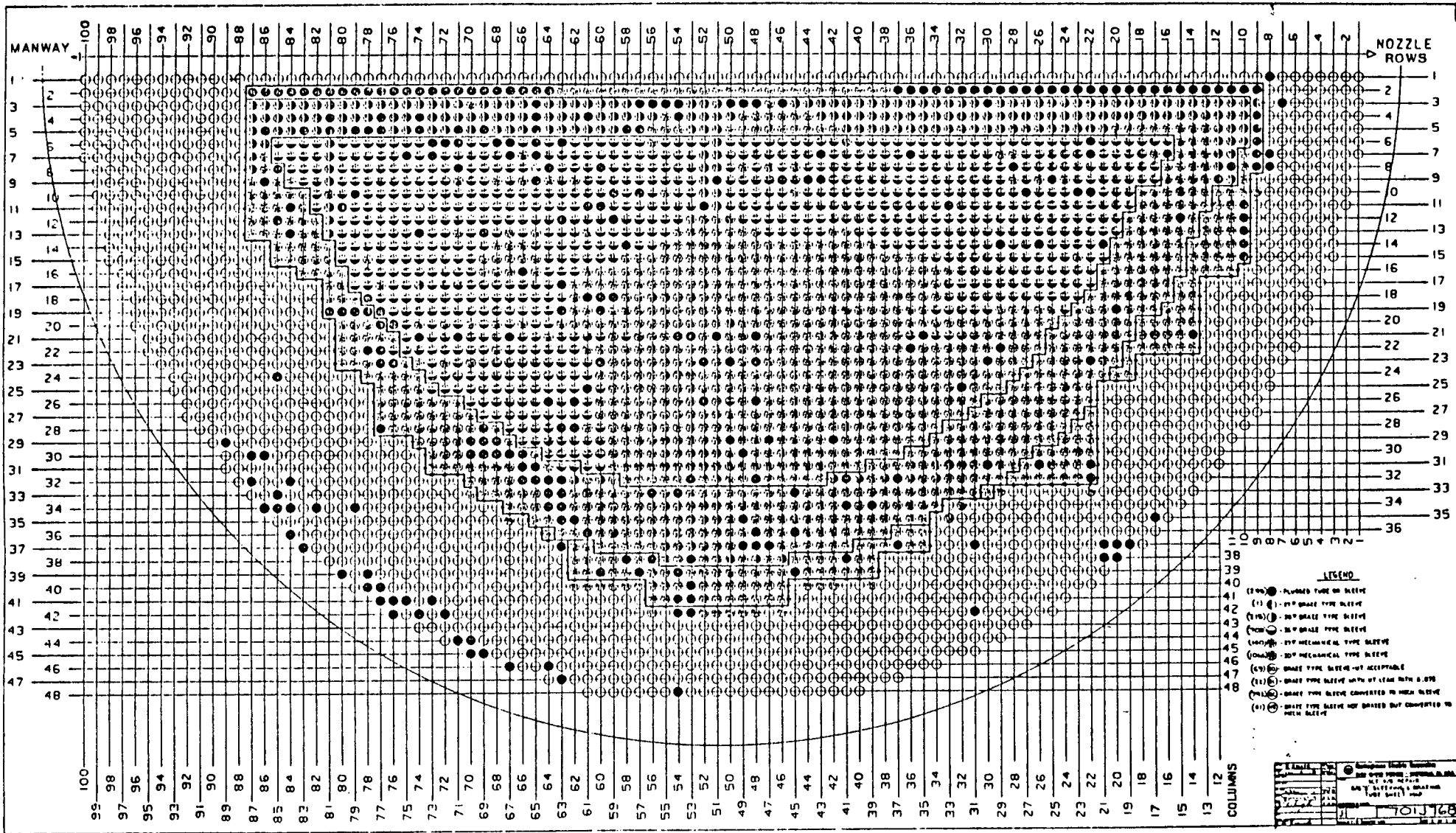
Sleeving Repair Inspection

Tables and Figures



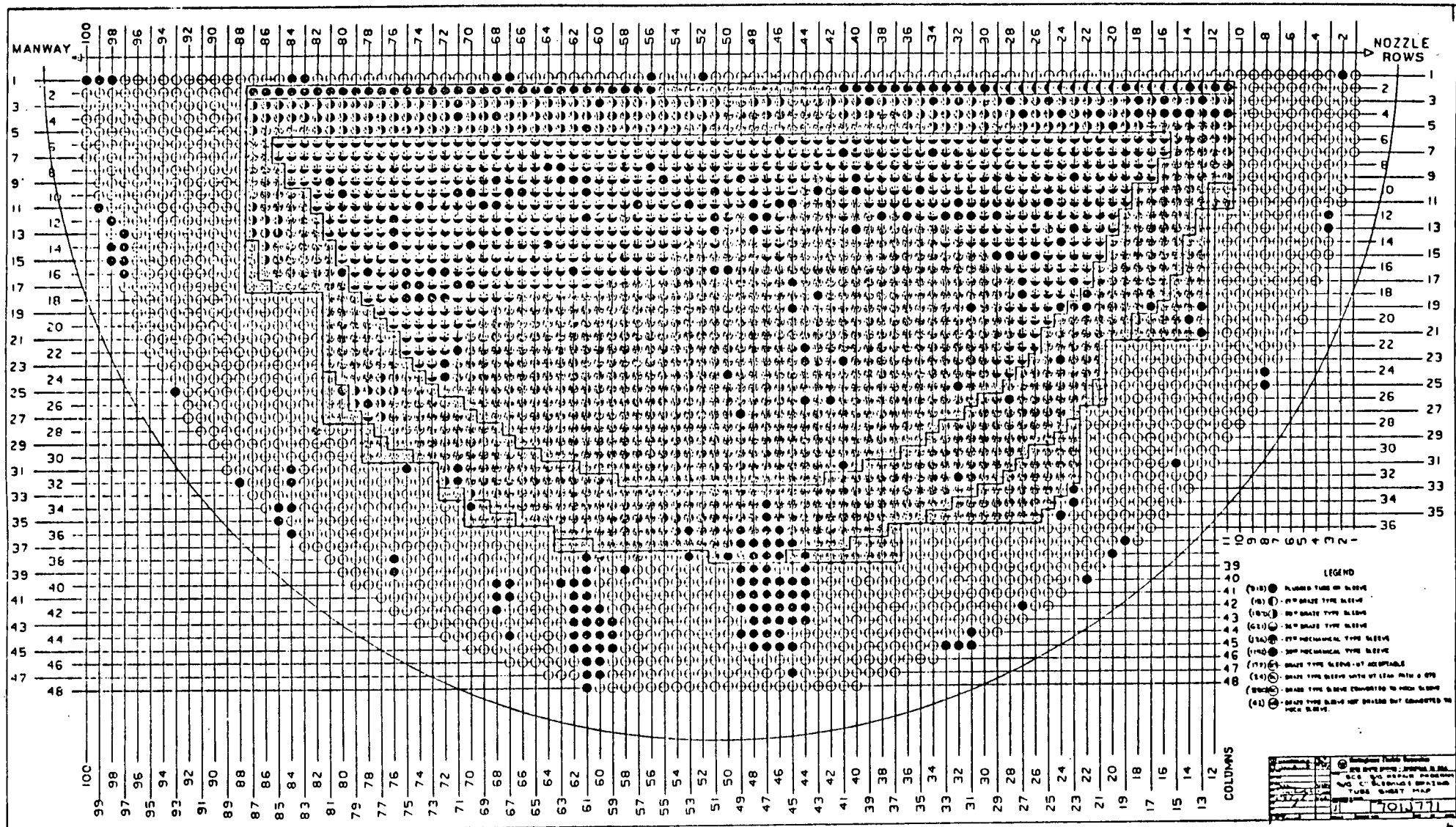
SG-A 1981 SLEEVING REPAIR BOUNDARY

FIGURE A-1



SG-B 1981 SLEEVING REPAIR BOUNDARY

FIGURE A-2



SG-C 1981 SLEEVING REPAIR BOUNDARY

FIGURE A-3

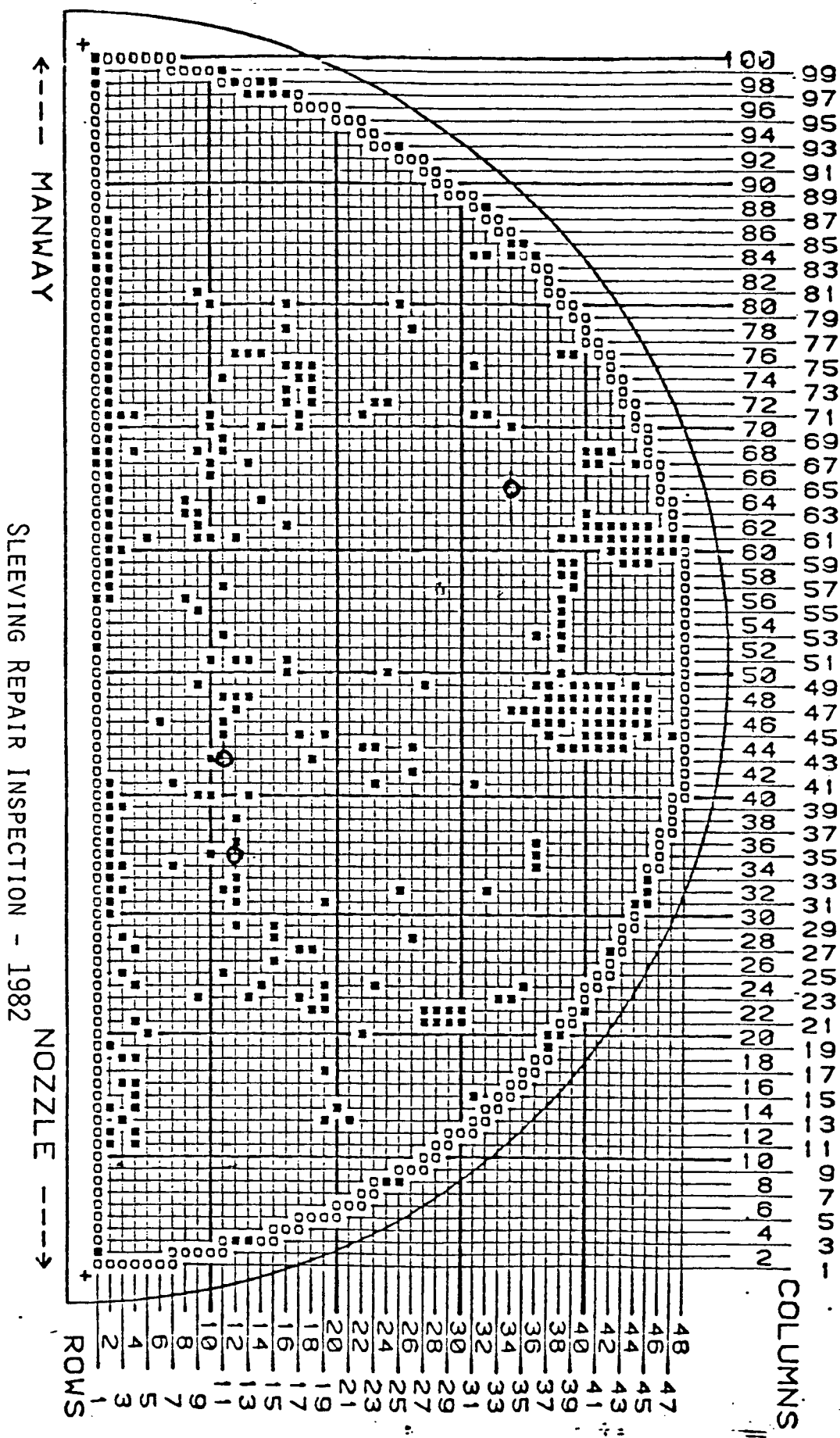
FIGURE A-4

SERIES 27

LEAKING TUBES - SECONDARY SIDE LEAKAGE TEST

○ - DENOTES LEAKING TUBE

SCE-C  
INLET



SLEEVING REPAIR INSPECTION - 1982



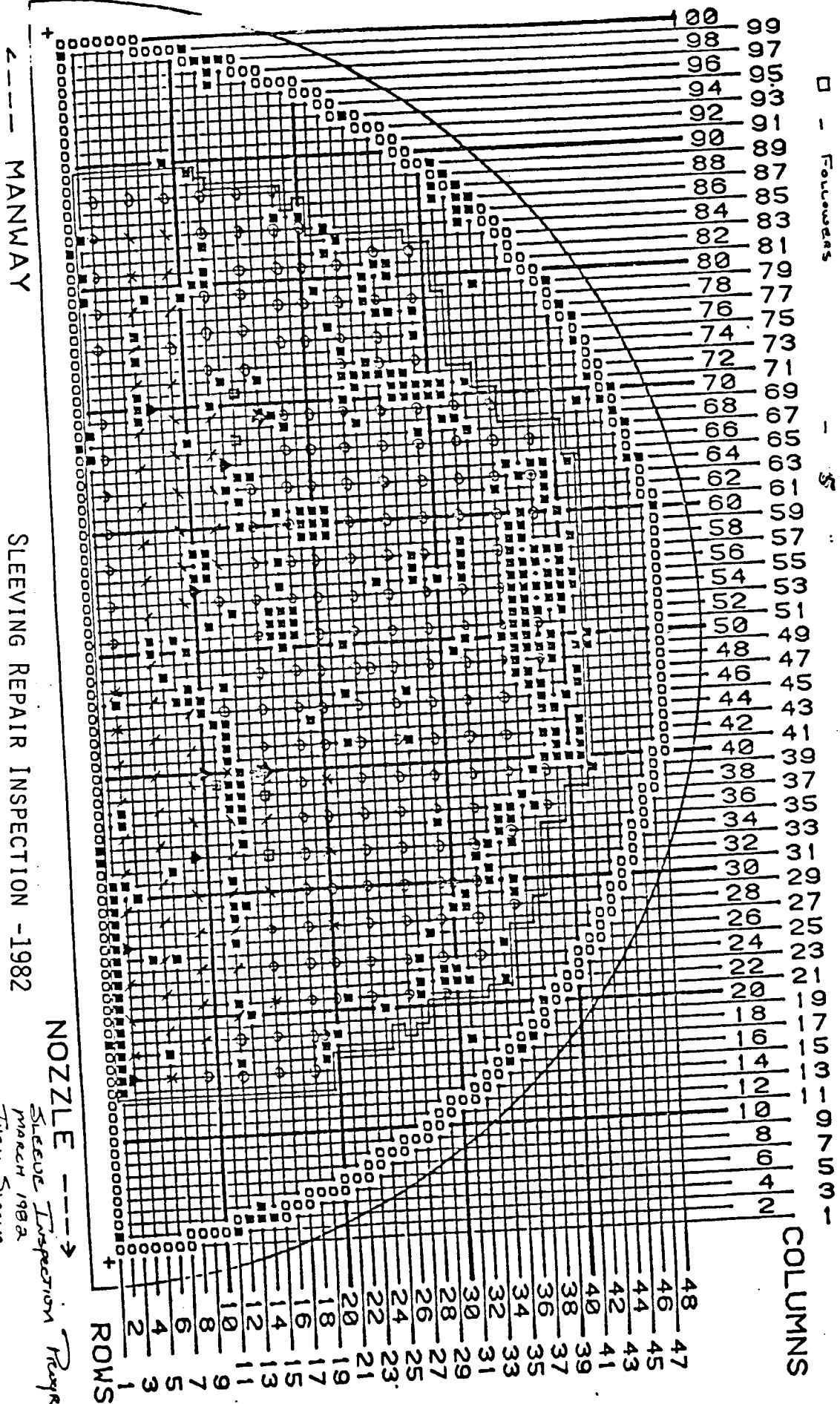
FIGURE A-5

SLEEVED TUBE INSPECTION PATTERN

- △ - GRADED LEAK LIMITERS - 7 SLEEVES
- - Mechanical - 186 "
- - GRADE COVERED - 45 "
- X - No GRADE Covering - 11 "
- - GRADE ONLY - 16 "
- ☆ - LEADERS - 2 "
- - FOLLOWERS - 5 "

SERIES 27

SCE-A



SLEEVING REPAIR INSPECTION - 1982

NOZZLE →  
Sleeve Inspection Program  
March 1982  
True Sleeve.

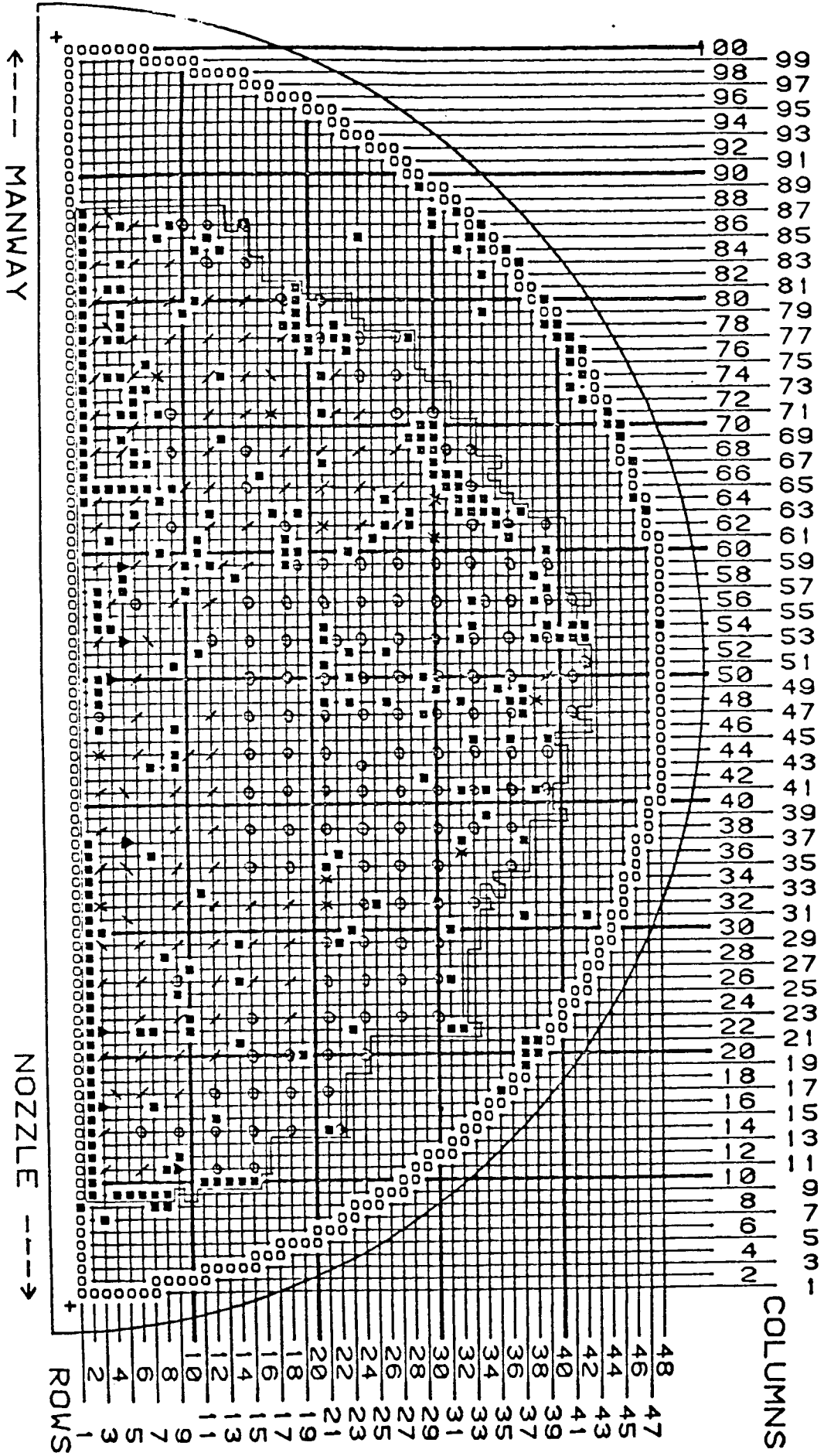
FIGURE A-6

SLEEVED TUBE INSPECTION PATTERN

- △ - Braised Lead Linerless
- - Mechanical
- ∩ - Braze Converter
- x - No Braze Converter
- ∟ - Braze Only

SERIES 27

SCE-B



SLEEVED TUBE INSPECTION - 1982

MANWAY ←

NOZZLE →

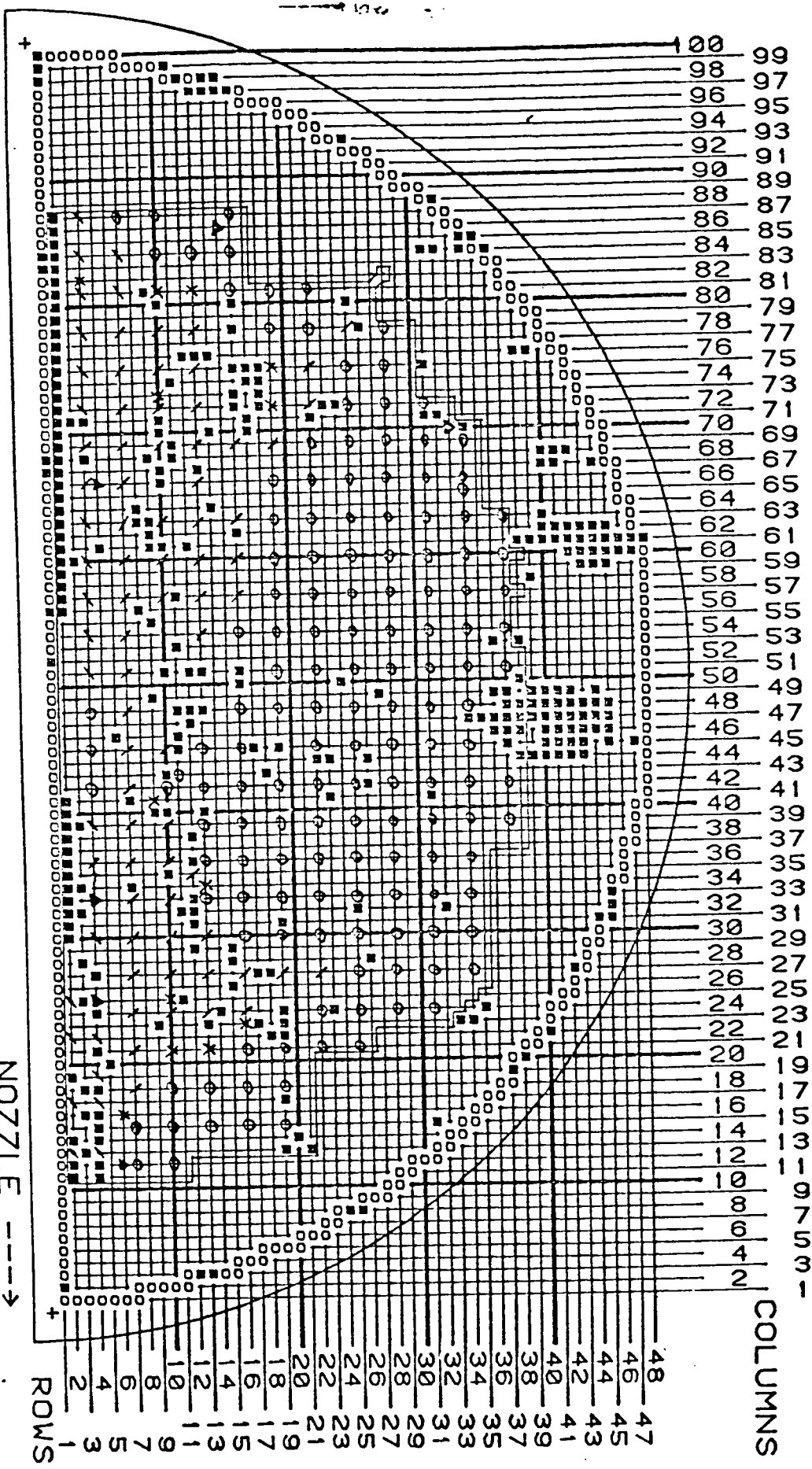
COLUMNS

ROWS

FIGURE A-1  
SLEEVED BE INSPECTION PATTERN  
SG-C

A - Brazed Leak Limiters - 6 Sleeves  
 O - Mechanical - 147 "  
 / - Brazed Converter - 62 "  
 X - No Brazed Converter - 13 "  
 / - Brazed Only - 24 "

SERIES 27  
 SCE-C  
 Inlet



MANWAY ←  
 SLEEVING REPAIR INSPECTION - 1982

NOZZLE →  
 Sleeve Inspection  
 March 1982  
 thru Sleeve

TABLE A-1  
SLEEVING INSPECTION SUMMARY

<u>Sleeve Type</u>	<u>S/G</u>	<u>Number of Sleeve Type in Steam Generator</u>	<u>Number of Sleeve Type Inspected in each Steam Generator</u>
Brazed only	A	117	16
	B	69	11
	C	177	23
Brazed Converted	A	333	45
	B	792	101
	C	580	63
No Braze Converted	A	53	10
	B	41	11
	C	42	15
Leak Limiter	A	54	7
	B	22	7
	C	24	6
Mechanical	A	1685	187
	B	1206	142
	C	1318	147

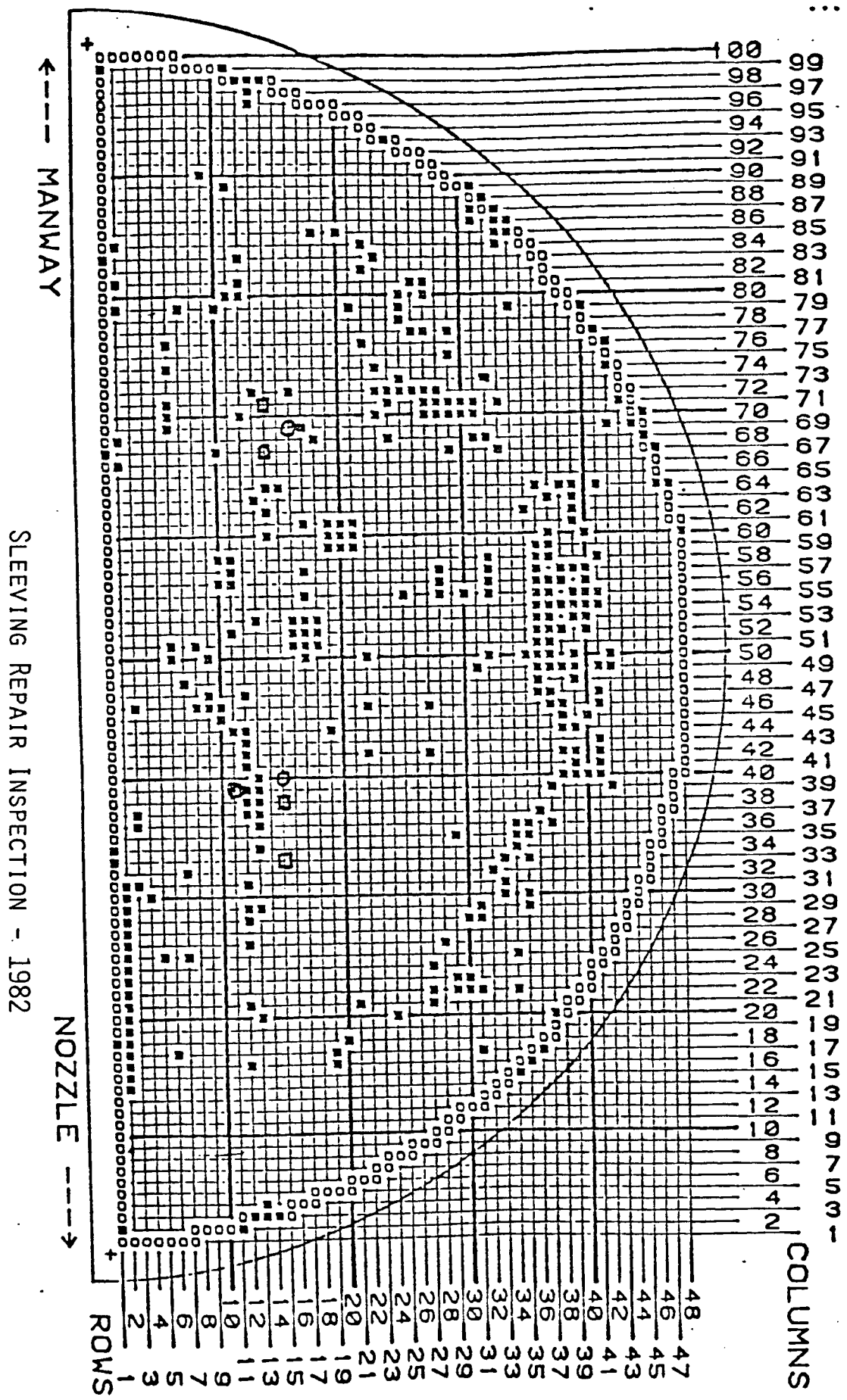
SCALE R TUBE = 2  
D. FOLLOWER TUBE = 5

FIGURE A-8  
LEADER - FOLLOWER PROGRAM

SG-A

SERIES 27

SCE-A  
INLET



SLEEVE REPAIR INSPECTION - 1982

MANWAY

NOZZLE

COLUMNS

ROWS

FIGURE A-9

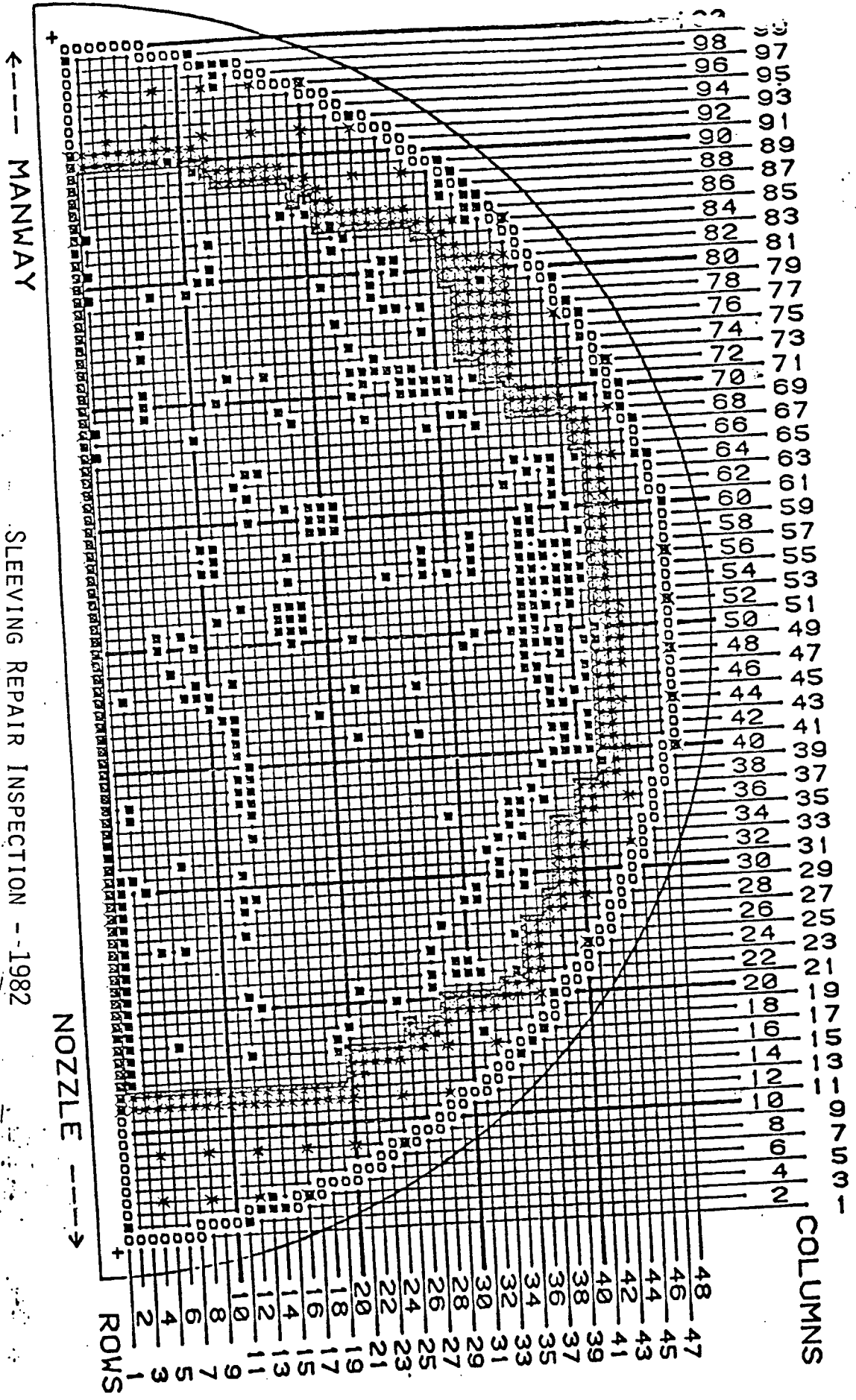
NON-SLEEVED TUBE INSPECTION PATTERN

SERIES 27

TUBES INSPECTED: X=422 TUBES

SG-A

SCE-A  
INLET



MANWAY ←

SLEEVEING REPAIR INSPECTION --1982

NOZZLE →

COLUMNS

ROWS

FIGURE A-10

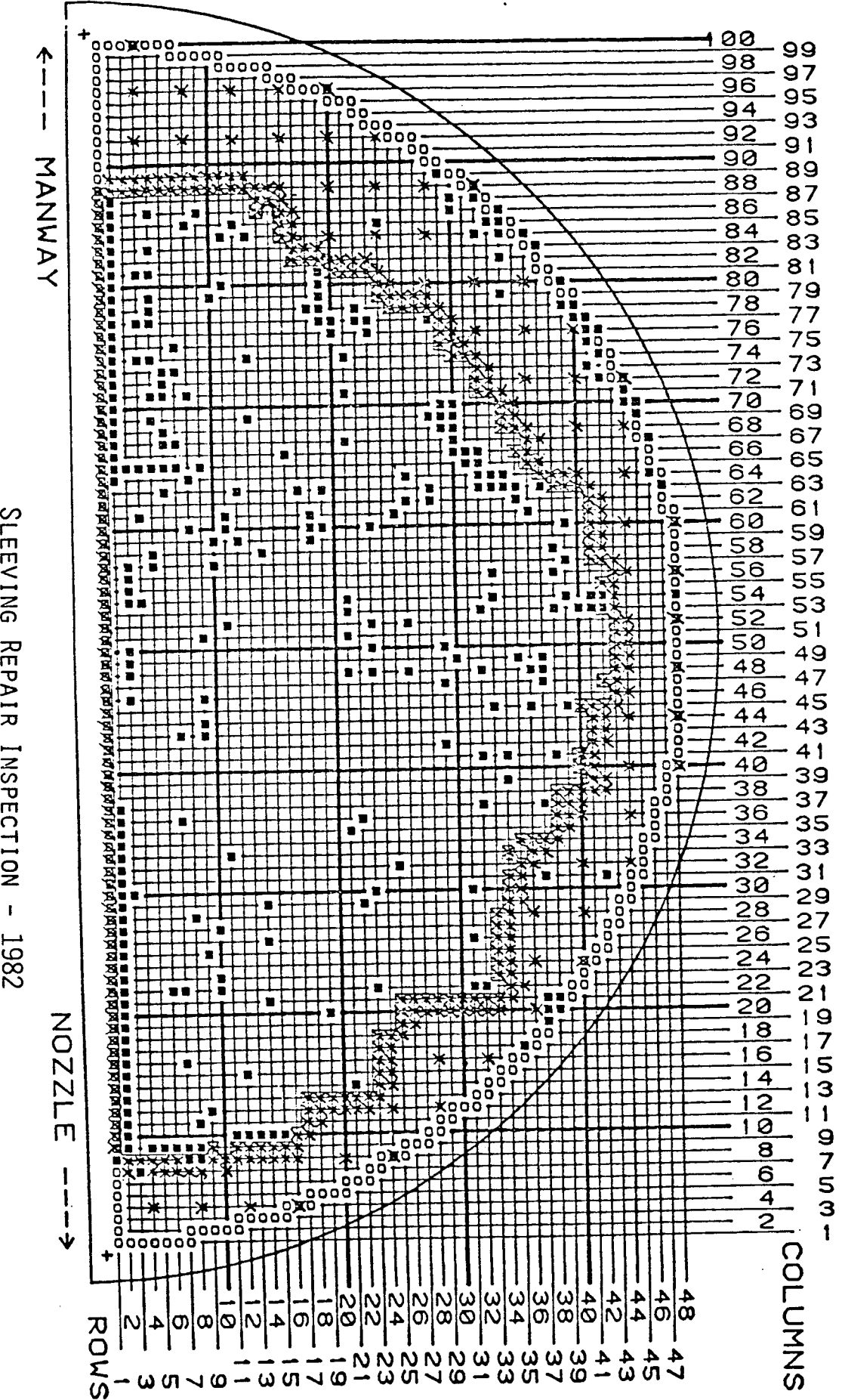
NON-SLEEVED TUBE INSPECTION PATTERN

SG-B

SERIES 27

TUBES INSPECTED: X=396

SCE-B  
INLET



SLEEVING REPAIR INSPECTION - 1982

FIGURE A-11

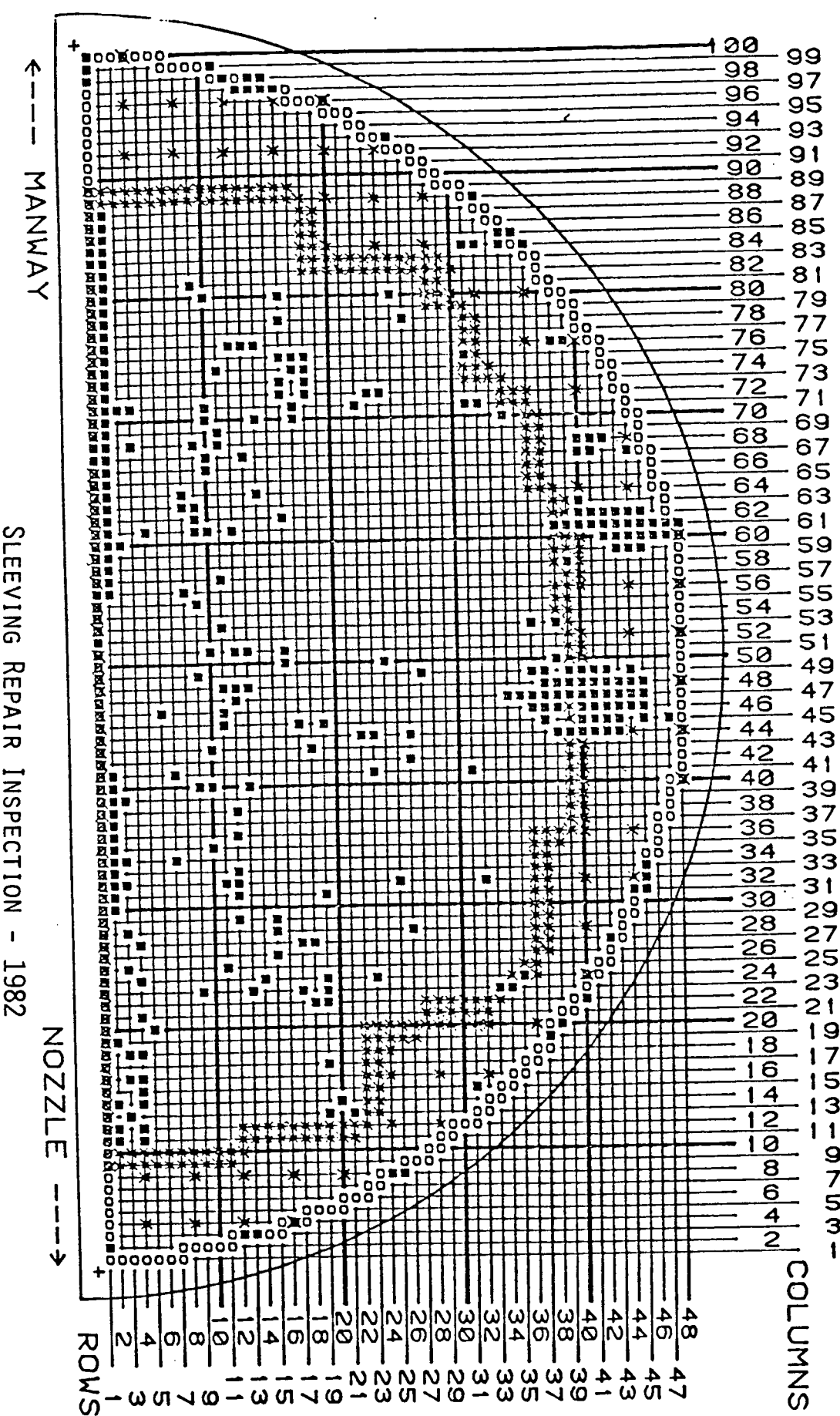
NON-SLEEVED TUBE INSPECTION PATTERN

SG-C

SERIES 27

TUBES INSPECTED: X=394

SCE-C  
INLET



SLEEVING REPAIR INSPECTION - 1982



FIGURE A-12

NON-SLEEVED TUBE INSPECTION

IGA INDICATIONS AT TOP OF TUBESHEET

SG-C

SERIES 27

INDICATIONS BY 4X4 AND RPC = 7

SCE-C

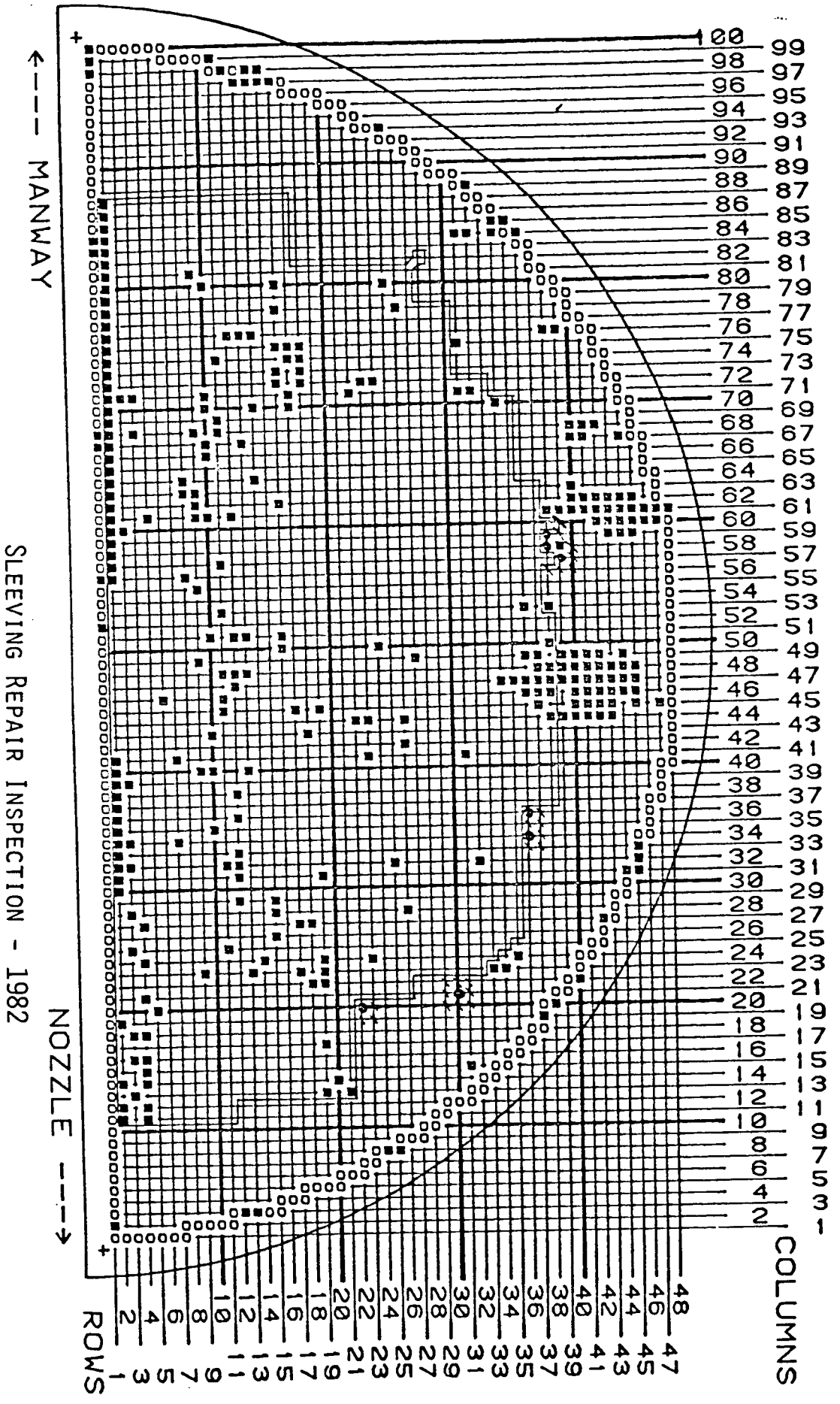
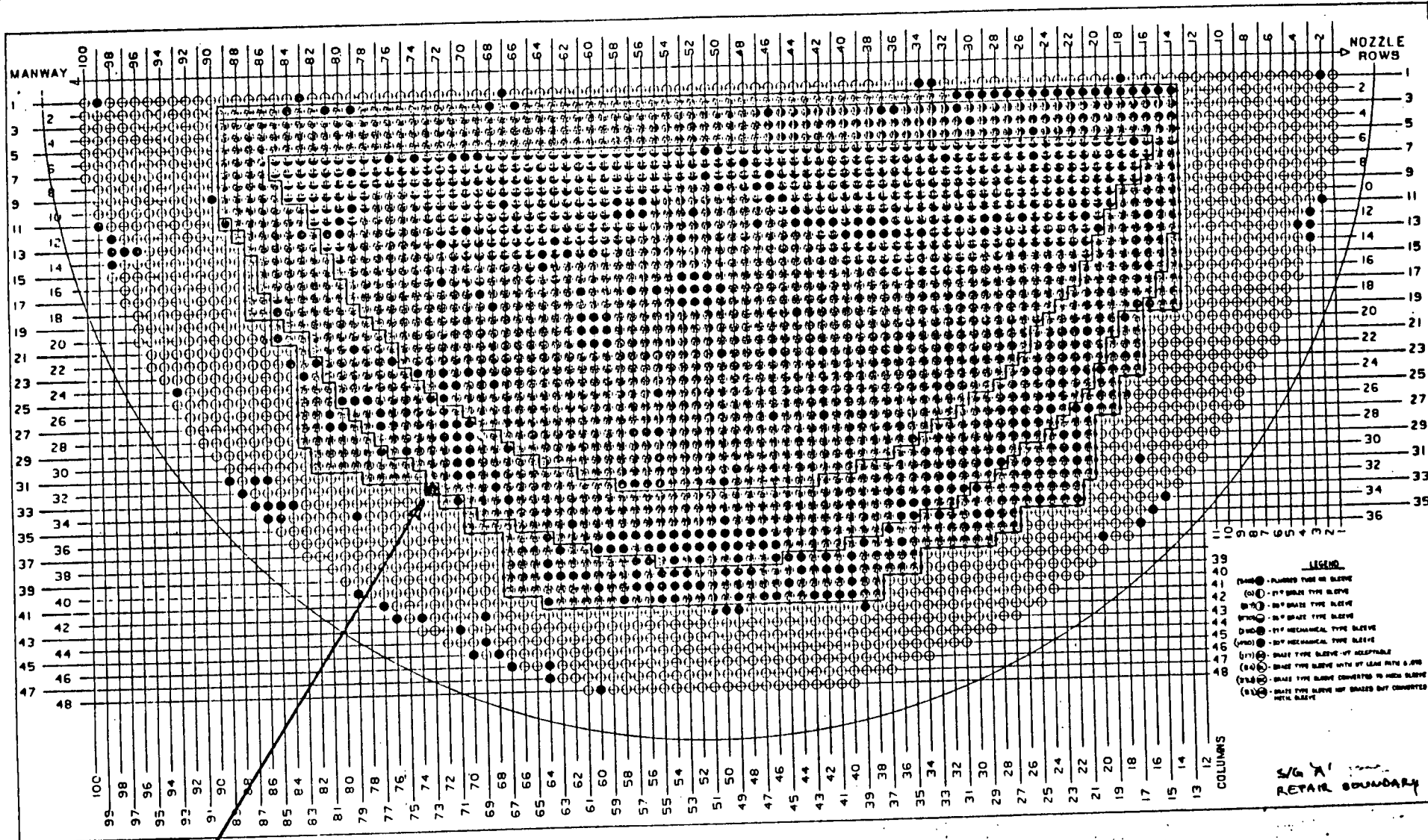


TABLE A-2

COMPARISON OF 1980 and 1982  
Surface Coil Eddy Current Data  
Top of Tube Sheet--Hot Leg Side

	<u>1980</u>	<u>1982</u>
A. SG-A		
1. Tubes Inspected	2315	422
2. No. of Indications		
< 20%	194	1*
≥ 20% < 50%	106	0
≥ 50%	354	0
B. SG-B		
1. Tubes Inspected	2145	396
2. No. of Indications		
< 20%	198	0
≥ 20% < 50%	92	0
≥ 50%	176	0
C. SG-C		
1. Tubes Inspected	2787	394
2. No. of Indications		
< 20%	282	6
≥ 20% < 50%	112	1
≥ 50%	324	0

\*By 4x4 EC Coil



1982 PLUGGING

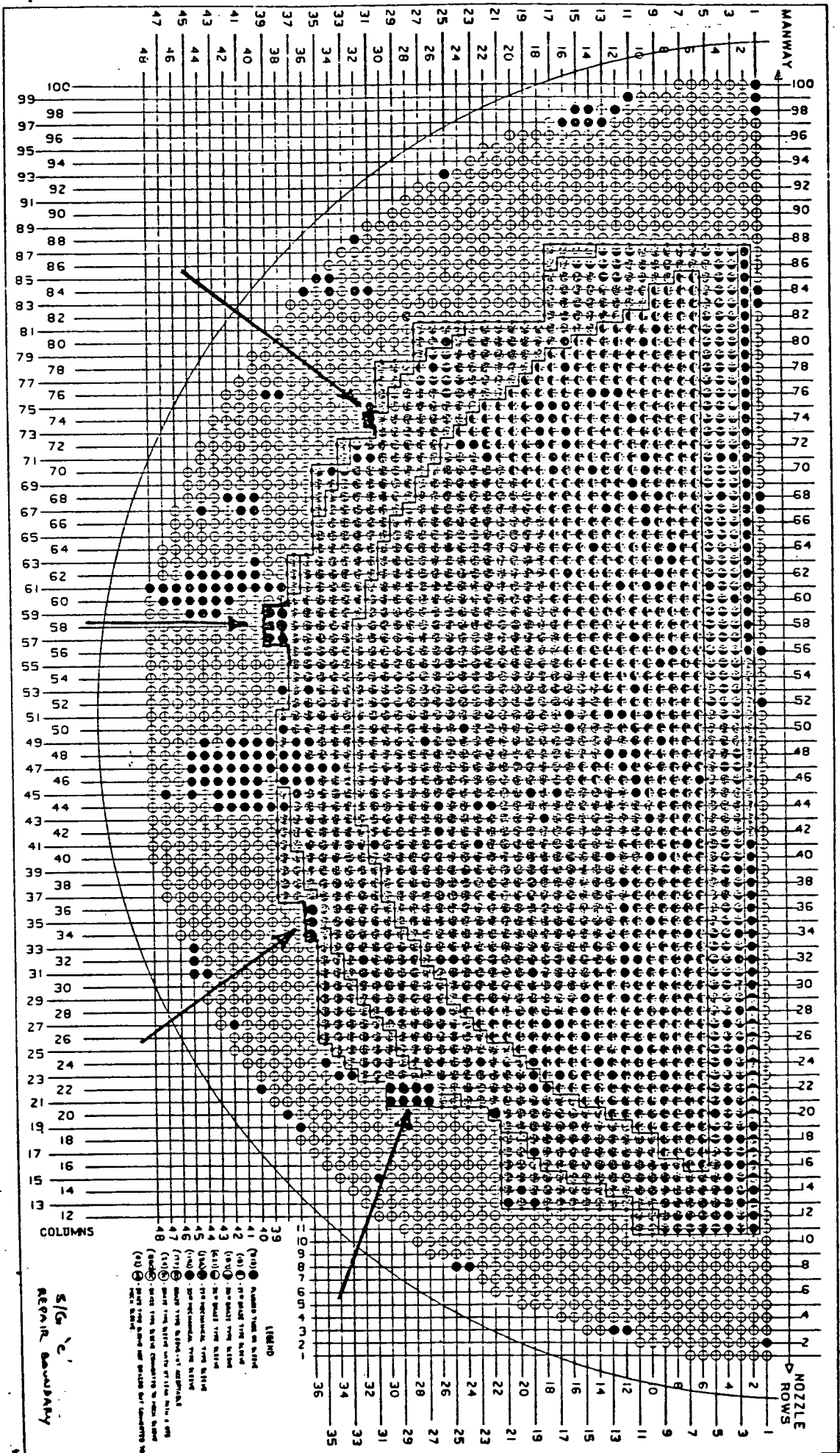
PLUGGING REPAIR DUE TO IGA INDICATIONS IN NON-SLEEVED TUBES

FIGURE A-13

SG-A

SLEEVING REPAIR INSPECTION - 1982

SG A  
RETAIN BOUNDARY



~ 1982 PLUGGING

PLUGGING REPAIR DUE TO IGA INSPECTION OF NON-SLEEVED TUBES SG-C

FIGURE A-14

SLEEVING REPAIR INSPECTION - 1982

APPENDIX B

Technical Specification Inspection  
Tables, Figures and Photographs

FIGURE B-1

GENERAL INSPECTION PATTERN SG-C

Errors of Trans Inspected - INLET (Does not Include Gauge Program)

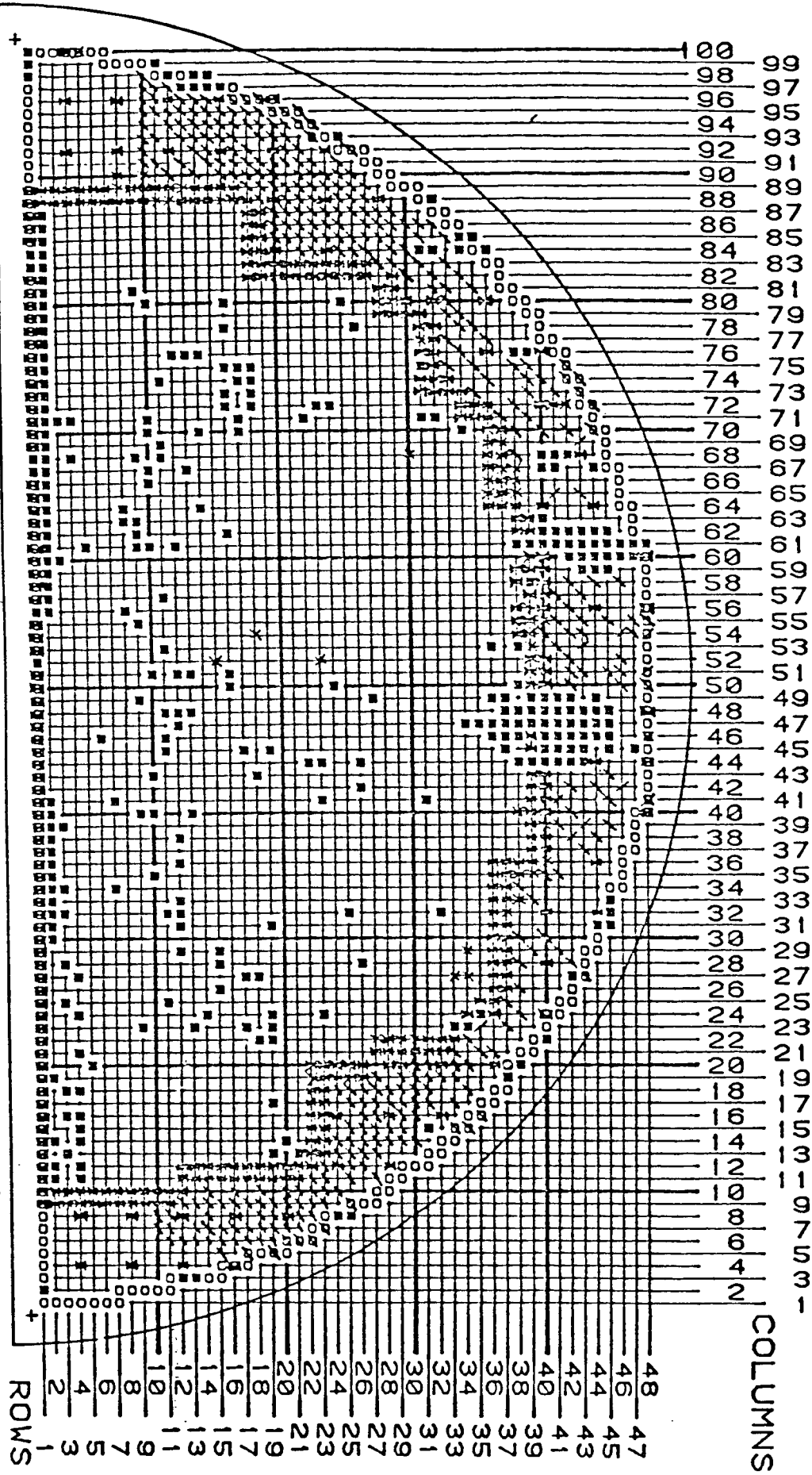
SERIES 27

1 - COMPLETED through U-Bend - 348

SCE-C

1 - Previous AUI indications completed thru U bend. - 11  
 1 - Previous AUI indications completed thru 1st Support - 34 + 8 in slanted area  
 X - trans inspected thru 1st support to supplement 454 program - 394

INLET



COLUMNS

ROWS

MANWAY

NOZZLE

TECHNICAL SPECIFICATION INSPECTION - 1982

TABLE B-1  
COMPARISON OF WASTAGE INDICATIONS

Steam Generator A

A. Hot Leg

1. Number of Indications Compared Between 1980 and 1982 (4.3 EFPM)	3
2. Mean Indication Change Over 4.3 EFPM	-6.7%
3. Standard Deviation	5.7%
4. Calculated Mean Growth (%EFPM)	-1.9%EFPM

B. Cold Leg

1. Number of Indications Compared Between 1980 and 1982 (4.3 EFPM)	89
2. Mean Indication Change Over 4.3 EFPM	-2.4%
3. Standard Deviation	5.6%
4. Calculated New Growth (%EFPM)	-0.6%EFPM

Steam Generator B

A. Hot Leg

1. Number of Indications Compared Between 1980 and 1982 (4.3 EFPM)	9
2. Mean Indication Change Over 4.3 EFPM	-0.7%
3. Standard Deviation	7.5%
4. Calculated New Growth (%/EFPM)	-0.2%EFPM

Steam Generator C

A. Hot Leg

1. Number of Indications Compared Between 1980 and 1982 (4.3 EFPM)	27
2. Mean Indication Change Over 4.3 EFPM	-0.9%
3. Standard Deviation	4.8%
4. Calculated New Growth (%/EFPM)	-0.2% EFPM

Table B-1 continued

B. Cold Leg

1. Number of Indications Compared Between 1980 and 1982 (4.3 EFPM)	29
2. Mean Indication Change Over 4.3 EFPM	-4.4%
3. Standard Deviation	6.3%
4. Calculated New Growth	-1.0%/EFPM

All Three Steam Generators (Hot and Cold Legs Combined)

1. Number of Indications Compared Between 1980 and 1982 (4.3 EFPM)	157
2. Mean Indication Change Over 4.3 EFPM	-2.5%
3. Average Standard Deviation	6.0%
4. Calculated New Growth	-0.6%EFPM



FIGURE 2

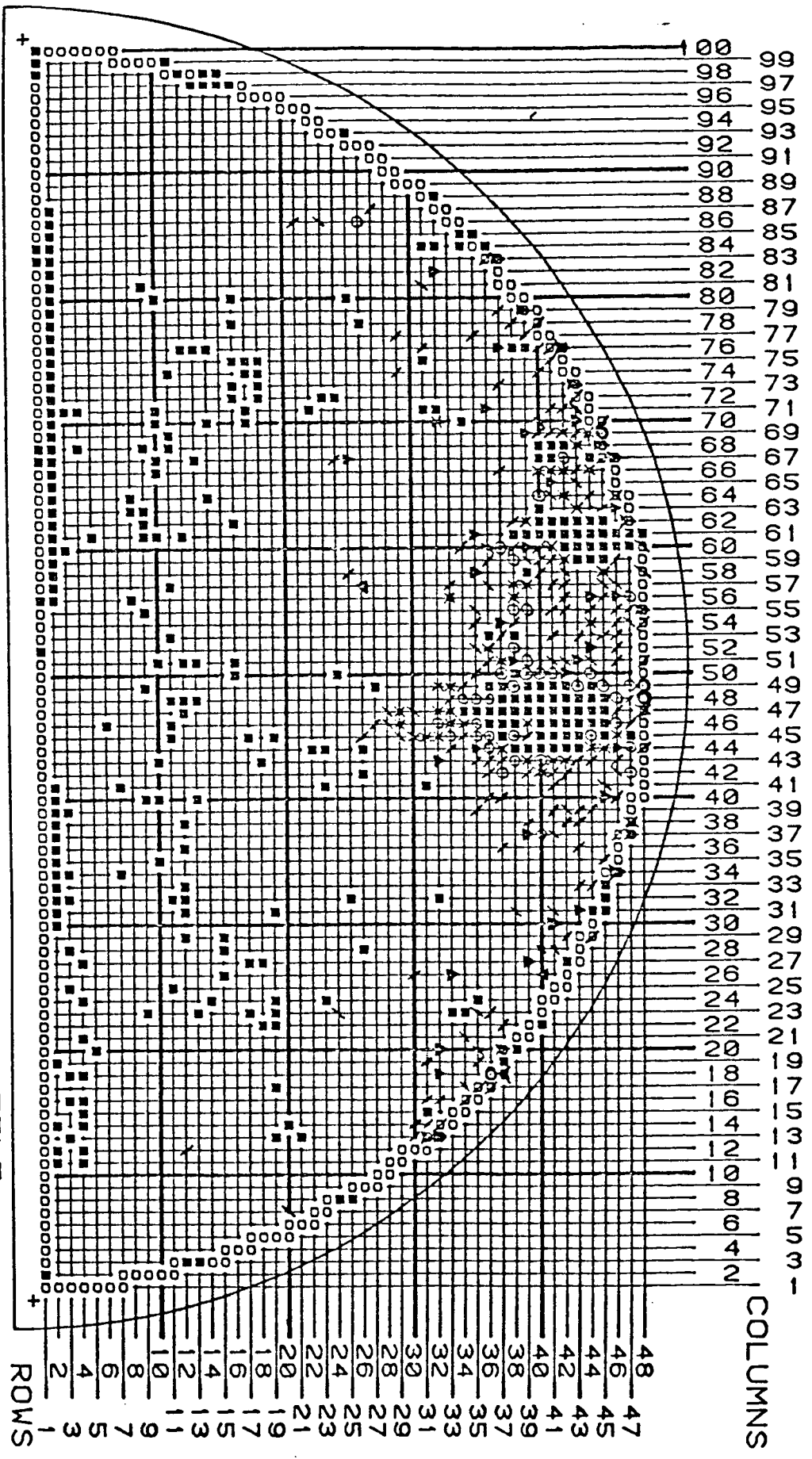
AVB INSPECTION PATTERN SG-C

AVB INDICATIONS (From HL and CL)

- / - 220% - 38 fuses
- \ - 20-29% - 118 "
- ▲ - 42% - 42 "
- - 40-49% - 42 fuses
- ▼ - 650 - 3 fuses
- X - 30-39% - 44 "

SERIES 27

SCE-C



TECHNICAL SPECIFICATION INSPECTION - 1982

TABLE B-2

COMPARISON OF 1982 VS 1980 AVB INDICATIONS


SG-C

Steam Generator C

1. Number of Indications Compared With Previous Inspection Results	373
2. Mean Indication Change Since Last Inspection	-2.0%
3. Standard Deviation	3.5%
4. Calculated New Growth Rate	-0.05%/EFPM

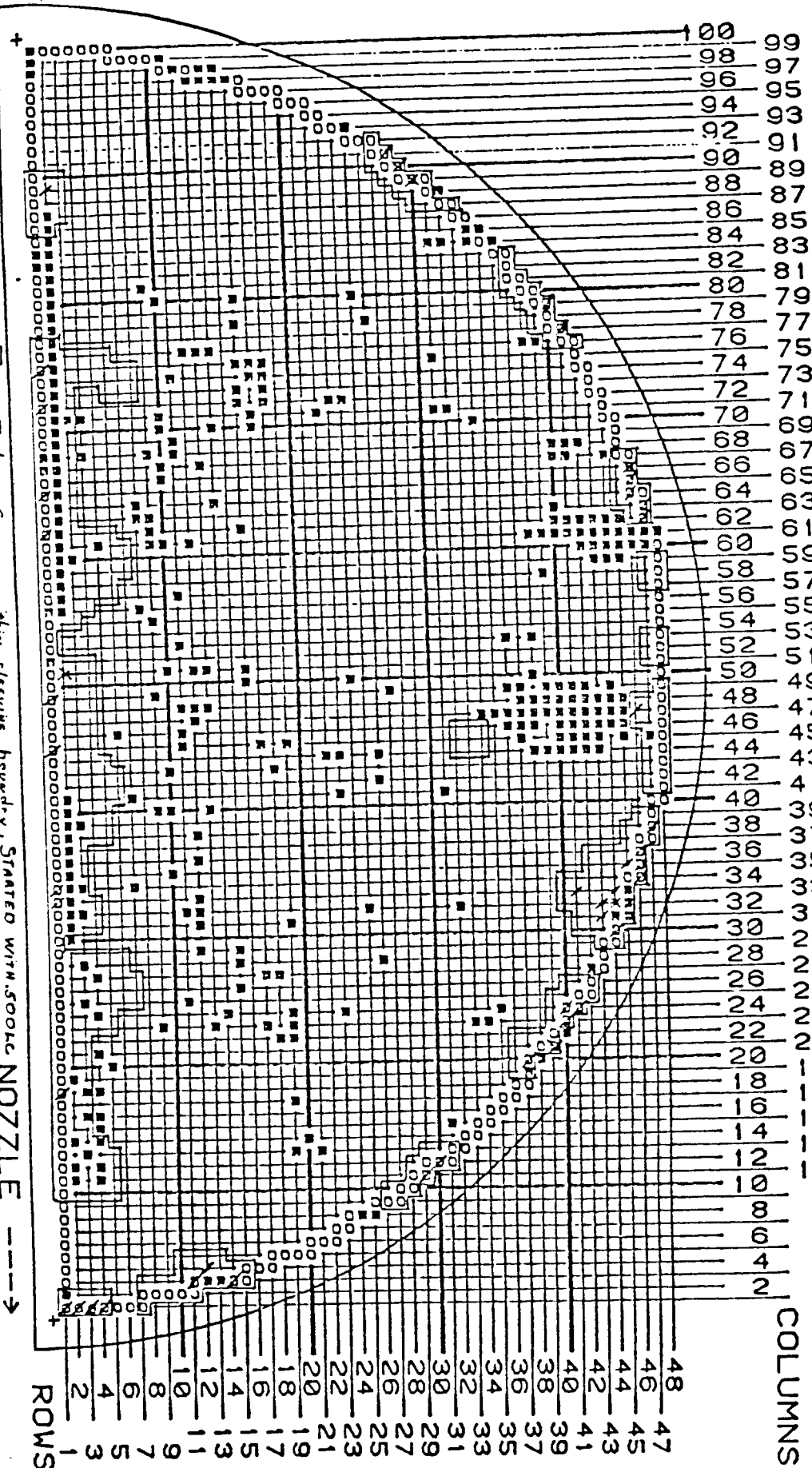
FIGURE B-3

GAUGING PATTERN - SG-C HOT LEG


 Gauge thru top suggest w/S60 SF, any restricts thru should be gauged down w/500c 460 cc and 400c. Tubes between R2 thru R9 and columns 10 thru 80 have sleeves in them, those tubes have to be gauged starting with a Snowprobe and gauges down to use 400c

SERIES 27  
SGE-C

1 - RESTRICTS .560 PROBE PASSES .500 PROBE (41) X - RESTRICTS .500 PROBE PASSES .460 PROBE (6)  
 INLET



TECHNICAL SPECIFICATION INSPECTION

1982

Gauging Program  
March 1982

Figure B-4: Restriction Locations, SG-C Hot Leg

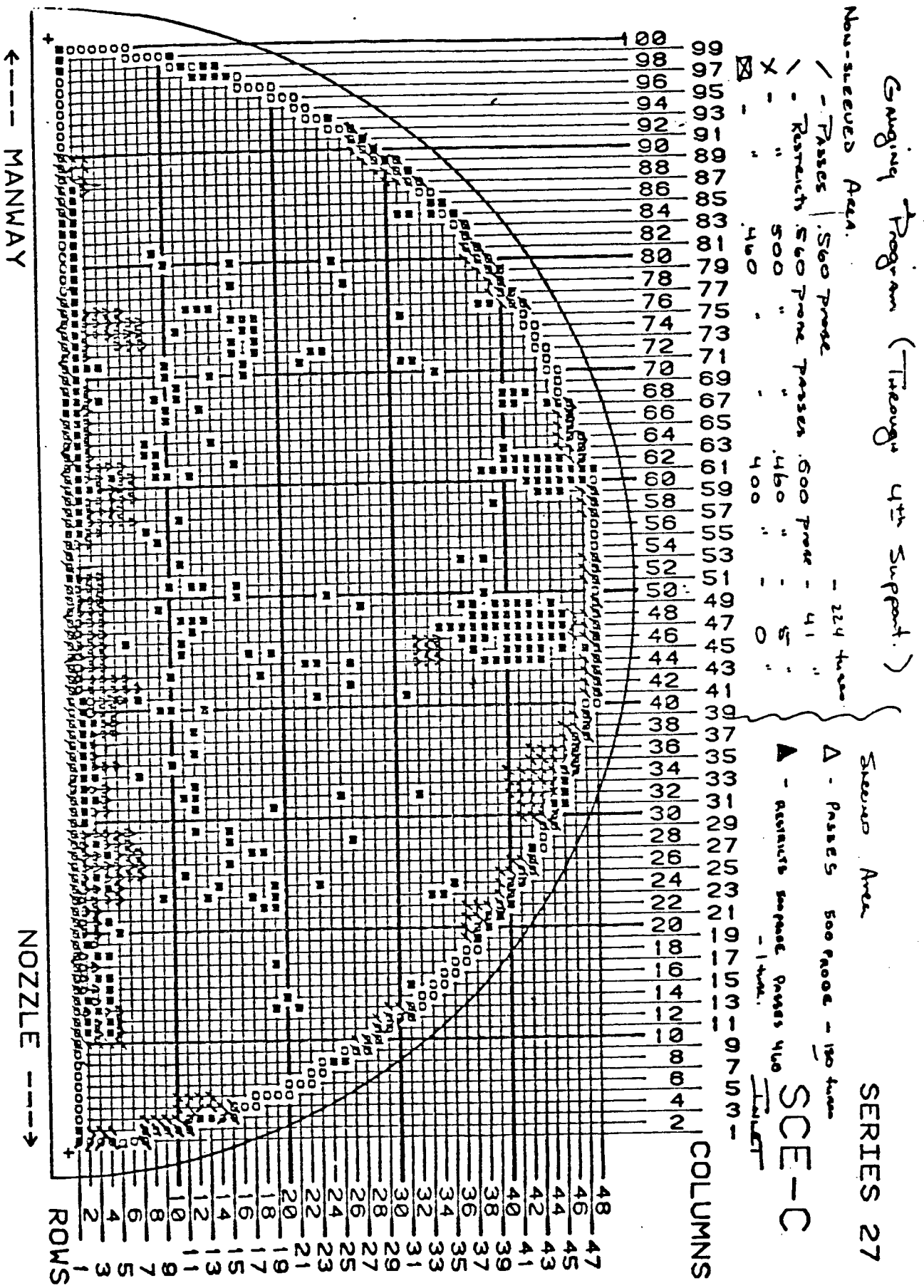


FIGURE B-5: GAUGING PROGRAM, SG-C COLD LEG

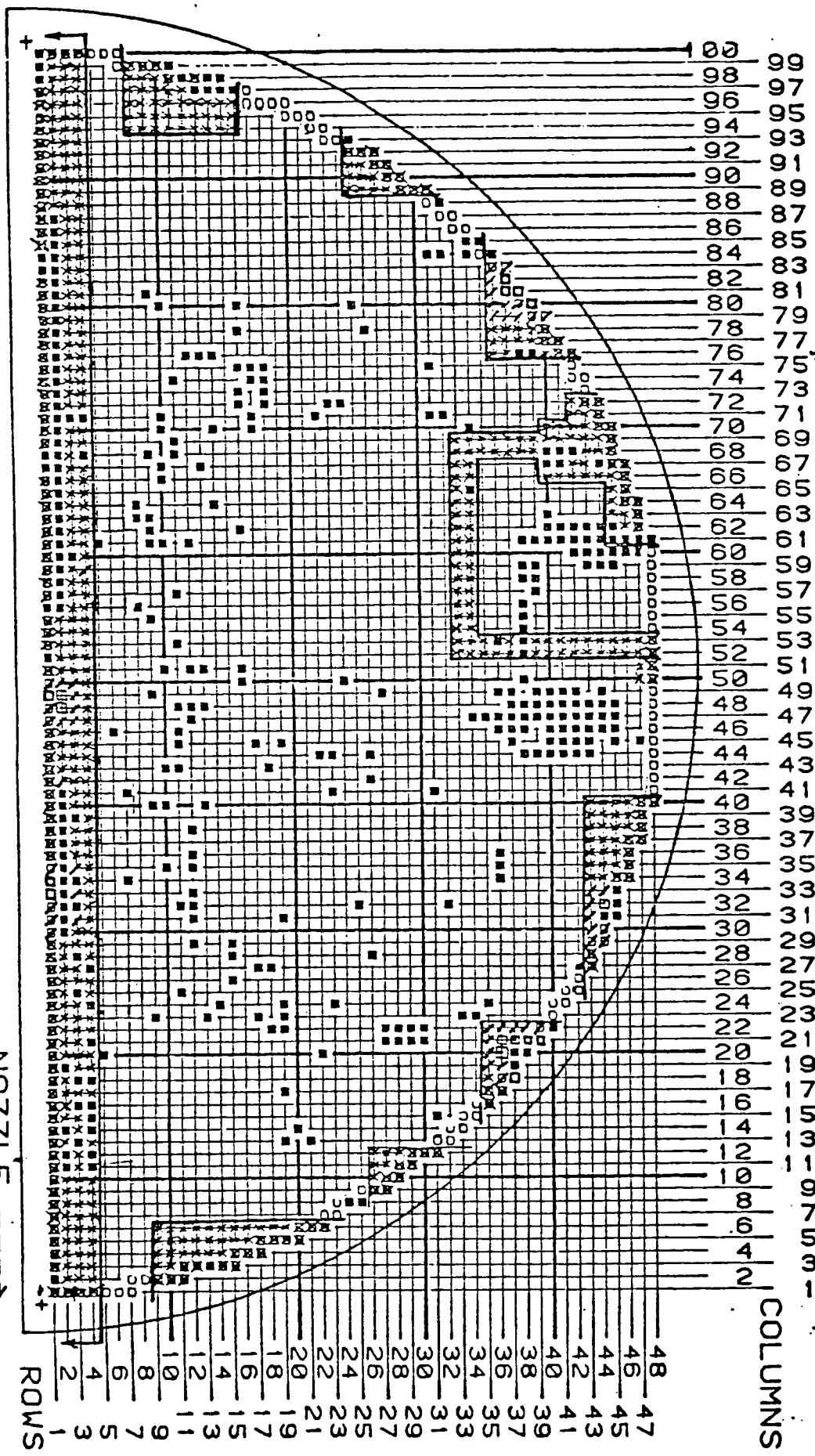
X - TESTED THRU 4<sup>th</sup> TSP

✓ - TESTED BUT RESTRICTED - (SEE RESTRICTION & LIBERATION MAPS)

□ - GAUGED March 82 - PASSED SLD  
 □ - GAUGED March 82 - RESTRICTED

SERIES 27

SCE-C  
 OUTLET



TECHNICAL SPECIFICATION INSPECTION - 1982

FIGURE B-6: RESTRICTION LOCATIONS, SG-C COLD LEG

/- RESTRICTED w/560

X- RESTRICTED w/500

SERIES 27

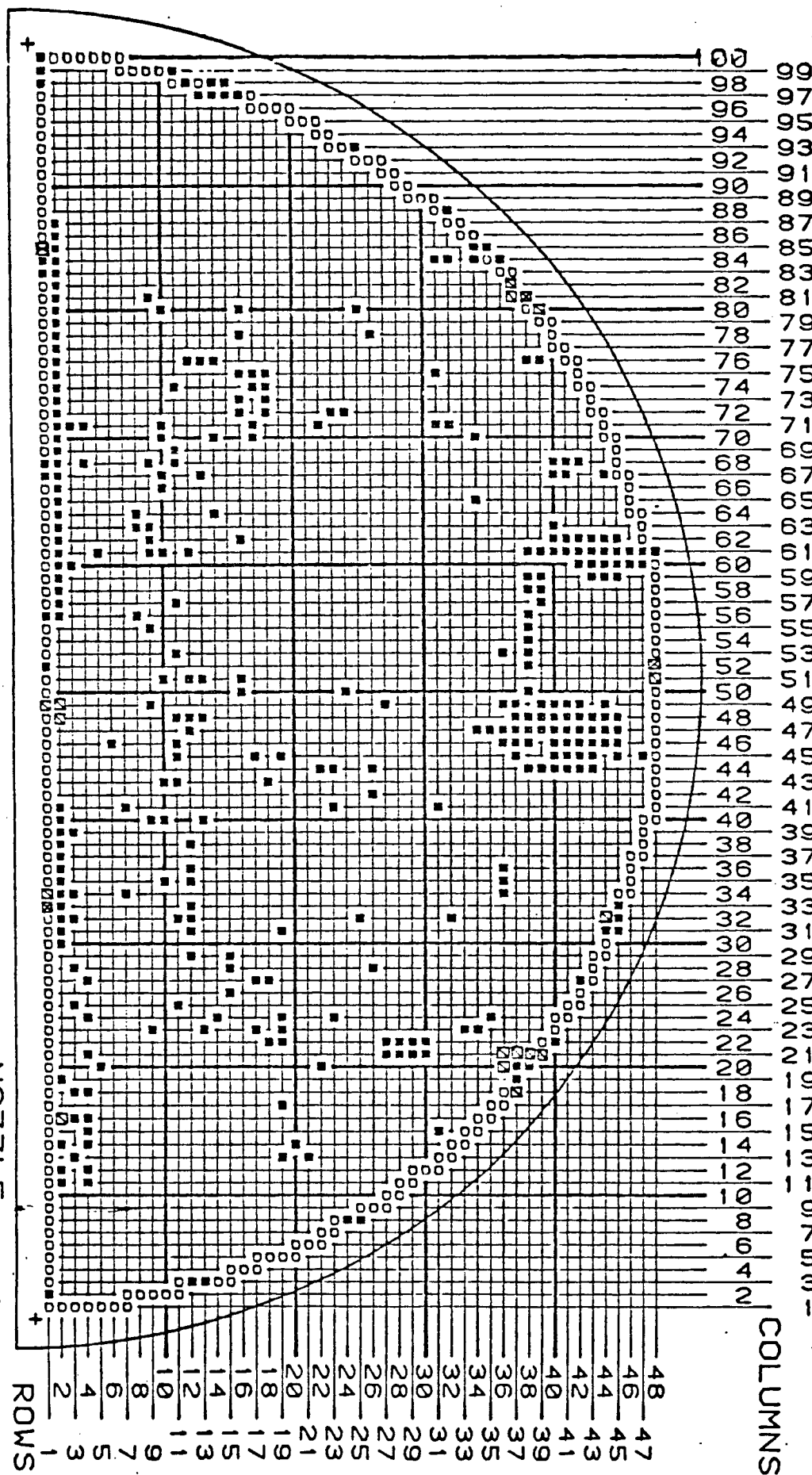
(16 TUBES) □- RESTRICTED w/560 PASSED 500

⊠- RESTRICTED w/500, PASSED 460 (3 TUBES)

⊞- RESTRICTED w/460

⊞- RESTRICTED w/460 PASSED 400 (1 TUBE)

SCE-C  
OUTLET



TECHNICAL SPECIFICATION INSPECTION - 1982

FIGURE B-7: GAUGING PROGRAM, SG-A COLD LEG

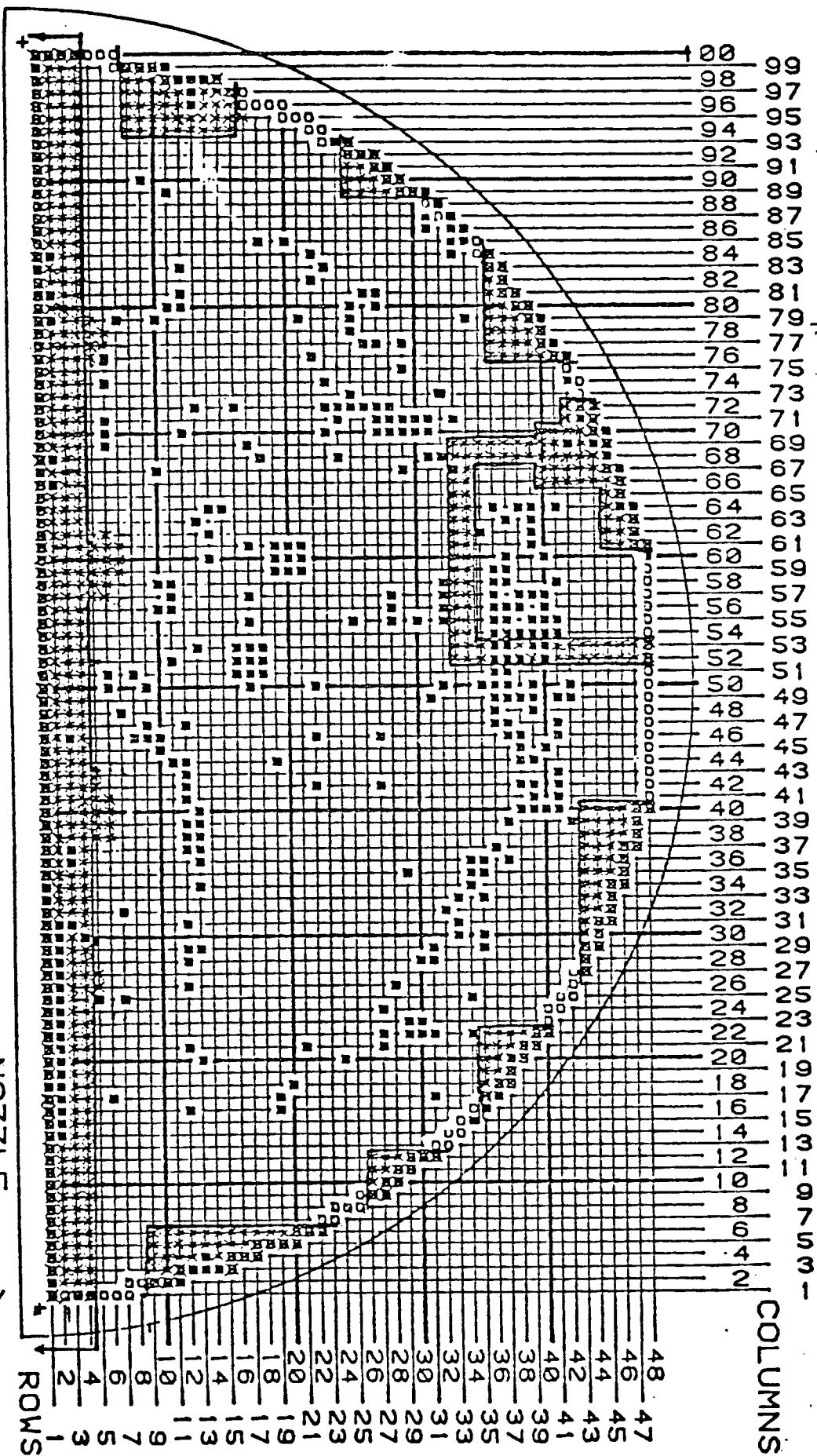
7A

X-TESTED THRU 4" TSP

X-TESTED BUT RESTRICTED - (SEE RESTRICTION LOCATION MAP)

SERIES 27

SCE-A  
OUTLET

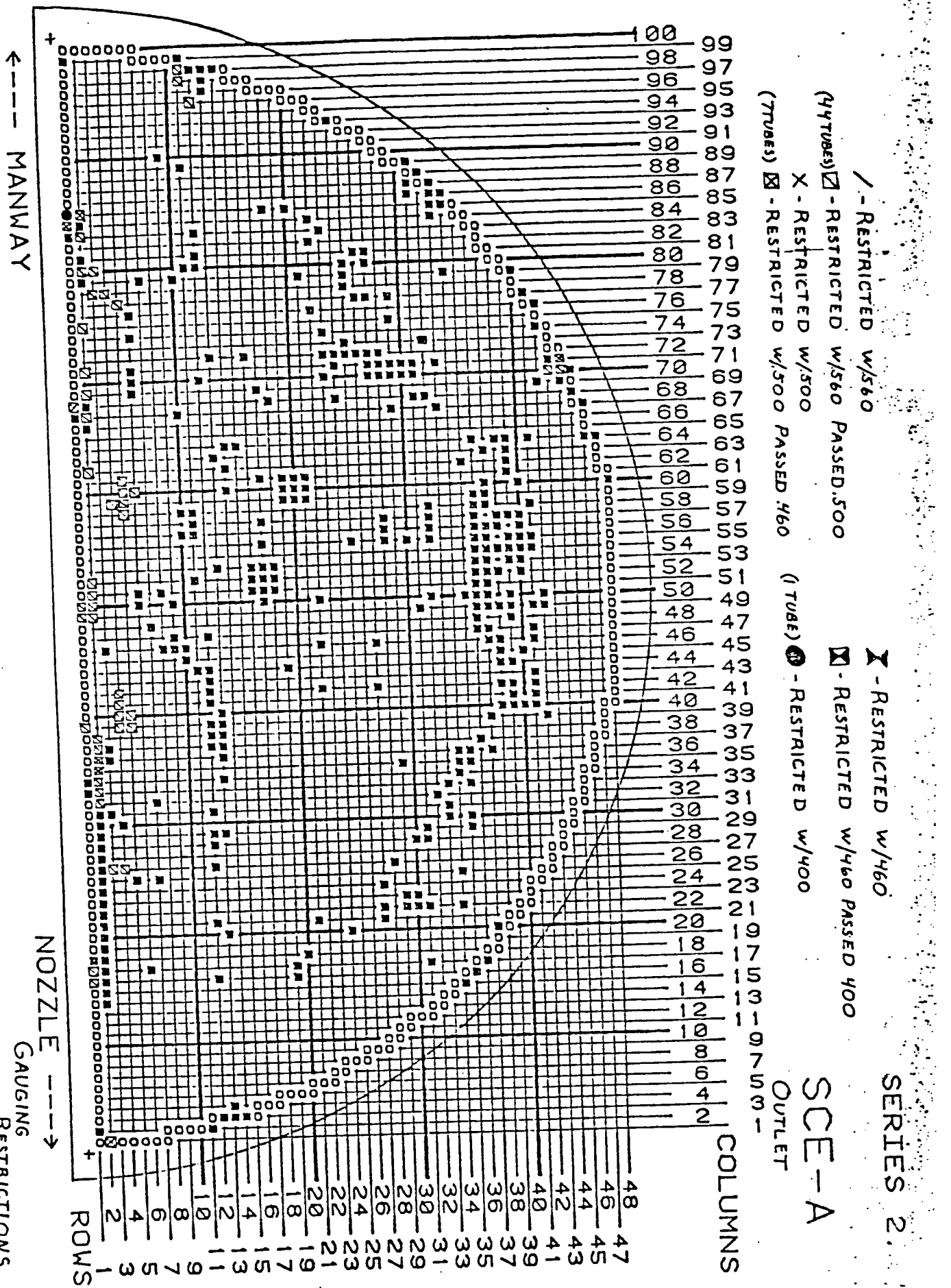


747 TUBES - 70 PLUGS = 677 TUBES TO BE TESTED THRU 4" TSP

TECHNICAL SPECIFICATION INSPECTION 1982

GAUGING

FIGURE B-8: RESTRICTION LOCATIONS, SG-A COLD LEG



SERIES 2

SG-A

OUTLET

COLUMNS

ROWS

TECHNICAL SPECIFICATION INSPECTION - 1982



TABLE B-3

1982 STEAM GENERATOR GAUGING RESULTS

I. SG-A

A. NUMBER OF TUBES GAUGED THROUGH 4TH SUPPORT PLATE

<u>HOT LEG</u>	<u>COLD LEG</u>
0	677

B. TUBE RESTRICTIONS

<.400	N/A	1
.400-.460	N/A	0
.460-.500	N/A	7
.500-.560	N/A	44
.560-.580	N/A	0

II. SG-C

A. NUMBER OF TUBES GAUGED THROUGH 4TH SUPPORT PLATE

451	704
-----	-----

B. TUBE RESTRICTIONS

<.400	0	0
.400-.460	0	3
.460-.500	6	5
.500-.560	221	29
.560-.580	224	54

FLOW SLOT PHOTOGRAPHS  
STEAM GENERATORS A and C

The photographs which follow were taken during the 1982 steam generator inspection. Prints of the photographs were given to the NRC during the May 12, 1982 meeting in Bethesda.

In addition to the photographs, support plate maps at flow slot locations are provided showing the location of support plate cracks as determined from the photographs.

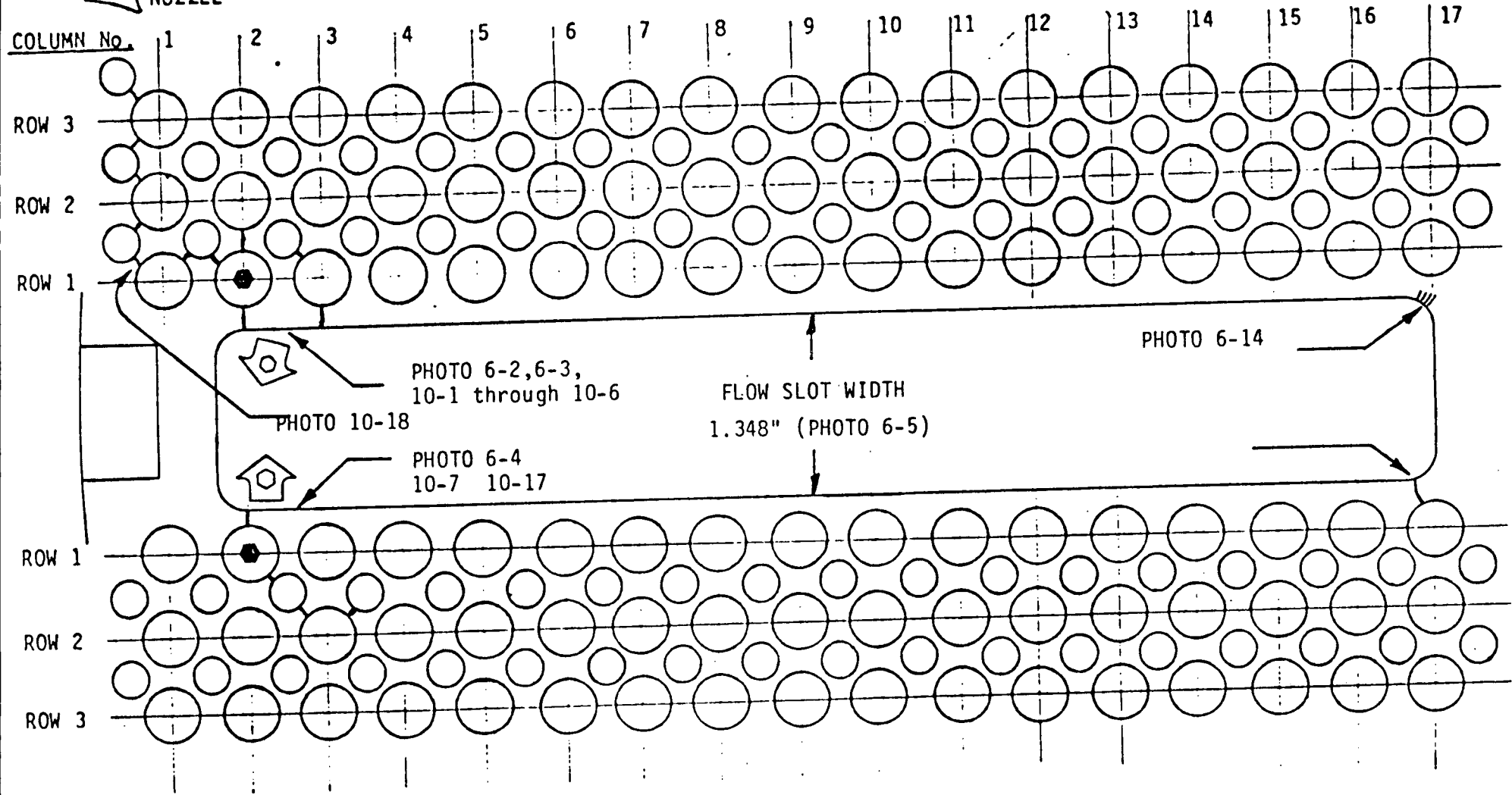
FLOW SLOT EXAMINATION DATA

FLOW SLOT No.1 NOZZLE SIDE



COLD LEG SIDE

MANWAY 

 NOZZLE



HOT LEG SIDE

-  DISPLACEMENT
-  PLUGGED TUBE

STEAM GENERATOR A  
FIRST SUPPORT PLATE

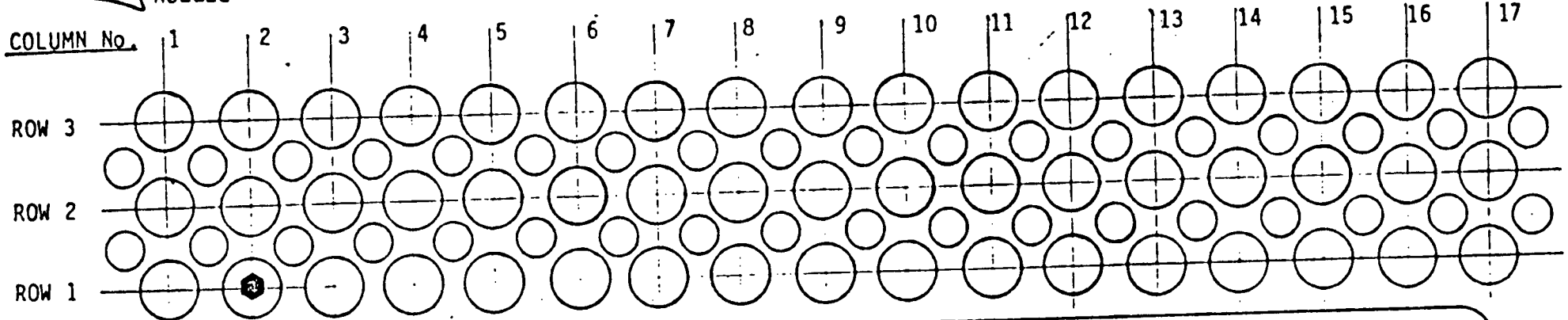
FLOW SLOT EXAMINATION DATA


FLOW SLOT No.1 NOZZLE SIDE

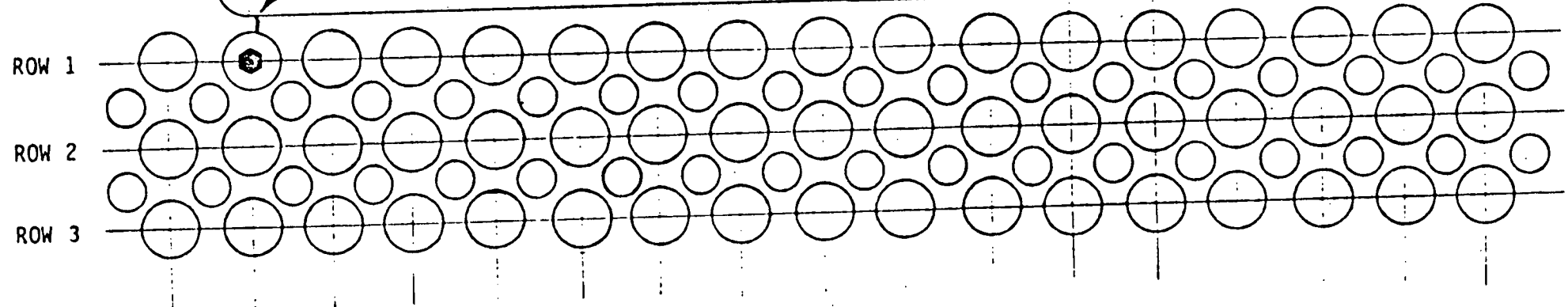
COLD LEG SIDE

MANWAY 


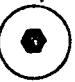
 NOZZLE



 PHOTO 6-6,6-9



HOT LEG SIDE

-  DISPLACEMENT
-  PLUGGED TUBE

STEAM GENERATOR A  
SECOND SUPPORT PLATE

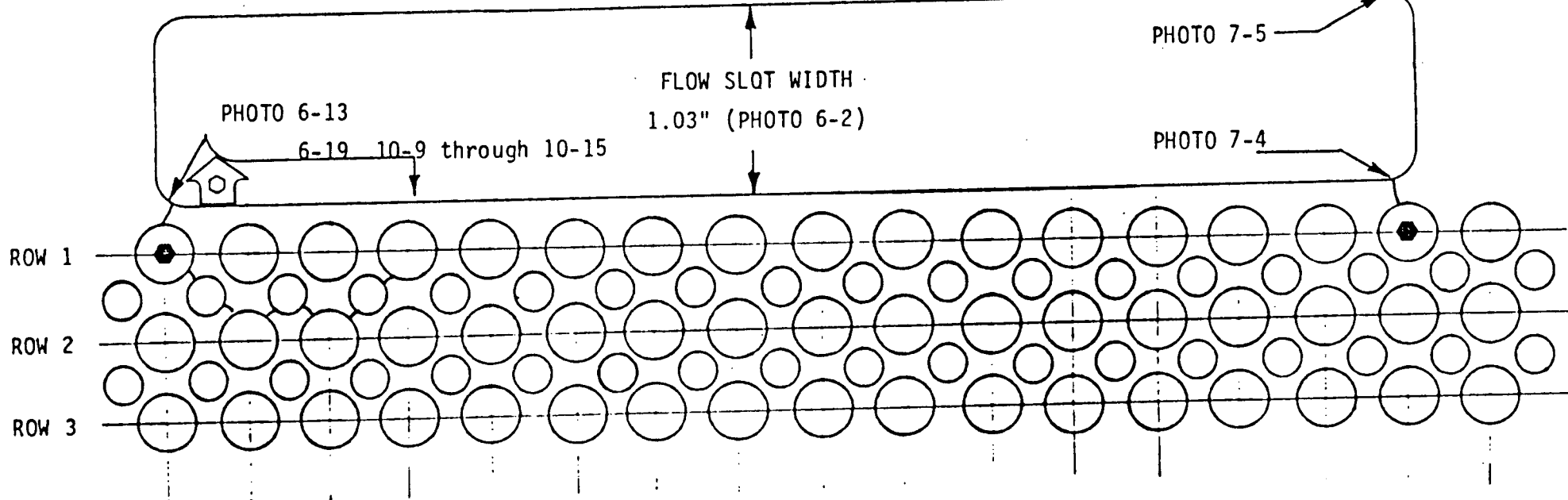
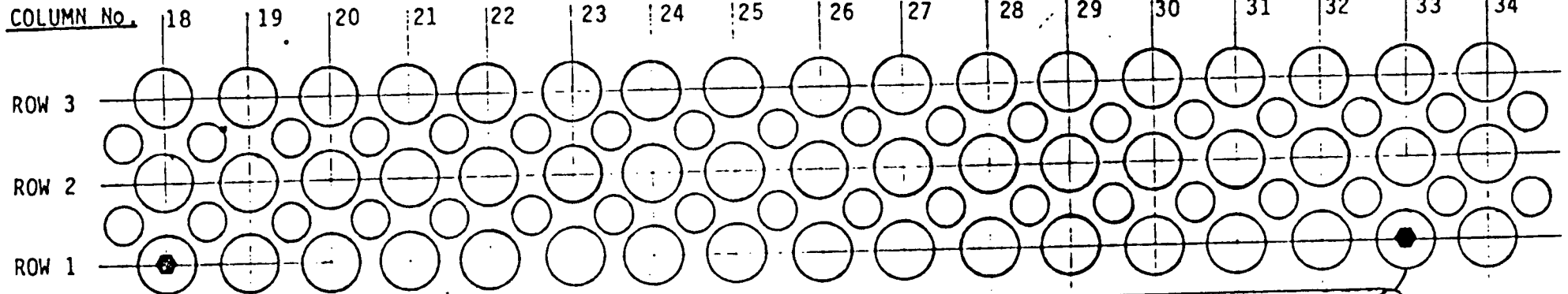
FLOW SLOT EXAMINATION DATA

FLOW SLOT No.2 NOZZLE SIDE

COLD LEG SIDE

MANWAY 

 NOZZLE



HOT LEG SIDE



DISPLACEMENT

PLUGGED TUBE

STEAM GENERATOR A  
FIRST SUPPORT PLATE

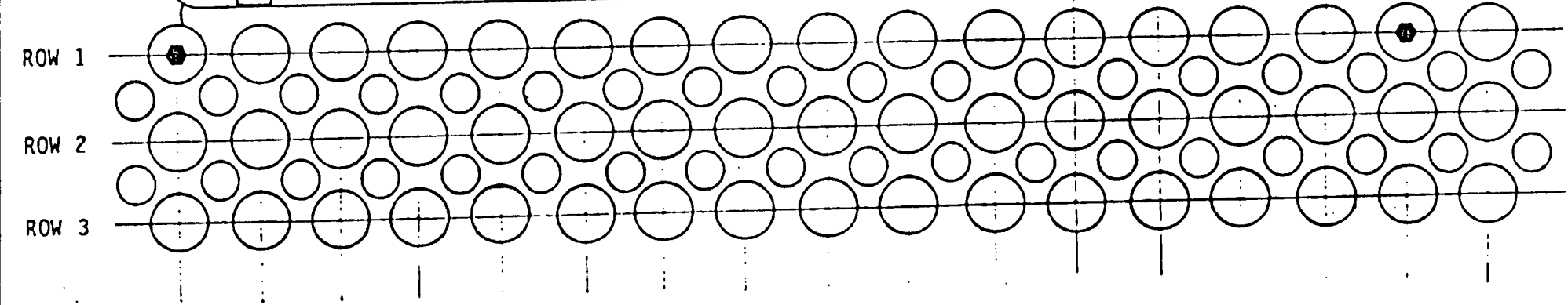
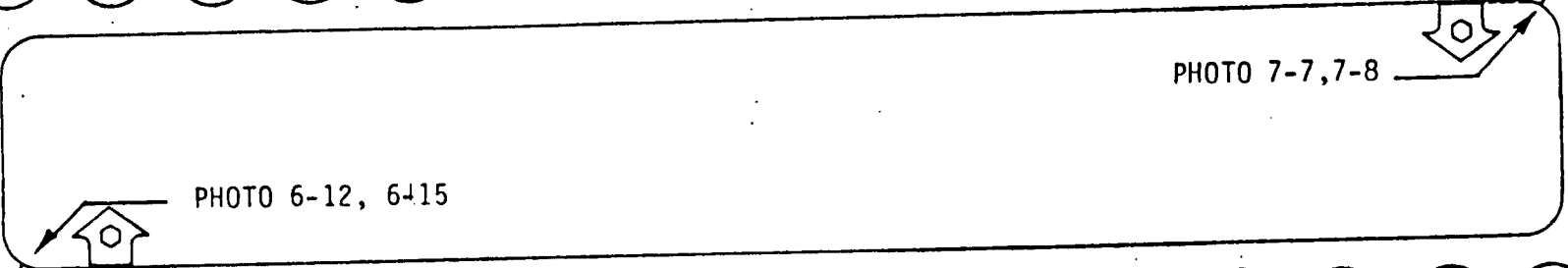
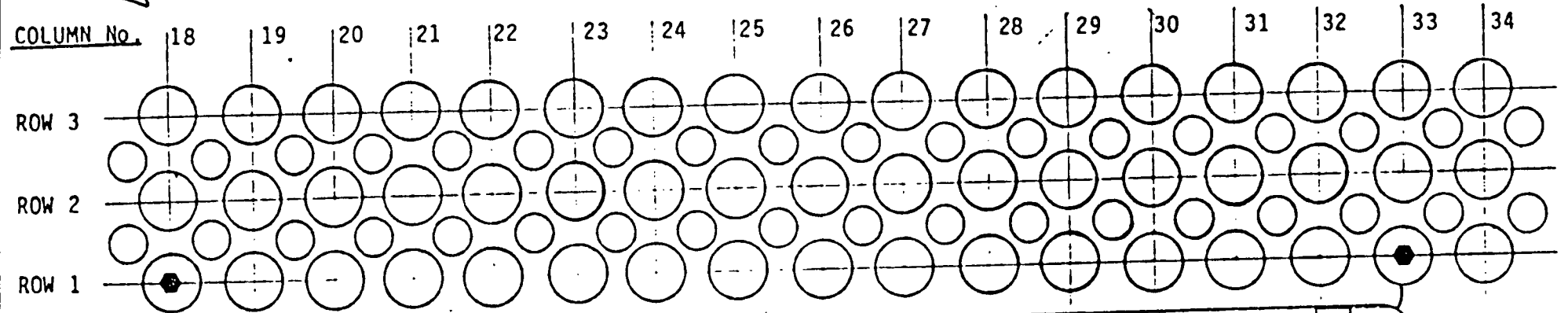
FLOW SLOT EXAMINATION DATA

FLOW SLOT No.2 NOZZLE SIDE



COLD LEG SIDE

MANWAY 

 NOZZLE



HOT LEG SIDE

-  DISPLACEMENT
-  PLUGGED TUBE

STEAM GENERATOR A

SECOND SUPPORT PLATE

FLOW SLOT EXAMINATION DATA

FLOW SLOT No.3 NOZZLE SIDE

COLD LEG SIDE

MANWAY 

 NOZZLE

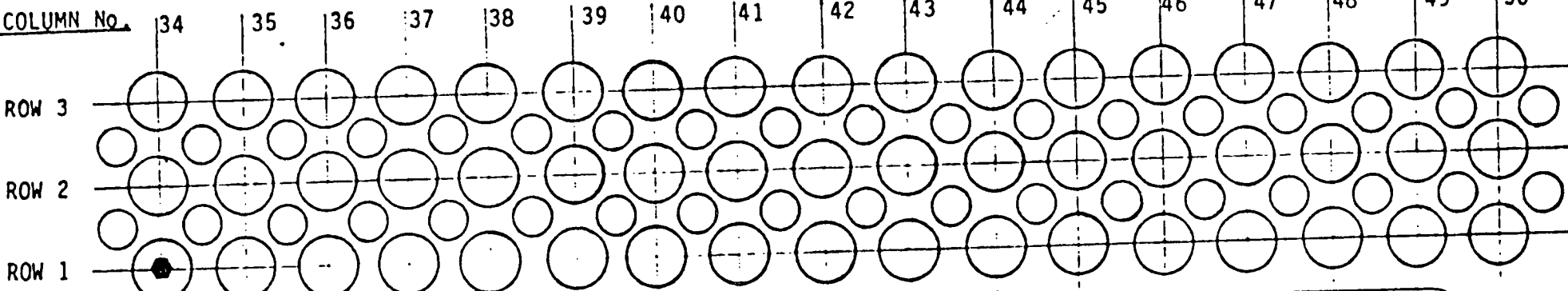
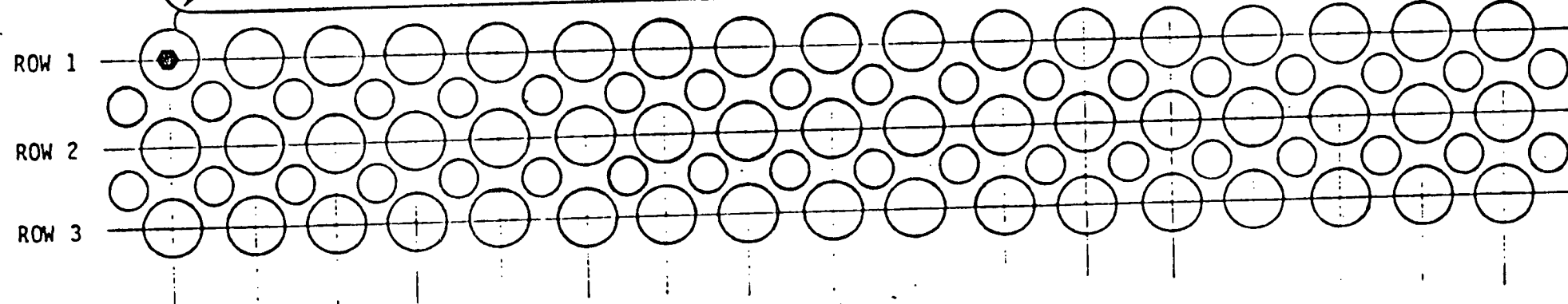


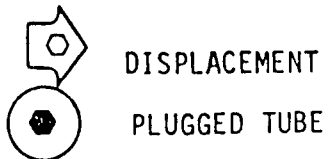
PHOTO 7-9

FLOW SLOT WIDTH  
.984" (PHOTO 7-11)

PHOTO 7-10



HOT LEG SIDE



STEAM GENERATOR A

FIRST SUPPORT PLATE

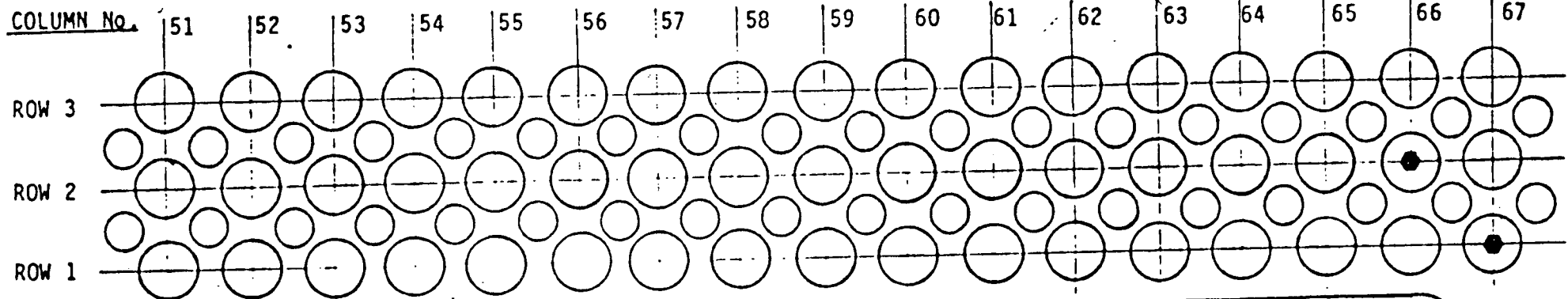
FLOW SLOT EXAMINATION DATA

FLOW SLOT No.3 MANWAY SIDE

COLD LEG SIDE

MANWAY 

 NOZZLE

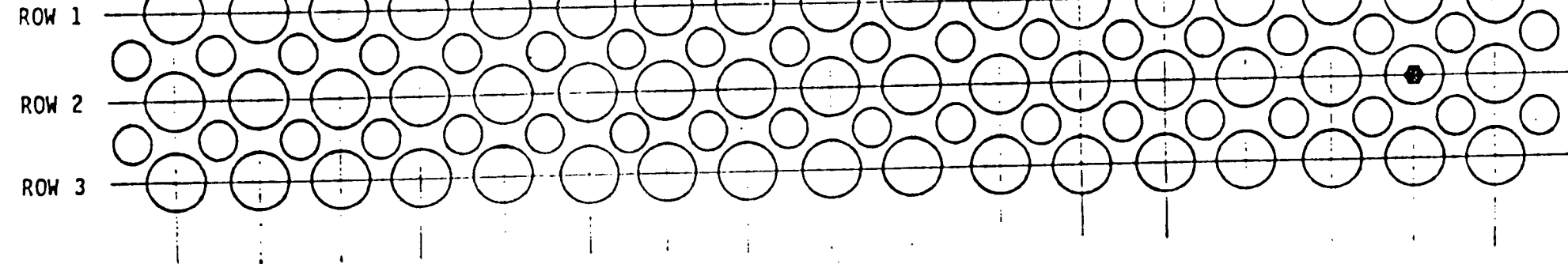


FLOW SLOT WIDTH

.930" (PHOTO 8-19)

PHOTO 8-18

PHOTO 8-17



HOT LEG SIDE

STEAM GENERATOR A

FIRST SUPPORT PLATE



DISPLACEMENT



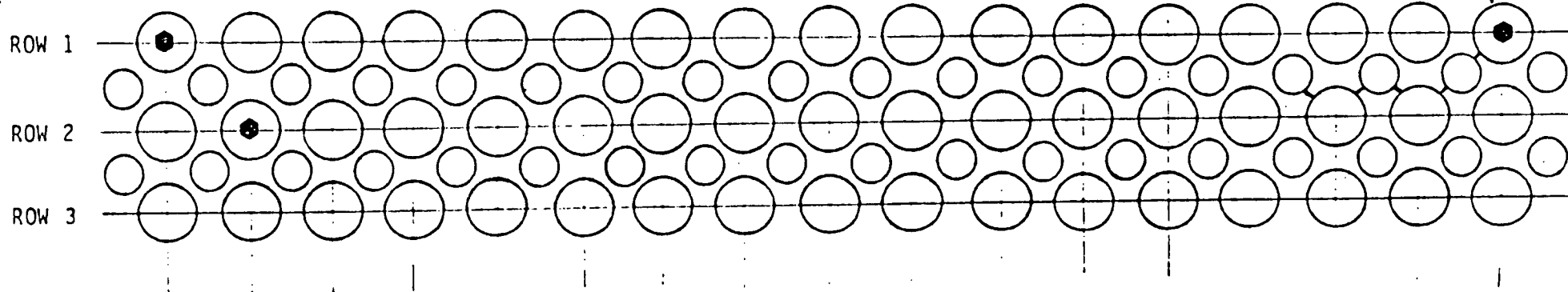
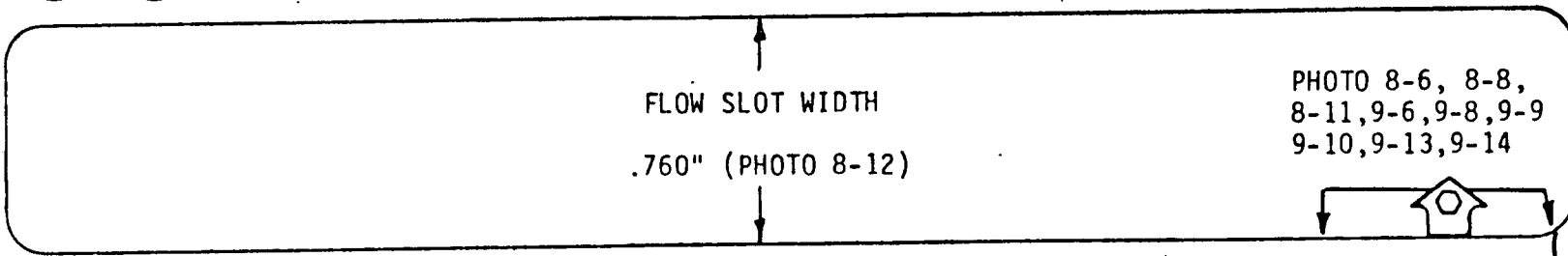
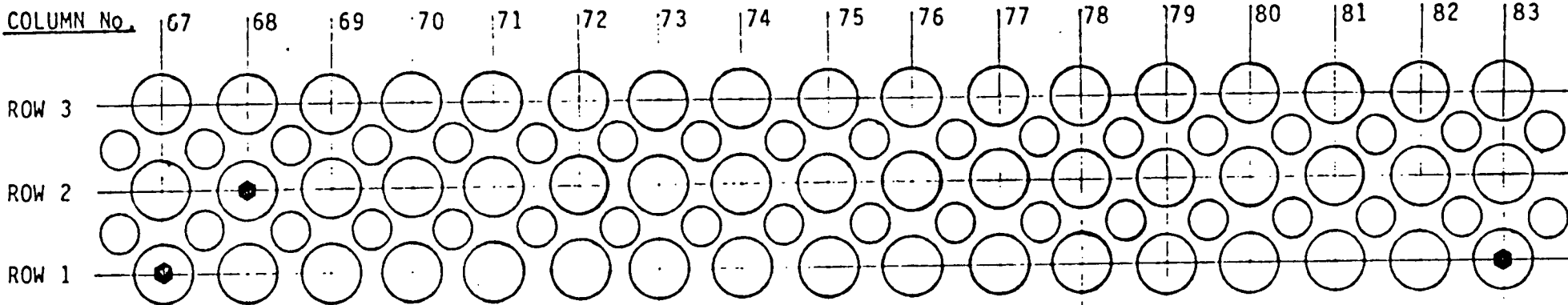
PLUGGED TUBE



FLOW SLOT EXAMINATION DATA

FLOW SLOT No.2 MANWAY SIDE

COLD LEG SIDE



HOT LEG SIDE

STEAM GENERATOR A  
FIRST SUPPORT PLATE



DISPLACEMENT




PLUGGED TUBE

FLOW SLOT EXAMINATION DATA

FLOW SLOT No.2 MANWAY SIDE

COLD LEG SIDE

MANWAY 

 NOZZLE

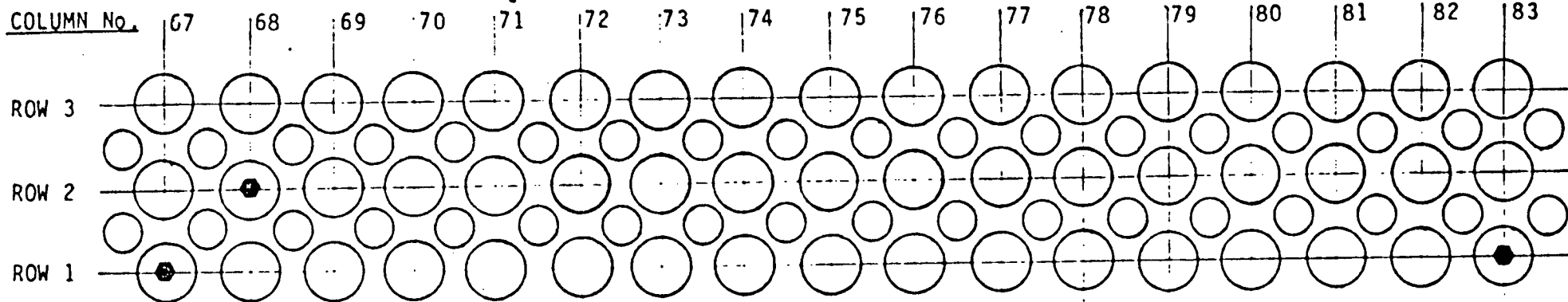
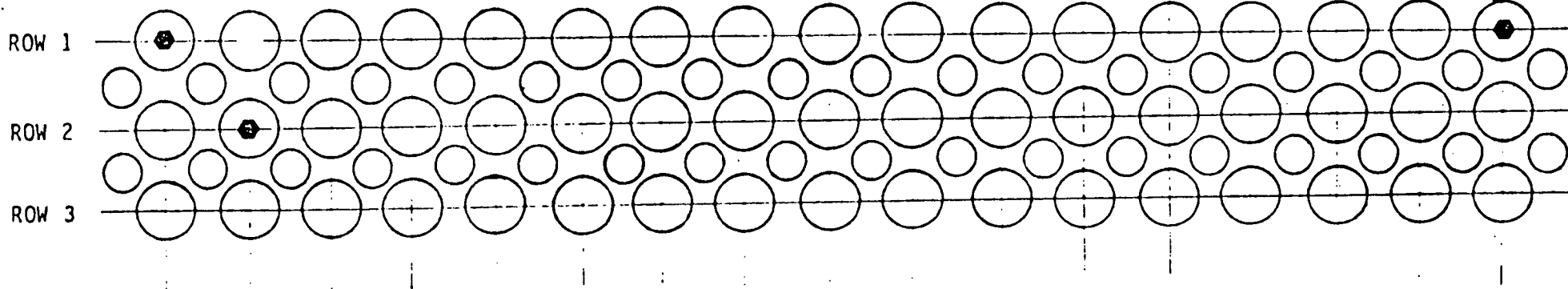


PHOTO 8-14 



HOT LEG SIDE

STEAM GENERATOR A  
SECOND SUPPORT PLATE



DISPLACEMENT

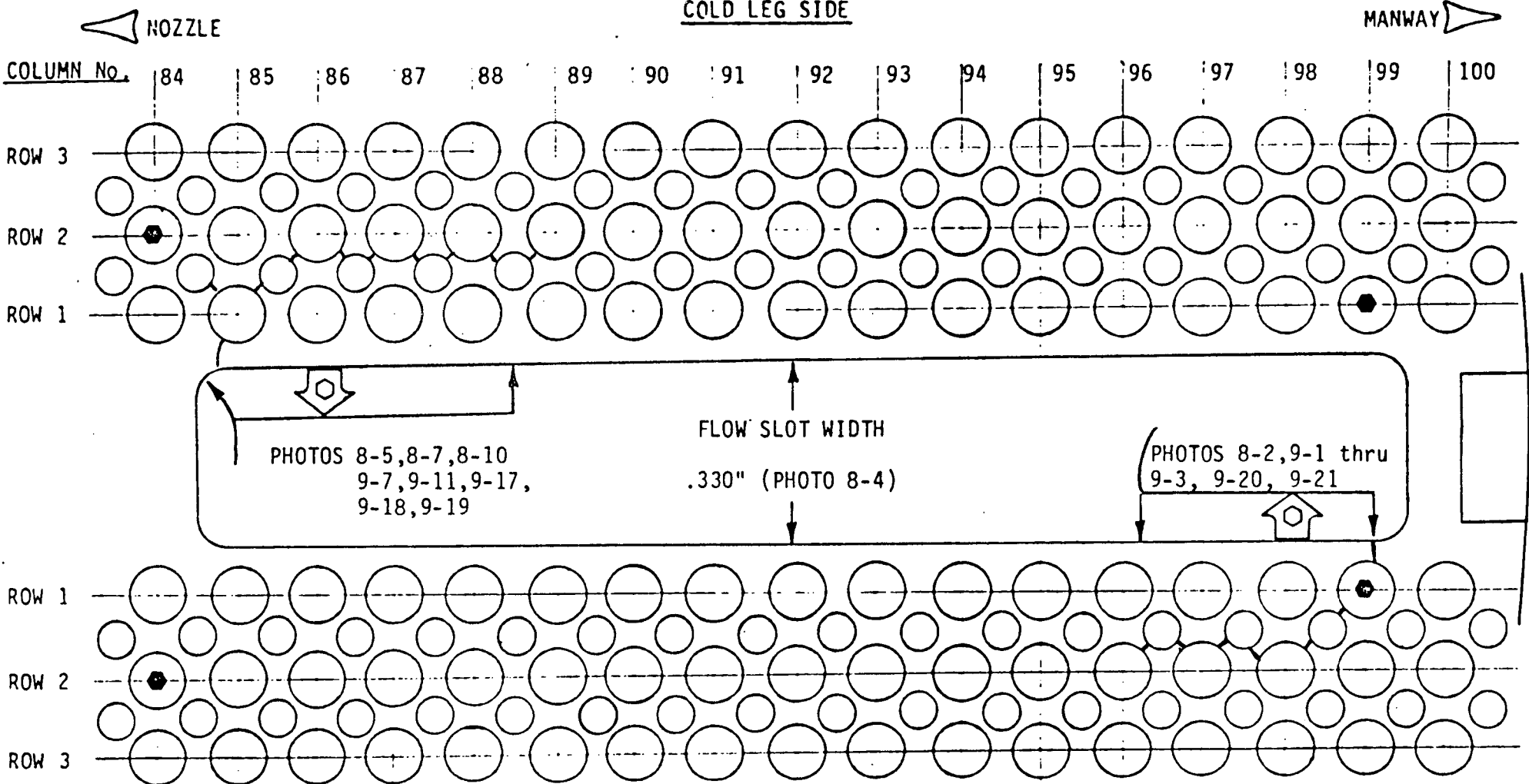


PLUGGED TUBE

FLOW SLOT EXAMINATION DATA

FLOW SLOT No.1 MANWAY SIDE



COLD LEG SIDE



HOT LEG SIDE

STEAM GENERATOR A

FIRST SUPPORT PLATE

-  DISPLACEMENT
-  PLUGGED TUBES

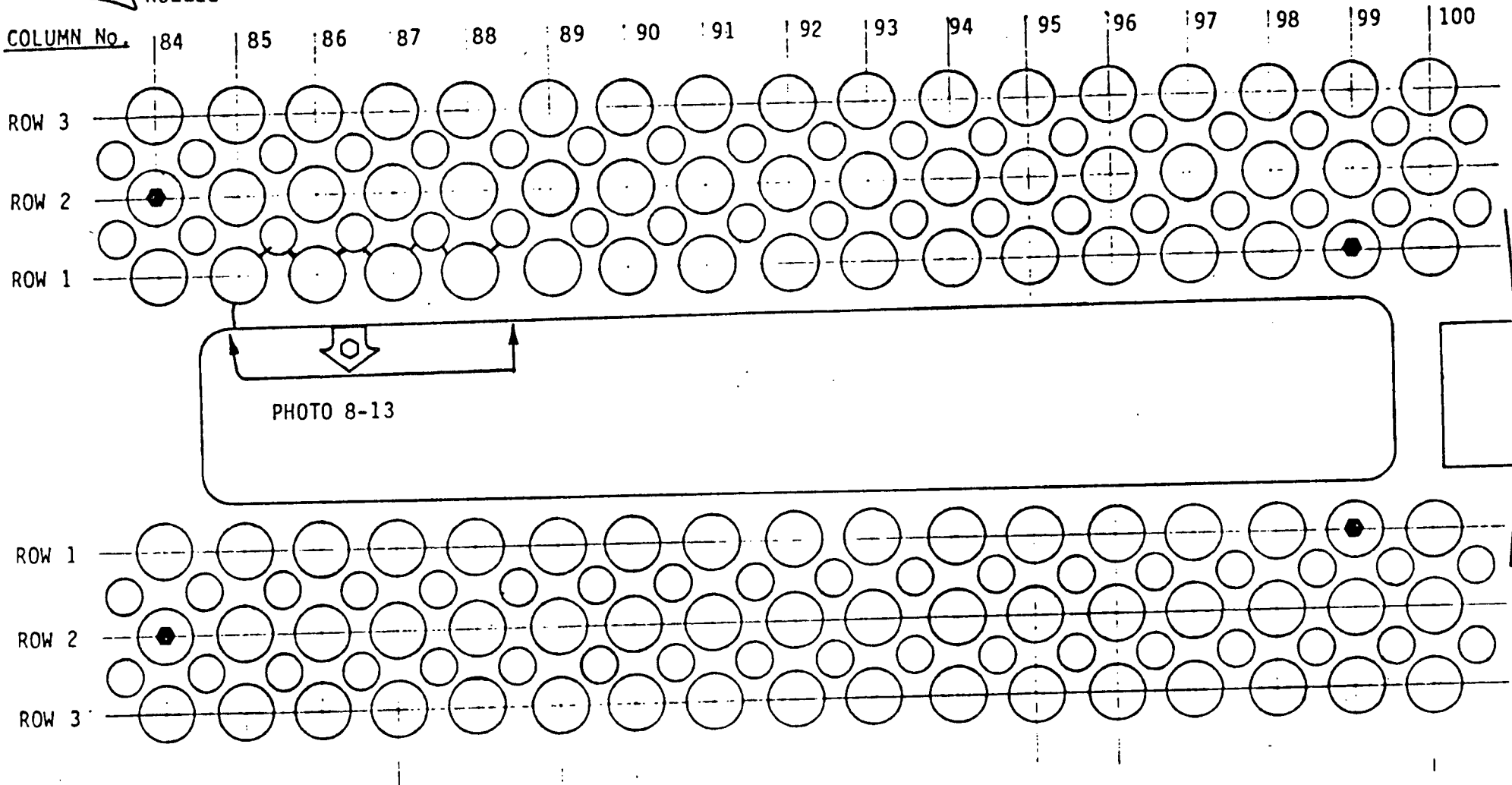
FLOW SLOT EXAMINATION DATA

FLOW SLOT No.1 MANWAY SIDE

COLD LEG SIDE

MANWAY 

 NOZZLE



HOT LEG SIDE

STEAM GENERATOR A

SECOND SUPPORT PLATE



DISPLACEMENT



PLUGGED TUBES

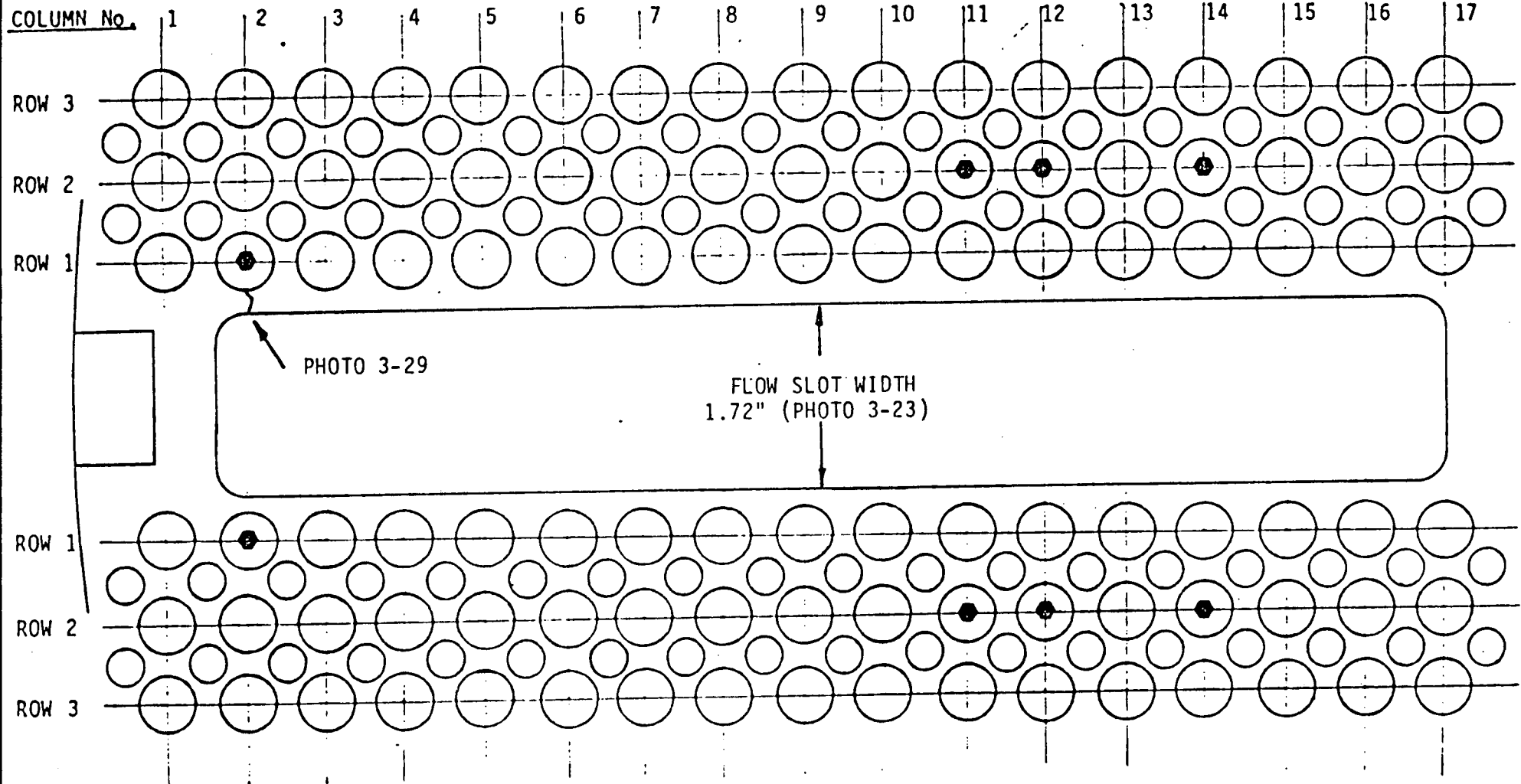
FLOW SLOT EXAMINATION DATA

FLOW SLOT No.1 NOZZLE SIDE



COLD LEG SIDE

MANWAY 

 NOZZLE



HOT LEG SIDE

-  DISPLACEMENT
-  PLUGGED TUBE

STEAM GENERATOR C  
FIRST SUPPORT PLATE

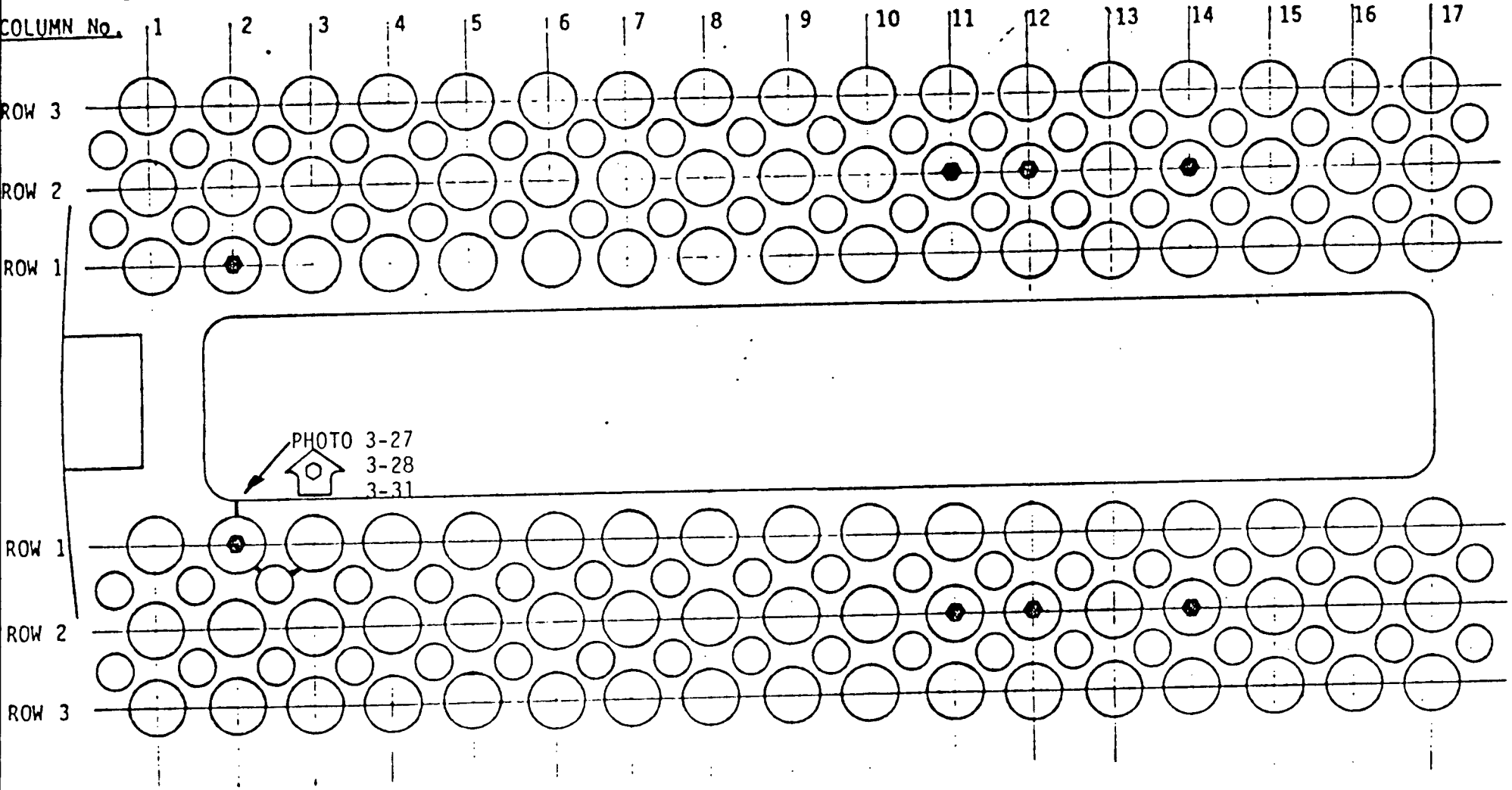
FLOW SLOT EXAMINATION DATA

FLOW SLOT No.1 NOZZLE SIDE

COLD LEG SIDE

MANWAY 

 NOZZLE



HOT LEG SIDE



DISPLACEMENT



GAGED TUBE

STEAM GENERATOR r  
SECOND SUPPORT F E

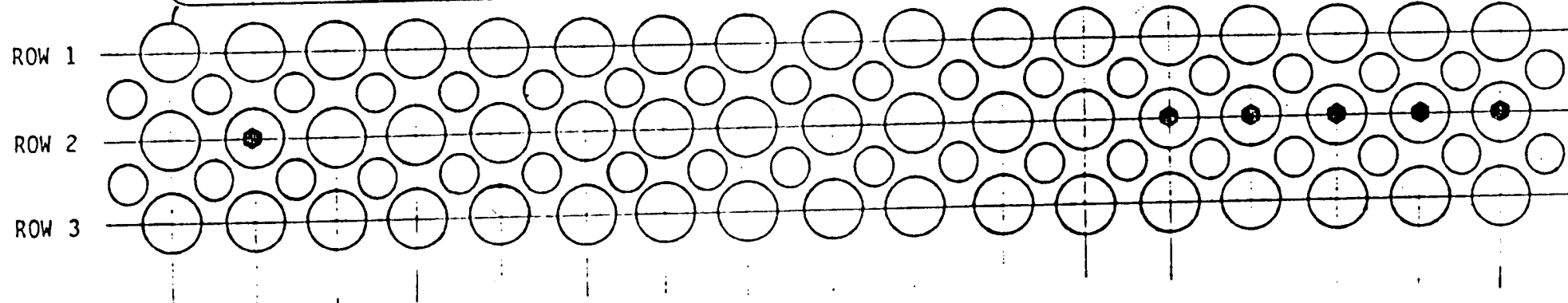
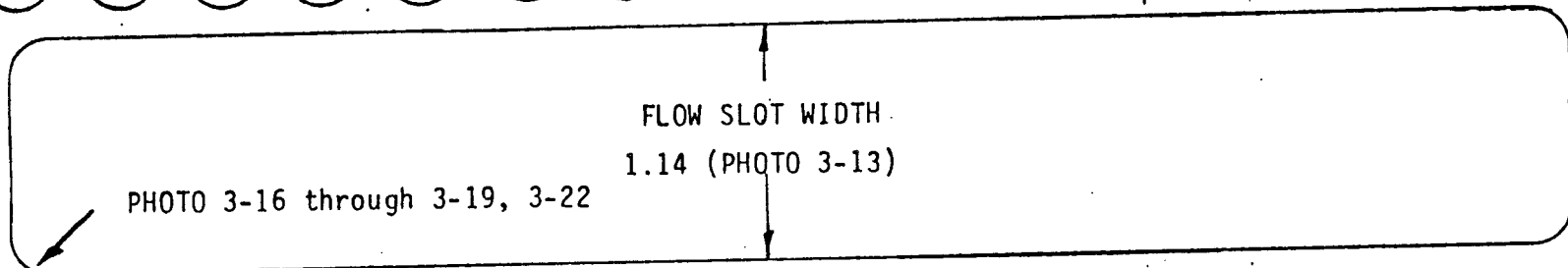
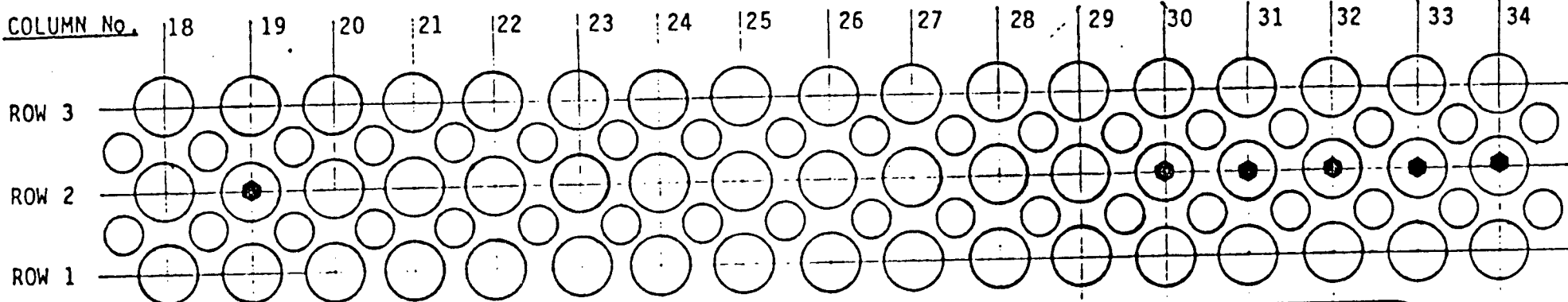
FLOW SLOT EXAMINATION DATA



FLOW SLOT No.2 NOZZLE SIDE

COLD LEG SIDE

MANWAY 

 NOZZLE



-  DISPLACEMENT
-  PLUGGED TUBE

HOT LEG SIDE


STEAM GENERATOR C  
FIRST SUPPORT PLATE

FLOW SLOT EXAMINATION DATA

FLOW SLOT No.2 NOZZLE SIDE

COLD LEG SIDE

MANWAY 

NOZZLE 

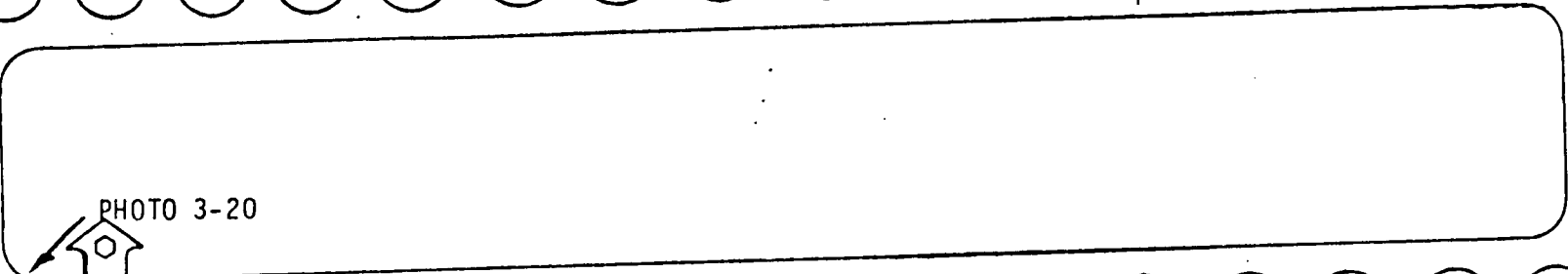
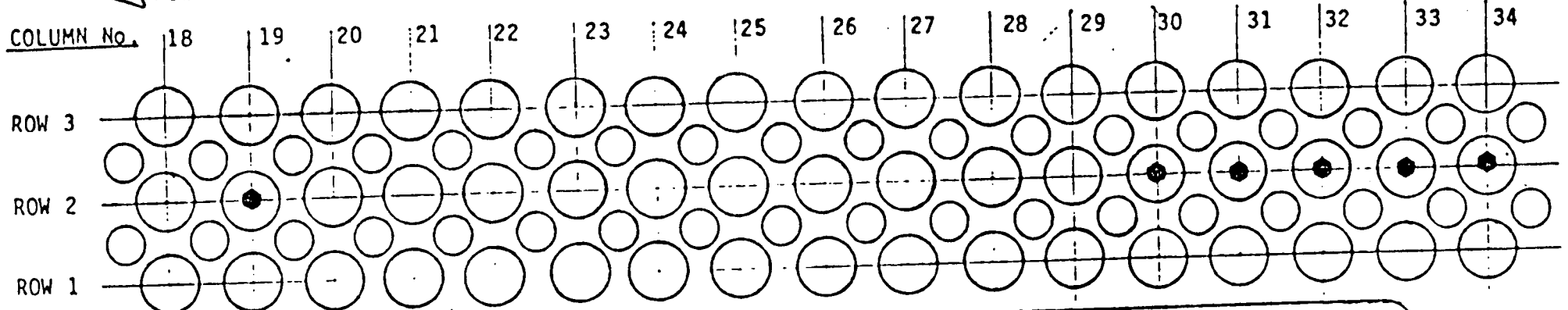
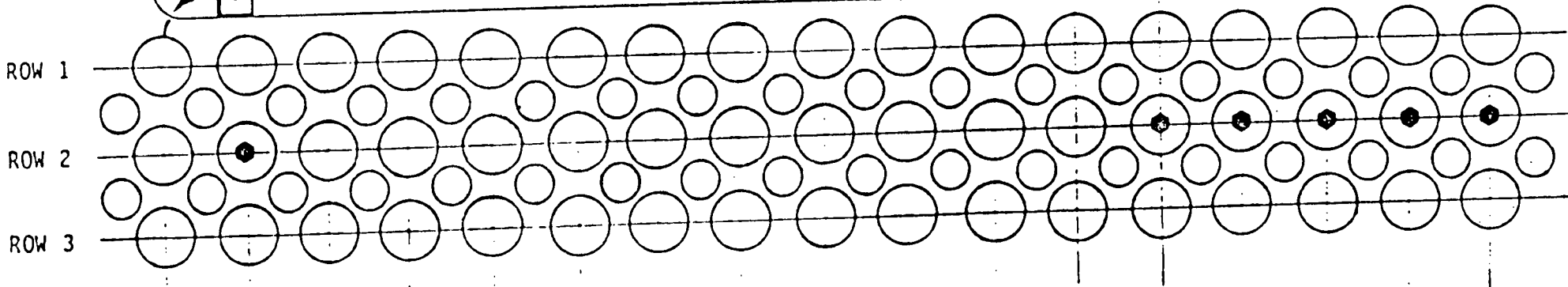


PHOTO 3-20



HOT LEG SIDE



DISPLACEMENT



PLUGGED TUBE

STEAM GENERATOR C \_\_\_\_\_  
SECOND SUPPORT P E \_\_\_\_\_




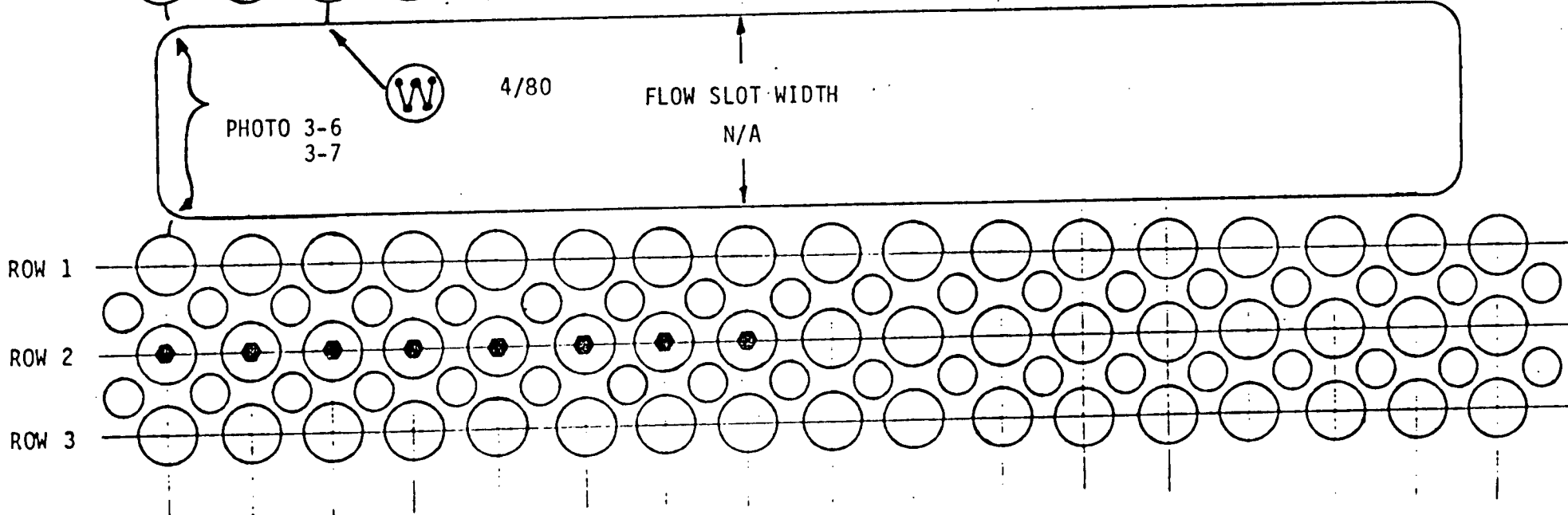
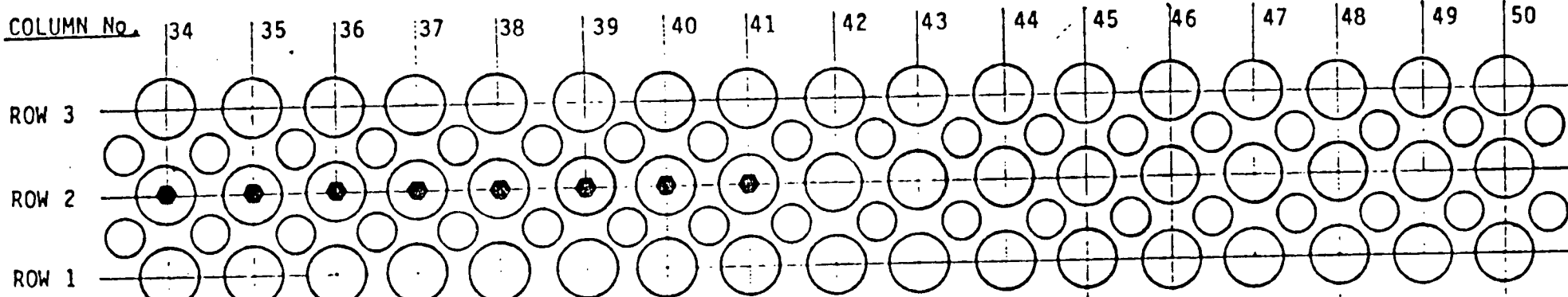
FLOW SLOT EXAMINATION DATA

FLOW SLOT No.3 NOZZLE SIDE



COLD LEG SIDE

MANWAY 

 NOZZLE



HOT LEG SIDE

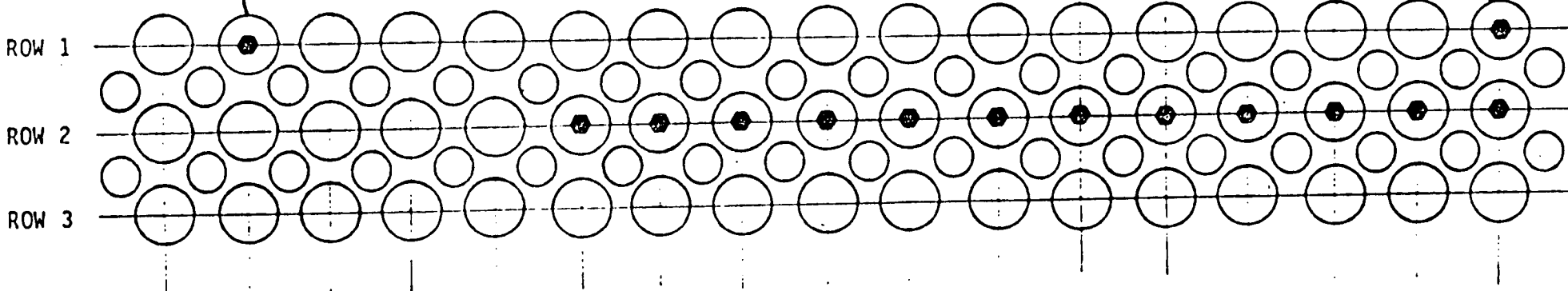
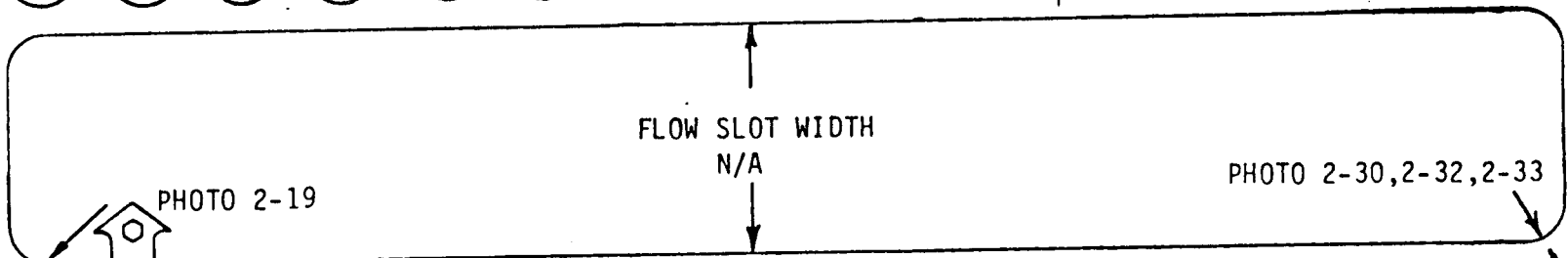
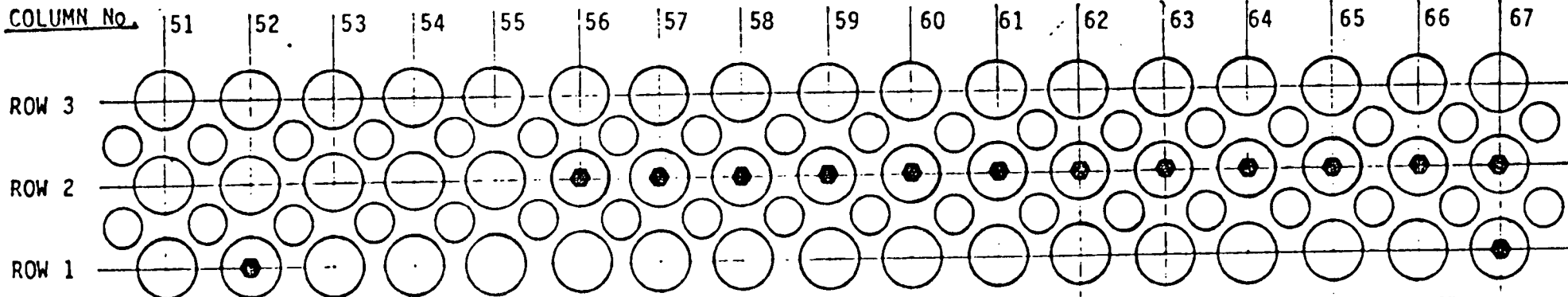
-  DISPLACEMENT
-  PLUGGED TUBE

STEAM GENERATOR C  
FIRST SUPPORT PLATE



FLOW SLOT EXAMINATION DATA

FLOW SLOT No.3 MANWAY SIDE

COLD LEG SIDE



HOT LEG SIDE

-  DISPLACEMENT
-  PLUGGED TUBE


STEAM GENERATOR C  
FIRST SUPPORT PLATE

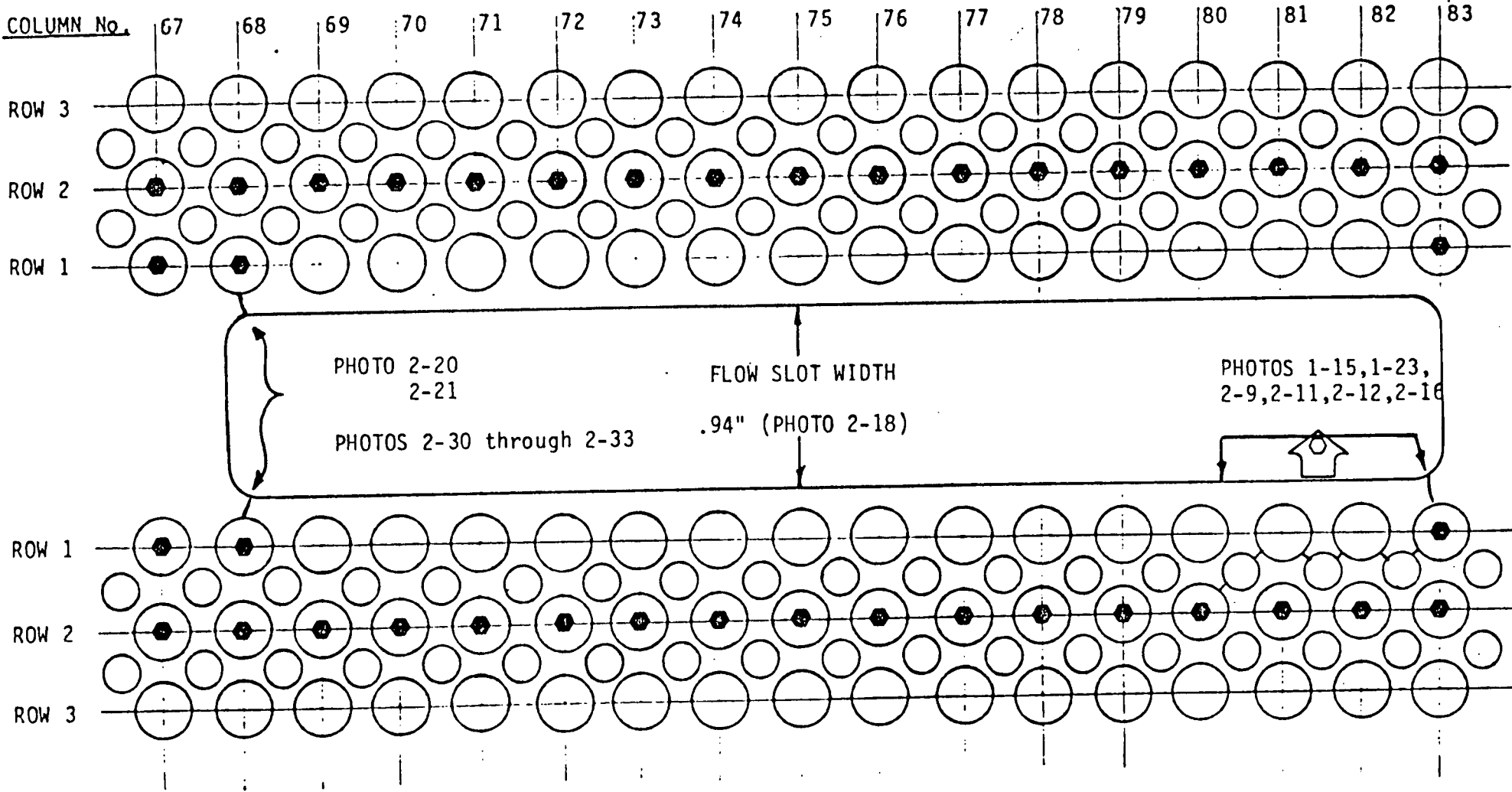
FLOW SLOT EXAMINATION DATA

FLOW SLOT No.2 MANWAY SIDE

COLD LEG SIDE

MANWAY 

 NOZZLE



HOT LEG SIDE



DISPLACEMENT

PLUGGED TUBE

STEAM GENERATOR C  
FIRST SUPPORT PLATE

FLOW SLOT EXAMINATION DATA

FLOW SLOT No.2 MANWAY SIDE

COLD LEG SIDE

NOZZLE

MANWAY

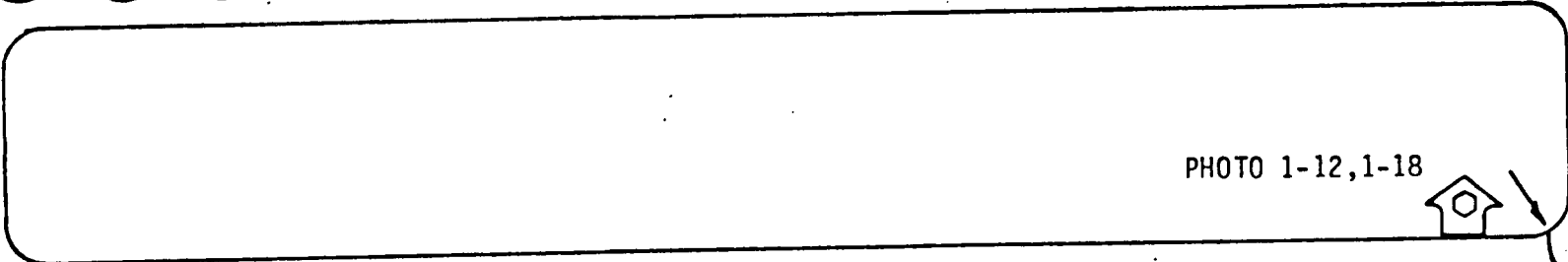
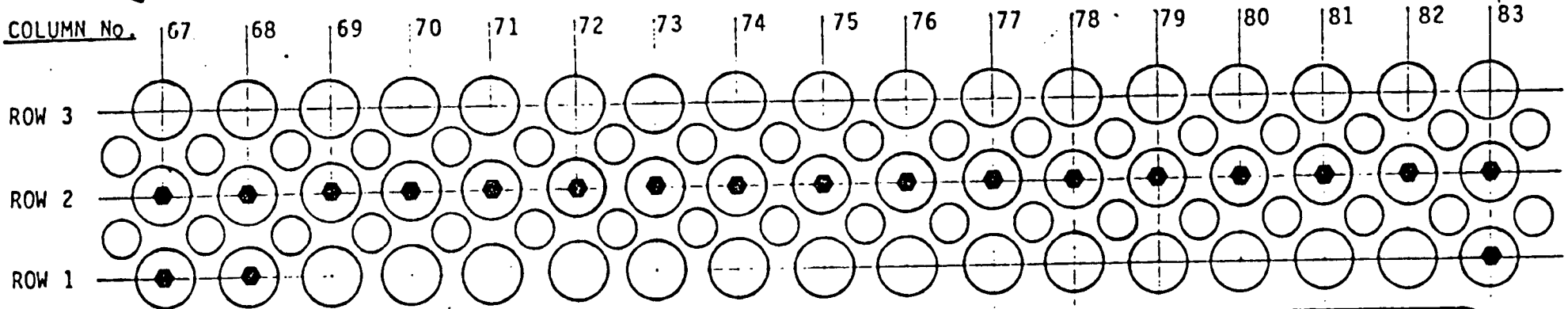
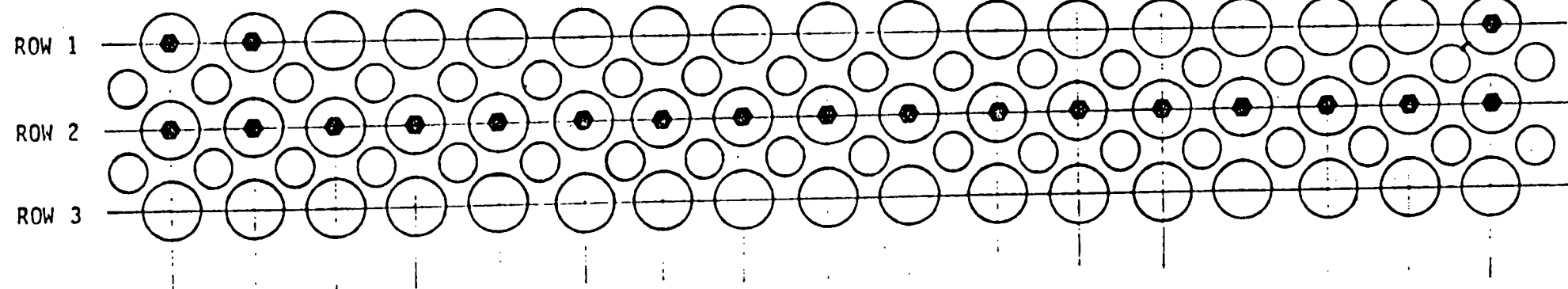


PHOTO 1-12, 1-18



HOT LEG SIDE

DISPLACEMENT

PLUGGED TUBE


STEAM GENERATOR C  
SECOND SUPPORT PLATE

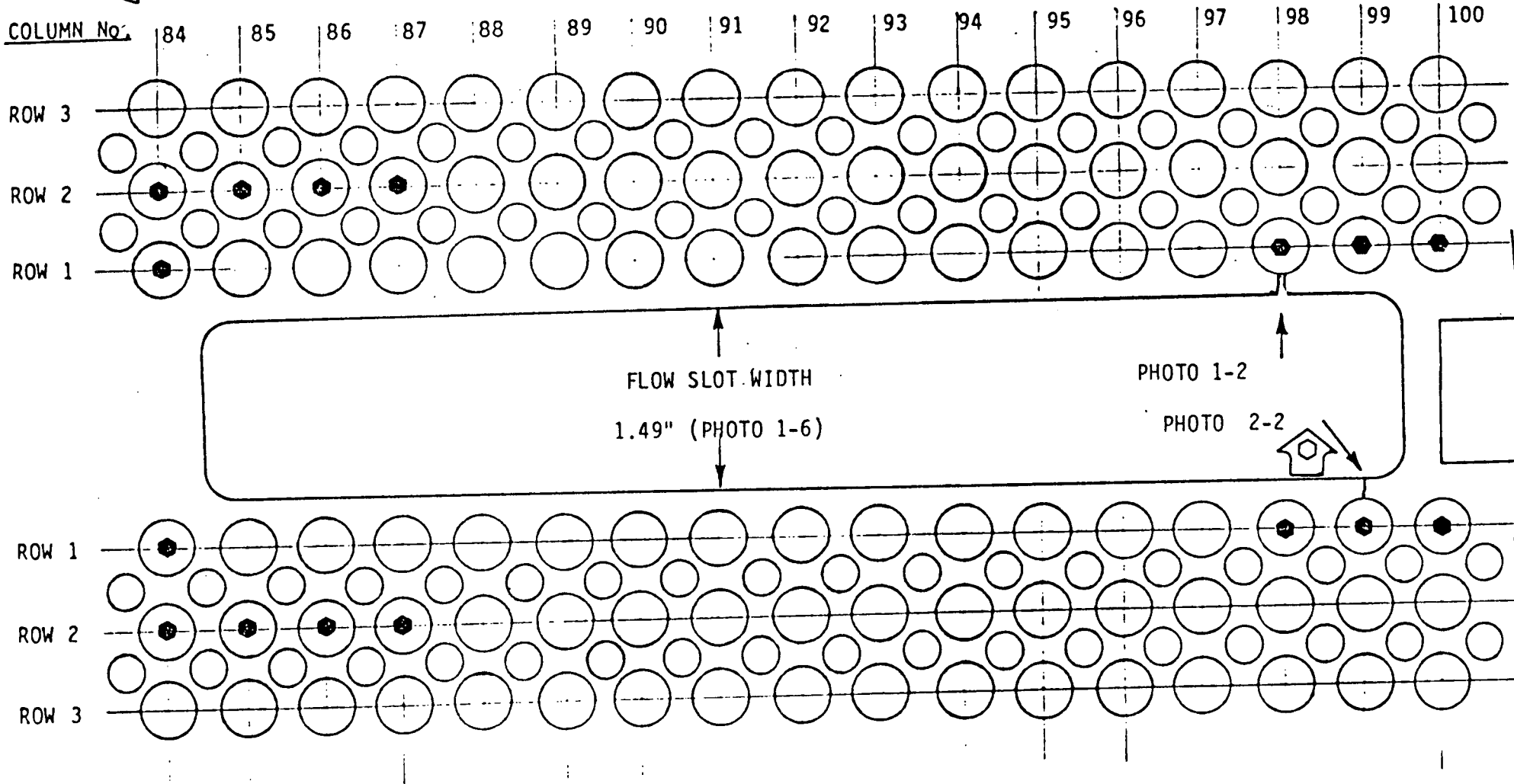
FLOW SLOT EXAMINATION DATA

FLOW SLOT No.1 MANWAY SIDE

COLD LEG SIDE

MANWAY 

 NOZZLE





FLOW SLOT WIDTH  
1.49" (PHOTO 1-6)

PHOTO 1-2  
PHOTO 2-2

HOT LEG SIDE

STEAM GENERATOR C  
FIRST SUPPORT PLATE

-  DISPLACEMENT
-  PLUGGED TUBE

FLOW SLOT EXAMINATION DATA

FLOW SLOT No.1 MANWAY SIDE

COLD LEG SIDE

MANWAY 

 NOZZLE

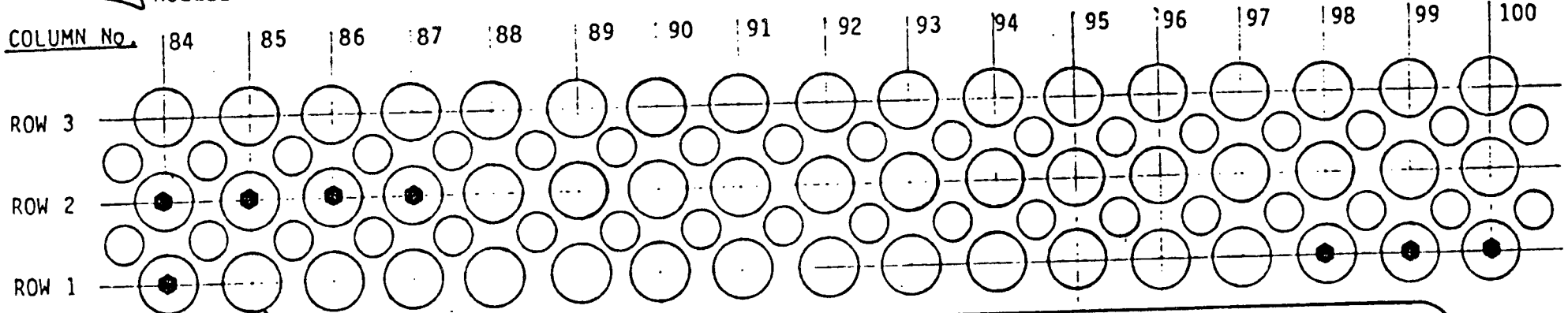
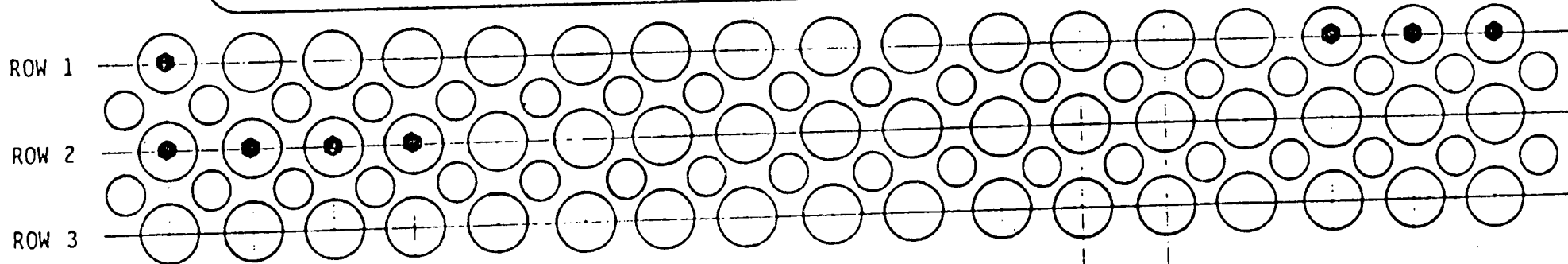


PHOTO 1-18, 1-22, 1-26

2-10, 2-13, 2-17



HOT LEG SIDE

STEAM GENERATOR C  
SECOND SUPPORT PLATE



DISPLACEMENT



PLUGGED TUBE

TABLE B-4  
 EDDY CURRENT INSPECTION OF TUBES AT  
 CRACKED SUPPORT PLATE REGIONS

SG-C OUTLET

<u>Row-Column</u>	<u>Indication</u> *	<u>Remarks</u> **
1 - 15	NDD	Slight dent at #1 TSP
2 - 15	NDD	
3 - 15	NDD	
1 - 16	NDD	Dent at #1 & 2 TSP's
1 - 17	NDD	Dent at #1 & 2 TSP's
2 - 17	NDD	
3 - 17	< 20 %	2" ATS
1 - 32	NDD	Dent at #1 & 2 TSP's
1 - 35	NDD	Dent at #1 & 2 TSP's
1 - 47	NDD	Dent at #1 & 2 TSP's
2 - 47	< 20 %	1" ATS
3 - 47	32 %	2" ATS
1 - 48	NDD	Dent at #1 & 2 TSP's
3 - 48	NDD	
3 - 49	39 %	2½" ATS
1 - 50	NDD	Dent at #1 & 2 TSP's
2 - 50	NDD	
3 - 50	22 %	2" ATS
1 - 86	NDD	Dent at #2 TSP
1 - 87	NDD	Dent at #2 TSP

\* NDD = No detectable degradation

\*\* TSP - Tube Support Plate

ATS - Above Tube Sheet

*Robert L. Cloud and Associates, Inc.*

---



DYNAMIC RESPONSE OF SCE (MODEL 27)  
STEAM GENERATOR TUBES  
WITH PARTIAL SUPPORT  
NORMAL OPERATION AND STEAMLINE BREAK

REVISION 0

August 30, 1982

P 120-5

Robert L. Cloud Associates, Inc.

125 University Avenue  
Berkeley, California 94710  
(415) 841-9296

20 Main Street  
Cotuit, Massachusetts 02635  
(617) 428-3258



DYNAMIC RESPONSE OF SCE (MODEL 27)  
STEAM GENERATOR TUBES WITH PARTIAL SUPPORT

NORMAL OPERATION AND STEAMLINE BREAK

REVISION 0

Prepared by: Jan Hong Long Date: 9/1/82

Verified by: Curtis J. Chia Date: 9/1/82

Approved by: R L Cloud Date: 9/1/82

## Table of Contents

	<u>Page</u>
List of Tables	
List of Figures	
1.0 Introduction	1
Purpose	1
Background	1
Summary of Analysis	2
2.0 Method of Analysis	3
2.1 The SG Tube Model	4
2.1.1 Support Conditions	4
2.1.2 Gap Condition	6
2.1.3 Simulated Loads	8
2.1.3.1 Simulated Normal Load	8
2.1.3.2 Simulated Steamline Break (SLB) Loads	9
2.2 Method of Computation	12
3.0 Results and Discussion	13
3.1 Results	13
3.1.1 Normal Operation	13
3.1.2 Steamline Break (SLB) Accident	15
3.2 Discussion	16
4.0 Conclusions	17
5.0 References	18
6.0 Tables 1 Through 6	19
7.0 Figures 1 Through 30	26
Appendix A - Modal Analyses of SG Tubes	A-1
Appendix B - Convergence Criteria	A-4

List of Tables

<u>Table No.</u>	<u>Title</u>	<u>Page</u>
1	Node Definitions for Case A	20
2	Node Definitions for Case B	21
3	Node Definitions for Case C	22
4	Node Definitions for Case D	23
5	Node Definitions for Case F	24
6	Conversion Table for Time Step, N	25

## List of Figures

<u>Figure No.</u>	<u>Title</u>	<u>Page</u>
1	Tube Support Conditions	27
2	Nodal Point Locations for Case A	29
3	Nodal Point Locations for Case B	30
4	Nodal Point Locations for Case C	31
5	Nodal Point Locations for Case D	32
6	Nodal Point Locations for Case E	33
7	Nodal Point Locations for Case F	34
8	One-Way Support	35
9	Simulated Normal Load $F(t)$	36
10	Dynamic Response of Node 11 for Case A during Normal Operation	37
11	Dynamic Response of Node 11 (at first TSP) for Case B with No Lateral Load during Normal Operation	38
12	Dynamic Response of Node 11 (at first TSP) for Case B with Lateral Load during Normal Operation	39
13	Dynamic Response of Node 11 for Case C during Normal Operation	40
14	Dynamic Response of Node 19 for Case C during Normal Operation	41
15	Dynamic Response of Node 11 (at first TSP) for Case D with No Lateral Load during Normal Operation	42
16	Dynamic Response of Node 20 (at second TSP) for Case D with No Lateral Load during Normal Operation	43

List of Figures, (Cont.)

<u>Figure No.</u>	<u>Title</u>	<u>Page</u>
17	Dynamic Response of Node 11 (at first TSP) for Case D with Lateral Load during Normal Operation	44
18	Dynamic Response of Node 20 (at second TSP) for Case D with Lateral Load during Normal Operation	45
19	Dynamic Response of Node 15 for Case D with Lateral Load during Normal Operation	46
20	Simulated SLB Loads $F(x,t)$ at Nodes 2-5, 7, 8, 9, 10, 12 for Case E	47
21	Simulated SLB Loads $F(x,t)$ at Nodes 13, 14, 15, 16, 17, 18 for Case E	48
22	Simulated SLB Loads $F(x,t)$ at Nodes 20, 21, 22, 23, 24, 25 for Case E	49
23	Simulated SLB Loads $F(x,t)$ at Node 26 for Case E	50
24	Dynamic Response of Node 11 for Case E in a SLB Accident	51
25	Dynamic Response of Node 11 (at first TSP) for Case F with Lateral Load in a SLB Accident	52

List of Figures, (Cont.)

<u>Figure No.</u>	<u>Title</u>	<u>Page</u>
26	Dynamic Response of Node 11 for Case C in a SLB Accident	53
27	Dynamic Response of Node 19 for Case C in a SLB Accident	54
28	Dynamic Response of Node 11 (at first TSP) for Case D with Lateral Load in a SLB Accident	55
29	Dynamic Response of Node 20 (at second TSP) for Case D with Lateral Load in a SLB Accident	56
30	Dynamic Response of Node 17 for Case D with Lateral Load in a SLB Accident	57

## 1.0 INTRODUCTION

This report analyzes the possibility of fretting and wear in the SCE (Model 27) steam generator (SG) tubes in a nuclear power plant. Fretting is a form of corrosion-assisted wear that consists of largely mechanical metal removal. Fretting occurs relatively slowly and is associated with small motions of contacting surfaces.

### Purpose

This report specifically analyzes fretting and wear motion in SG tubes that are only partially supported at the tube support plates (TSP) during normal operation of the plant and in a steamline break (SLB) accident condition. This partial support results from cracks which may occur at the TSP tube holes where the SG tubes pass through. The purpose of this analysis was to determine the vibration amplitude of the SG tube in contact with cracked TSPs. The amount of vibrational amplitude would indicate the potential for fretting and wear.

### Background

In a typical SCE (Model 27) power plant steam generator, over three thousand SG tubes exist. These U-shaped SG tubes are bundled, welded to the tube sheet at the bottom of the steam generator, and supported by four horizontal tube support plates. High temperature reactor coolant flows into the channel head at the bottom of the steam generator, through the SG tubes, and back to the channel head. A partition plate divides the channel head into inlet and outlet sections.

During normal plant operation, non-radioactive water penetrates the tube bundle through a 6.38 inch wrapper opening. The water turns into a mixture of water and steam as it travels up the steam generator. The flow of the fluid around the tube bundle may induce vibrations to the tubes. Three identified types of flow-induced vibration mechanisms [1]\* are possible: fluidelastic excitation, vortex shedding, and turbulence. For this analysis, turbulence is assumed to be the main cause of tube vibration, since turbulence is the main consideration in predicting the long term wear of the SG tubes under normal operating conditions [1].

\* Numbers in square brackets designate References at end of report.

### Summary of Analysis

This analysis shows that vibration amplitude is considerably reduced when cracked tube support plates contributing one-way support are considered in the steam generator tube model. Vibration amplitude is even further reduced when a lateral load or force is added to the steam generator tube model at the tube support plate location.



## 2.0 METHOD OF ANALYSIS

In this analysis, the vibration amplitude of the SG tube subjected to a simulated load is obtained on a time history basis. There are two types of simulated loads, namely, the simulated normal load and the simulated SLB load. The simulated normal load represents the force acting on the tube under normal operating conditions. SLB load is the transient force in a steamline break blowdown event. The force is a function of time and was derived on the basis that it should produce equivalent amplitudes of vibration in the linear case as determined by Westinghouse [2, 3, 4]. In other words, the load was calibrated against the Westinghouse analysis.

The simulated normal load is applied at the section of the SG tube that is exposed to the wrapper opening. This simulated force is applied for a duration of 1.1 seconds. For the steamline break (SLB) accident, the simulated load is applied to the SG tube for 1.489 seconds. The loads described above are applied to SG tubes both without tube support plate (TSP) support and with partial TSP support.

At the SG tube and TSP interface, the tube vibrational amplitude is obtained by two methods. The first describes the application of a lateral load. The second describes a situation where there is no lateral load at the SG tube - TSP junction.

## 2.1 THE SG TUBE MODEL

The SG tube is modeled as a two-dimensional beam with one end fixed. Six different support conditions (Cases A to F) are evaluated as described below and shown in Figure 1. The four conditions correspond to:

- o a 91.8 inch tube without a TSP
- o a 91.8 inch SG tube with a TSP that provides partial support
- o a 137.7 inch SG tube without TSPs
- o a 137.7 inch SG tube with two TSPs providing partial support
- o a 137.7 inch SG tube without a TSP
- o a 137.7 inch SG tube with a TSP that provides partial support

### 2.1.1 Support Conditions

For all six cases, five closely spaced nodes are placed in the model at the region of the tube that is exposed to the wrapper opening; three closely spaced nodes are placed at each TSP and two more at the far end.

Case A corresponds to a clamped-simply supported SG tube with the first TSP missing. This case is a linear problem and serves as the basis for calibration of the normal load. Figure 2 shows the nodal point locations for Case A.

Case B simulates an SG tube with a cracked first TSP providing one-way support at mid-span. Two more nodes are placed in the center of the beam to account for the interface between the SG tube and the TSP. Figure 3 shows nodal point locations for Case B.

Case C is similar to Case A, but has a longer length. It represents a clamped-simply supported SG tube with the first and second TSPs missing. Figure 4 shows the nodal point location for Case C.

Case D consists of a beam divided in thirds by two one-way supports. This represents an SG tube with two cracked TSPs. Two more nodes have been placed at each of the two partial support locations to account for the supports. Figure 5 shows nodal point locations for Case D.

Case E is a modification of Case A for the steamline break (SLB) accident condition. The beam is divided into two sections by the two-way support. This case is used for calibration of the SLB load. Figure 6 shows the nodal point locations for Case E.

Case F is similar to Case E, but has a cracked first TSP providing one-way support at the lower section. Figure 7 shows nodal point locations for Case F.

### 2.1.2 Gap Condition

When the SG tube has only one-way support, it may maintain or break physical contact with the cracked TSP. This situation results in a gap condition which applies in Cases B, D and F. Figure 8 shows a SG tube with a one-way support. This one-way support is modeled by a gap together with a spring and a damper connected to the ground as shown in Figures 3, 5 and 7.

In the model, three parameters are used: namely, k (spring constant), c (damping coefficient), and d (gap size).

#### Spring Constant k

The k value of the spring is based upon the stiffness of the surfaces in contact.

k is assumed to be equal to  $AE/L$

where,

A = half the metal area  
E = modulus of elasticity  
L = support plate thickness

k is equal to  $2.8 \times 10^6$  lb/in. for cases B, D and F.

#### Damping Coefficient c

The damping coefficient of the damper is calculated by first determining the critical damping coefficient,  $c_{cr}$ , of a small section of the SG tube with length .6252 inch.  $c_{cr}$  is calculated using the following assumption [5]:

$$c_{cr} = 2\sqrt{\frac{kW}{g}} \quad (1)$$

where,

W = combined tube weight x L

To give the damping coefficient,  $c_{cr}$  is multiplied by a factor of 2%. The damping coefficient, c, of the gap condition has a value of .57 lb-sec/in.

### Gap Size d

To determine the gap size  $d$ , two options are considered: no lateral load and a pre-existing lateral load. When there is no lateral load, the value of  $d$  is zero. When there is a lateral load, the displacement ( $d$ ) of the SG tube must be calculated.

For Case B, a static force of  $P$  lb. is applied at the middle of the single span SG tube and the displacement,  $\delta$  inches, is calculated using the following formula [6]:

$$\delta = \frac{7 PL^3}{768 EI} \quad (2)$$

To calculate for the gap interference as a result of the lateral load, the negative value of the displacement is used.

$$d = - \delta \quad (3)$$

For Case D,  $P_1$  lb. and  $P_2$  lb. are the static forces applied at the first and second TSP locations respectively; and  $\delta_1$  inches and  $\delta_2$  inches are the corresponding displacements.

The amount of displacement is calculated using the following equations [6]:

$$\delta_1 = A (10 P_1 + 11.5 P_2) \quad (4)$$

$$\delta_2 = A (11.5 P_1 + 20 P_2) \quad (5)$$

where,

$$A = \frac{a^3}{81 EI} \quad \text{and } a = 45.9 \text{ inches.}$$

To calculate for the gap interferences as a result of the lateral loads, the negative values of the displacements are used for Case D in the same manner as for Case B.

### 2.1.3 Simulated Loads

#### 2.1.3.1 Simulated Normal Load

Under normal operating conditions, water enters through a wrapper opening. The water is heated as it flows up the steam generator turning into a mixture of water and steam. The movement of the mixture may induce vibration in the SG tubes. Tubulent excitation is assumed to be the main cause of this excitation, as discussed in Section 1.0.

Under turbulent excitation, narrow-band random vibration response of the SG tube is anticipated at about the tube's natural frequency in the fluid [1]. To simulate this anticipated response, a combination of sine functions is used to represent the forcing. The forcing function,  $F(t)$ , is given in the following equation:

$$F(t) = S [\text{Sin} (\frac{1}{2} \omega t) + \text{Sin}(\omega t) + \text{Sin}(2\omega t)] \quad (6)$$

where,

$S$  = scaling factor

$\omega$  = forcing frequency

For cases A to D, one frequency is used as the forcing frequency. This frequency is derived from the longest single span tube, which is shown by Case C.

To find  $\omega$ , a modal analysis of Case C was done. The results, which are given in Appendix A, show the lowest natural frequency for Case C to be 5.524374 Hz. Therefore, 5 Hz. is used for  $\omega$  and

$$\omega = 2 \pi f = 2 \pi (5) = 31.42 \text{ rad/sec.} \quad (7)$$

After  $\omega$  is found,  $S$ , the scaling factor, must be calculated. Tube vibration amplitudes for both Cases A and C were already determined by Westinghouse, using their flow-induced vibration analyses methodology. The results were found to be as follows [2]:

Case A      Maximum amplitude =  $3.5 \times 2 = 7$  mils

Case C      Maximum amplitude =  $3.5 \times 6 = 21$  mils

The maximum response amplitude Westinghouse determined for Case A provides the reference for this analysis where different values for  $S$  were substituted in Equation 6 until the stipulated 7 mils maximum response was reached.

$S$  was found to be equal to .5 lb. The corresponding maximum amplitudes for Cases A and C are 7.2 mils and 19.4 mils, respectively. This calibration ensures that  $F(t)$  in Equation (6) provides an excitation equivalent to the Westinghouse linear model.

The plot of the time history of  $F(t)$  for  $t \in [0, 1.1]$  sec. is shown in Figure 9. Note that the maximum forcing amplitude is about 1.1 lbs.

After  $F(t)$  is found, it is then applied at nodes 2 through 5 of the model. These nodes correspond to the region of the tube at the wrapper opening.

#### 2.1.3.2 Simulated Steamline Break (SLB) Loads

For the steamline break (SLB) accident condition, the following assumptions are used.

- o a complete severance of the pipe (steamline) and the pipe centerline is offset by at least the pipe diameter
- o no choking of flow through the steam nozzle
- o the SLB forcing function is in the shape of a triangular pulse

The SLB forcing function is derived making use of the momentum flux time histories obtained by MPR Associates, Inc. [7]. Five different sets of momentum flux time histories  $M_1(t)$  to  $M_5(t)$  were generated. These time histories were then multiplied by a scaling factor  $\bar{S}$  to get the forcing histories in pounds force. The corresponding forcing histories are denoted by  $F_1(t)$  to  $F_5(t)$ , where

$F_1(t)$  = SLB load at the region of the tube exposed to the wrapper opening

$F_2(t)$  = SLB load at mid section between the tube sheet and the first tube support plate (TSP)

$F_3(t)$  = SLB load at the first TSP location

$F_4(t)$  = SLB load at the second TSP location

$F_5(t)$  = SLB load at the third TSP location

Assuming a linear distribution, the SLB loads at other locations of the tube are calculated by the following formula

$$\bar{X} = (1 - \frac{x}{L}) F_A + \frac{x}{L} F_B \quad (8)$$

where,

$\bar{X}$  = SLB loads at node n

$F_A$  = given SLB load at first governing node

$F_B$  = given SLB load at last governing node

x = distance of node n from first governing node

L = distance between first and last governing nodes

The SLB loads are then applied along the span of the SG tube as shown in Figures 6 and 7. The same set of loads are also applied to Cases C and D for the broken lower two support plates conditions.

The vibration amplitudes for both Cases E and C (SLB) were determined by Westinghouse and the results were found to be as follows [4]:

Case E            Maximum amplitude = .155 in

Case C (SLB)    Maximum amplitude = .213 in



These maximum response amplitudes provide the reference where different values for  $\bar{S}$ , the scaling factor, were used until the stipulated maximum responses were reached. This calibration again ensures that the SLB loads provide an excitation equivalent to the Westinghouse linear model.

$\bar{S}$  was found to be equal to .00049 for Case E and this value is used for both Cases E and F in the calculation. Similarly, for both Cases C (SLB) and D (SLB),  $\bar{S}$  was found to be equal to .000029. The corresponding maximum amplitudes for Cases E and C (SLB) are .1542 inch and .2147 inch, respectively.

There are a total of 19 SLB loads and the forcing time step histories for Case E are shown in Figures 20, 21, 22 and 23 (see Table 6).

A modal analysis of Case E was done and the results are given in Appendix A.

## 2.2 METHOD OF COMPUTATION

To find the resulting vibration amplitudes, a computer analysis was performed for all cases once the forcing function had been determined. Reduced Linear Transient Dynamic Analysis (KAN=5) of the computer code "ANSYS (Rev. 3)" was used together with the following assumptions and conditions:

- 1) a structural damping of 2.5% was assumed for the SG tube.
- 2) The time history analysis for normal operation was done for  $t \in [0, 1.1]$  sec. For SLB accident condition the analysis was done for  $t \in [0, 1.489]$  sec.
- 3) The integration time step [ITS] was chosen to ensure accuracy for the numerical solutions. The ITS was constant throughout the analysis (see Appendix B).
- 4) Seventeen master degrees of freedom in the y-direction were specified for Cases A and B, twenty-five for Cases C and D, and twenty-four for Cases E and F.
- 5) No reference temperature was used in the calculations.

### 3.0 RESULTS AND DISCUSSION

#### 3.1 RESULTS

The vibration behavior of the SG tube was obtained at the TSP locations for all the previously mentioned cases. The results are summarized as follows:

##### 3.1.1 Normal Operation

###### Case A

For Case A there is no TSP at mid-span. The maximum negative displacement  $y_{\max}^{(A)}$  of the SG tube within the time interval of interest occurred at node 13 and

$$y_{\max}^{(A)} = - 7.2342 \times 10^{-3} \text{ in.} \quad (9)$$

If there was a TSP, it would be placed at node 11. A plot of the displacement time history for node 11 is used as a reference for Case B and shown in Figure 10.

###### Case B With No Lateral Load

For Case B with no lateral load, the gap size,  $d$ , is 0 in., as discussed in Section 2.1.2. For comparison, the same Case A scale as shown in Figure 10 is applied to the displacement time history plot of node 11 which is given in Figure 11.

The maximum positive displacement of node 11 is  $.11024 \times 10^{-5}$  in.

###### Case B With Lateral Load

For Case B with a lateral load, the gap interference equals  $-.0026$  in. which corresponds to a static load of  $.0786$  lb., according to Equation 2.

The displacement time history given in Figure 12 was plotted for node 11 using the same Case A scale.

### Case C

For Case C there are no TSPs except at the far end of the SG tube. The maximum displacement  $y_{\max}^{(C)}$  of the SG tube occurred in node 16 which is 15.7 inches below the second TSP location.

$$y_{\max}^{(C)} = .19365 \times 10^{-1} \text{ in.} \quad (10)$$

The displacement time history plots of the first and second TSP locations which correspond to nodes 11 and 19 are shown in Figures 13 and 14, respectively.

### Case D With No Lateral Load

For Case D with no lateral load, the gap size  $d$  is 0 inches.

The displacement time histories were plotted for the two TSPs which correspond to nodes 11 and 20. These time histories used the same scale as Case C and are shown in Figures 15 and 16.

The maximum positive displacements of nodes 11 and 20 were found to be  $.74839 \times 10^{-6}$  inch and  $.56445 \times 10^{-9}$  inch, respectively.

### Case D With Lateral Load

For Case D with lateral loads, the gap interference,  $d$ , equals  $-.0027$  inch for the first TSP and  $-.0039$  inch for the second TSP. The interferences correspond to static loads of about .024 lb. and .021 lb., respectively.

The displacement time histories of the TSPs were plotted using the same scale as Case C and are shown in Figures 17 and 18.

For this case, the maximum negative displacement took place in node 15 as shown in Figure 19. This time history plot for node 15 provides a comparison with the time history plots of the TSPs shown in Figures 17 and 18.

### 3.1.2 Steamline Break (SLB) Accident

#### Case E

For Case E there is no first TSP. The maximum displacement  $y_{\max}^{(E)}$  of the SG tube within the time interval of interest at node 11 is equal to

$$y_{\max}^{(E)} = .15415 \text{ in.} \quad (11)$$

A plot of the displacement time history for node 11 is used as a reference for Case F and shown in Figure 24.

#### Case F With Lateral Load

For Case F with a lateral load, a gap interference of  $-.0013$  in. was used.

The displacement time history given in Figure 25 was plotted for node 11 using the same Case E scale.

#### Case C (SLB)

For Case C (SLB), the maximum displacement  $y_{\max}^{(\bar{C})}$  of the SG tube occurred in node 17 and

$$y_{\max}^{(\bar{C})} = .21468 \text{ in.} \quad (12)$$

The displacement time history plots of the first and second TSP locations which correspond to nodes 11 and 19 are shown in Figures 26 and 27, respectively.

#### Case D (SLB) With Lateral Load

For Case D (SLB) with lateral loads, the gap interference equals  $-.00135$  inch for the first TSP and  $-.00195$  inch for the second TSP.

The displacement time histories of the TSPs were plotted using the same scale as Case C (SLB) and are shown in Figures 28 and 29.

For this case, the maximum negative displacement took place in node 17 as shown in Figure 30. This time history plot for node 17 provides a comparison with the time history plots of the TSPs shown in Figures 28 and 29.

### 3.2 DISCUSSION

When the tube support plate (TSP) is added to the SG tube, the vibration amplitude is considerably reduced as can be seen by comparing Figures 10 and 11, 13 and 15, and 14 and 16.

When the lateral load is added to the SG tube at the TSP location, the vibration amplitude is even further reduced as seen by comparing the following groups: Figures 10, 11 and 12; Figures 13, 15 and 17; Figures 14, 16 and 18; Figures 24 and 25; Figures 26 and 28; and Figures 27 and 29.

Figures 12, 17, 18, 25, 28 and 29 show vibrational amplitudes for the SG tubes at the TSPs when the lateral load is added.

For Case B with a lateral load, the static load of .0786 lb. was used to calculate the maximum displacement at node 11 (the TSP location). This displacement was found to be about .3 mil as shown in Figure 10. Here displacement is measured from the initial position of the node at time zero.

For Case D with a lateral load, two static loads, .024 lb. and .021 lb. were used to calculate the maximum displacements at nodes 11 and 20 (the two TSP locations). These displacements were found to be about 2 mils at the first and .1 mil at the second as shown in Figures 15 and 16.

For Case F with a lateral load, the maximum displacement at node 11 was found to be about 6 mils as shown in Figure 25.

For Case D (SLB) with lateral loads, the maximum displacements at nodes 11 and 20 (the two TSP locations) are .2 mil and .0004 mil, respectively.

As can be seen from the plots of the SLB response, the major portion of the excitation and the response is uni-directional rather than oscillatory in nature. The one-way support at the TSP can be seen to effectively control the motion of the tubes and therefore the possibility of unstable fluid-elastic oscillation is believed negligible.

#### 4.0 CONCLUSIONS

This analysis shows that results obtained by considering a total absence of support at cracked TSP locations are excessively conservative. Consideration of the true non-linear behavior of the tube-TSP junction shows that the relative motion is very small at the junction.

These response amplitudes are reduced when lateral loads on the SG tube model at the TSP locations are considered. Lateral deformation which implies existence of a lateral load is noticeable in photographs of actual steam generator tubes taken at nuclear power plants. Thus, the possibility for fretting at the cracked TSPs during normal operation is negligible.

The results of this analysis show that the same general situation prevails when SLB loads are considered. There is a marked difference in response of the tubes between the case of an assumed absence of the TSP and the case of partial support that would exist at a deteriorated TSP. When partial support is considered, the mode shapes are different and the response is greatly reduced. The possibility of fretting, wear, or unstable vibration occurring in the short interval of maximum response to the SLB is negligibly small.

## 5.0 REFERENCES

1. Connors, H. J., "Flow-Induced Vibration and Wear of Steam Generator Tubes", Nuclear Technology, Vol. 55, Nov. 1981.
2. "Steam Generator Tube Vibration Analyses. San Onofre Nuclear Generating Station Unit 1." Appendix G. 1978 NRC Submittal by SCE.
3. "SCE UNIT I STEAM GENERATOR. Flow-induced Vibration Analysis to Evaluate Potential for Propagation of Pre-Existing IGA in Non-sleeved Tubes." Attachment to CA-AEA-114. June 30, 1982.
4. "SCE UNIT #1 STEAM GENERATOR. Update of Tubing Evaluation Subject to SLB Loads." Westinghouse meeting material. August 12, 1982.
5. Timoshanko, S., Young, D. H. and Weaver, W. Jr., Vibration Problems in Engineering. Fourth Edition, Wiley.
6. McNeese, D. C. and Hoag, A. L., Engineering and Technical Handbook. Prentice-Hall.
7. "Hydraulic Analysis of Postulated Steam Line Break for SCE (Model 27) Steam Generator." Volume One of Three Volumes. MPR-743, MPR Associates, Inc. (Aug. 1982).
8. Roark, R. J. and Young, W. C., Formulas for Stress and Strain. Fifth Edition, McGraw-Hill.





Section 6.0

Tables

Node No.	X (In.)	Y (In.)
1	0	0
2	1.595	0
3	3.190	0
4	4.785	0
5	6.380	0
6	14.044	0
7	21.708	0
8	29.372	0
9	37.036	0
10	44.700	0
11	45.900	0
12	47.100	0
13	54.350	0
14	61.600	0
15	68.850	0
16	76.100	0
17	83.350	0
18	90.600	0
19	91.800	0

Table 1

Node Definitions for Case A

Node No.	X (In.)	Y (In.)
1	0	0
2	1.595	0
3	3.190	0
4	4.785	0
5	6.380	0
6	14.044	0
7	21.708	0
8	29.372	0
9	37.036	0
10	44.700	0
11	45.900	0
12	45.900	.38
13	47.100	0
14	54.350	0
15	61.600	0
16	68.850	0
17	76.100	0
18	83.350	0
19	90.600	0
20	91.800	0
21	45.900	0

Table 2  
Node Definitions for Case B

Node No.	X (In.)	Y (In.)
1	0	0
2	1.595	0
3	3.190	0
4	4.785	0
5	6.380	0
6	14.044	0
7	21.708	0
8	29.372	0
9	37.036	0
10	44.700	0
11	45.900	0
12	47.100	0
13	54.350	0
14	61.600	0
15	68.850	0
16	76.100	0
17	83.350	0
18	90.600	0
19	91.800	0
20	93.000	0
21	100.250	0
22	107.500	0
23	114.750	0
24	122.000	0
25	129.250	0
26	136.500	0
27	137.700	0

Table 3  
Node Definitions for Case C

Node No.	X (In.)	Y (In.)
1	0	0
2	1.595	0
3	3.190	0
4	4.785	0
5	6.380	0
6	14.044	0
7	21.708	0
8	29.372	0
9	37.036	0
10	44.700	0
11	45.900	0
12	45.900	.38
13	47.100	0
14	54.350	0
15	61.600	0
16	68.850	0
17	76.100	0
18	83.350	0
19	90.600	0
20	91.800	0
21	91.800	.38
22	93.000	0
23	100.250	0
24	107.500	0
25	114.750	0
26	122.000	0
27	129.250	0
28	136.500	0
29	137.700	0
30	45.900	0
31	91.800	0

Table 4  
Node Definitions for Case D

Node Number	x (in.)	y (in.)
1	0	0
2	1.595	0
3	3.190	0
4	4.785	0
5	6.380	0
6	14.044	0
7	21.708	0
8	29.372	0
9	37.036	0
10	44.700	0
11	45.900	0
12	45.900	.38
13	47.100	0
14	54.350	0
15	61.600	0
16	68.850	0
17	76.100	0
18	83.350	0
19	90.600	0
20	91.800	0
21	45.900	0
22	93.000	0
23	100.250	0
24	107.500	0
25	114.750	0
26	122.000	0
27	129.250	0
28	136.500	0
29	137.700	0

Table 5  
Node Definitions for Case F

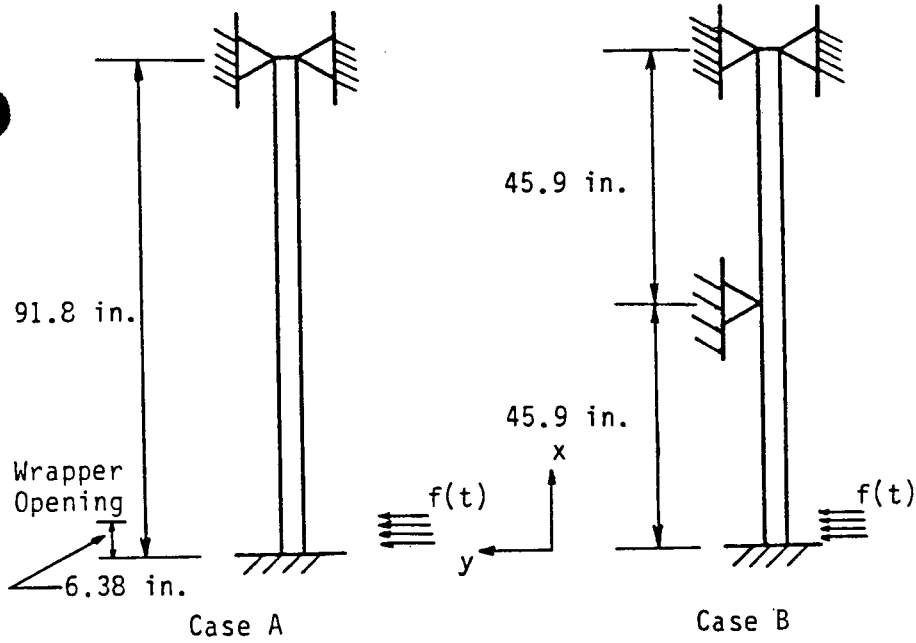
Time Step, N	Time (sec)
0	0
10	.032
20	.085
30	.169
40	.268
50	.472
60	.683
70	.859
80	1.063
90	1.292
100	1.489

Table 6  
Conversion Table for Time Step, N



Section 7.0  
Figures





Parameters:

Beam is tube filled with water

OD = .75 in., ID = .64 in.

$E = 29.2 \times 10^6$  lb/in<sup>2</sup>

$\rho_{\text{metal}} = .28$  lb/in<sup>3</sup>

$\rho_{\text{water}} = 3.61 \times 10^{-2}$  lb/in<sup>3</sup>

$I = 7.3 \times 10^{-3}$  in<sup>4</sup> [8]

Combined Tube Weight =  
 $4.52 \times 10^{-2}$  lb/in.

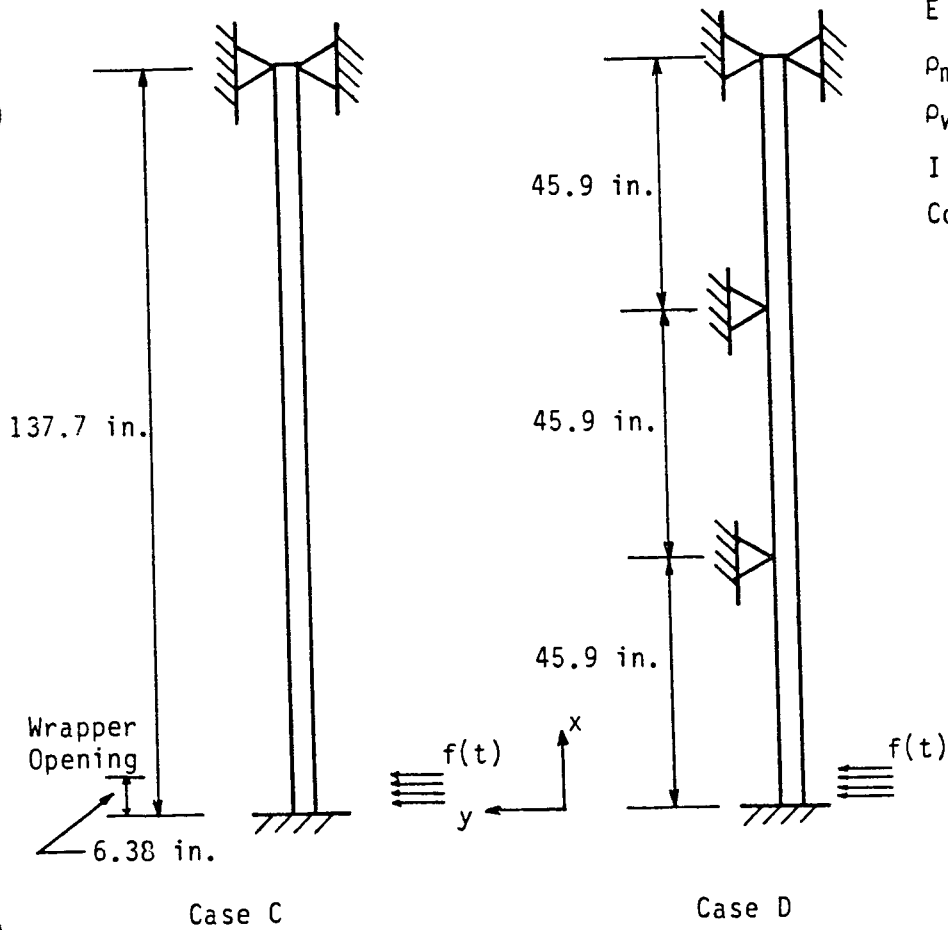
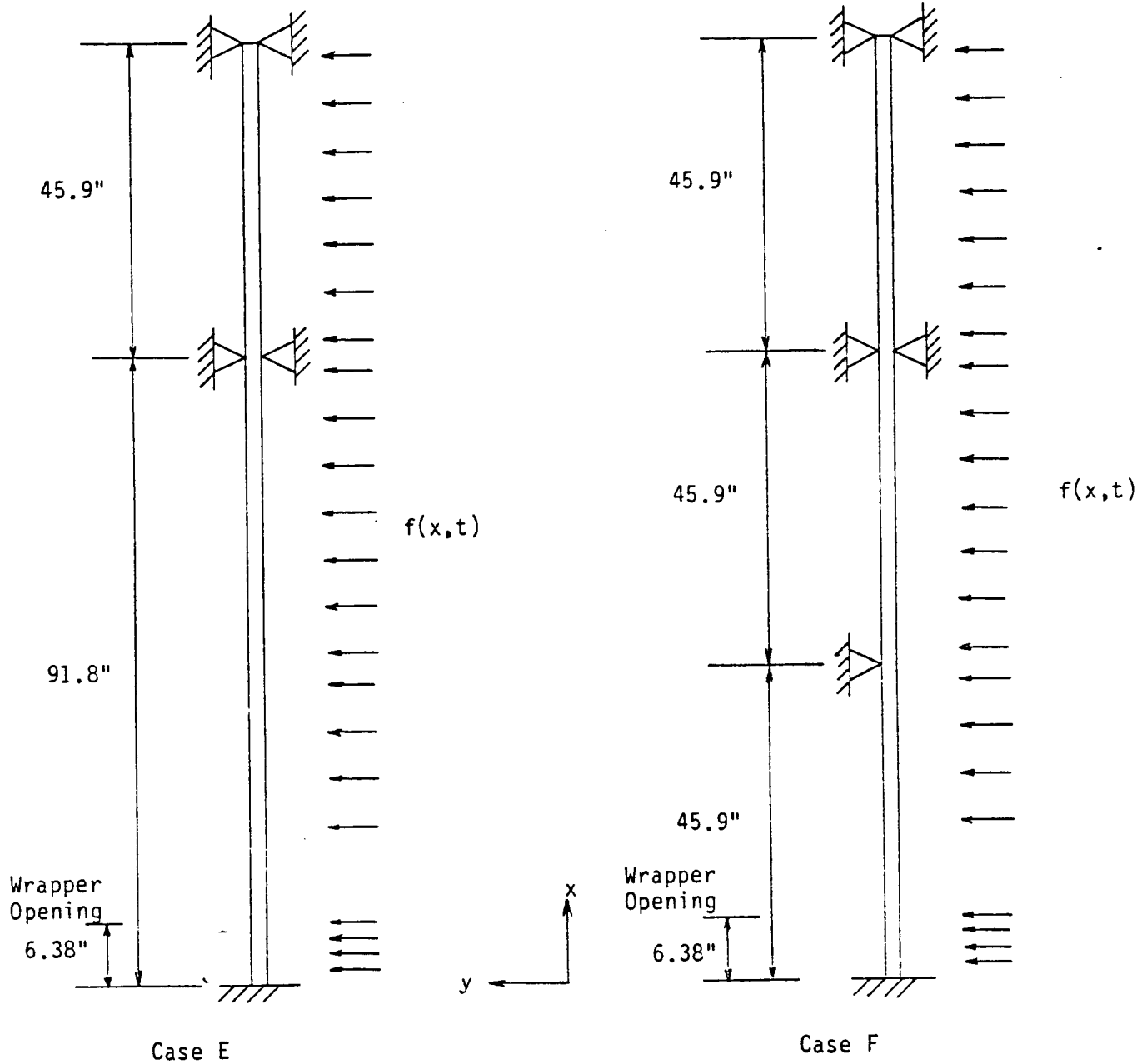


Figure 1

Tube Support Conditions



Parameters:

Beam is tube filled with water

OD = .75 in., ID = .64 in.

$E = 29.2 \times 10^6$  lb/in<sup>2</sup>

$\rho_{\text{metal}} = .28$  lb/in<sup>3</sup>

$\rho_{\text{water}} = 3.61 \times 10^{-2}$  lb/in<sup>3</sup>

$I = 7.3 \times 10^{-3}$  in<sup>4</sup> [8]

Combined Tube Weight =  $4.52 \times 10^{-2}$  lb/in.

Figure 1 (Continued)

Tube Support Conditions

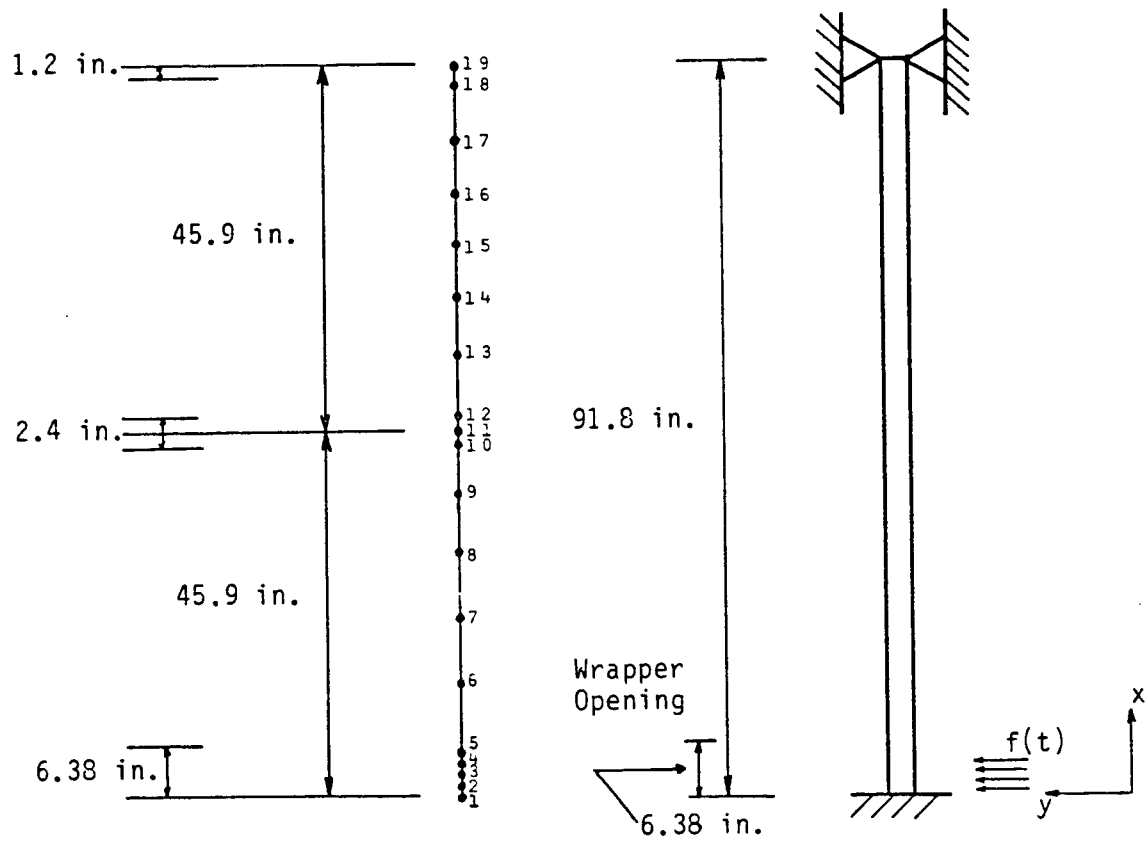


Figure 2  
 Nodal Point Locations for Case A

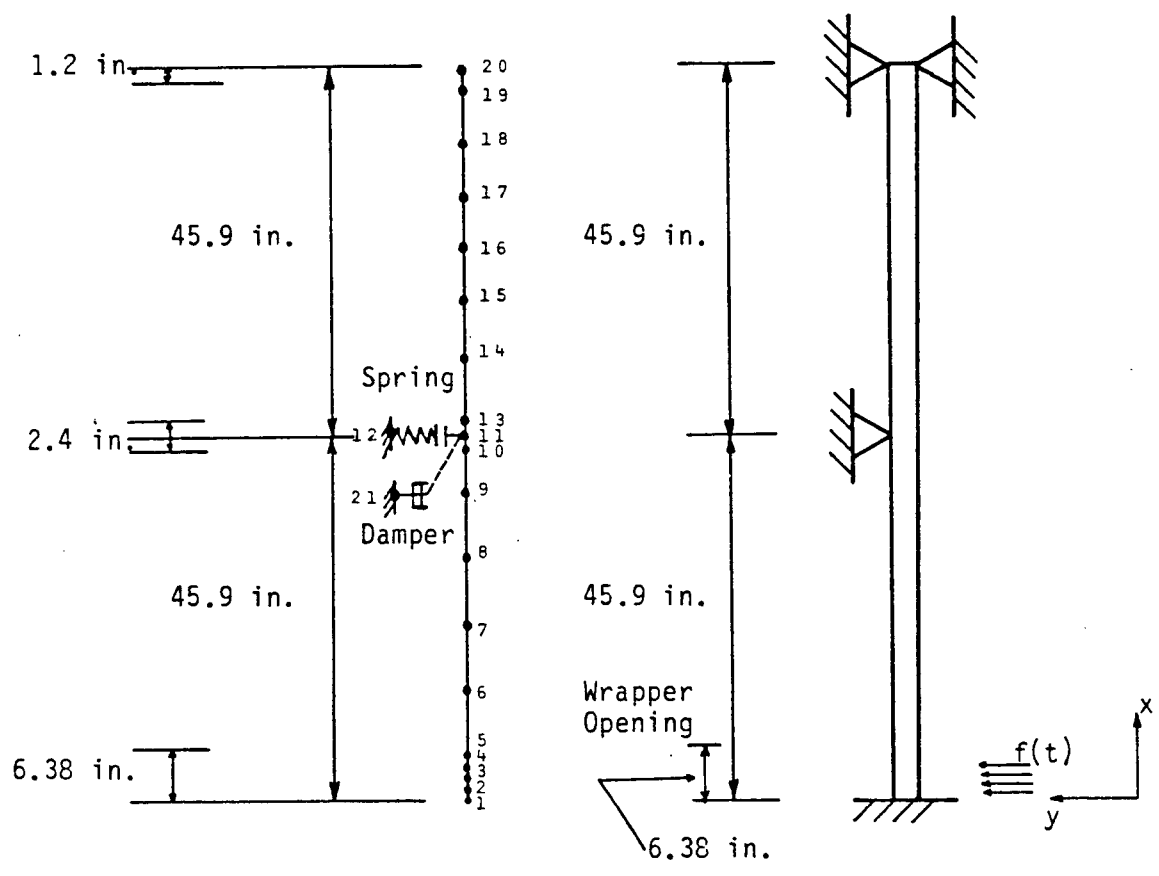


Figure 3  
 Nodal Point Locations for Case B

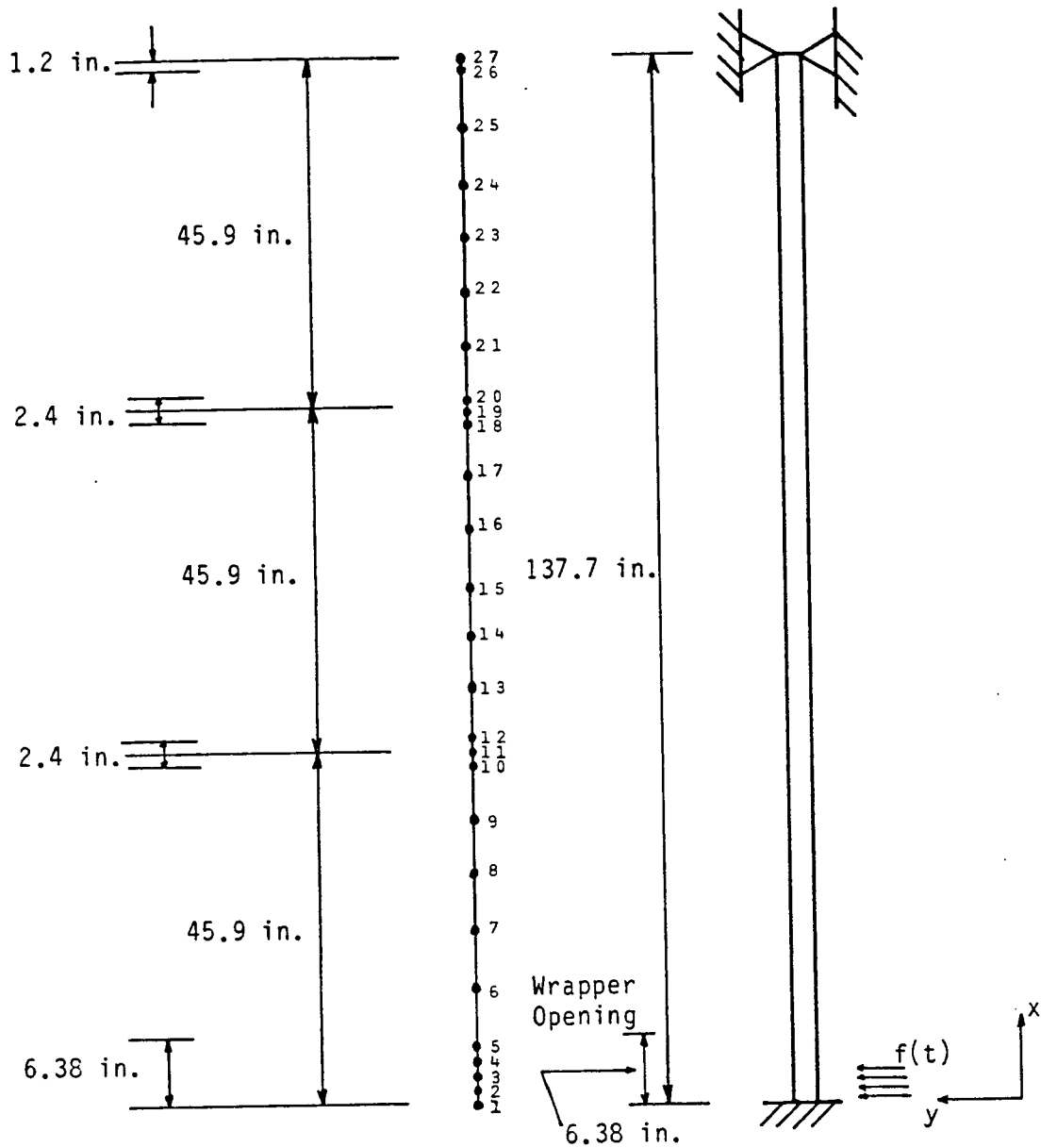


Figure 4  
 Nodal Point Locations for Case C

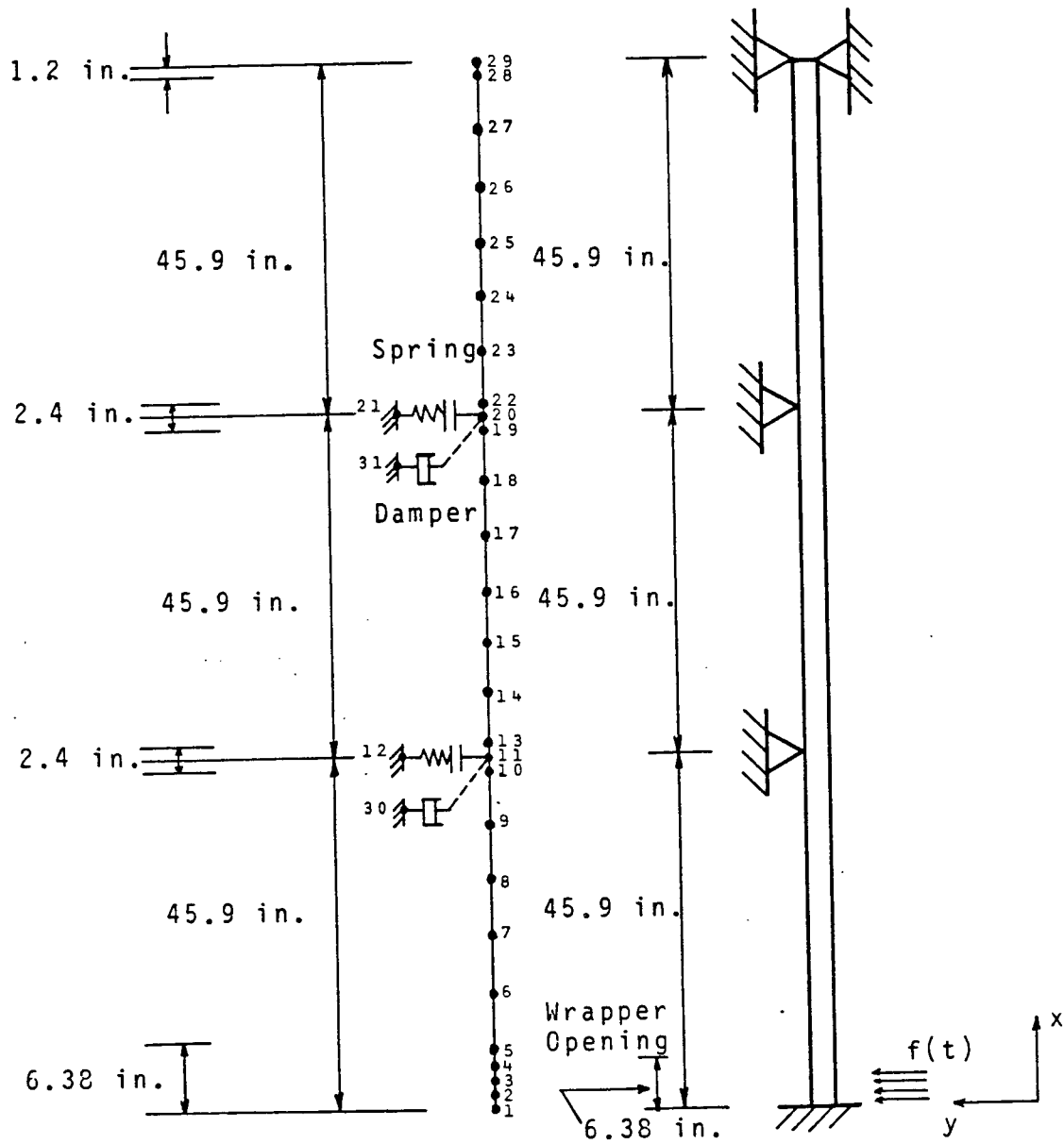


Figure 5  
 Nodal Point Locations for Case D

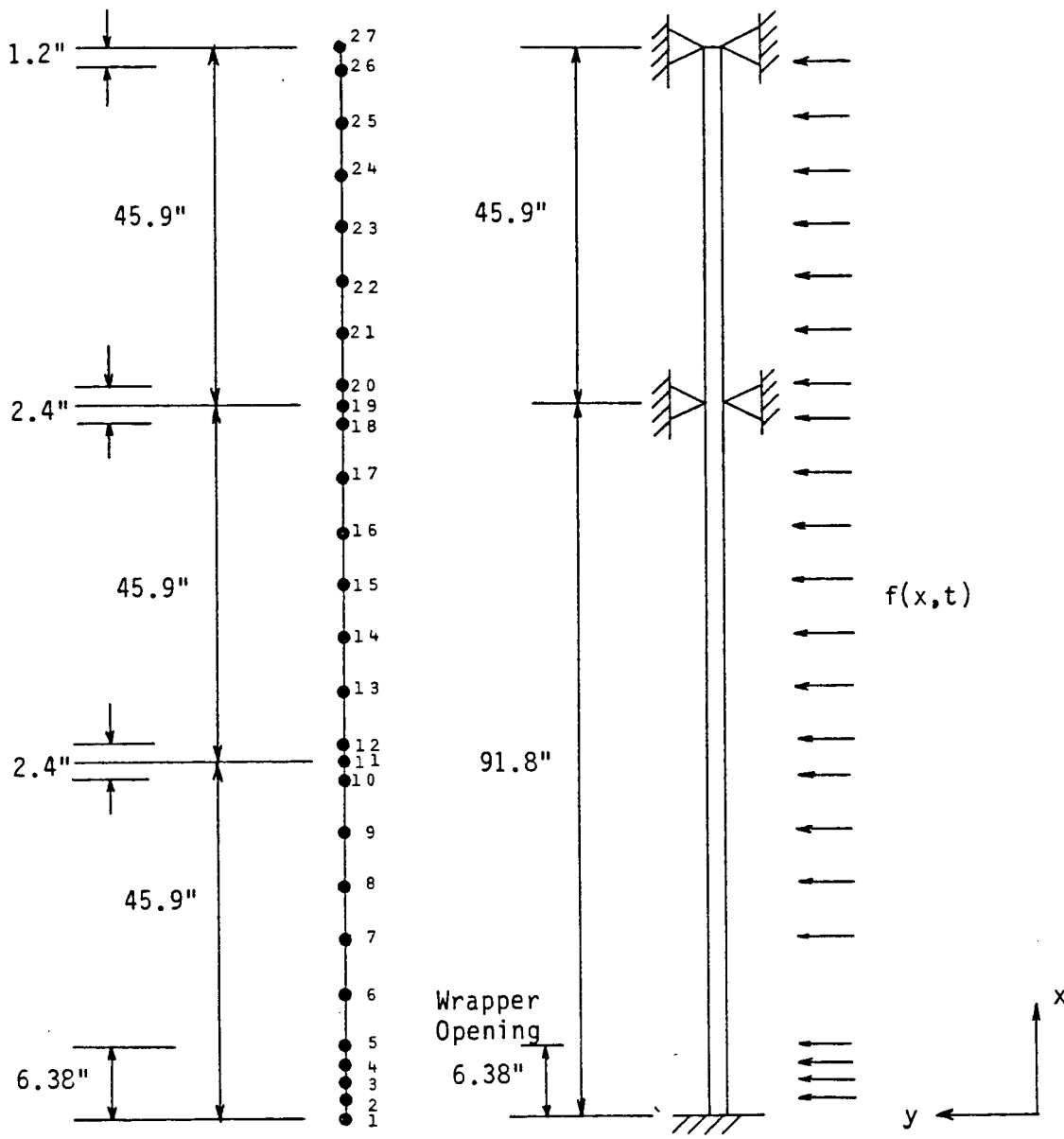


Figure 6  
 Nodal Point Locations for Case E

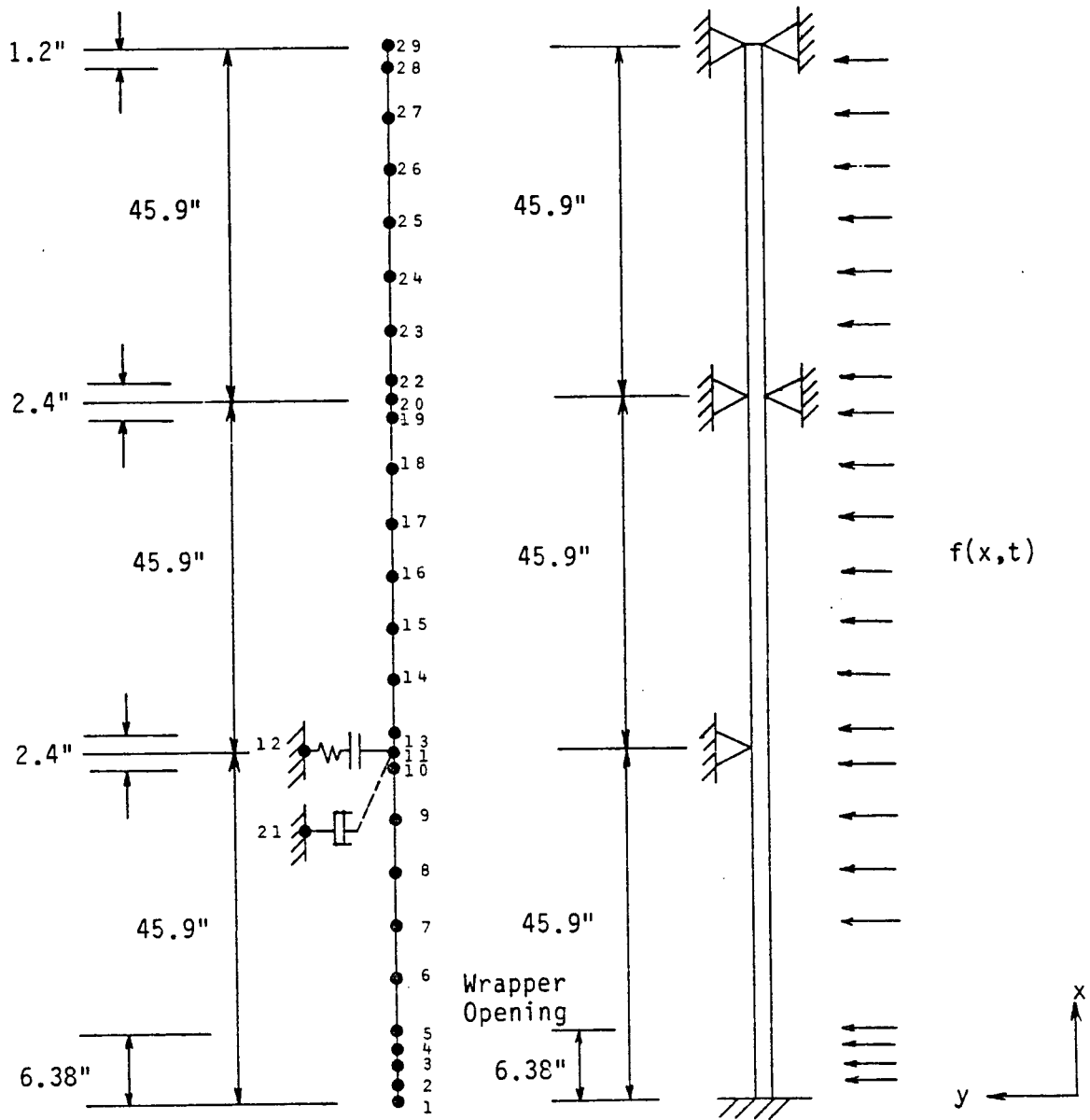


Figure 7

Nodal Point Locations for Case F



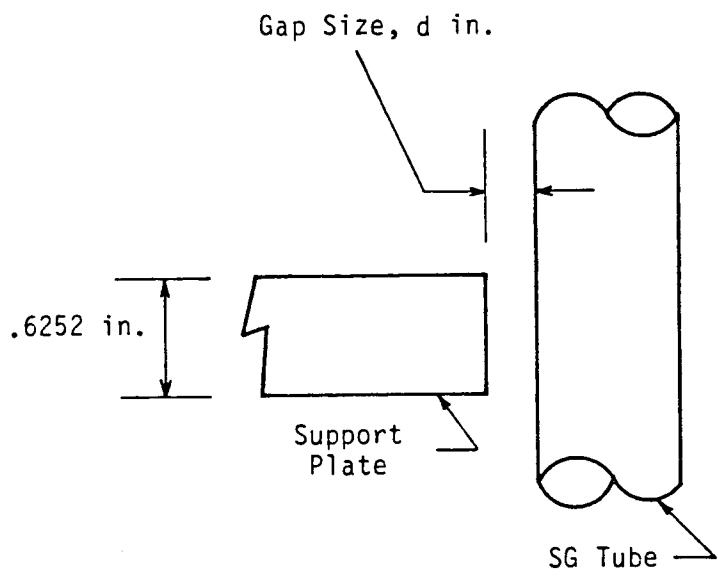


Figure 8  
One-Way Support

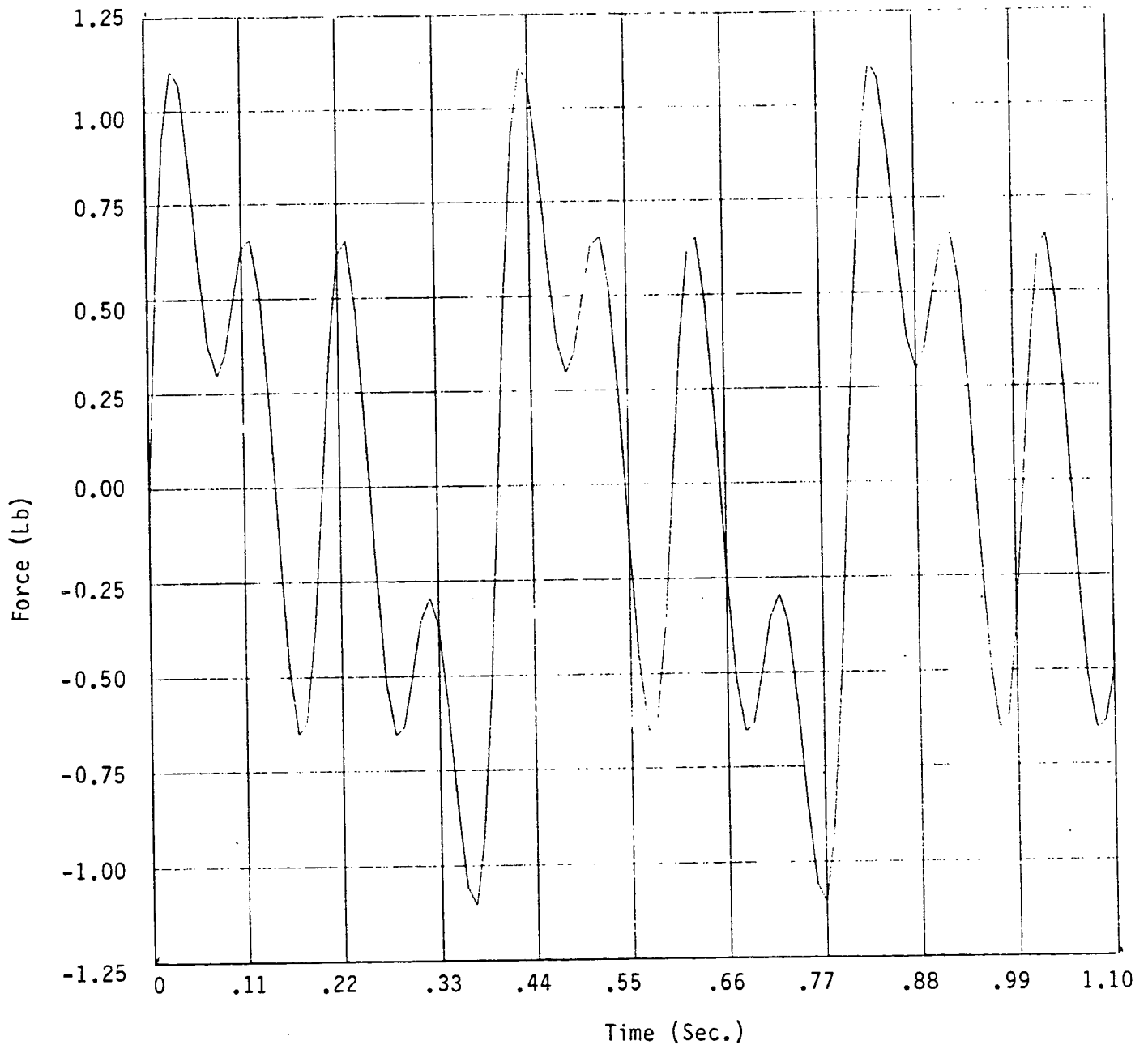


Figure 9  
Simulated Normal Load  $F(t)$

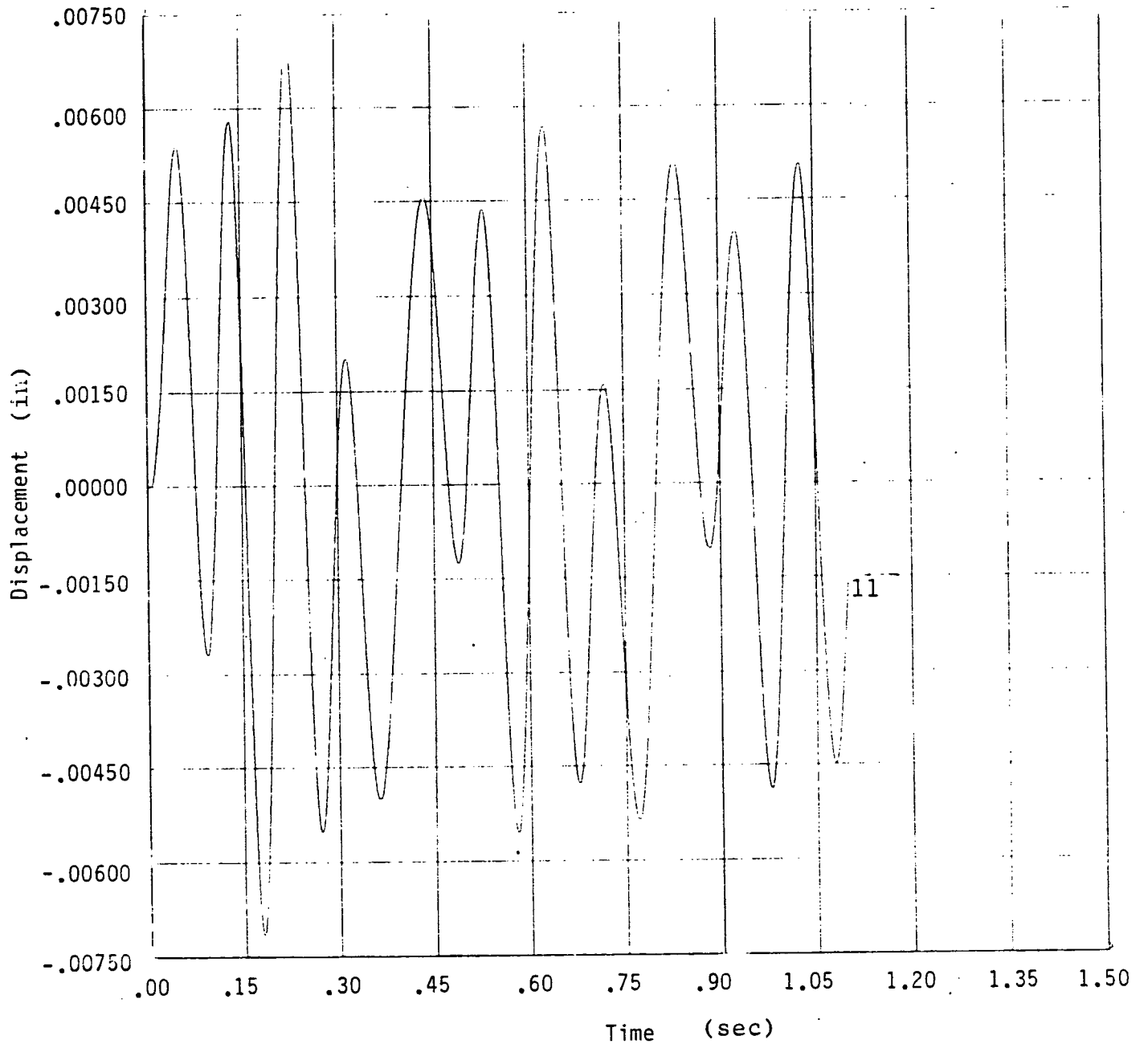


Figure 10  
 Dynamic Response of Node 11 for Case A  
 During Normal Operation

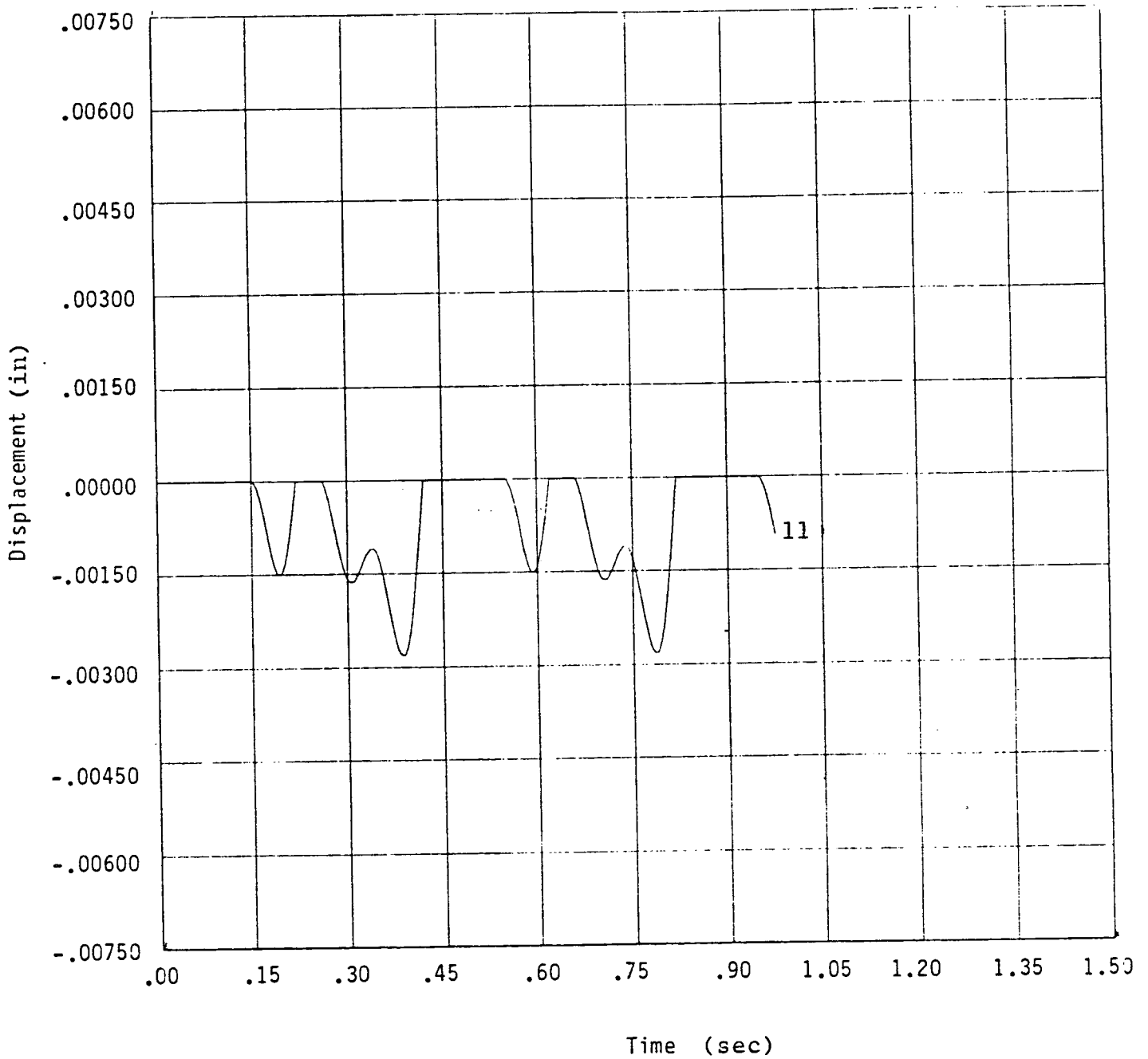


Figure 11  
 Dynamic Response of Node 11 (at first TSP) for Case B  
 With No Lateral Load During Normal Operation

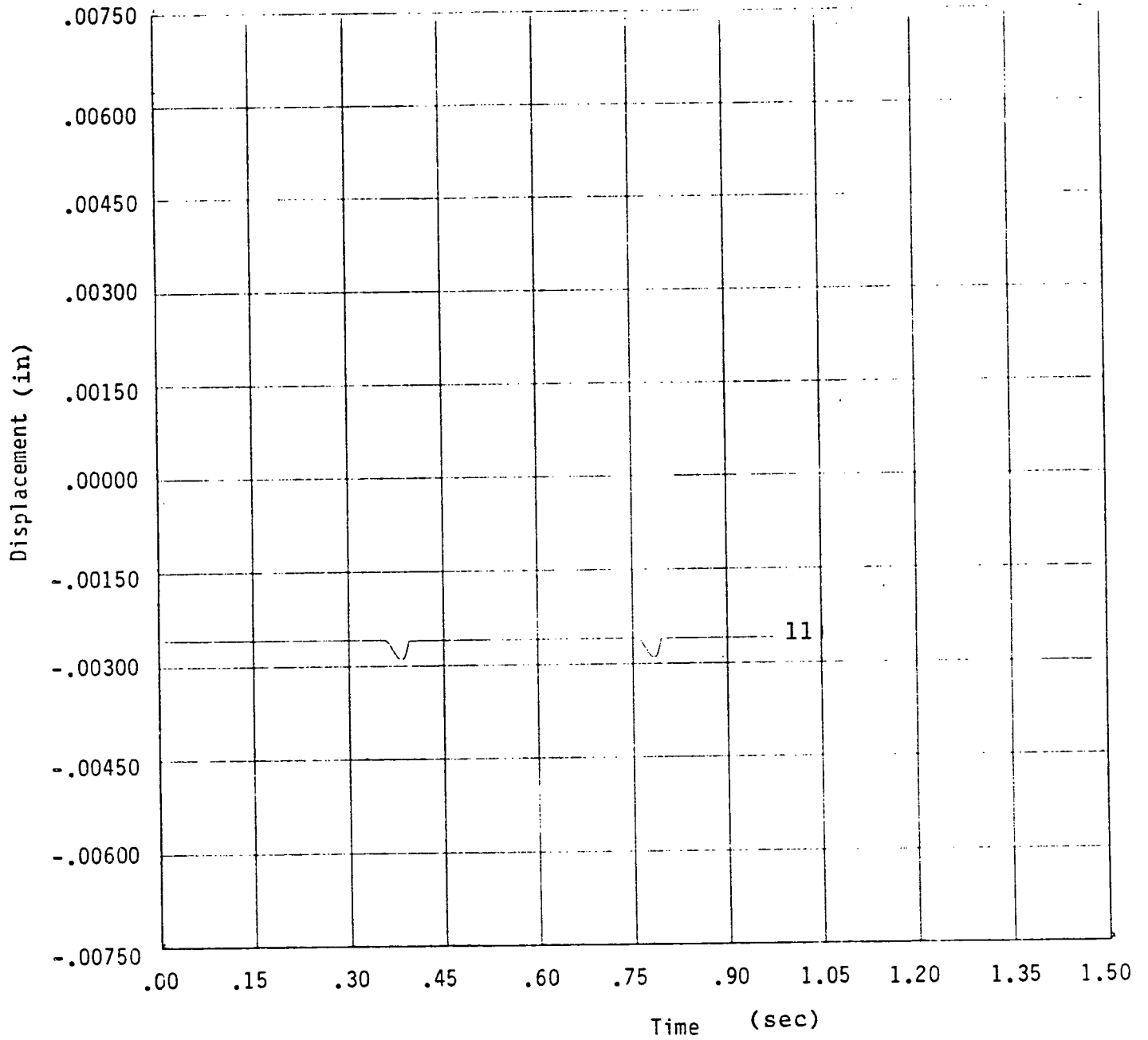


Figure 12

Dynamic Response of Node 11 (at first TSP) for Case B  
with Lateral Load During Normal Operation

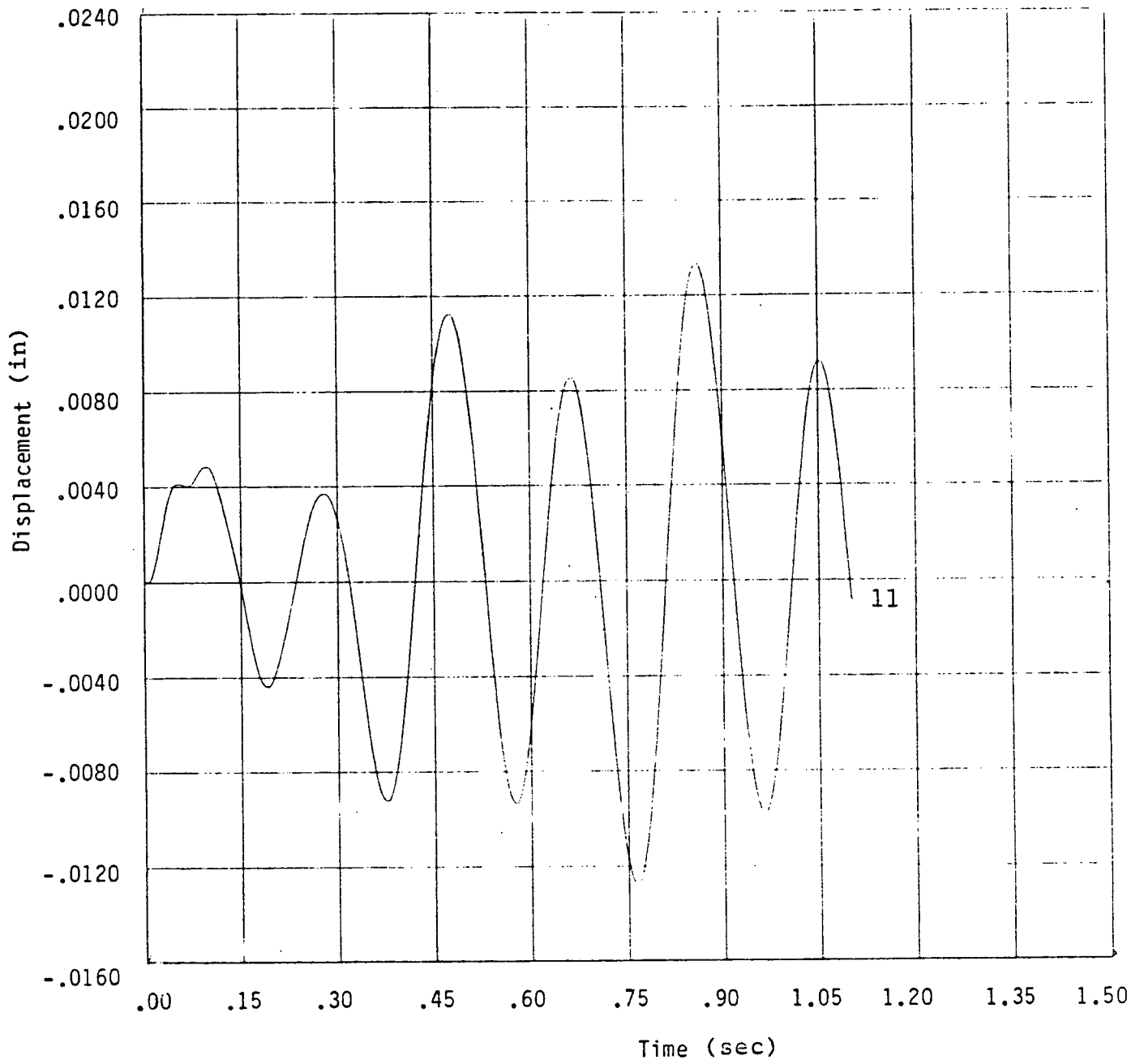


Figure 13  
 Dynamic Response of Node 11 for Case C  
 During Normal Operation

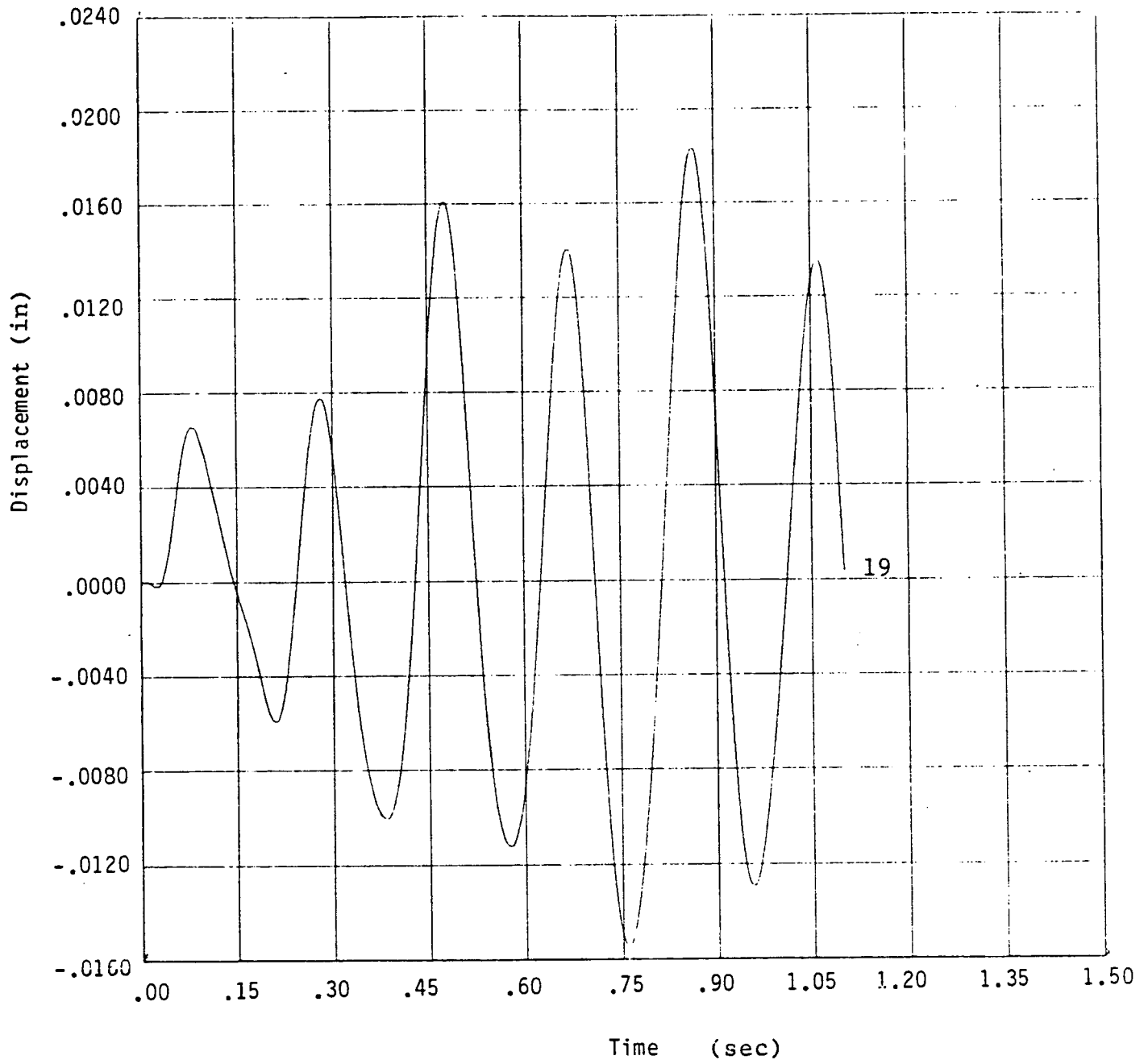


Figure 14  
 Dynamic Response of Node 19 for Case C  
 During Normal Operation

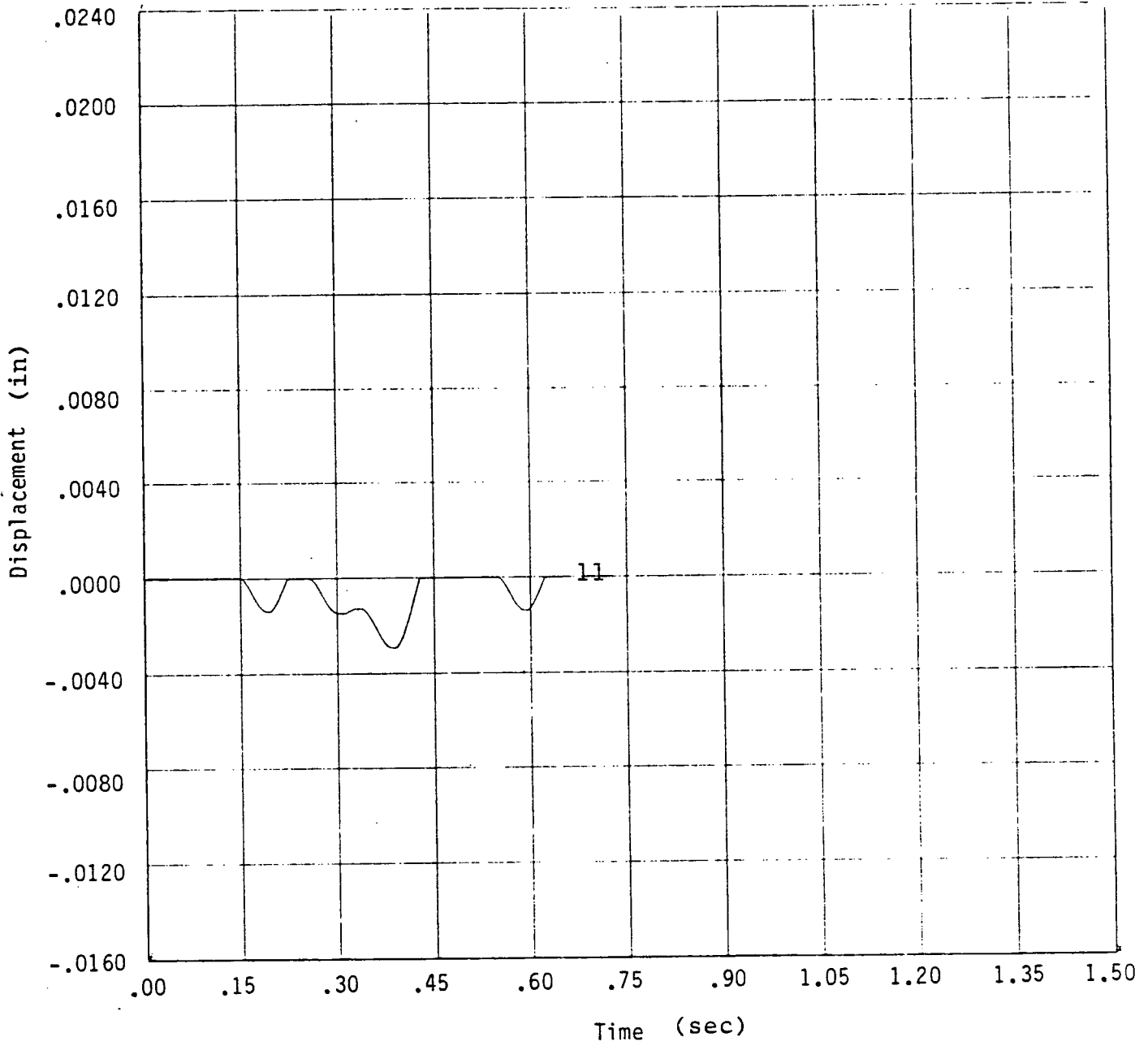


Figure 15  
 Dynamic Response of Node 11 (at first TSP)  
 for Case D with No Lateral Load during Normal Operation



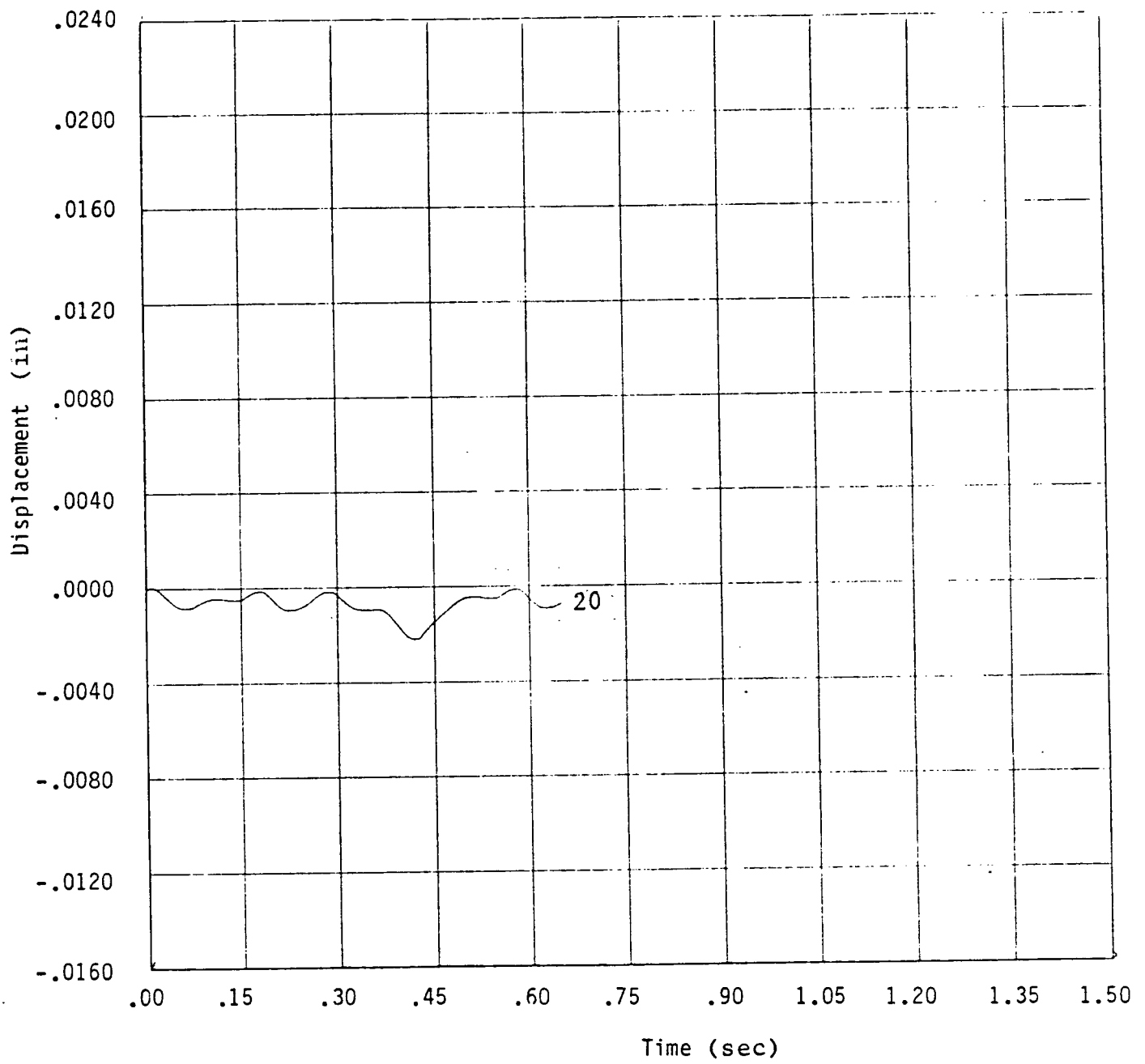


Figure 16  
 Dynamic Response of Node 20 (at second TSP) for Case D  
 with No Lateral Load During Normal Operation

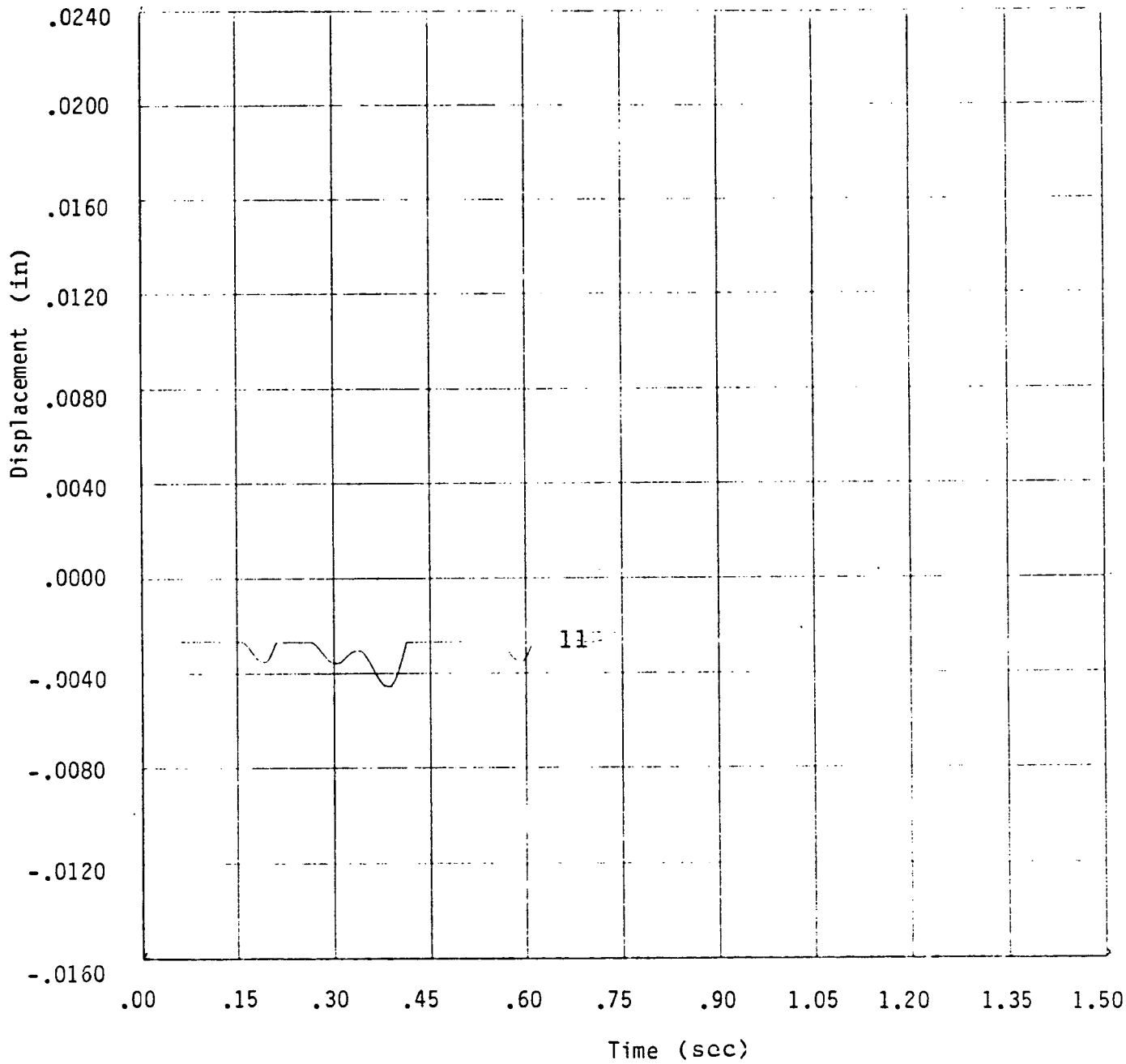


Figure 17

Dynamic Response of Node 11 (at first TSP) for Case D  
with Lateral Load During Normal Operation

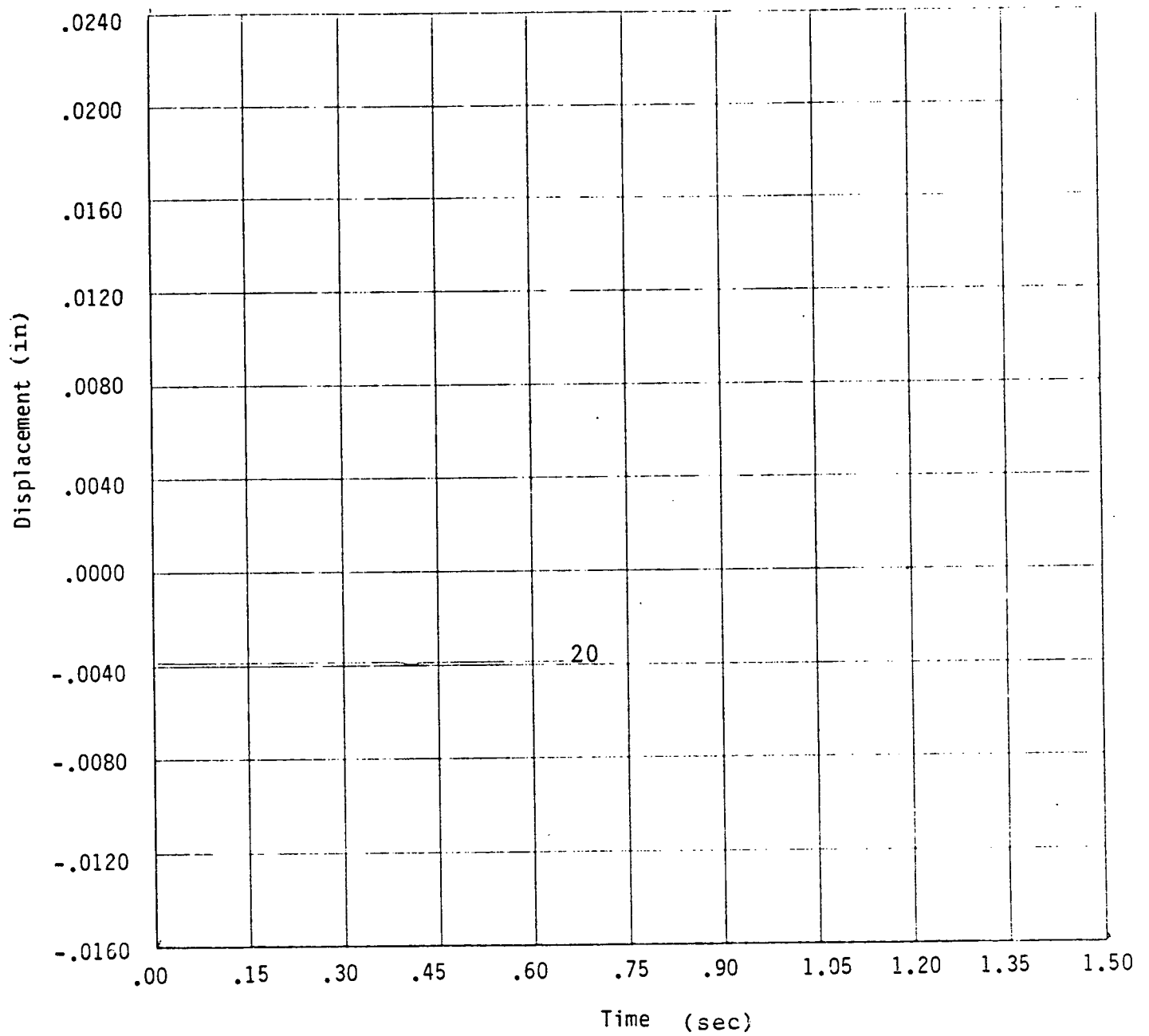


Figure 18

Dynamic Response of Node 20 (at second TSP) for Case D  
with Lateral Load During Normal Operation

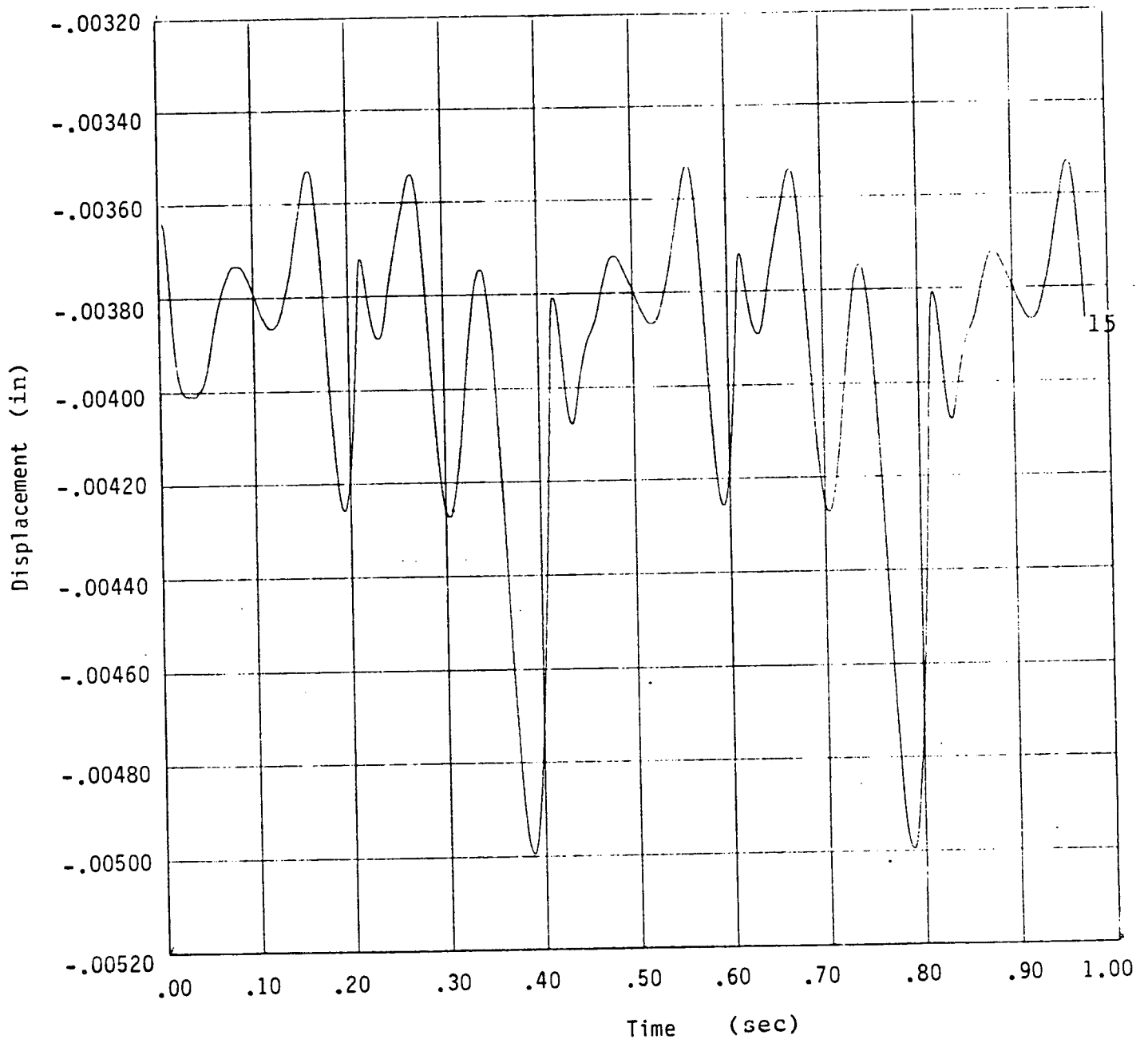


Figure 19  
 Dynamic Response of Node 15 for Case D with Lateral Load  
 During Normal Operation

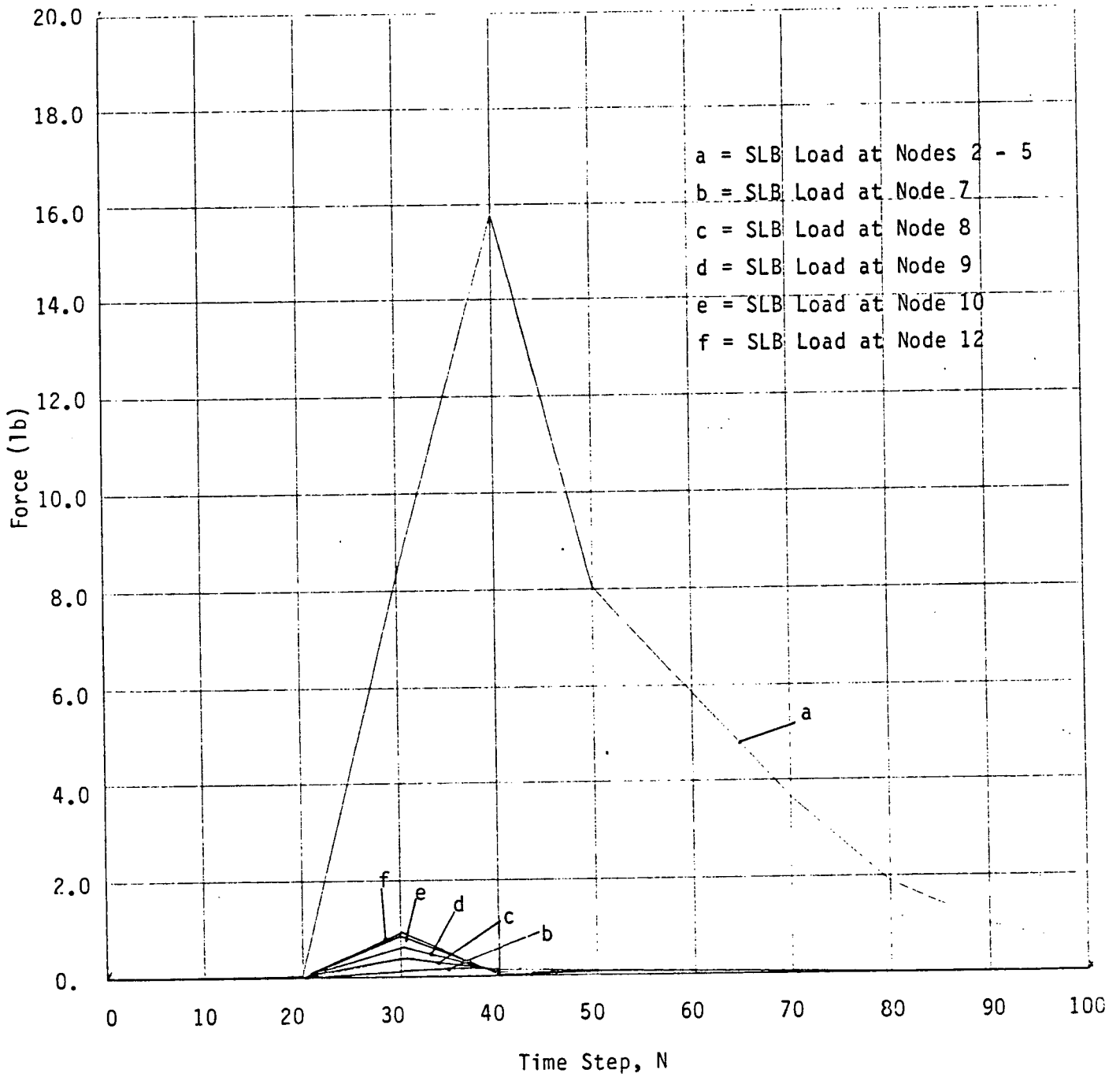


Figure 20  
 Simulated SLB Loads  $F(x,t)$  at Nodes 2-5, 7, 8, 9, 10, 12  
 for Case E

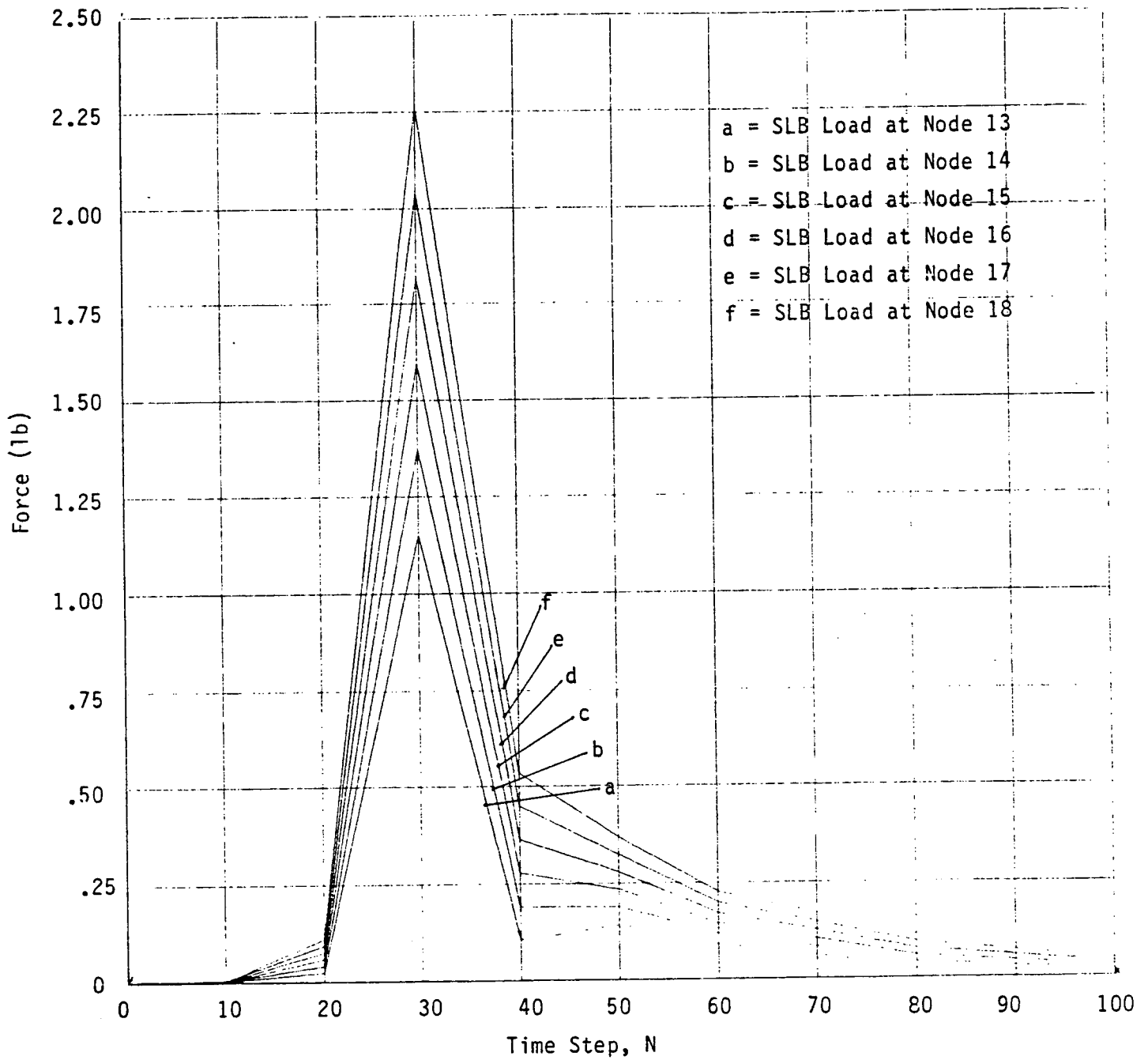


Figure 21  
 Simulated SLB Loads  $F(x,t)$  at Nodes 13, 14, 15, 16, 17, 18  
 for Case E

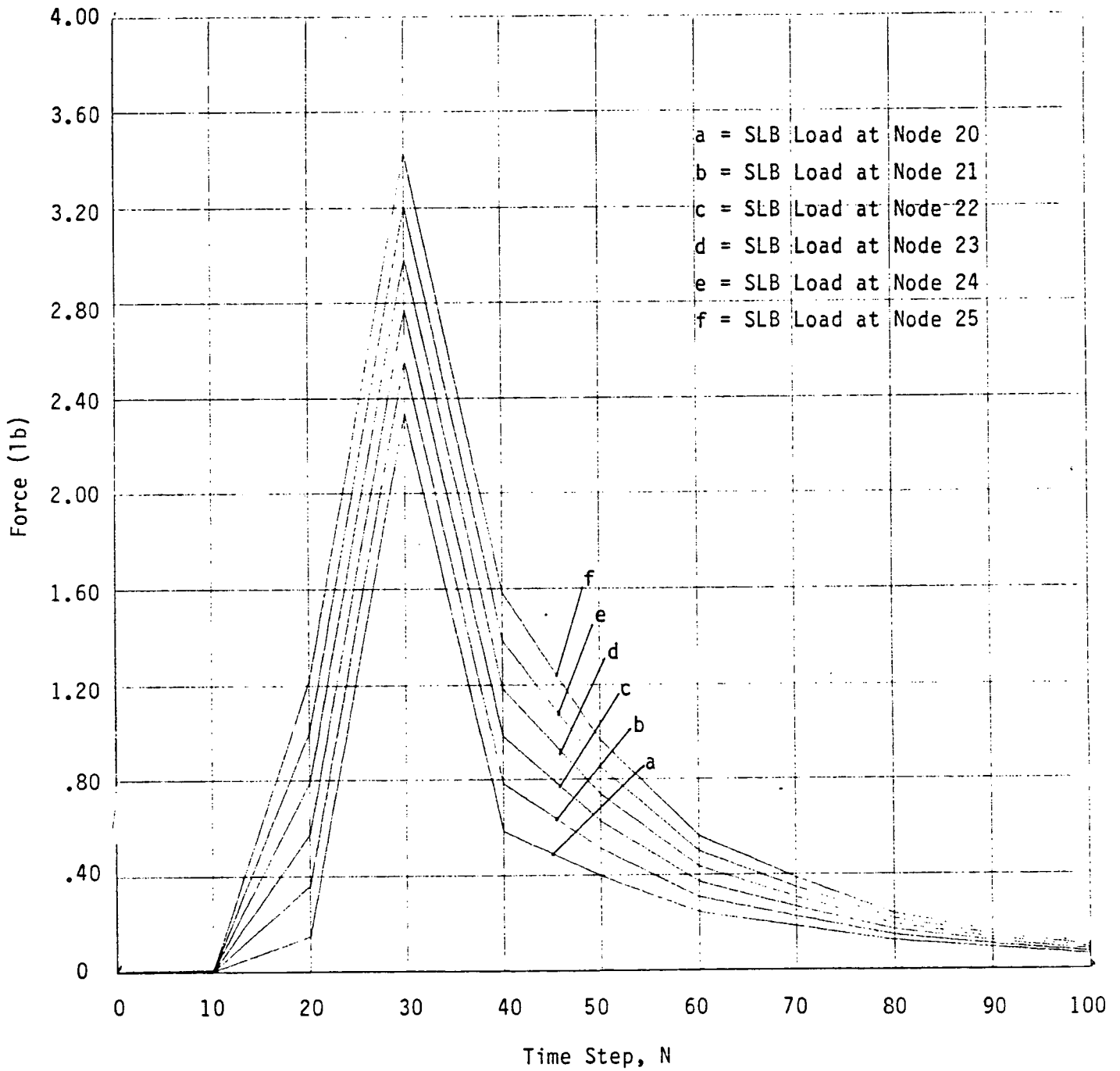


Figure 22  
 Simulated SLB Loads  $F(x,t)$  at Nodes 20, 21, 22, 23, 24, 25  
 for Case E

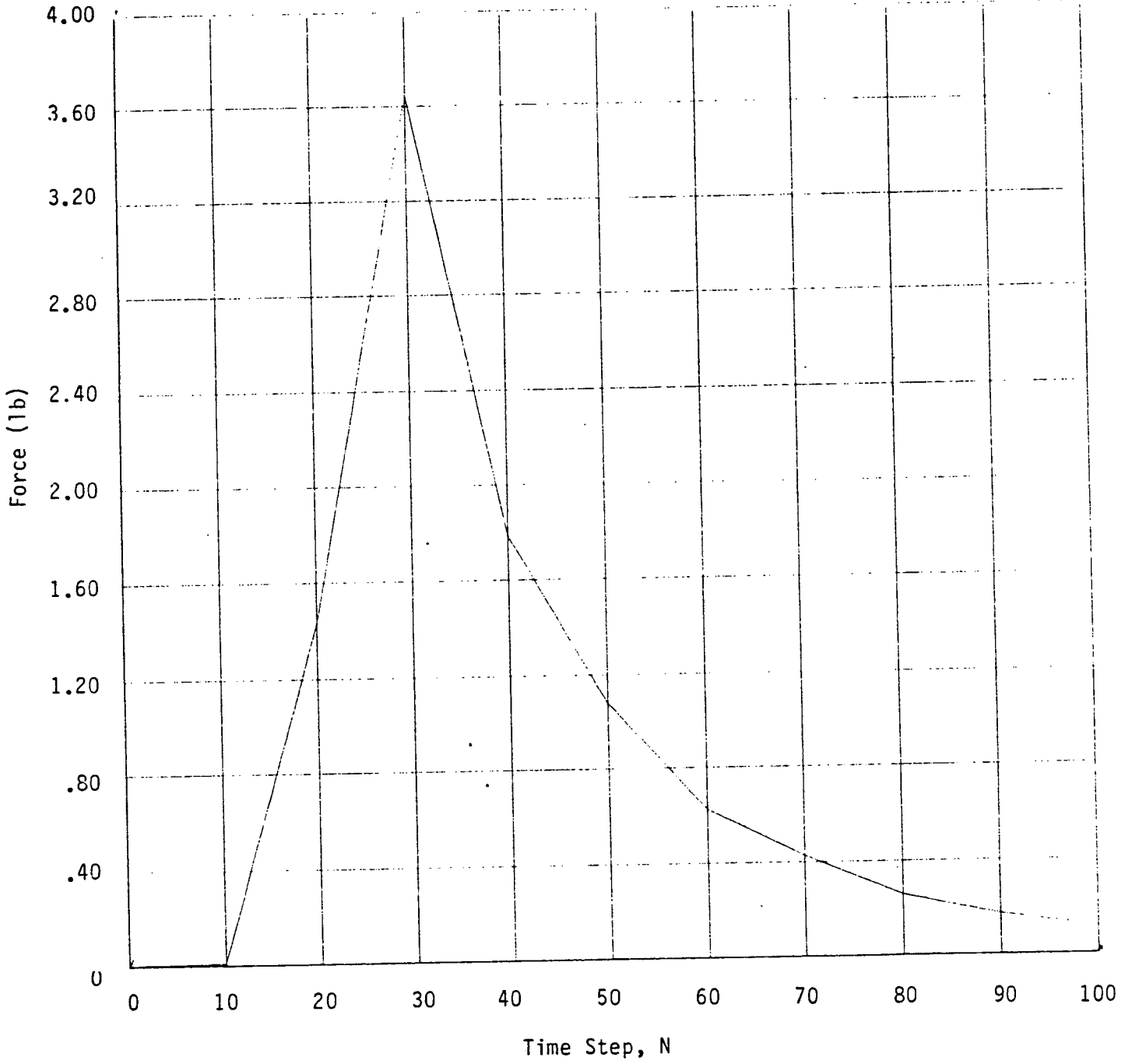


Figure 23  
 Simulated SLB Load  $F(x,t)$  at Node 26 for Case E



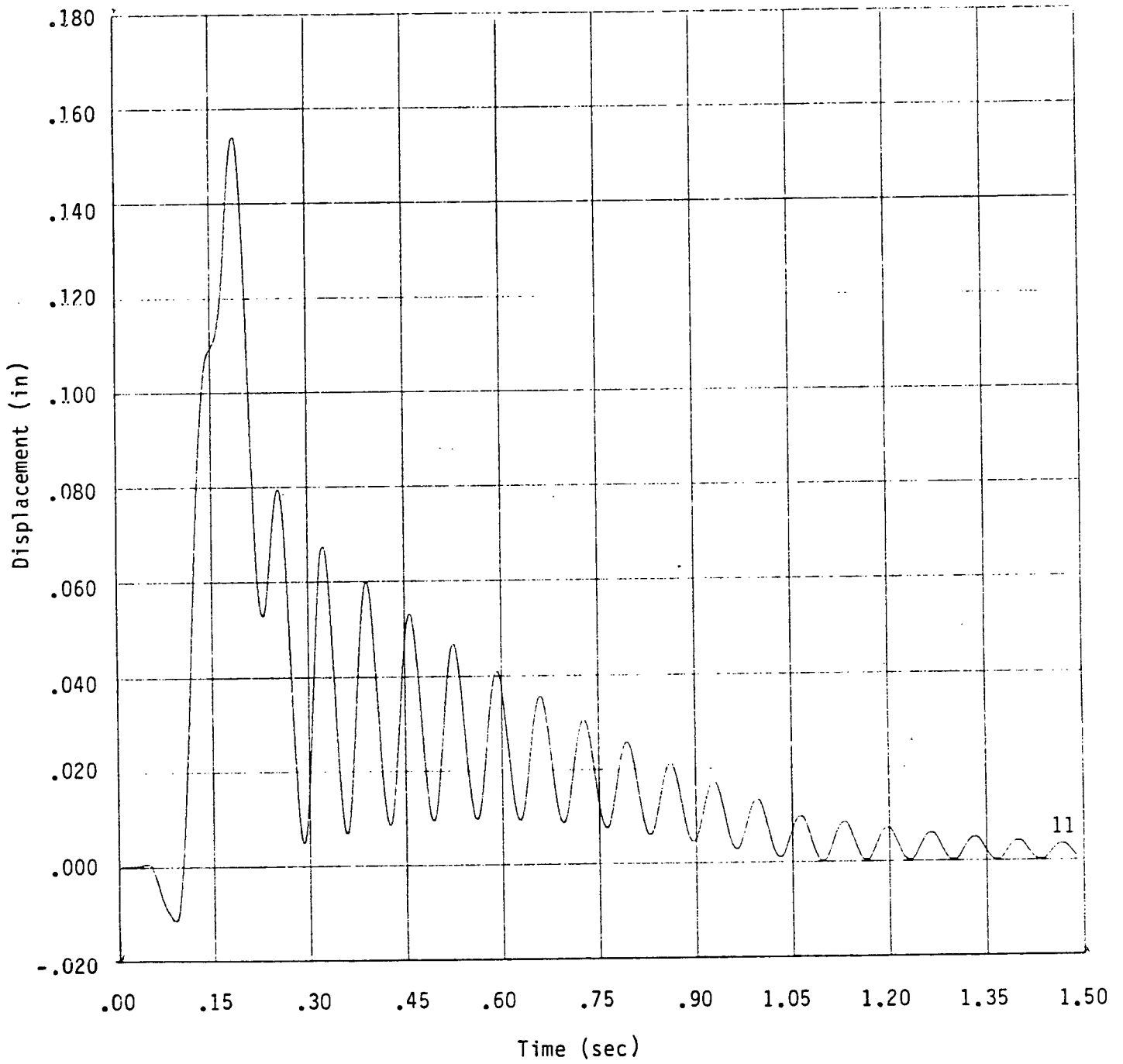


Figure 24  
 Dynamic Response of Node 11 for Case E in a SLB Accident

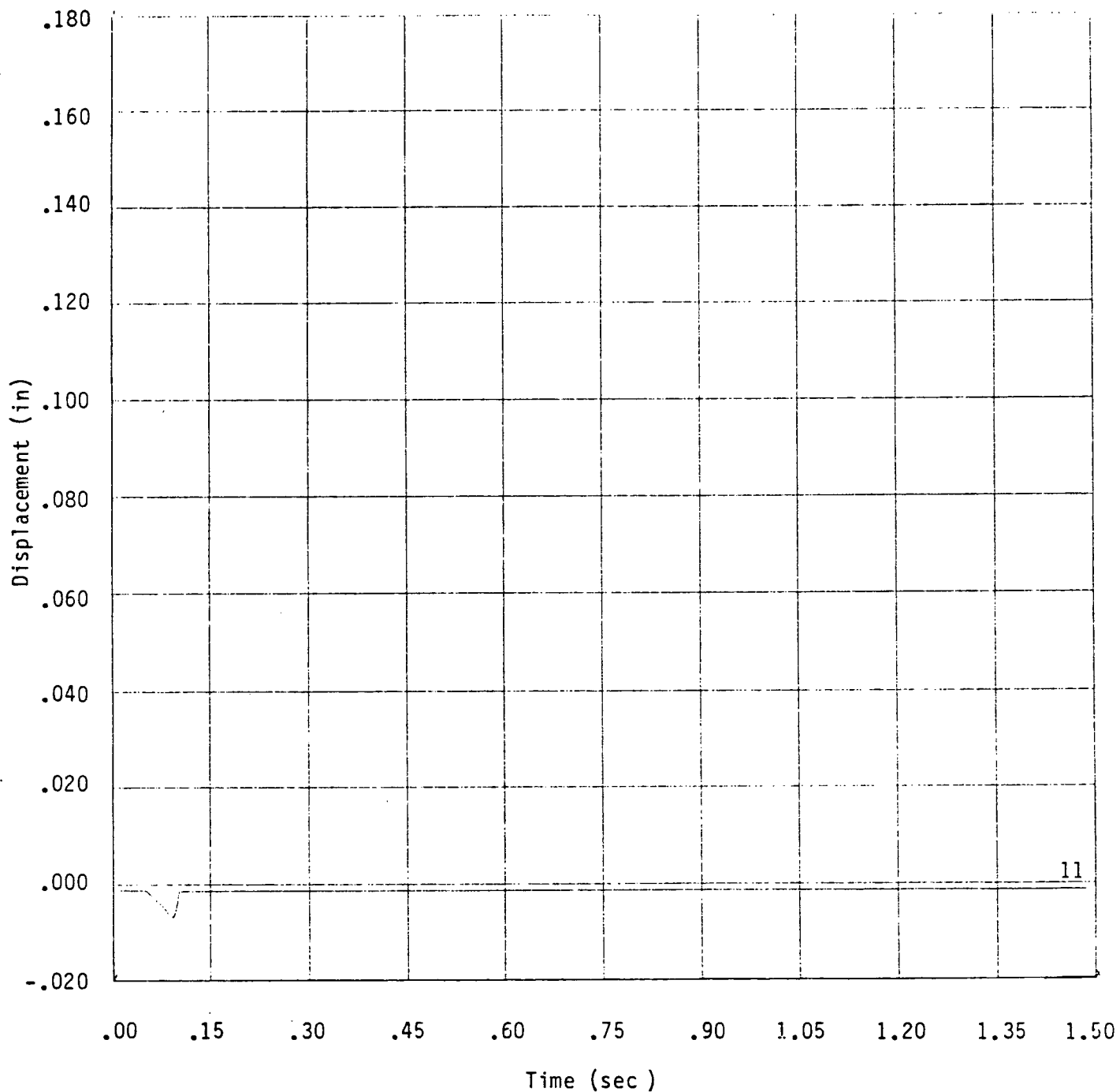


Figure 25  
 Dynamic Response of Node 11 (at first TSP) for  
 Case F with Lateral Load in a SLB Accident

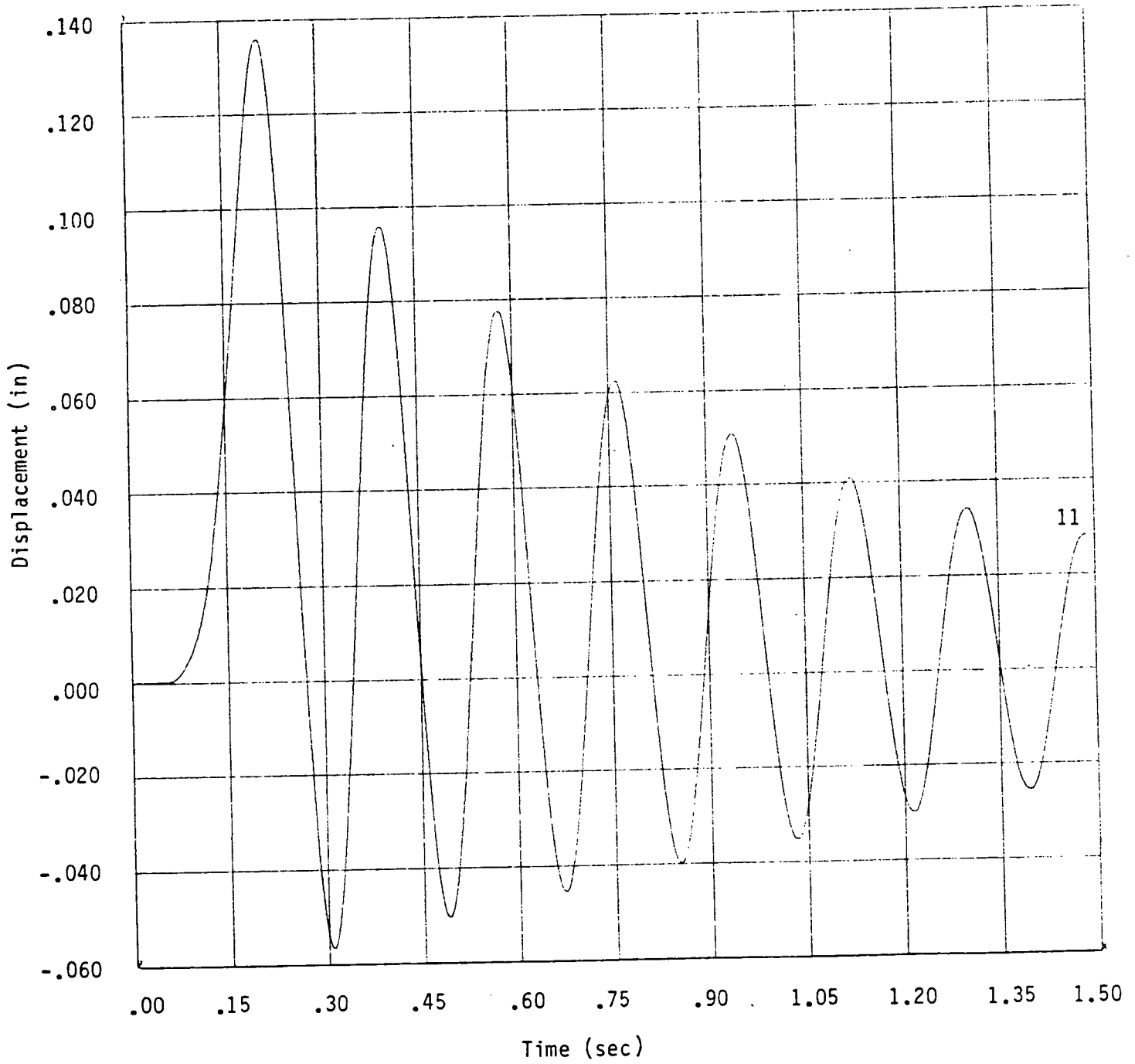


Figure 26

Dynamic Response of Node 11 for Case C in a SLB Accident

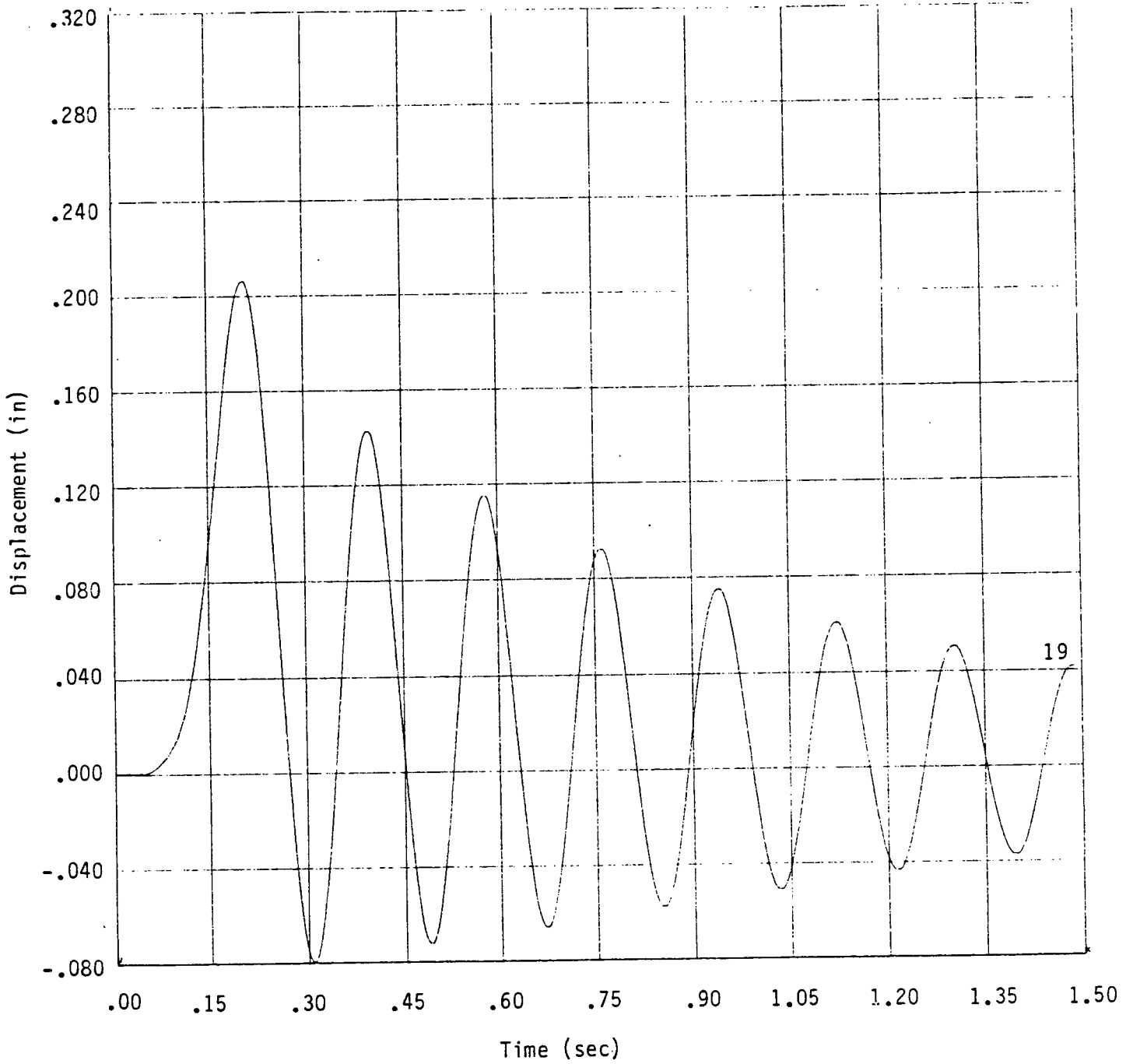


Figure 27  
 Dynamic Response of Node 19 for Case C in a SLB Accident

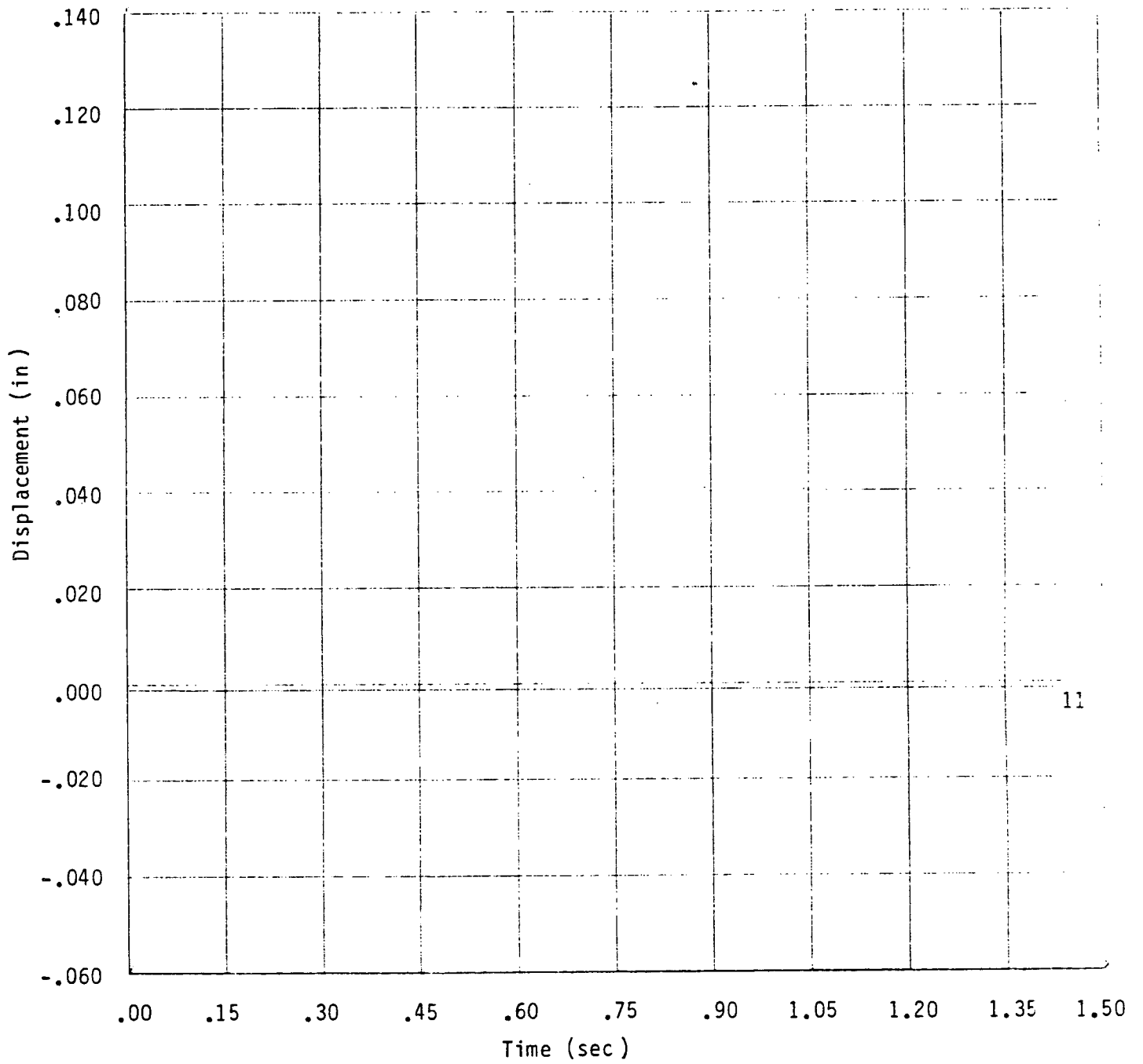


Figure 28  
 Dynamic Response of Node 11 (at first TSP) for Case D  
 with Lateral Load in a SLB Accident

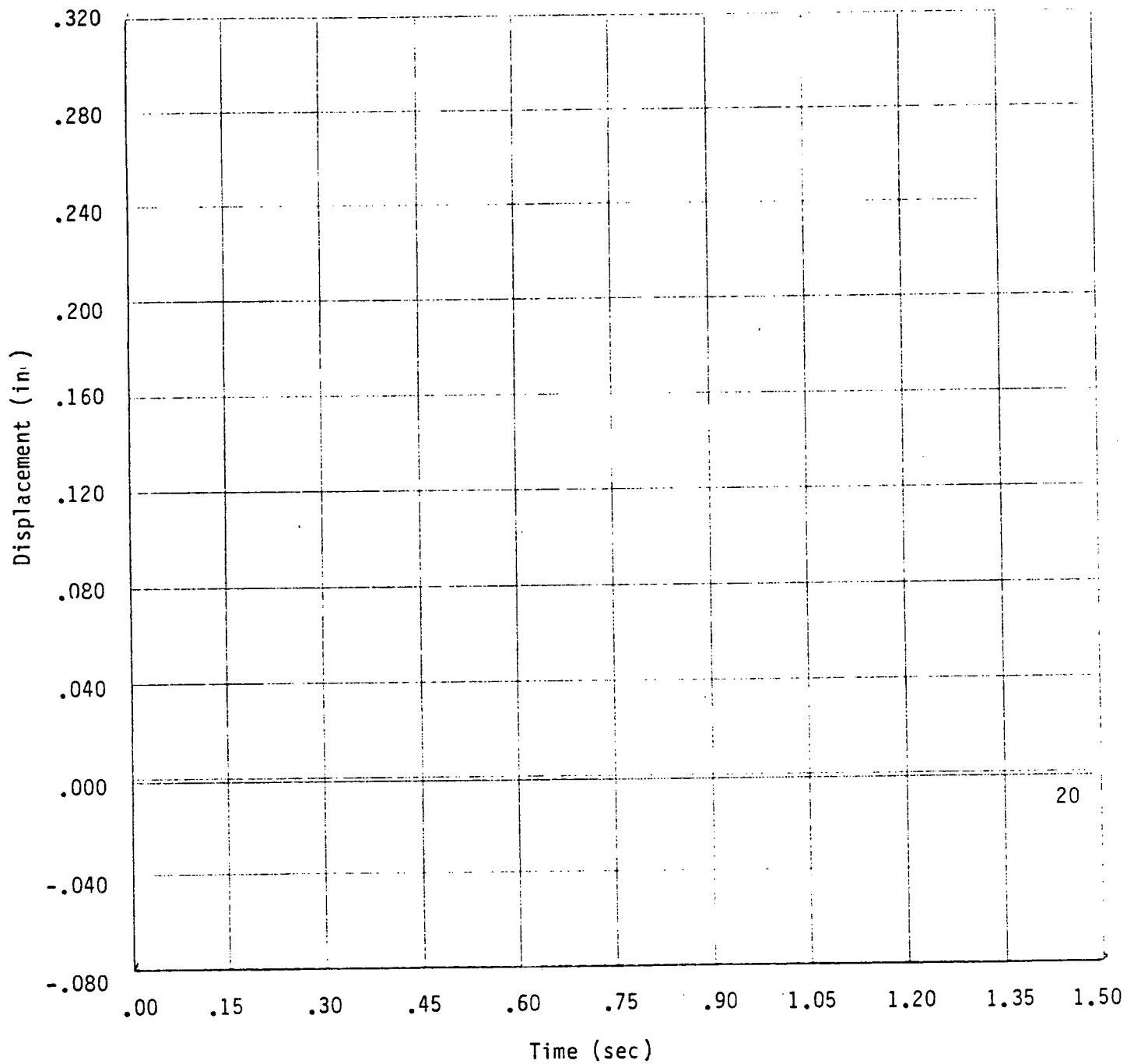


Figure 29  
 Dynamic Response of Node 20 (at second TSP) for Case D  
 with Lateral Load in a SLB Accident

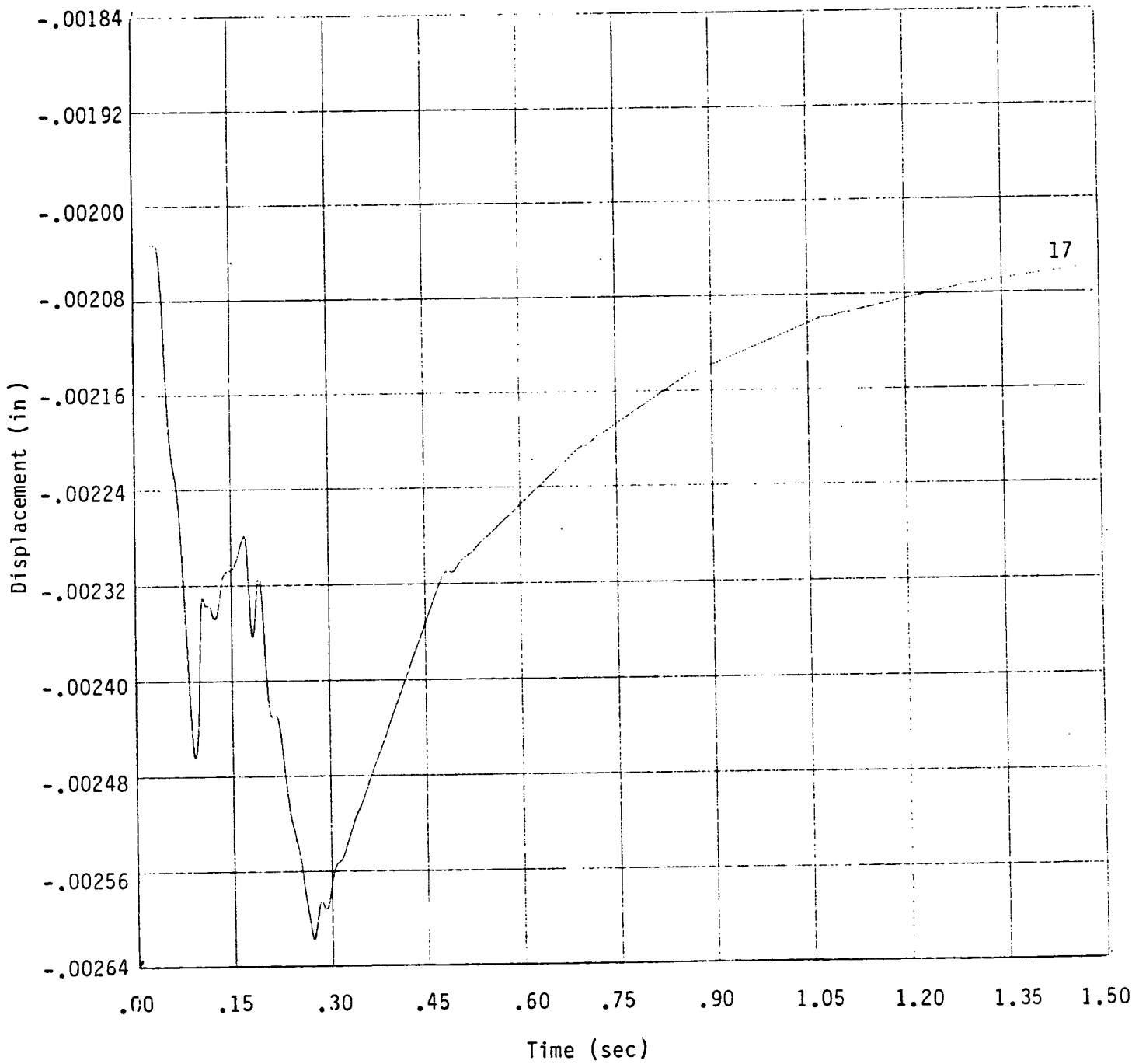


Figure 30  
 Dynamic Response of Node 17 for Case D  
 with Lateral Load in a SLB Accident

APPENDIX A

MODAL ANALYSES OF SG TUBES



- a) For Case C, the complete set of natural frequencies corresponding to the 25 specified master degrees of freedom are as follows:

Natural Frequency Solution

<u>Mode</u>	<u>Frequency (cycles/sec)</u>
1	5.524374
2	17.90185
3	37.34966
4	63.87145
5	97.47959
6	138.2036
7	186.1123
8	241.3499
9	304.1023
10	374.8354
11	454.2819
12	543.1718
13	642.4467
14	753.0001
15	882.3129
16	999.6721
17	1093.769
18	1530.959
19	1610.940
20	1723.903
21	2447.432
22	4569.556
23	4747.049
24	6781.431
25	15755.59

b) For Case E, the complete set of natural frequencies corresponding to the 24 specified master degrees of freedom are as follows:

Natural Frequency Solutions

<u>Mode</u>	<u>Frequency (cycles/sec)</u>
1	14.88889
2	36.26899
3	49.71783
4	90.10558
5	136.1008
6	161.2601
7	229.5932
8	300.8732
9	338.4097
10	437.6427
11	538.0695
12	590.9967
13	729.8453
14	873.9440
15	942.6322
16	1064.577
17	1530.816
18	1603.457
19	1722.881
20	2447.409
21	2793.258
22	4581.285
23	6781.430
24	15755.59

APPENDIX B  
CONVERGENCE CRITERIA

For Cases A, C, E and C (SLB) ITS = .0001 sec.

For Cases B, D, F and D (SLB) ITS = .000025 sec.

For Case D with lateral load, several values of ITS were used and the results are summarized in the following.

(1) ITS = .00005 sec.

Maximum negative displacements of node 11 and 20 within the time interval of interest are:

$$Y_{11} = -.46287 \text{ E-02 in.}$$

$$Y_{20} = -.40409 \text{ E-02 in.}$$

(2) ITS = .000025 sec.

Maximum negative displacements of nodes 11 and 20 within the time interval of interest are:

$$Y_{11} = -.46244 \text{ E-02 in.}$$

$$Y_{20} = -.40367 \text{ E-02 in.}$$

The two sets of maximum negative displacements [(1) and (2)] differ from each other by about  $4 \times 10^{-6}$  in. and therefore convergence of solutions is established at ITS .000025 sec.

The ITS for cases other than D were also verified for accuracy of solutions.

APPENDIX C

Responses to NRC Requests  
For Additional Information

## APPENDIX C

### Table of Contents

---	Introduction
	Agenda from May 12, 1982 SCE/NRC Meeting
C.1	Review of Reference Joint Design
C.2	Review of Dissolution Phenomenon
C.3.1	Flow Induced Vibration Analysis
C.3.2	Steam Line Break Analysis
C.3.3	Revision to Sleeving Repair Report
C.4	NDE Capabilities of Reference Joint / Safety Assessment

## INTRODUCTION

The viewgraphs displayed and discussed at the SCE/NRC Steam Generator Review Meeting in Bethesda, Maryland, on May 12, 1982, are presented in this submittal with accompanying explanatory text.

Proprietary information has been designated by brackets.

The NRC requested additional information at the meeting. The information requested and its location within this report are as follows:

- Appendix C.3.3, Volume I - Conclusions Pertinent to Section 6.3.10, "Flow Induced Vibration" of Steam Generator Repair Report, San Onofre Unit 1, SE-SP-40 (80) Rev. 1, March 1981.
- Appendix E, Part II, Volume II - Sketch of Wrapper Support Bar, San Onofre, Unit 1.
- Appendix E, Part V, Volume II - List of Peripheral and Row 1 Tubes Plugged Prior to 1982 at San Onofre Unit 1.

SCE/NRC MEETING  
STEAM GENERATOR REVIEW  
MAY 12, 1982

\*\*\*

ANNOTATION OF THE WESTINGHOUSE PRESENTATION  
TO THE NRC AND ADDITIONAL REQUESTED MATERIALS

\*\*\*



A G E N D A

SCE/NRC MEETING  
STEAM GENERATOR REVIEW

May 12, 1982

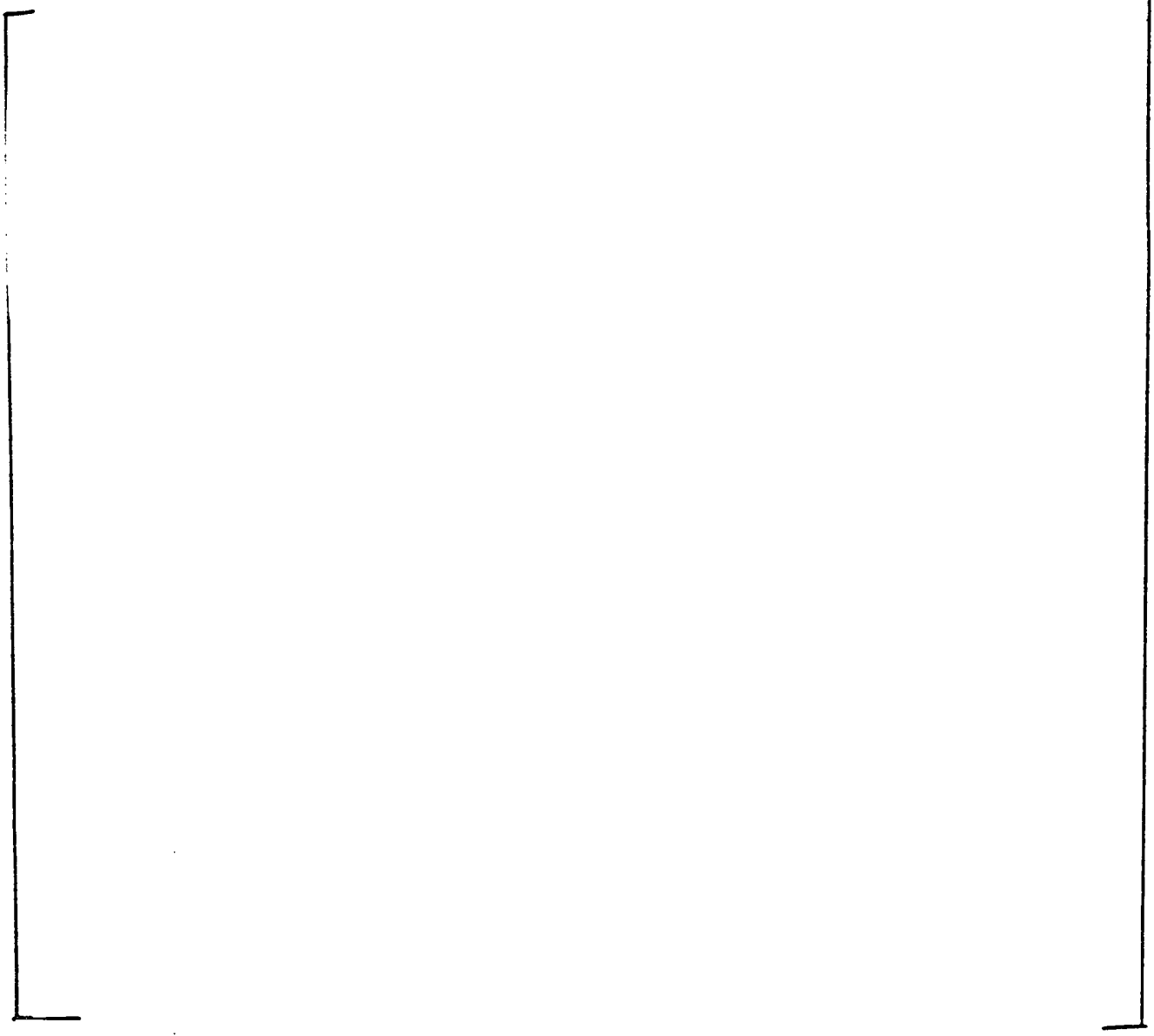
1. Review of the Reference Joint Design and Joint Fabrication Procedures
2. Review of Dissolution Phenomenon
  - 2.1 Description of the dissolution phenomenon (we would also like to see metallographic photographs of severe dissolution and actual lab specimens)
  - 2.2 Causative factors for the introduction of these defects
  - 2.3 Specific problems encountered at San Onofre
  - 2.4 Input values for relevant fabrication parameters for each of the tubes which leaked as a result of dissolution
  - 2.5 Corrective actions taken following the occurrence of problem
  - 2.6 The basis for the corrective actions
  - 2.7 Baseline eddy current and ultrasonic results for the tubes which leaked
  - 2.8 Current NDE capabilities to detect sleeve and tube wall dissolution
3. Review of Tube/Sleeve Structural Integrity Requirements
4. Review of NDE Capability of Tube and Sleeve
  - 4.1 Reference Joint  
Expansion Transitions  
Sleeve Ends

- 4.2 Magnetite Influence
- 4.3 Masking of IGA
- 4.4 Development Status
  - 4.4.1 "D" Coil
  - 4.4.2 UT
  
- 5. Review of Safety Assessment (including consideration of ECT uncertainties, tube integrity considerations, and potential for axial and lateral loadings during normal and accident conditions)
  
- \*6. Review of Results of Recently Completed Steam Generator Tube Inspections
  
- \*7. Review of Support Plate Flow Slot Deformation and Cracking
  
- \*8. Review of Foreign Material Inspection

\*Not included in this compilation.

AGENDA ITEM 1 - REVIEW OF THE REFERENCE JOINT DESIGN AND JOINT FABRICATION PROCEDURES

a,b,c



REFERENCE JOINT DESIGN

a,b,c

£

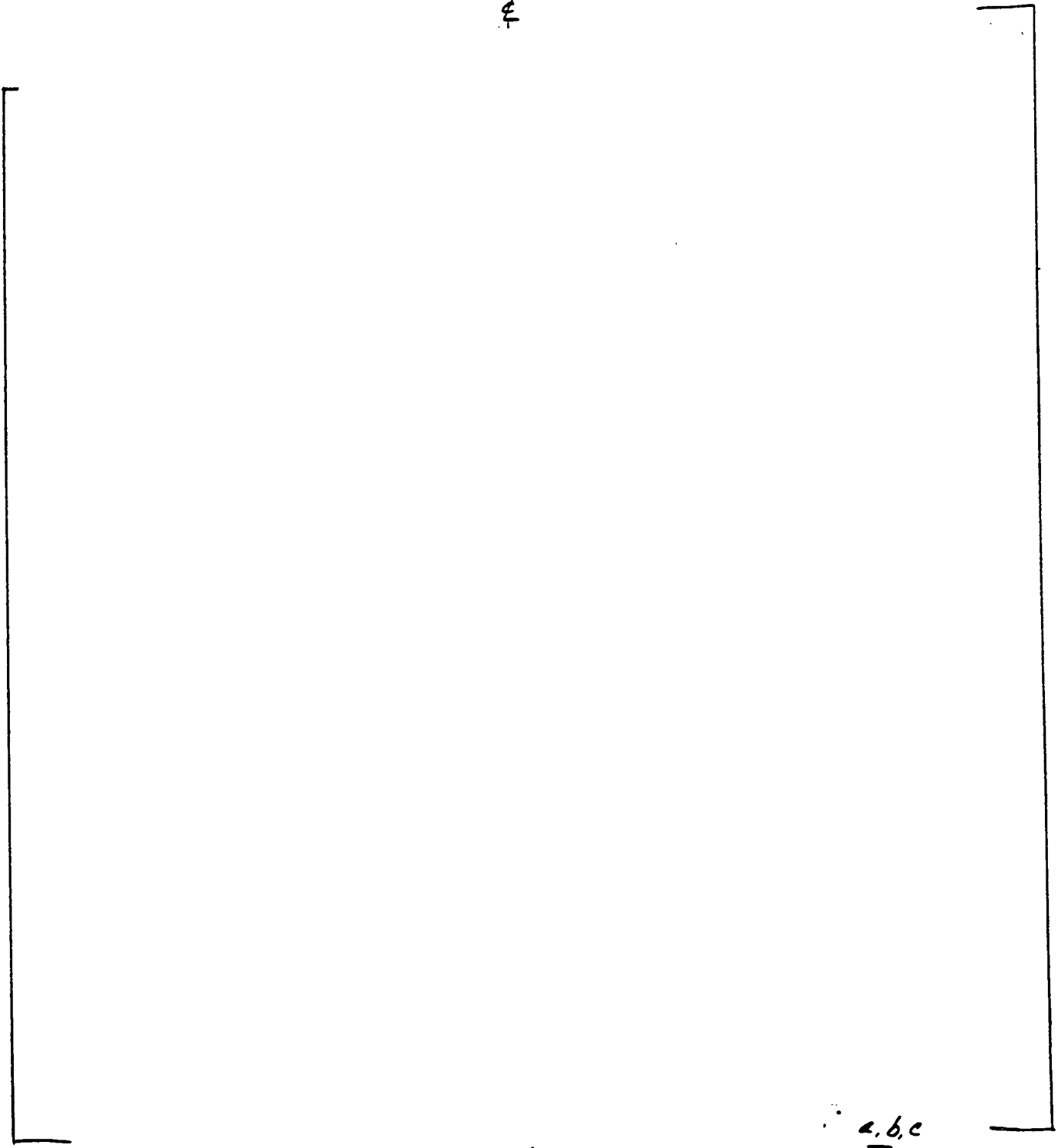


FIGURE 1-1 [

a,b,c ]

TABLE 1-1

REFERENCE JOINT FABRICATION PROCEDURE

a,b,c



## AGENDA ITEM 2 - REVIEW OF DISSOLUTION PHENOMENON

### AGENDA ITEM 2.1 - DESCRIPTION OF THE DISSOLUTION PHENOMENON

In the case of excessively high braze temperature and time, dissolution between I-600 and braze alloy may occur. A summary description of the dissolution phenomenon is presented in Table 2.1-1.

In order to further understand the dissolution phenomenon, a laboratory program was conducted in support of the field evaluations performed at San Onofre (refer to Table 2.1-2). The laboratory effort was focused on determining braze conditions that would result in dissolution of the tubes and/or sleeves and on the development of nondestructive methods of identifying tubes and/or sleeves that may have undergone significant dissolution.

During this laboratory program relationships between soak currents, braze cycle lengths and dissolution were developed.

2,b,c

] Radiography and metallography were employed to evaluate the tube/sleeve dissolution. Results are presented in Figures 2.1-1 to 2.1-3. Figure 2.1-1 is a plot of maximum outer tube-wall thinning based on metallography as a function of soak current. [

] <sup>a,b,c</sup> (refer to Figure 2.1-2). Figure 2.1-3 shows the relationship between outer tube and sleeve dissolution for specimens brazed with a controlled ramp and soak current. In addition to metallographic examination, tensile and internal pressurization tests were performed to evaluate joint integrity. Tensile results met all ASME Code

requirements. Results of internal pressurization tests are shown in Figure 2.1-4. [

] <sup>a,b,c</sup> Metallographic photographs showing outer tube and sleeve dissolution for both normal and high current brazing cycles are presented in Figures 2.1-5 and 2.1-6. Conclusions based on the metallographic examination are presented in Table 2.1-3.

Plugging criteria were established on the basis of the laboratory tests and the development of an eddy current procedure for the detection of sleeve penetration.

TABLE 2.1-1

DESCRIPTION OF DISSOLUTION PHENOMENON

- o DISSOLVING OF THE INCONEL ALLOY 600 TUBE  
AND/OR SLEEVE BY THE [ a,b,c ]  
BRAZE.
  
- o EXTENT OF DISSOLUTION IS RELATED TO [ a,b,c ]
  
- o [ a,b,c ]  
WILL ACCELERATE THE DISSOLUTION.
  
- o THE AREA MOST SUSCEPTIBLE IS THE [ a,c ]  
AREA.



TABLE 2.1-2

LABORATORY EFFORT (DISSOLUTION)

- o DIRECTED TOWARD:
  - DETERMINING BRAZE CONDITIONS THAT WOULD RESULT IN DISSOLUTION OF THE TUBES AND/OR SLEEVES.
  - THE DEVELOPMENT OF NON-DESTRUCTIVE METHODS OF IDENTIFYING TUBES AND/OR SLEEVES THAT MAY HAVE UNDERGONE SIGNIFICANT DISSOLUTION.
  
- o RELATIONSHIPS BETWEEN [ a, b, c ] AND DISSOLUTION WERE DEVELOPED.
  
- o RESULTS SHOWED [ a, b, c ]

TABLE 2.1-3  
CONCLUSIONS BASED ON LABORATORY TESTS  
FOR EVALUATING TUBE/SLEEVE DISSOLUTIONS

a, b, c



[ a,b,c] (AS OF MAY 7, 1981)

a,b,c

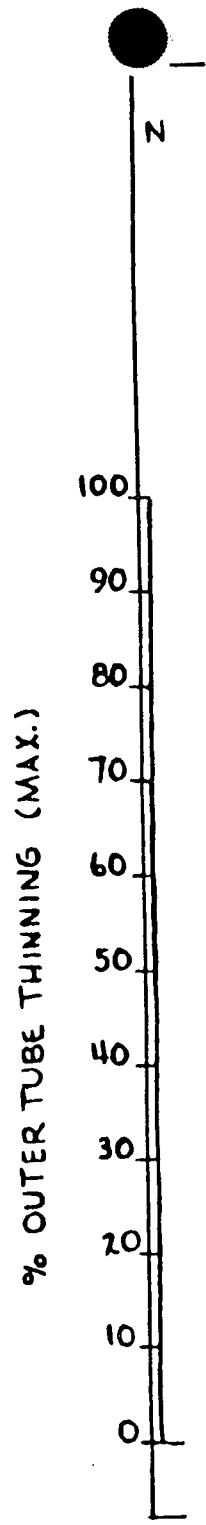
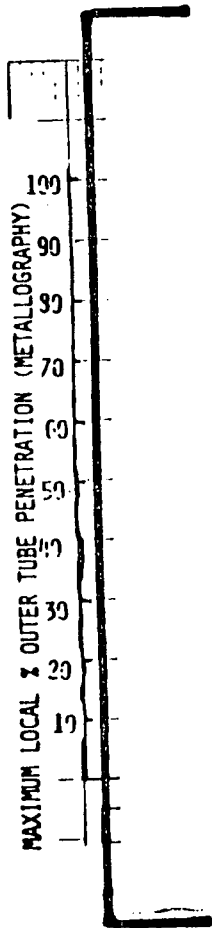



FIGURE 2.1-2

TUBE PENETRATION VS. [ a, b, c ] FOR LABORATORY SPECIMENS



a, b, c



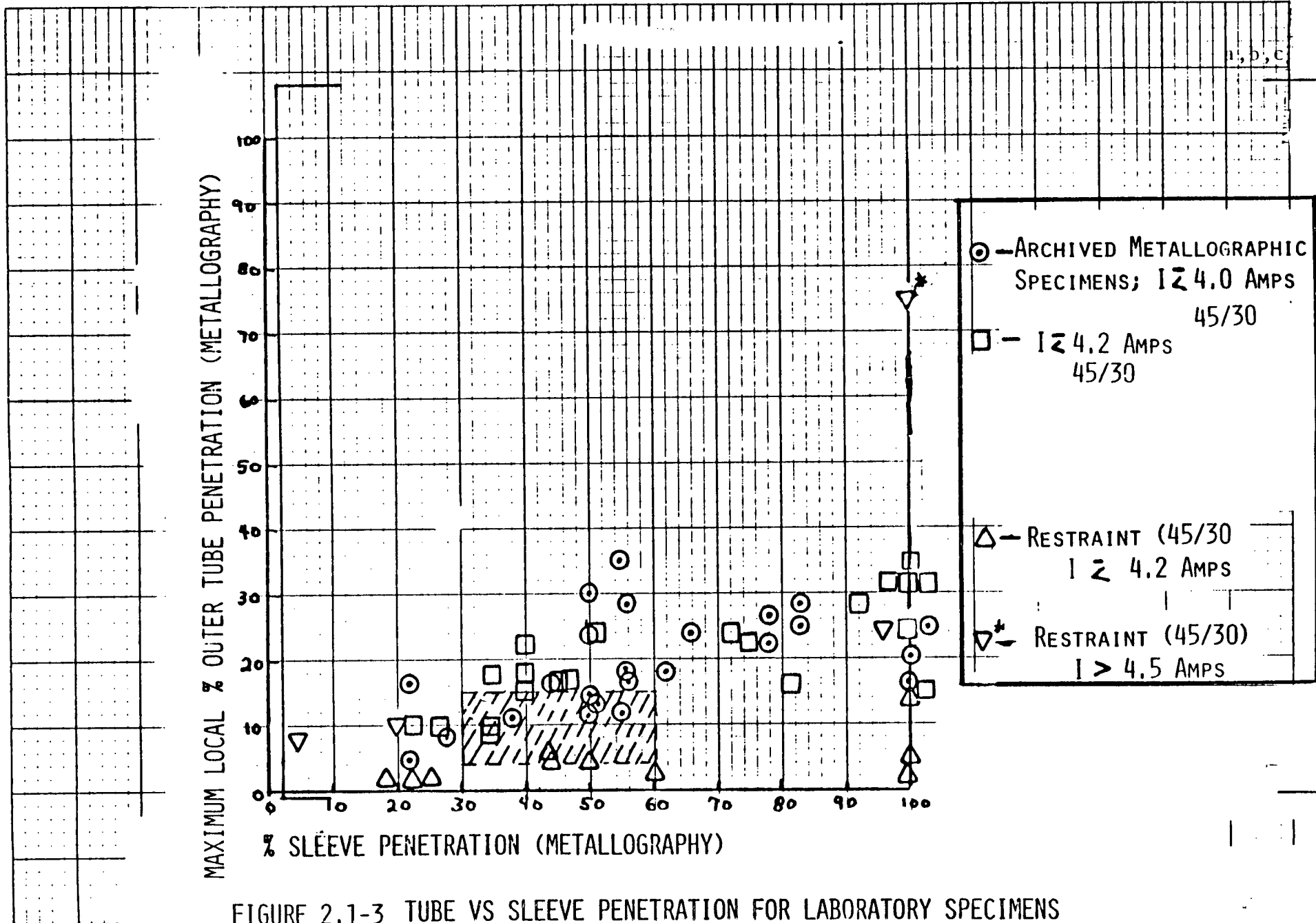


FIGURE 2.1-3 TUBE VS SLEEVE PENETRATION FOR LABORATORY SPECIMENS BRAZED WITH A CONTROLLED RAMP AND SOAK CURRENTS

a, b, c

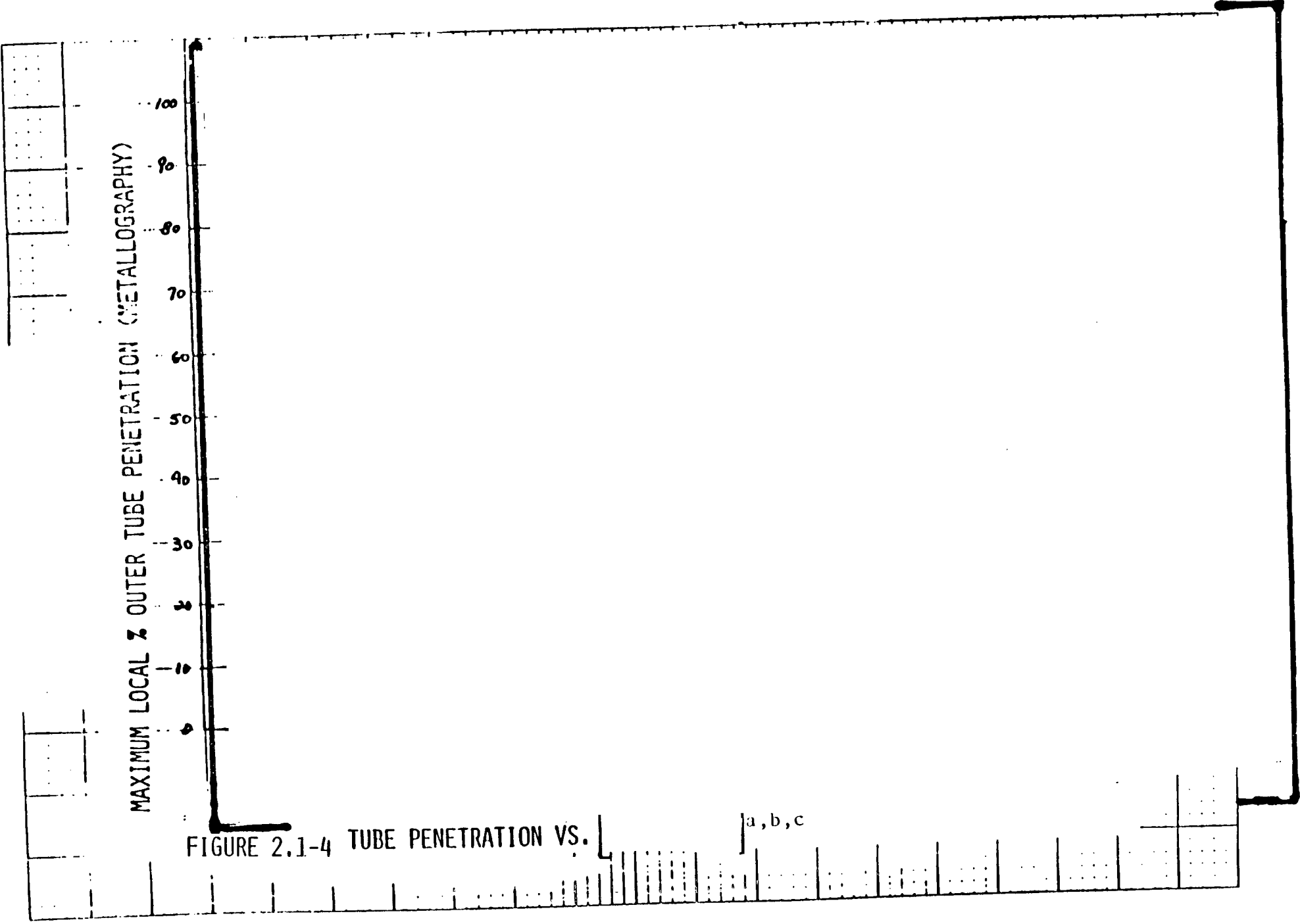
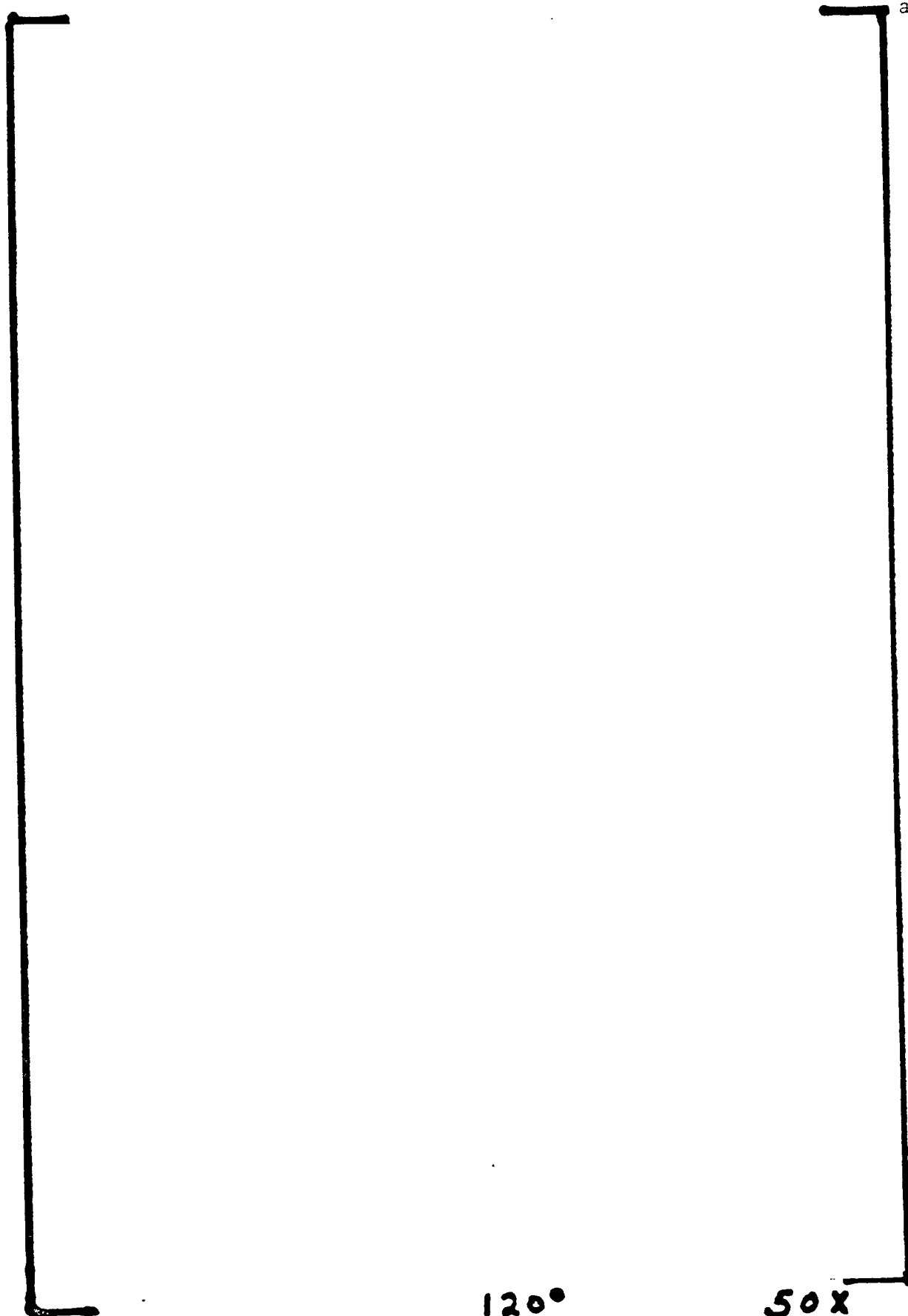


FIGURE 2.1-4 TUBE PENETRATION VS.



a,b,c

120°

50x

FIGURE 2.1-5 METALLOGRAPHIC SECTION SHOWING TUBE DISSOLUTION  
OBSERVED AT [ ]<sub>a,b,c</sub>

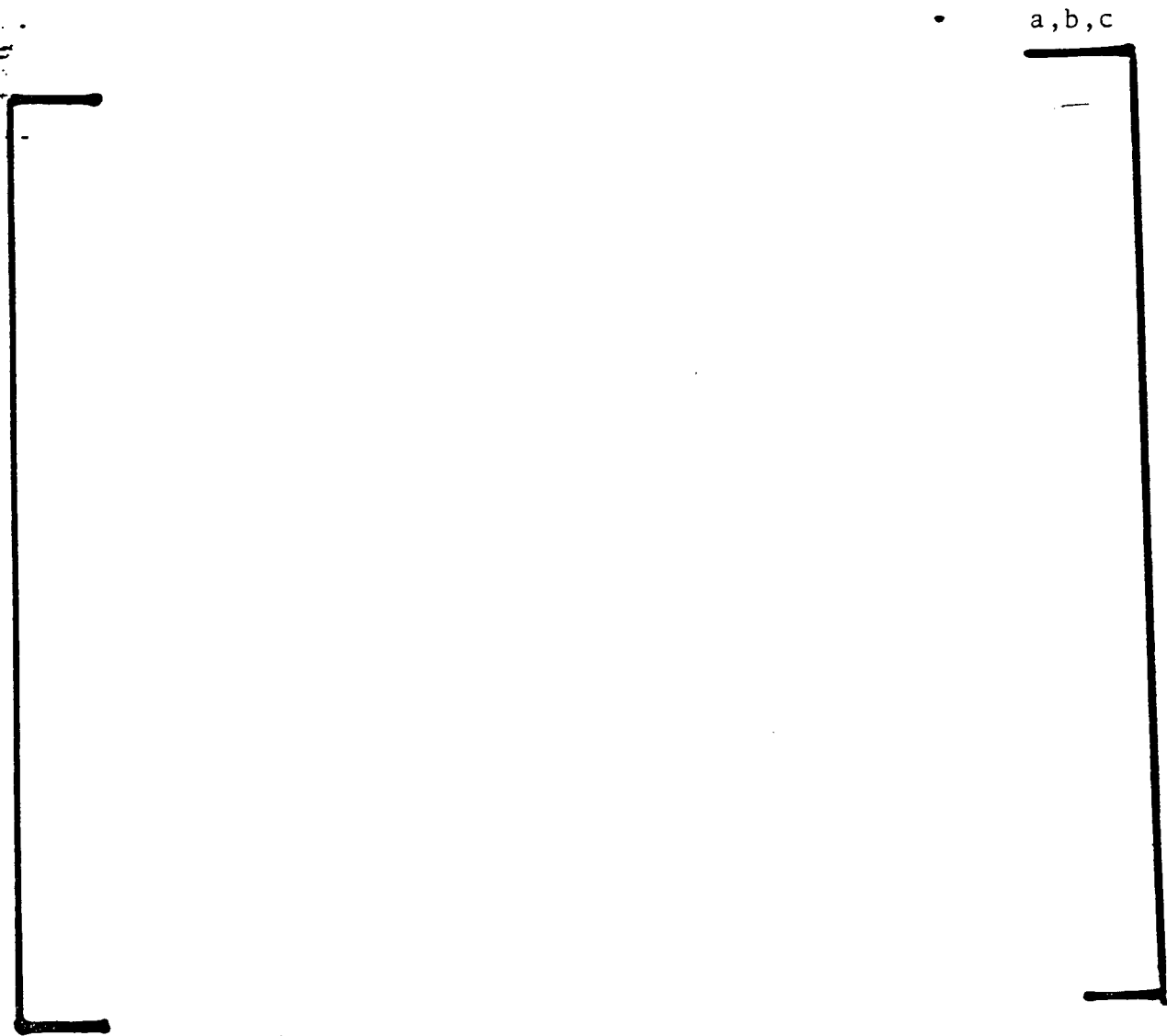


FIGURE 2.1-6 METALLOGRAPHIC SECTION SHOWING MAXIMUM LOCAL  
TUBE DISSOLUTION OBSERVED FOR A [ ]  
] a,b,c



AGENDA ITEM 2.2 - CAUSATIVE FACTORS FOR THE INTRODUCTION OF DISSOLUTION

Based on the results of the laboratory program previously discussed (Agenda Item 2.1), [

a,b,c  
]

The plate current vs. time and ID temperature vs. time relationships for various boundary conditions are shown in Figures 2.2-1 and 2.2-2. Curve A represents the plate current and ID temperature responses for the reference process. If the heat sink characteristics of the outer tube changes from the reference condition, i.e., air to that of an improved conductor, then Curve B might apply. Curve C would apply to an intermediate heat sink condition.

For these various boundary conditions, the integrated area under each curve will vary. As the magnitude of this integrated plate current versus time area increases, Figure 2.2-1, the likelihood for observing appreciable dissolution increases.

TABLE 2.2-1

CAUSATIVE FACTORS FOR THE  
INTRODUCTION OF DISSOLUTION

a, b, c



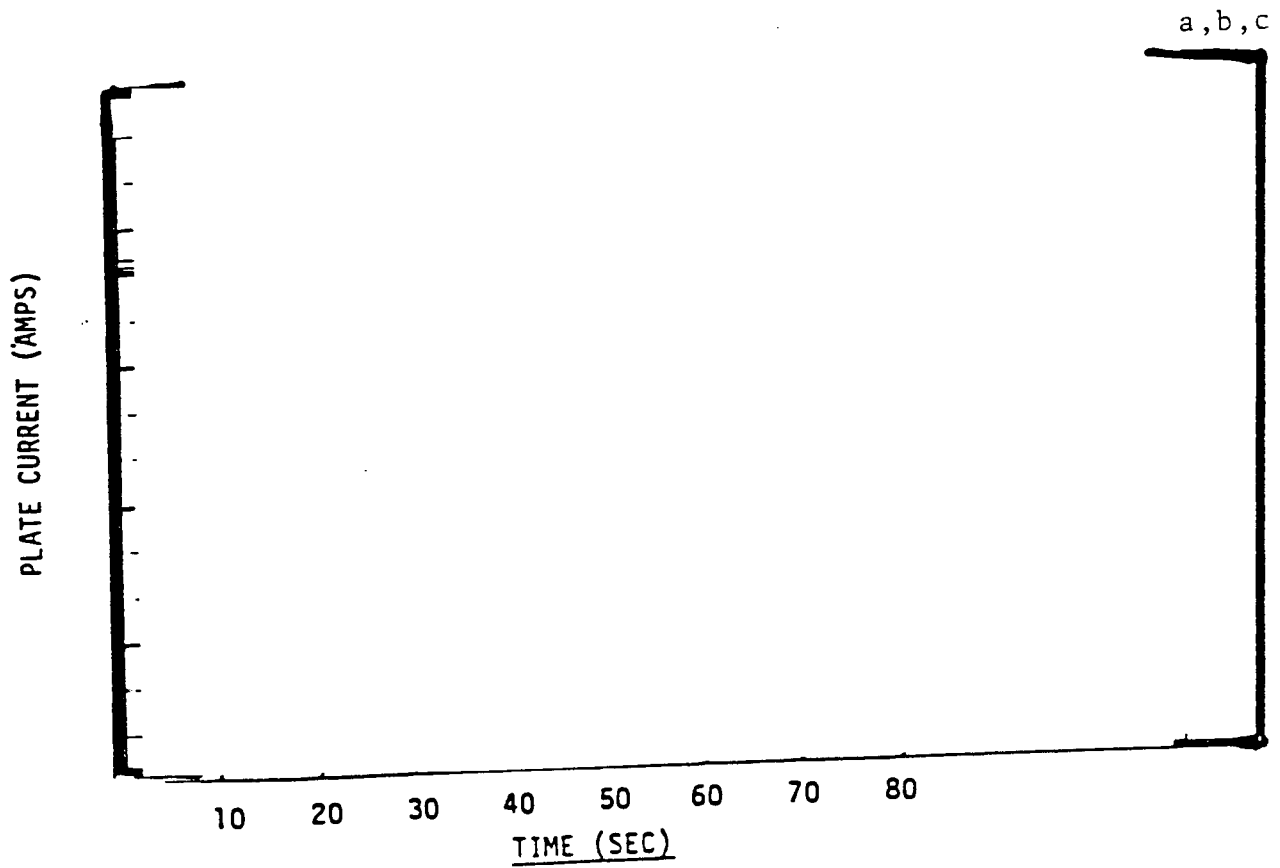


FIGURE 2.2-1 - SCHEMATIC OF CURRENT VS. TIME RELATIONSHIP FOR VARIOUS BOUNDARY CONDITIONS

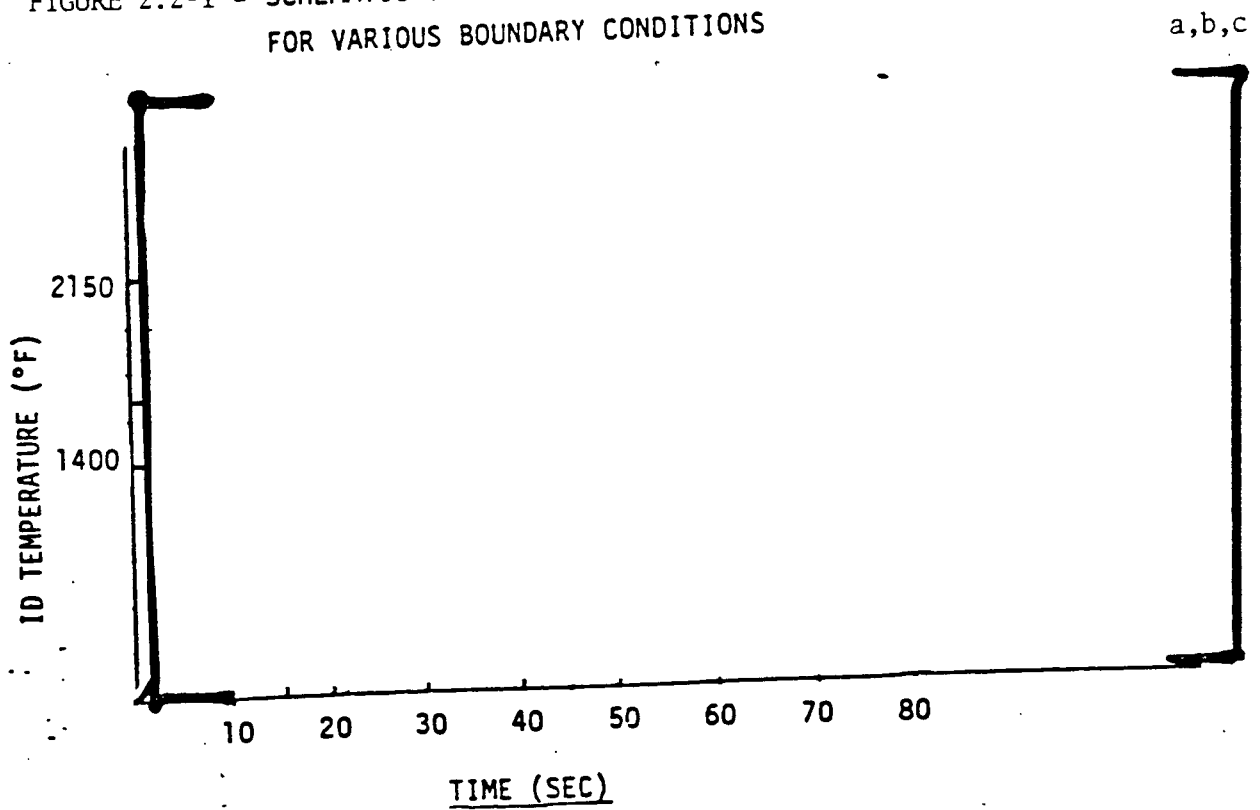
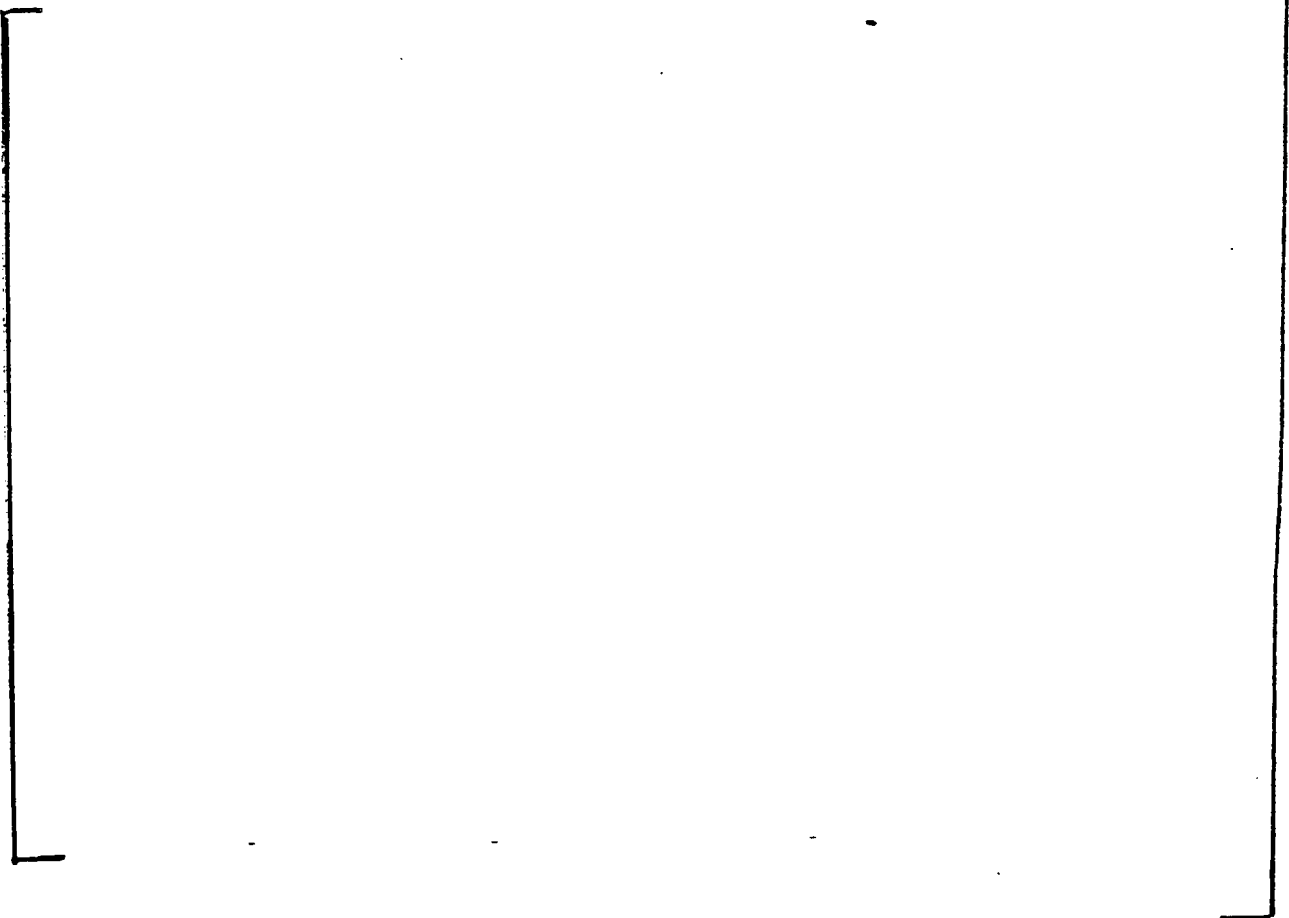


FIGURE 2.2-2 - SCHEMATIC OF TEMPERATURE VS. TIME FOR VARIOUS BOUNDARY CONDITIONS

AGENDA ITEM 2.3 - SPECIFIC PROBLEMS ENCOUNTERED AT SAN ONOFRE

Isolated incidences [ ] were encountered at San Onofre (refer to Table 2.3-1). An analysis of the brazing data was performed on the seven leaking tubes which were found on April 27, 1981, when the secondary side water level was raised above the top of the sleeves. Five of the seven were characterized by [ ] as summarized below. The other two were [ ] sleeves which did not exhibit [ ] Fiber optic inspection indicated some [ ] distortion in a circumferential direction in one sleeve and an unidentified bright spot in the [ ] of the second sleeve. Without pulling these tubes/sleeves for additional examination, it was not possible to determine the actual cause of leakage. These two [ ] tubes were subsequently plugged.\*



Based on the above analysis, all field braze parameters were reviewed and checked for the above characteristics, [ ]<sup>a,b,c</sup>

---

\*Due to the schedular delays that were being encountered in the process of field [ ]<sup>a,b,c</sup> inspection of brazed joints, the decision was made to forego this inspection and either plug or convert the remaining brazed sleeves with a mechanical roll. As a result, all [ ]<sup>a,b,c</sup> non-inspected sleeved tubes with brazed joints were to be plugged because the short vertical distance from the braze to the suspected region of IGA was insufficient to allow the mechanical conversion. The two in question were not inspected by the [ ]<sup>a,b,c</sup> technique and were, therefore, scheduled to be plugged.

TABLE 2.3-1

SPECIAL SITUATIONS ENCOUNTERED AT SAN ONOFRE

Isolated incidences of:

a,b,c

-- [ ]  
--  
--

[ ]

AGENDA ITEM 2.4 - INPUT VALUES FOR RELEVANT FABRICATION  
PARAMETERS FOR EACH OF THE TUBES WHICH LEAKED AS A RESULT  
OF DISSOLUTION

The fabrication parameters for "the seven" leaking tubes are presented in Table 2.4-1.

AGENDA ITEM 2.5 - CORRECTIVE ACTIONS

As a result of the preceding findings, an investigation was initiated to determine the conditions that result in [ ]<sup>a,b,c</sup> penetration and/or leakage of the subject tubes. The effort was initially focused on determining brazing conditions that can result in degradation of the sleeves or tubes and on the development of nondestructive methods of identifying tubes and/or sleeves that may have undergone significant degradation. Based on the results of the laboratory tests and the development of an eddy current procedure, plugging criteria were developed and applied (refer to Table 2.5-1). The number of tubes plugged in each steam generator and the fabrication parameters for each of these tubes are presented in Tables 2.5-2 and 2.5-3.



TABLE 2.4-1

FABRICATION PARAMETERS FOR "THE SEVEN" LEAKING TUBES

<u>ROW</u>	<u>COL</u>	<u>SLEEVE LENGTH, INCH</u>	<u>TOTAL CYCLE TIME*</u>	<u>PLATE CURRENT (A)</u>	<u>SOAK CURRENT* (A)</u>	<u>SOAK TEMP. (°F)</u>
<u>STEAM GENERATOR B</u>						a, b, c
6	9	[				]
7	9					
8	11					
<u>STEAM GENERATOR C</u>						a, b, c
10	70	[				]
14	24					
18	73					
18	74					

\*BASED ON REVIEW OF STRIP CHARTS  
 \*\*SOAK TEMPERATURE REACHED, BUT NOT MAINTAINED

TABLE 2.5-1

SITE PLUGGING CRITERIA:

- o ALL BRAZES MADE WITH A SOAK CURRENT  
[>4.5 AMPS.<sup>a,b,c</sup>]
  
- o ALL BRAZES MADE WITH A SOAK CURRENT  
FROM [4.0 TO 4.5<sup>a,b,c</sup>] AMPS INDICATING  
SLEEVE PENETRATION BASED ON EC.
  
- o ALL BRAZES MADE WITH A SOAK CURRENT  
[<4.0<sup>a,b,c</sup>] AMPS AND INDICATING SLEEVE  
PENETRATION BELOW [RESERVOIR<sup>a,b,c</sup>]  
BASED ON EC.

TABLE 2.5-2

TUBES PLUGGED DUE TO  
VERIFICATION EC EVALUATION  
OF BRAZED SLEEVES

<u>S/G</u>	<u>NUMBER OF TUBES</u>
A	9
B	30
C	42

TABLE 2.5-3

SCE - STEAM GENERATOR - A

a, b, c



TABLE 2.5-3 (CONT.)

SCE - STEAM GENERATOR - B

a,b,c

- con't -

TABLE 2.5-3 (CONT.)

SCE - STEAM GENERATOR - B (con't)

a,b,c

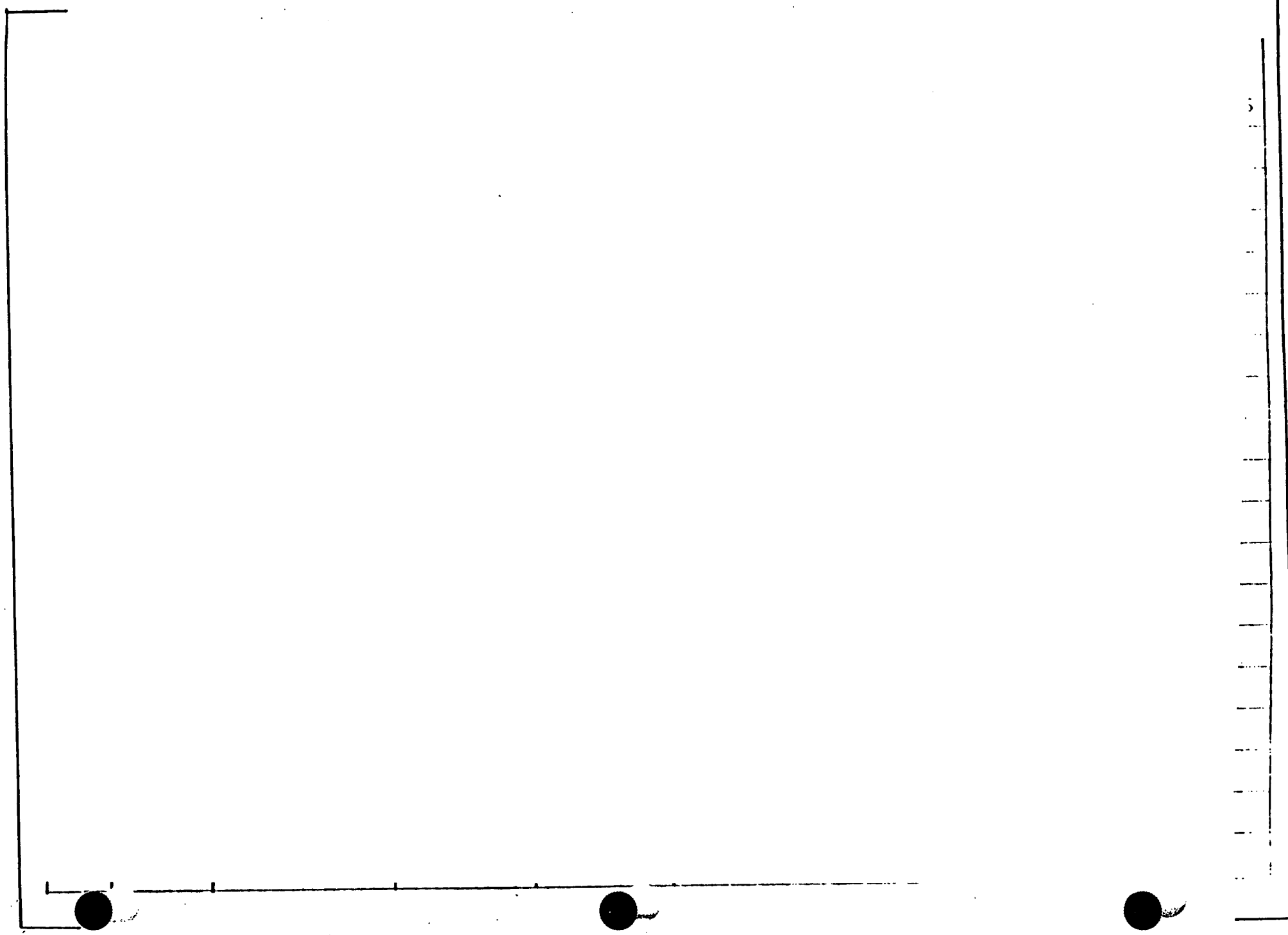


TABLE 2.5-3 (CONT.)

SCE - STEAM GENERATOR - C

a,b,c

- con't -

TABLE 2.5-3 (CONT.)

SCE - STEAM GENERATOR - C (con't)

a,b,c



TABLE 2.5-3 (CONT.)

SCE - STEAM GENERATOR - C (con't)

a,b,c

A large empty rectangular frame with three binder holes at the bottom edge. The frame is defined by a thin black line. The holes are located at approximately the bottom-left, bottom-center, and bottom-right corners of the frame.

AGENDA ITEM 2.6 - THE BASIS FOR THE CORRECTIVE ACTIONS

Since [ ]<sup>a,b,c</sup> outer tube thinning is the maximum allowable in this unit, the plugging criteria are based on the test data analysis which showed that (1) the degradation of the outer tube wall in excess of [ ]<sup>a,b,c</sup> is most likely to occur when the braze joint, in the restrained state, is subjected [ ]<sup>a,b,c</sup> (2) the degradation of the outer tube wall in excess of [ ]<sup>a,b,c</sup> can occur on braze joints, [ ]<sup>a,b,c</sup>

[ ]<sup>a,b,c</sup> Also the development of nondestructive test showed that eddy current is capable of detecting [ ]<sup>a,b,c</sup> penetration as well as penetration of the sleeve below [ ]<sup>a,b,c</sup> Pressure tests also indicated that tubes brazed at soak currents up to [ ]<sup>a,b,c</sup> were capable of sustaining [ ]<sup>a,b,c</sup>

The basis for the corrective actions are presented in Table 2.6-1. In addition to the basis shown in this table, field pressure tests were conducted to verify the structural integrity of the field brazes. Seven field brazed sleeves with soak currents ranging from [ ]<sup>a,b,c</sup> were hydro tested, in-situ, at 3000 psi (nominal). All seven tubes successfully passed the 18 minute hydro test (refer to Table 2.6-2).

TABLE 2.6-1

BASIS FOR THE CORRECTIVE ACTIONS

1. [ a,b,c ] outer tube thinning is the maximum allowable.
2. Based on current data, degradation of the outer tube wall in excess of [ a,b,c ] may occur when the braze joint, in the restrained state, is subjected to soak currents of [ a,b,c ] amps or greater.
3. Based on current data, degradation of the outer tube wall in excess of [ a,b,c ] may occur on braze joints, in the restrained state, when the [ a,b,c ] is penetrated and the soak current is [ a,b,c ] amps or greater.
4. Eddy current is capable of detecting [ a,b,c ] penetration as well as penetration of the sleeve below the [ a,b,c ]
5. Pressure tests indicate that tubes brazed at soak currents up to [ a,b,c ]

TABLE 2.6-2

FIELD PRESSURE TESTING OF  
SELECTED BRAZED JOINTS

- o Field brazed sleeves with soak currents ranging from [ a,b,c ] were hydro tested, in-situ, at 3000 psi (nominal).
  
- o All seven tubes successfully passed the 18 minute hydro test.

AGENDA ITEMS 2.7 AND 2.8 - BASELINE EDDY CURRENT AND UT RESULTS

The normal bobbin eddy current procedure, described in Table 2.7-1, was observed to be ineffective for sleeve inspection. Subsequent development efforts on a test procedure for sleeving inspection focused on the [ ]<sup>a,b,c</sup> area as well as the sleeve itself, Table 2.7-2. The procedure involved a [ ]<sup>a,b,c</sup> eddy current method using a [ ]<sup>a,b,c</sup> eddy current probe. The tests were performed at [ ]

[ ]<sup>a,b,c</sup> Refer to Table 2.7-3.

This test was applied to samples which were produced at various brazing power levels. [ ]<sup>a,b,c</sup> braze samples with various out of process parameters were examined in the course of the investigation. For reference, Figure 2.7-1 shows the eddy current results on a set of four samples that were brazed with a properly controlled brazing cycle. Figure 2.7-2 shows the eddy current results of some of the samples from one of the out of process test matrices. In this set of experiments the brazing cycle consisted of [ ]

[ ]<sup>a,b,c</sup>

Another set of experiments was performed with the ends of the tube restrained during the brazing process. Figure 2.7-3 shows the eddy current results for two of the samples used in evaluating the influence of excessive heat applied to a restrained tube.

The eddy current response of the [ ]<sup>a,b,c</sup> region of the sleeve is extremely complex. At [ ]<sup>a,b,c</sup> the response is essentially independent of the [ ]<sup>a,b,c</sup> condition. With a few exceptions, however, the eddy current signals at [ ]

[ ]<sup>a,b,c</sup> showed the ability to identify sleeves which were degraded. The [ ]<sup>a,b,c</sup> eddy current measurements of the samples show that the sleeves which have undergone degradation in the [ ]<sup>a,b,c</sup> region produce eddy current signals of large amplitude and a phase of less than 90°, Figure 2.7-2. These sleeves that had undergone degradation below the [ ]<sup>a,b,c</sup> produce eddy current signatures with multiple lobes, Figure 2.7-3.

As a result of these observations a data evaluation procedure relying on the [ ]<sup>a,b,c</sup> data was developed. Some typical field eddy current responses are shown in Figure 2.7-4. Note that these data are similar to those generated in the laboratory under normal brazing conditions, Figure 2.7-1. Examples of four sleeves which have signals that are suggestive of degradation are shown in Figure 2.7-5. Three of these tubes were confirmed leakers. Table 2.7-4 summarizes the inspection of leaking tubes.

The description of the [ ]<sup>a,b,c</sup> capabilities are discussed in Agenda Item 4.6.2.

TABLE 2.7-1

INSPECTION OF LEAKERS

o BASELINE INSPECTION

BOBBIN COIL - MULTIPLE FREQUENCY PROCEDURE

- |    |   |                    |   |
|----|---|--------------------|---|
| -- | [ | ] <sup>a,b,c</sup> | - HIGH GAIN FOR SLEEVE INTEGRITY          |
| -- |   |                    | - TUBE INSPECTION, EXPANSION VERIFICATION |
| -- |   |                    | - HARDROLL REGION, TRANSITION REGION      |
| -- |   |                    | - TRANSITION REGIONS                      |

RESULTS INCONCLUSIVE FOR DISSOLUTION.

TABLE 2.7-2

INSPECTION FOR DISSOLUTION

[ ]<sup>a,b,c</sup>

SLEEVE



TABLE 2.7-3

EDDY CURRENT TEST DEVELOPED FOR DISSOLUTION

- [ <sup>a, b, c</sup> BOBBIN ]  
INSPECTION
- LABORATORY SIMULATIONS
- DETECTS SLEEVE WALL PENETRATION IN THE  
BRAZE REGION
- PROCEDURE APPLIED TO ALL BRAZES

TABLE 2.7-4

INSPECTION OF LEAKING TUBES

o [ ]<sup>a,b,c</sup>

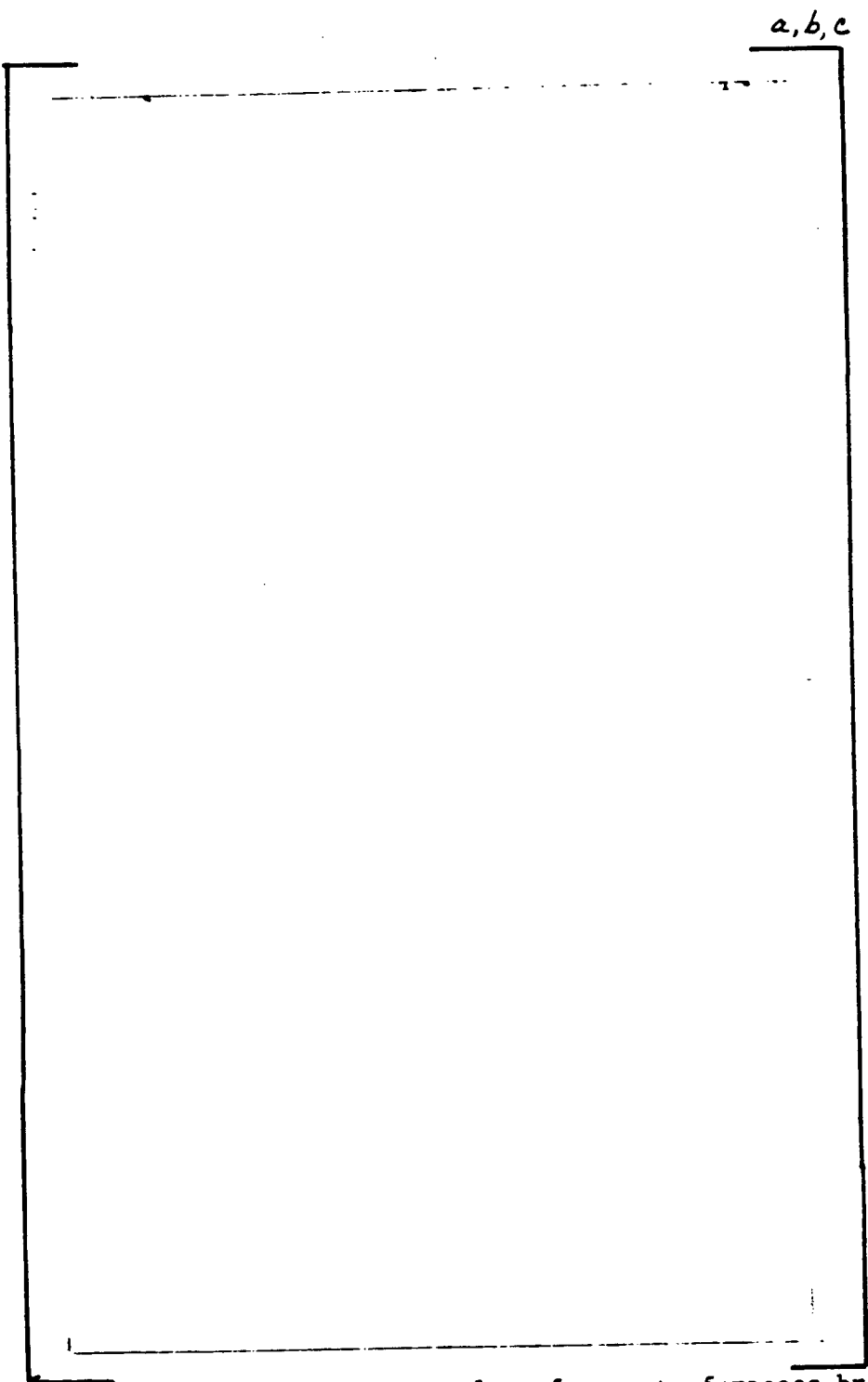
o RESULTS (SG C ONLY)

ALL LEAKING TUBES  
IDENTIFIED.

a, b, c

Eddy current responses of four samples brazed with correct  
brazing cycle.

FIGURE 2.7-1



a, b, c

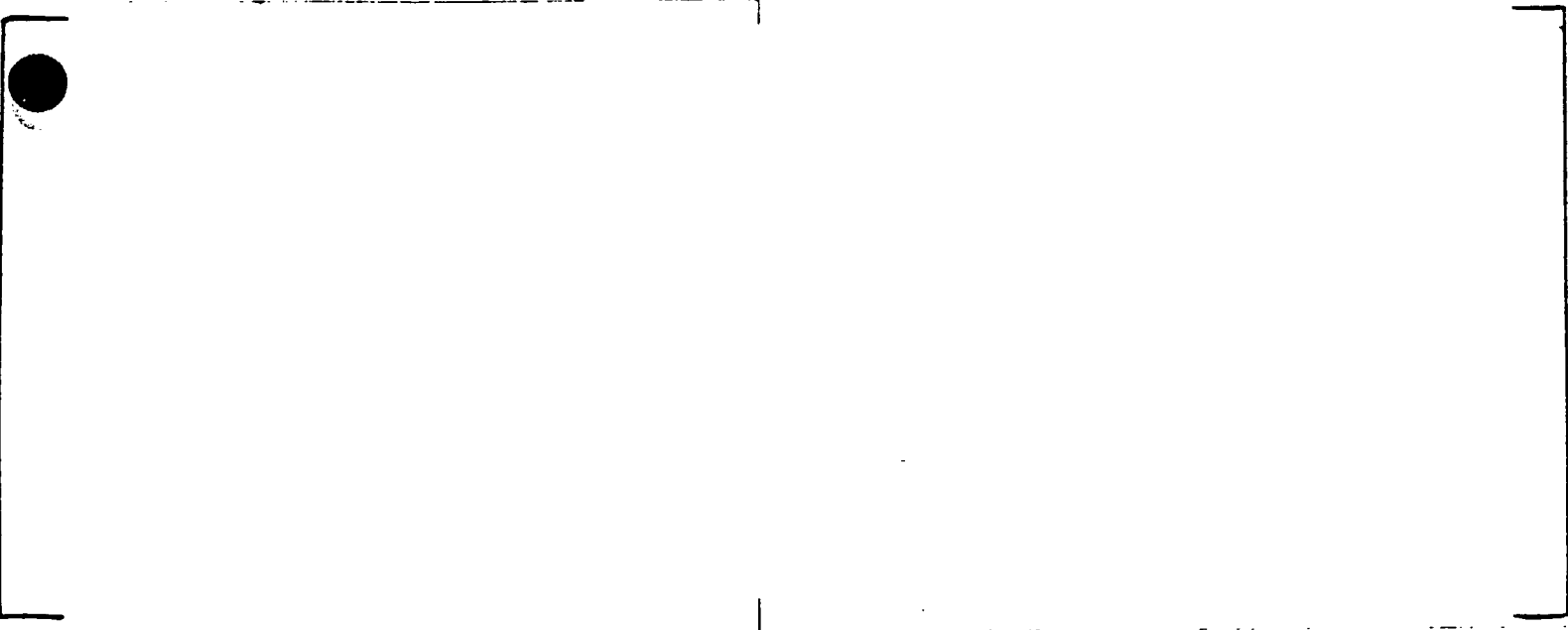
a. [ ]<sup>a, b, c</sup>  
 No visible indication

b. [ ]<sup>a, b, c</sup>  
 No visible indication

Eddy current results of an out of process brazing study in which the soak power was varied by varying the D.C. input current to the brazing power supply from [ ]<sup>a, b, c</sup>

FIGURE 2.7-2

a, b, c



f. [ ]<sup>a, b, c</sup>

Single axial opening the width of the  
[ ]<sup>a, b, c</sup>

Single axial opening the width of the  
[ ]<sup>a, b, c</sup>

g. [ ]<sup>a, b, c</sup>

Two axial openings the width of the  
[ ]<sup>a, b, c</sup>

FIGURE 2.7-2 (CONTINUED)

a,b,c

FIGURE 2.7-3

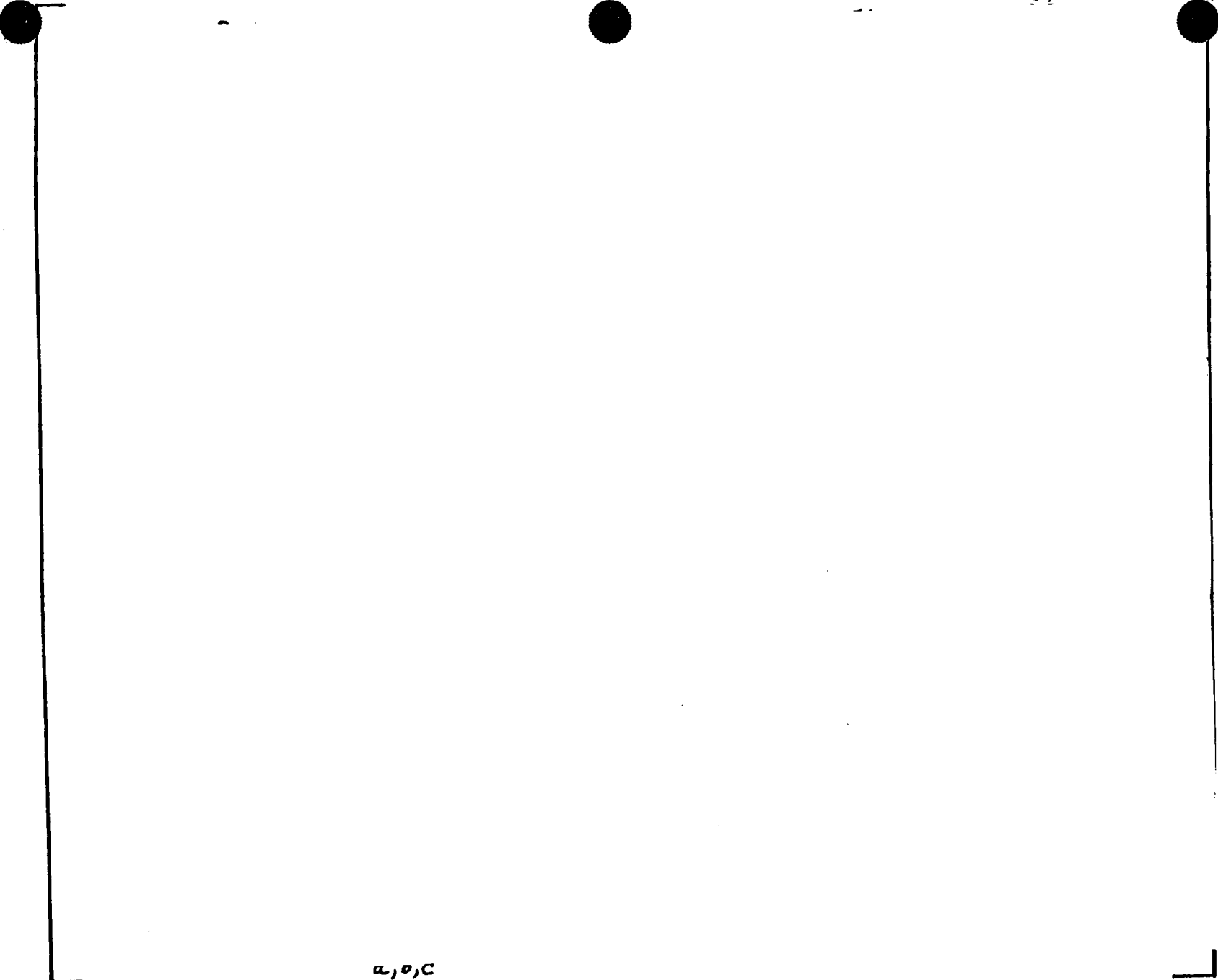
Eddy current response of two samples which displayed degradation  
below the braze [ ]<sup>a,c,e</sup>



Typical [ *a, b, c* ] eddy current response from field data.

FIGURE 2.7-4

1. 3, 5, 6



a, b, c

[ eddy current responses from field data that indicate sleeve degradation.  
Three of these assemblies are confirmed leakers.

FIGURE 2.7-5



SAN ONOFRE NUCLEAR POWER PLANT  
UNIT 1 (SCE) STEAM GENERATOR

Flow-induced Vibration Analysis to Evaluate Potential  
for Propagation of Pre-existing Cracks in a Degraded,  
Non-Steeved Peripheral Tube

EA-82-007

September, 1982

APPROVED BY:



M. R. Patel, Manager  
Auxiliary Equipment Analysis  
Nuclear Technology Division

WESTINGHOUSE ELECTRIC CORPORATION  
NUCLEAR ENERGY SYSTEMS  
PITTSBURGH, PA 15230

## 1.0 INTRODUCTION

This evaluation addresses structural integrity of non-sleeved tube-ends on the hotleg subject to normal and secondary side blowdown flow-induced loading conditions. Based on the inspection history of the units, it is assumed that (1) localized tube degradation could occur near the tube sheet on the hot leg, and (2) as a consequence of denting and restrictions in steam generators A and C, ligament cracking could exist resulting in partial loss of lateral support at the lower one support plate and, possibly also, a second tube support plate (TSP) on the inner row tubes.

Effects of pressure and dynamic fluid forces associated with full power normal operation and a postulated secondary side blowdown event were evaluated to determine if pre-existing cracks in degraded non-sleeved tube ends could propagate and lead to a double-ended tube rupture. Blowdown loadings during both a Main Steam Line Break (SLB) and a Feed Line break (FLB) were considered. In both blowdown cases, the tubing is subjected to maximum Flow-Induced Vibration (FIV) and tube-baffle interaction loads during the initial phase of the blowdown followed by a maximum primary-to-secondary pressure differential  $\Delta p$  of 2560 psig. Since the SLB results in higher blowdown rates, and consequently, larger axial and bending tube loads compared to a FLB case, the blowdown evaluation was based on SLB loads. The SLB blowdown loads were based on the considerations of actual conditions of the steam generators which affect the flow path. These include tube denting and consequent loss of flow area through the tube-to-tube support plate hole annuli, sludge pile, and location of the downcomer resistance plate (DRP) which affects the flow area across the plate through the downcomer annulus.

For tubing evaluation subject to the SLB blowdown loads, the depth of penetration in the degraded region was assumed to be uniform and equal to 60% (that is, 40% remaining) of nominal 0.055 inch wall\*. This was based on a 50% plugging margin and a 10% allowance for continued operation.

---

\*For tube evaluation under normal operating loads, the depth of penetration used was 73% of nominal. This was based on minimum required wall associated with design-basis maximum primary-to-secondary pressure differential.

It is noted that based on operating history of these and similar other units, presence of IGA has been associated with sludge pile regions only. Thus, observed IGA has always been in the interior of the tube bundle; to date no IGA has been observed on the peripheral tubes. The assumption of uniform degradation used in the subject evaluation, therefore, does not imply IGA. Rather, the assumption is used to conservatively bound the loss of structural capability of the tubing due to degradation in the vicinity of the tubesheet.

## 2.0 TUBE INTEGRITY REQUIREMENTS

Consideration of flow-induced vibration and the SLB blowdown loads impose the following additional requirements for tube integrity evaluation.

- (1) Fatigue due to FIV stresses during either normal operation or the SLB blowdown\*. For normal operation, the predominant consideration is low amplitude - high cycle fatigue, whereas during a postulated SLB blowdown, the consideration is primarily high amplitude-low cycle fatigue. The FIV stresses during normal operation are mainly due to cross-flow turbulence excitation. However, during a SLB blowdown, the fluid loads include the dynamic drag forces in addition to turbulent excitation. The effects of these two components of fluid loading were analyzed independent of each other and the resultant tube response was calculated conservatively by combining the peak responses on an absolute basis.

The fatigue evaluation was performed conservatively using the ASME Code approach. To account for the presence of any embedded crack(s), a conservatively assumed value of 4.0 for the stress concentration factor (SCF) was used in computing the peak stresses.

- (2) Steam line break being a faulted condition, it is required that the primary membrane ( $P_m$ ) and membrane-plus-bending ( $P_m + P_b$ ) stress intensities be limited to the allowables in accordance with Appendix F of Section III of the ASME Code.

Using the code minimum properties at 600°F, namely,

$$S_m = 26.67 \text{ ksi, and}$$

$$S_u = 80.00 \text{ ksi,}$$

the allowable primary stress intensities are given by

$$P_m = \text{Smaller of } (2.4 S_m, 0.7 S_u) = 56000 \text{ psi, and}$$

$$P_m + P_b = 1.3 P_m = 72800 \text{ psi,}$$

---

\*It is to be noted that according to the design rules in Section III of the ASME Code, a fatigue evaluation for faulted condition loading is not required.

the multiplier 1.3 being the shape factor for a thin cylinder.

The primary stress intensity evaluation was performed considering the combined influence of pressure, tube-baffle interaction, and FIV loadings during the SLB event. The axial tube loads due to tube-baffle interaction were obtained from a separate analysis, Reference (1)\*. The flow-induced tube moments included effects of both the fluid drag forces and turbulent excitation. These were obtained from detailed tube analyses using the worst case blowdown loads from Reference (2).

---

\*References are listed at the end of the report.

### 3.0 FIV ANALYSIS MODELS AND ASSUMPTIONS

In the analysis models, the region of tube degradation (on tube OD) on the hot leg at the tubesheet was simulated conservatively by a uniformly thinned section. As indicated earlier, this is to conservatively bound the loss of structural capability of the tube due to its OD degradation. It is noted that operating experience to date does not support evidence of any IGA on peripheral tubes away from sludge accumulation. The axial length of the degraded section was assumed to be 2.0 inches. The depth of degradation was assumed equal to 60% of nominal wall (that is, 40% remaining wall) based on the plugging margin of 50% and a 10% allowance for continued operation.

The lower two support plates in steam generators A and C have undergone extensive flow-slot hour-glassing as a result of tube denting. Recent visual examinations and photographic data have indicated some ligament cracking and islanding in the vicinity of the flow slots, and the potential for partial loss of support for the tubes\*. Based on the photographic evidence, the potential loss of support is limited to the first row tubes only. However, for analytical evaluation, it is conservatively assumed that (1) the loss of support may extend up to some of the second row tubes at both lower support plates, and (2) some of the tubes beyond the second row may also be subject to loss of lateral support at the first (from the tubesheet) TSP. In steam generator B, no flow slot hour-glassing and/or tube restrictions exists. Therefore, no loss of support is assumed for SG-B tubing.

The first 13 rows in these units do not have antivibration bar (AVB) supports in the U-bends. Hence, a total of three separate U-tube models were analyzed. In subsequent discussions, the three models are referred to as the 2nd row model (U-bend radius  $R = 2.906$  inch) the 13th row model ( $R = 14.25$  inch) and the 48th or outermost row ( $R = 50.34$  inch) model.

\*This condition is believed to have existed since the early seventies. Based on the operating history, the tube configuration is stable during normal operation. Since the analysis code used has only linear capabilities, partial loss of support cannot be simulated. Tubes partially supported by cracked ligament(s) were analyzed conservatively assuming total loss of lateral support.

The tube was assumed fixed at the top of the tube sheet. At TSP interfaces, in-plane and out-of-plane (with respect to U-bend) translational degrees of freedom (DOF) were restrained to simulate lateral support, where applicable. At the AVB's, the tube was restrained against out-of-plane translation and rotation. The material density for tubing was adjusted to account for the hydro-dynamic mass effects of the primary and secondary fluids.

### 3.1 FIV Mechanisms

Three mechanisms of tube vibration in fluids are recognized: fluid-elastic excitation, turbulence and vortex shedding. All are included in the analysis code FLOVIB which was used in the present work. The forcing function was input in the form of secondary velocity and density distribution along the tube length. For turbulence excitation, both axial and cross-flow velocities were included.

Of the three mechanisms identified with flow induced vibrations, in closely spaced tube arrays, the considered predominant mechanisms are turbulence and fluid-elastic excitation. Turbulence excitation causes narrow band random vibration of tubes at about the natural frequency of the tubes in the fluid. The vibration amplitudes vary randomly in time and direction. Turbulence is thought to be the main cause of tube vibration in steam generators when the possibility of fluid-elastic excitation has been eliminated, Reference (3) and (4). Vibration amplitudes due to axial flow turbulence are typically two to three orders of magnitude lower than those due to cross-flow turbulence.

Amplitudes of vibration due to vortex shedding were not considered to be applicable, since vortex shedding is essentially a boundary layer phenomena, and any condition that tends to disrupt the boundary layer will, in all probability, reduce the amplitude of vibration. Laboratory tests have shown no indications of resonance peaks due to vortex shedding in closely spaced tube arrays in the region of the wrapper opening and the tube sheet, Reference (3). In most of the research investigations regarding vortex shedding, the flow velocity approaching the tube and/or any array of tubes has a relatively uniform velocity profile and low level of turbulence. However, in a operating steam generator as the flow enters through the wrapper opening, the fluid flow becomes

turbulent and the axial component of the velocity is thought to disrupt the boundary layer on the tube and the formation of vortices generated by the flow perpendicular to the tube. Although research continues to be done for vortex shedding in tube bundles, it may be considered a second order mechanism since significant cross-flow impinges on only a small portion of the tube in the region of the tube sheet.



#### 4.0 NORMAL OPERATING LOAD EVALUATION

For normal operation, the velocities and densities were obtained from a detailed three-dimensional thermal-hydraulic analysis using the THEFT code, Reference (5). Figure 1 shows a typical schematic of the finite element tube model along with the velocity and density distribution during full power, steady-state normal operation. For the FIV analysis, 1.3% damping was assumed consistent with the subcooled flow conditions in the degraded region. (In the upper region of the tube bundle with low density mixture, typical of high quality steam, the expected damping is 3.8%).

Results of flow-induced vibration analysis and high-cycle fatigue evaluation are summarized in Table 1 for peripheral tubes in the 2nd row, 13th row and the outermost row. The analytically predicted fluid-elastic stability ratios ranged from 0.24 to 0.59 for these configurations. It is to be noted that the analytically calculated vibration amplitudes and stresses correspond to a root mean square (RMS) excitation. For an actual flow field in a typical steam generator, cross-flow turbulence causes narrow-band random vibration of tubes. Based on experimental observations, the ratio of peak-to-RMS amplitude is approximately  $[3.5]^{a,b,c}$ . In addition to this ratio, in computing the peak value of  $S_a$ , a factor of 4.0 was assumed to account for the stress concentration effects of any pre-existing cracks. The calculated  $S_a$  was finally adjusted for the actual versus code fatigue curve values of elastic modulus, E.

Because of the lack of AVB support in the U-bends, the vibration response of the 2nd and the 13th row tubing in the lower region of the tube bundle was influenced by the motion in the U-bend. The impact of the U-bend on lower region dynamic response reduced somewhat as the lateral support at lower plate(s) was removed.

In contrast, for the outermost row tube, because of AVB support in the U-bend, the vibration modes in the lower region of the tube bundle and the U-bend remained uncoupled for all cases analyzed.

From the viewpoint of fatigue evaluation, the peripheral tubes in the 2nd row with assumed loss of lateral support at the lower two plates are most limiting. The maximum calculated  $S_a$  for this case is approximately [2.0 ksi]<sup>a,b,c</sup>. This is significantly less than the high-cycle fatigue endurance limit of 13.7 ksi corresponding to  $10^{10}$  cycles\* (For a 40 year design basis, with the highest predominant frequency of 6.7 Hz, the calculated number of RMS amplitude cycles is approximately  $10^{10}$ . The number of peak amplitude cycles will be lower).

Based on this limiting case, tubes with localized (uniform) degradation equal to 73% of nominal wall, and as-existing support plate configuration will not fail in fatigue due to flow-induced vibrations during normal operation.

---

\*Proposed high-cycle fatigue curve to the ASME Code Committee. This curve is corrected for the mean stress effect.

## 5.0 SLB BLOWDOWN LOAD EVALUATION

During the postulated SLB blowdown, the tubing is subjected to the following loads and stresses:

### 1. Fluid Drag Forces due to Cross-flow

Although these forces are dynamic in nature, the associated momentum flux during the peak loading is non-oscillatory as shown in Figure 2. Under the influence of this loading, the tube assumes an initial deflection and vibrates (due to the flow-induced vibrations) from this mean position. The tube bending moment due to the drag loading is primary in nature and included in the faulted condition primary stress evaluation.

### 2. Flow-induced Vibrations

As discussed earlier, of the three mechanisms identified with FIV, namely, fluid-elastic excitation, turbulence, and vortex shedding, turbulence is thought to be the main cause of vibration in steam generator tubing when the possibility of fluid-elastic instability has been eliminated. As long as a tube can vibrate without impacting a neighboring tube, the resulting stresses are primary in nature. The peak bending responses for primary stress evaluation were obtained by conservatively combining the peak FIV and drag force responses on an absolute basis. In computing the alternating stress intensities for the fatigue evaluation, a conservatively assumed stress concentration factor of 4.0 was applied to the peak bending stresses to account for the presence of any pre-existing cracks.

### 3. Axial Load Due to Tube-Baffle Interaction

The axial tube-baffle interaction load, in general, is secondary in nature and not required to be considered for faulted condition tube evaluation. However, if the tubes are assumed to provide axial restraint to the wrapper against the resultant SLB blowdown forces, the load distributed on an average basis on the total number of tubes interacting with the baffle is primary. From

a detailed tube-baffle interaction analysis in Reference (1), the primary axial load was determined to be less than 100 lbs. In the subsequent evaluation, a value of 100 lbs. was used for this load\*.

#### 4. Primary-to-Secondary Pressure Differential, $\Delta p$

The effect of the secondary side depressurization due to blowdown is to increase the  $\Delta p$  across the tubing from its steady-state operating condition  $\Delta p$ . However, the peak blowdown loads occur during the very early phase of the transient (typically 0.5 sec. or earlier) whereas the peak  $\Delta p = 2560$  psi represents essentially a quasi-steady state condition, typically 8 to 10 secs. following the initiation of the transient. Thus, the peak effects of these loads are fully decoupled. At the time the maximum  $\Delta p$  occurs, the blowdown loads are essentially (attenuated to) zero. From the viewpoint of both fatigue and primary stress intensities, the most limiting condition occurs when the blowdown loads peak; actual  $\Delta p$  at this time was used in computing the primary stress intensities.

#### 5.1 SLB Blowdown Loads and Tube Analyses

The fluid velocities and densities during the postulated SLB were obtained from a time-history, transient analysis using the TRANFLO code, Reference (2). Typical variations in the momentum flux\*\* during the transient are shown in Figure 2. It is to be noted that the maximum momentum flux at various locations in the tube bundle occur at different times during the blowdown. Also, the peak values of the momentum flux at various locations depend on a number of different parameters including the initial water level and initial power level. From the viewpoint of maximizing the combined effects of drag and FIV loads on the degraded tube region, the limiting blowdown case is one which yields the maximum momentum flux at the tube sheet.

\*As indicated by Figure 6.2 in Reference (1), all of the tube ends (7588) interact with the TSP corresponding to the peak wrapper load of 371 kips. Thus, a primary load of 100 lbs. per tube end would imply a conservatively assumed participation of less than 50% tube ends.

\*\*Momentum flux equals density times square of velocity, and is a measure of input energy for flow-induced vibrations.

The FIV analyses were performed for two different cases of blowdown loads. In the subsequent discussion, these are referred to as Case 18 and Case 19 per Reference (2). These cases are as follows:

Case 18: This case corresponds to the maximum momentum flux at the tubesheet for steam generators A and C.

Case 19: This case corresponds to the maximum momentum flux at the tubesheet for SG-B.

In addition to the initial water level and initial power level, the momentum flux distribution at the tube sheet is also very sensitive to the flow area through the downcomer resistance plate (DRP). For cases 18 and 19, the actual areas were computed using as-modified configurations based on field change records; the respective values are  $3.2 \text{ ft}^2$  (bounds SG - A and C) and  $3.5 \text{ ft}^2$  (SG - C). Additionally, the DRP was assumed to be flexible and allowed to deform due to the blowdown loads resulting in further increase in the flow area and momentum flux at the tube sheet.

For both cases, discharge coefficient of 1.0 was used based on the assumption of chocking of flow through the steam nozzle, thus representing an upper bound on momentum flux distribution.

Figures 3 and 4 show the momentum flux variations on the peripheral (and neighboring inner bundle) tubes due to the cross flow through the wrapper opening in steam generators A or C and B, respectively.

The velocity and density distributions corresponding to the time of maximum momentum flux for the two blowdown cases are shown in Figures 5 and 6, along with the FIV analysis model\*. Based on the density distributions, the flow field throughout the tube bundle is predominantly two-phase. Correspondingly, a damping ratio of 2.55% (average value of 1.3% for subcooled liquid and 3.8% for high quality steam) was used for the vibration analyses.

---

\*Node 11 represents the first TSP location for Row 2 and 13 tubes; the corresponding node for Row 48 tube is #10.

The effect of the dynamic drag force was evaluated independently of the FIV due to turbulent excitation. The drag force was computed based on the equation for hydraulic loss in a square tube array with 1.0303 inch pitch, Reference (6), and is given by:

$$F = \frac{0.276 \times 10^{-3}}{R_e^{.2}} \times \text{momentum flux}$$

where  $R_e = VD/\nu$

and  $D = \text{tube OD}, 0.75 \text{ inch}$

$V = \text{tube gap velocity in ft/sec, and}$

$\nu = \text{kinematic viscosity, } 0.145 \text{ ft}^2/\text{sec at } \sim 600^\circ\text{F}$

The tube deflections and moments at the tubesheet end were obtained statically using fixed-pinned beam formulas and peak drag forces. The effect of the dynamic nature of loading was accounted for by multiplying the statically obtained responses with appropriate dynamic load factors (DLF).

The DLFs were calculated using a single-degree-of-freedom assumption with the forcing function in the shape of a triangular pulse from Reference (7). The DLF is given as a function of  $t/\tau$  where  $t$  is the duration of the pulse and  $\tau$  is the fundamental period of the system. The smaller the ratio  $t/\tau$ , the larger the DLF. The largest periods of the tube spans (associated with the degraded tube region) are given by the reciprocals of corresponding bending frequencies which were obtained from the FIV analyses. The resultant DLF were calculated to be 1.0, 1.24 and 1.56 for the cases of all plates integral, first TSP removed, and first and second TSP removed, respectively.

## 5.2 Consideration of Fluid-Elastic Stability

Tube configurations with assumed loss of lateral support(s) were analytically predicted to be fluid-elastically unstable. The analytically calculated maximum stability ratio was 1.39. However, given the actual condition of the tube bundle geometry, the expected realistic magnitude of blowdown loadings, and the transient nature of the loads the analytically predicted unstable modes of significant amplitudes would not occur. This is

because of a number of conservatisms assumed in the analyses. The major ones are as follows:

- (1) Assumptions of instantaneous full break opening and discharge coefficient of 1.0 for blowdown analysis.
- (2) Full loss of tube support under the postulation of ligament cracking. A partial support will stabilize and/or limit the vibration amplitudes of analytically predicted unstable modes, thus making the tube response practically the same as if it were fully supported.
- (3) Assumption of uniform degradation around the circumference. Operating experience on degradation on peripheral tubes indicate that the degradation is nonuniform around the circumference. Thus, the load capacity of tubing in actual situations would be expected to be higher than assumed in the analysis. On the other hand, if degradation is indeed uniform, the present eddy-current technique over-estimates the actual magnitude, Reference (8).
- (4) The analyses were performed using peak momentum flux input. Figures 3 and 4, show the actual momentum flux variations during the blowdown. For such a short duration transient, the fluid-elastic response is expected to be more closely related to the RMS rather than the peak momentum flux distribution.
- (5) The magnitude of fluid-elastic excitation depends on the interaction response of neighboring tubes within an array. As shown on Figures 3 and 4, the fluid velocities and momentum flux drop off rapidly in the neighboring inner row tubes. Also, statistically it would be expected that some neighboring tubes are supported at lower plates and hence have higher response frequencies and lower vibration amplitudes. Therefore, the effective fluid-elastic excitation and the resultant stability ratio for an unsupported peripheral tube would be lower than predicted by the analysis.
- (6) Any large increase in the vibration amplitudes would cause an increase in structural damping which will dissipate the fluid-elastic energy and slow down the rate of amplitude build-up. Coupled

with the fact that the transient peak is of rather short duration, it is highly unlikely that large amplitudes typical of fluid-elastic instability would occur.

In the subsequent evaluation, drag and turbulence are considered to be the only primary mechanisms for tube bending.

### 5.3 Primary Stress Evaluation

As explained earlier, the primary stresses include: (1) the axial bending stresses due to fluid drag and superimposed FIV stresses (prior to tube-to-tube contact), (2) direct axial stresses due to tube-baffle interaction primary axial load  $P$ , and (3) membrane hoop and axial stresses due to the primary-to-secondary  $\Delta p$ .

For both blowdown cases (18 and 19), at the time of maximum momentum flux and wrapper blowdown loads,  $\Delta p \approx 1200$  psi. Based on the analyses in Reference (1), a conservative value of 100 lbs. is used for the primary tube-baffle interaction load. Since the bending stresses are significantly higher than the pressure and axial load stresses, the governing criterion for primary stress evaluation becomes

$$P_m + P_b \leq 72800 \text{ psi.}$$

Assuming average radial stress  $\sigma_r = -\Delta p$ , the governing criterion for maximum allowable bending moment becomes,

$$\frac{\Delta p R_m}{2t} + \frac{P}{A} + \frac{Mc}{I} + \Delta p = 72800, \text{ for tensile bending,}$$

$$\frac{\Delta p R_m}{t} + \frac{Mc}{I} - \frac{P}{A} = 72800, \quad \text{for compressive bending.}$$

where  $R_m$  = tube mean radius, in.

$A$  = cross-sectional area, in<sup>2</sup>

$I$  = moment of inertia, in<sup>4</sup>, and

$c$  = OD/2



For the case of a 40% remaining wall tube, the maximum allowable moment was calculated to be 418 in-lb.

Results of the primary stress evaluation are summarized in Tables 2 and 3 for steam generators A/C and B, respectively. As indicated by the results, the maximum ratio of actual to allowable bending moment (in the degraded region) is 0.92, and all configurations are acceptable in accordance with the ASME Code primary stress allowable. It is to be noted that, for configurations with loss of lateral support, the drag moments would reduce further if tubes were partially supported, thus providing significant additional margin.

#### 5.4 Fatigue Evaluation

As in the case of normal operating loads, the fatigue evaluation was performed conservatively using the ASME Code approach and a stress concentration factor of 4.0 to account for the presence of any cracks.

Results of the fatigue evaluation are summarized in Table 4. Note that this table lumps the limiting configurations from all three steam generators. The maximum fatigue usage occurred for Row 13 - one plate removed configuration and was calculated to be  $\sim 0.06$  per second of the transient. Since the analyses were based on peak momentum flux input and as seen from Figures 3 and 4, since the RMS value of the transient peak lasts for less than half a second, the maximum expected usage during the transient is less than 0.05. Thus, pre-existing degradation associated with a 40% remaining wall indication will not propagate into a double-ended tube rupture during the postulated SLB blowdown.

## 6.0 SUMMARY AND CONCLUSIONS

Structural integrity of unsleeved peripheral tubes under the assumption of uniform degradation localized near the tube sheet has been evaluated subject to the normal operating and worst case secondary side blowdown loads. The limiting blowdown loads occur during a postulated main steam line break since for this break a potentially larger break opening is available compared to a main feed line break.

Tube configurations with and without anti-vibration bar supports in the U-bend were evaluated. For a 2.0-inch long uniformly degraded region on the hot leg at the top of the tube sheet, the depth of penetration was assumed to be 60% of nominal wall based on the 50% plugging margin and a 10% allowance for continued operation\*. For tubing in steam generators A and C, the analyses accounted for the potential loss of lateral support (at the lower two plates for up to the second row tubes and at the first plate for all tubes beyond the second row tubes) due to flow slot hour-glassing and consequent ligament cracking. These support configurations conservatively bound the actual support conditions in the steam generators based on photographic evidence and visual examinations. In steam generator - B, no indications of tube restrictions and/or flow slot hour-glassing exist. The tubing in SG - B was therefore analyzed assuming integral supports.

The SLB blowdown loads were obtained conservatively assuming an instantaneous, double-ended break and a discharge coefficient of 1.0. In computing the fluid loads on the tubes, the most limiting effects of initial water level, initial power level, and changes in the flow areas due to tube denting and location and flexibility of the down-comer resistance plate were included.

The degraded tubing was evaluated for low amplitude-high cycle fatigue during normal operation. For the postulated SLB condition, the structural integrity evaluation considered both the primary stress intensity evaluation in accordance with the Appendix F requirements in Section III of the ASME Code and a (high amplitude - low cycle) fatigue

---

\*For tube evaluation under normal operating loads, the depth of penetration was conservatively assumed to be 73% of nominal wall consistent with the minimum required wall associated with the maximum primary-to-secondary pressure differential.

analysis to evaluate the potential of double-ended tube rupture due to the propagation of existing degradation under the influence of flow-induced stresses. The evaluation of primary stresses included the combined effects of primary-to-secondary pressure, bending moments due to flow-induced vibrations and fluid drag forces, and axial tube loads due to tube-baffle interaction.

For normal operation, all configurations analyzed were found to be acceptable. The maximum alternating stress intensity was calculated to be 1965 psi (for a peripheral tube in Row 2 with loss of support at both lower plates) versus the allowable high-cycle fatigue endurance limit of 13,700 psi.

For the SLB condition, tube configurations with assumed loss of lateral support(s) were predicted to be fluid-elastically unstable. The analytically calculated maximum stability ratio was 1.39. However, the analyses utilized a number of conservative assumptions, notably, the discharge coefficient of 1.0, loss of full lateral support at the lower plate(s), and uniform flow through the bundle corresponding to the peak momentum - flux during the transient. Under the influence of momentum flux distributions typical of that during a SLB (that is, a rather short peak duration and a significant decay in the peak values on the successive inner row tubes) the fluid-elastic response would tend to depend more on the RMS value rather than the peak momentum flux value. Also, any partial support would be sufficient to stabilize the vibration amplitudes, making the tube respond practically the same as if it were fully supported. Therefore, during an actual blowdown, fluid-elastic instability is not expected to occur.

The primary mechanisms for tube bending are thus, drag and turbulence. Conservatively combining the two effects on an absolute basis, the bending moment in the 60% uniformly degraded tube region ranged between 163 in-lb (Row 48 - all plates integral) and 386 in-lb. (Row 2 - lower two plates removed). The allowable moment in accordance with Appendix F of the code requirement is 418 in-lb. Thus, from the viewpoint of primary stress allowables, 40% remaining wall is acceptable even for the assumed limiting configuration.

Again, assuming the alternating stresses are associated with the calculated maximum moment of 386 in-lb, and a stress concentration factor of 4.0, the worst case fatigue usage based on the transient load distribution is expected to be  $\sim 0.05$ . Thus, pre-existing crack(s) associated with a 40% remaining wall indication will not propagate leading to tube failure under the influence of dynamic loads during a postulated SLB.

In summary, based on the analyses of primary and alternating stress effects, it is concluded that peripheral, unsleeved tubes with up to a 40% remaining wall indication and a potential loss of lateral support at the lower (one or two) support plates meet the applicable design requirements in Section III of the ASME Code.

## 7.0 REFERENCES

1. Bertsch, O. L., "Steam Line Break Analysis for the SCE San Onofre Power Plant Steam Generator Internals", WNEP-82-20, Westinghouse Nuclear Component Division, Pensacola, FL, August, 1982.
2. Hydraulic Analysis of Postulated Steam Line Break for SCE (Model 27) Steam Generator, MPR-743, MPR Associates, Inc., Washington D.C., August, 1982.
3. M. J. Pettigrew and D. J. Gorman, "Experimental Studies in Flow-Induced Vibration to Support Steam Generator Design, Part III. Vibration of Small Tube Bundles in Liquid and Two Phase Cross Flow", AECL 5804, June 1977.
4. H. J. Connors, "Flow-Induced Vibration and Wear of Steam Generators", Nuclear Technology Volume 55, November, 1981.
5. Letter SGPE-1521(82) from A. Y. Lee, "Velocity and Density Data", May 19, 1982, NTD, Pittsburgh, PA.
6. Idel'Chik, I.E., "Handbook of Hydraulic Resistance", Section 8, 1966.
7. Thomson, W. T., "Vibration Theory and Applications", Prentice Hall, Inc., 1965 (Figure 4-6).
8. Vagins, M., et. al., "Steam Generator Tube Integrity Program - Phase I Report", NUREG/CR-0718, September, 1979.

TABLE 1  
 SUMMARY OF FLOW INDUCED VIBRATION EVALUATION  
 PEAK TUBE RESPONSES DURING NORMAL  
 OPERATION

Analysis Case	Max. Amplitude, In. (node location)*	Highest Predominant Frequency, HZ	73% DEGRADED REGION+		
			Bending Moment in - lb	Bending Stress $\sigma$ psi	Alt. Stress Intensity, $S_a$ , psi **
1. 2nd Row Tube					
a) all plates integral	.0007 (16, 20)	33.0	.952	195.	803.
b) 1st TSP removed	.0049 (10)	14.1	2.24	459.	1892.
c) 1st & 2nd TSP removed	.0103 (12)	6.7	2.33	476.	1965.
2. 13th Row Tube					
a) all plates integral	.0046 (20)	36.9	1.45	297.	1224.
b) 1st TSP removed	.0049 (10)	14.1	2.31	472.	1948.
3. 48th Row Tube					
a) all plates integral	.0005 (12, 16, 20)	48.8	.875	179.	739.
b) 1st TSP removed	.0049 (10)	14.1	2.25	460.	1899.

a,b,c

\*Refer to Figure 1 for node locations

+ Simulated tube degradation in the form of (OD) thinning over a 2.0 inch length hot leg tube end at the top of the tubesheet.

\*\* $S_a = SCF \times \frac{E_{actual}}{E_{code}} \times \sigma$ , with  $SCF = 4.0$ ,  $E_{actual} = 29.2 \times 10^6$  psi and  $E_{code} = 28.3 \times 10^6$  psi

TABLE 2

SUMMARY OF PRIMARY STRESS EVALUATION OF A 40% REMAINING WALL  
PERIPHERIAL TUBE DURING A STEAM LINE BREAK  
SG. A and C - LOAD CASE 18, REFERENCE (2)

ANALYSIS CONFIGURATION	MAX. TUBE DEFLECTION, IN.			STABILITY RATIO	MOMENTS AT TUBESHEET, IN-LBS			RATIO** $M_t/M_A$
	NODE* No.	DRAG	PEAK TURBULENT AMPLITUDE		DRAG $M_d$	PEAK TURBULENCE $M_v$	TOTAL $M_t = M_d + M_v$	
1. 2nd Row Tube								
a) All plates integral.	8	0.056	0.0155	1.059	145	24	169	0.40
b) TSP 1 Removed	11	0.234	0.0511	1.235	250	33	283	0.68
c) TSP 1 & 2 Removed	13	0.521	0.0686	1.308	356	30	386	0.92
2. 13th Row Tube								
a) All plates integral	8	0.056	0.0161	1.057	145	36	181	0.43
b) TSP 1 Removed	11	0.234	0.0389	1.350	250	36	286	0.68
3. 48th Row Tube								
a) All plates integral	8	0.056	0.0102	0.585	145	18	163	0.39
b) TSP 1 Removed	10	0.234	0.0240	1.394	250	21	271	0.65

\* See Figure 5 for node locations. For Row 48 Model, node No. 10 corresponds to the first TSP location.

\*\*Maximum allowable total moment at the tubesheet,  $M_A = 418$  in-lbs. is based on ASME Section III, Appendix F Primary Stress Allowable of  $P_m + P_b = 72800$  psi,  $\Delta p = 1200$  psi and axial load  $P = 100$  lbs.

TABLE 3

SUMMARY OF PRIMARY STRESS EVALUATION OF  
A 40% REMAINING WALL PERIPHERAL TUBE DURING A STEAM LINE BREAK  
SG. B - LOAD CASE 19, REFERENCE (2)

ANALYSIS CONFIGURATION	MAX. TUBE DEFLECTION, IN.			STABILITY RATIO	MOMENTS AT TUBESHEET, IN-LBS.			RATIO** $M_t/M_A$
	NODE* NO.	DRAG	PEAK TURBULENT AMPLITUDE		DRAG $M_d$	PEAK TURBULENCE $M_v$	TOTAL $M_t = M_d + M_v$	
1. 2nd Row Tube a) All plates integral.	8	0.060	0.0156	0.983	157	24	181	0.43
2. 13th Row Tube a) All plates integral.	8	0.060	0.0160	1.058	157	35	192	0.46
3. 48th Row Tube a) All plates integral.	8	0.060	0.0105	0.601	157	18	175	0.42

\* See Figure 5 for node locations. For Row 48 Model, node No. 10 corresponds to the first TSP location.

\*\*Maximum allowable total moment at the tubesheet,  $M_A = 418$  in-lbs. is based on ASME Section III, Appendix F Primary Stress Allowable of  $P_m + P_b = 72800$  psi,  $\Delta p = 1200$  psi and axial load  $P = 100$  lbs.



TABLE 4

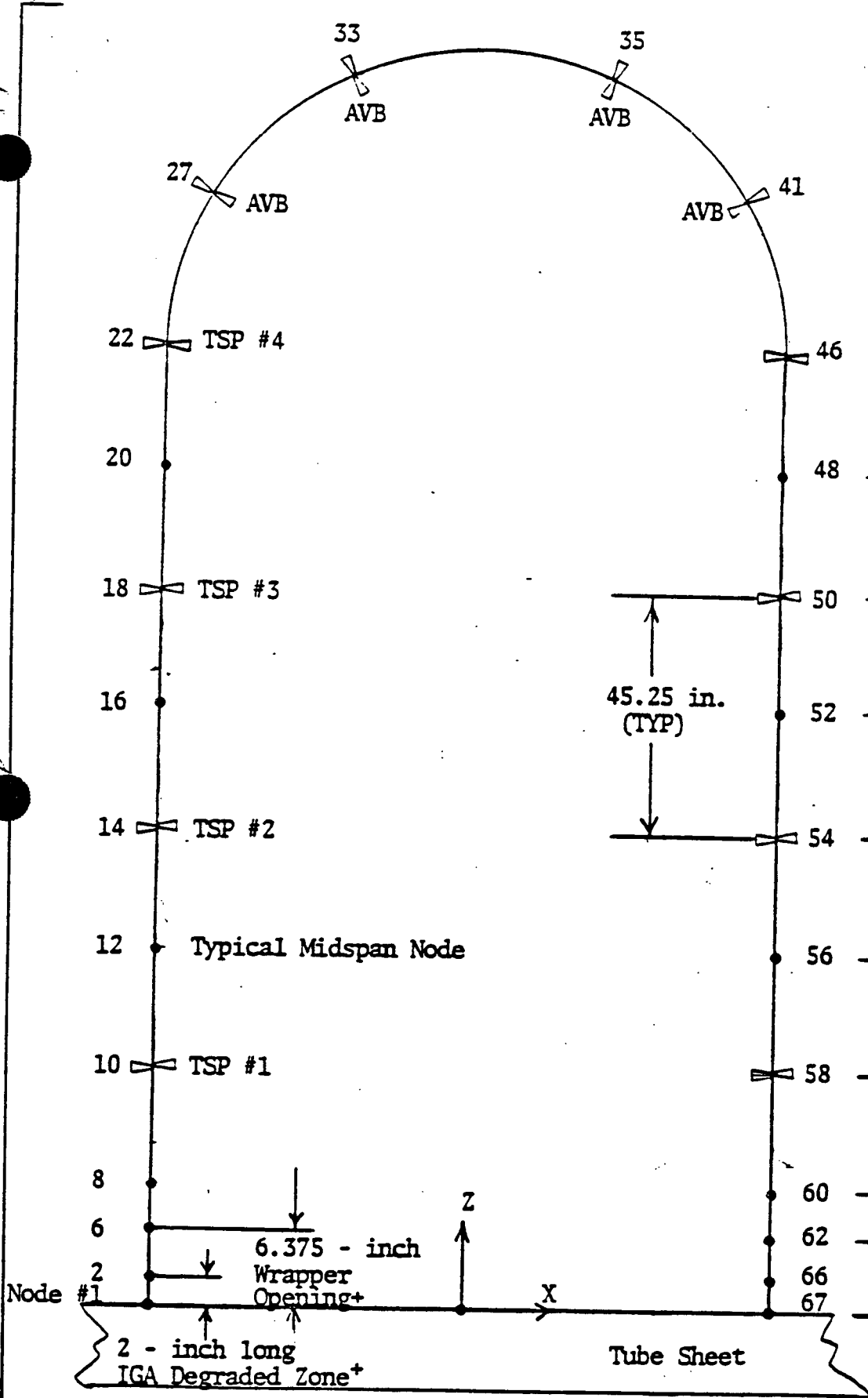
SUMMARY OF FATIGUE USAGE DUE TO SLB BLOWDOWN LOADS  
ON A 40% REMAINING WALL PERIPHERAL TUBE

ANALYSIS CONFIGURATION	MAXIMUM MOMENT M, IN. LB.	NOMINAL BENDING STRESS $\sigma$ , PSI	ALTERNATING STRESS INTENSITY* $S_a$ , PSI	ALLOWABLE CYCLES N	GOVERNING FREQUENCY FOR FIV f, HZ	FATIGUE USAGE PER SECOND OF TRANSIENT f/N
Row 2:						
a) All plates integral <sup>@</sup>	181	23869	107227	1058	37.10	.035
b) TSP 1 Removed	283	37320	167653	268	14.60	.054
c) TSP 1 and 2 Removed	386	50902	228748	114	6.86	.06
Row 13:						
a) All plates integral <sup>@</sup>	192	25319	113741	875	43.52	.05
b) TSP 1 Removed	286	37715	169427	260	14.58	.056
Row 48:						
a) All plates integral <sup>@</sup>	175	23081	103687	1186	46.00	.049
b) TSP 1 Removed	271	35737	160542	305	14.62	.048

$$*S_a = SCF \times \frac{E_{actual}}{E_{code}} \times \sigma \text{ with } SCF = 4.0, E_{actual} = 29.2 \times 10^6 \text{ psi. and } E_{code} = 26.0 \times 10^6 \text{ psi.}$$

<sup>@</sup>Only Applicable Cases for SG-B.

a, b, c



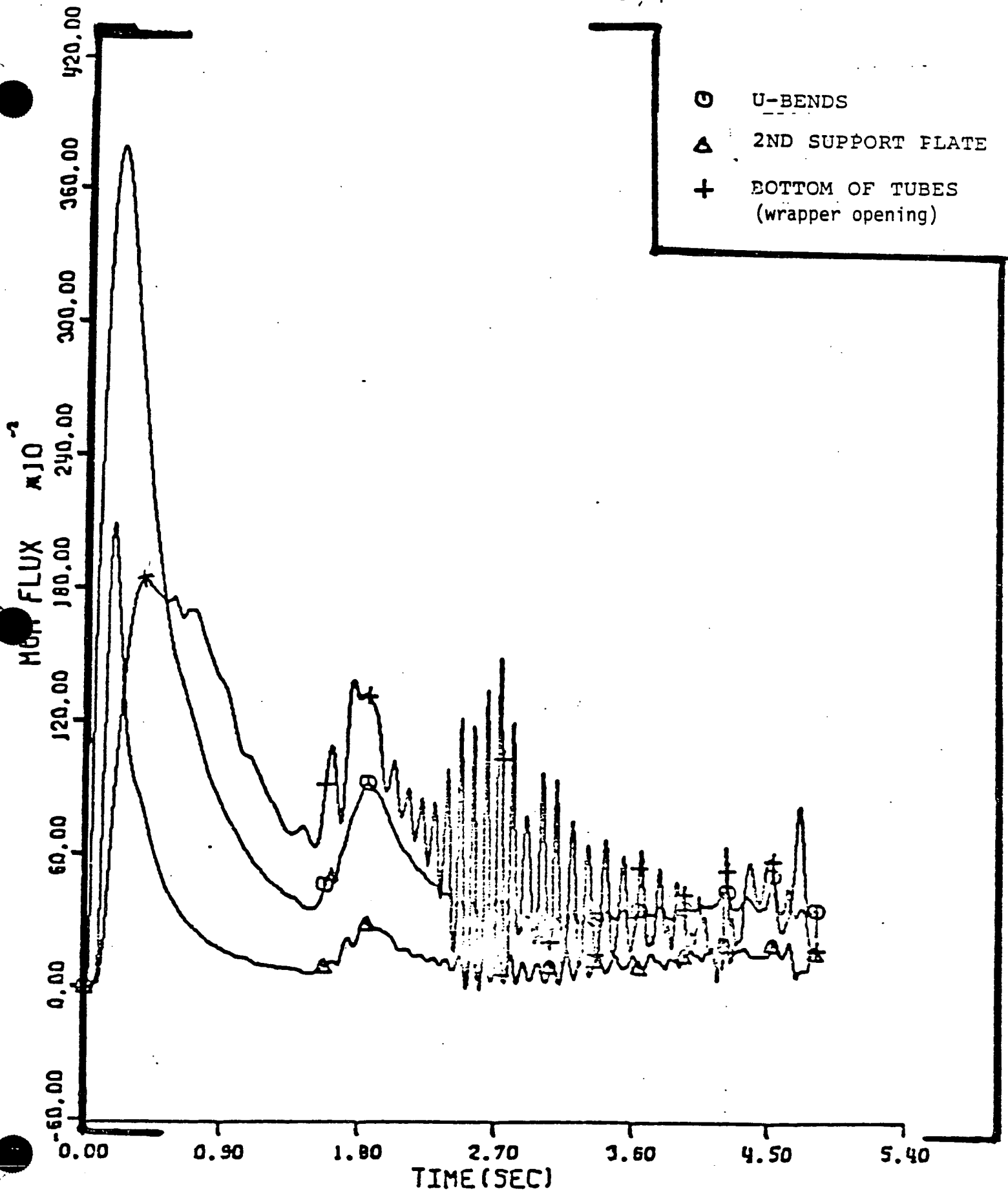
VELOCITY (Ft/Sec)	DENSITY (Lb/Ft <sup>3</sup> )
10.6* (average value over U-bend)	6.0
9.2	7.4
8.1	8.5
7.3	10.0
6.1	12.0
5.2	14.5
3.5	21.5
2.3	48.
1.92	48.
9.0*	48.

45.25 in.  
(TYP)

\*Radial Velocities,  
All Other Are Axial  
Or Parallel

+ Not to Scale

FIGURE 1 Schematic of a Finite Element Tube Model with Applicable Velocity and Density Distribution During Normal Operation.

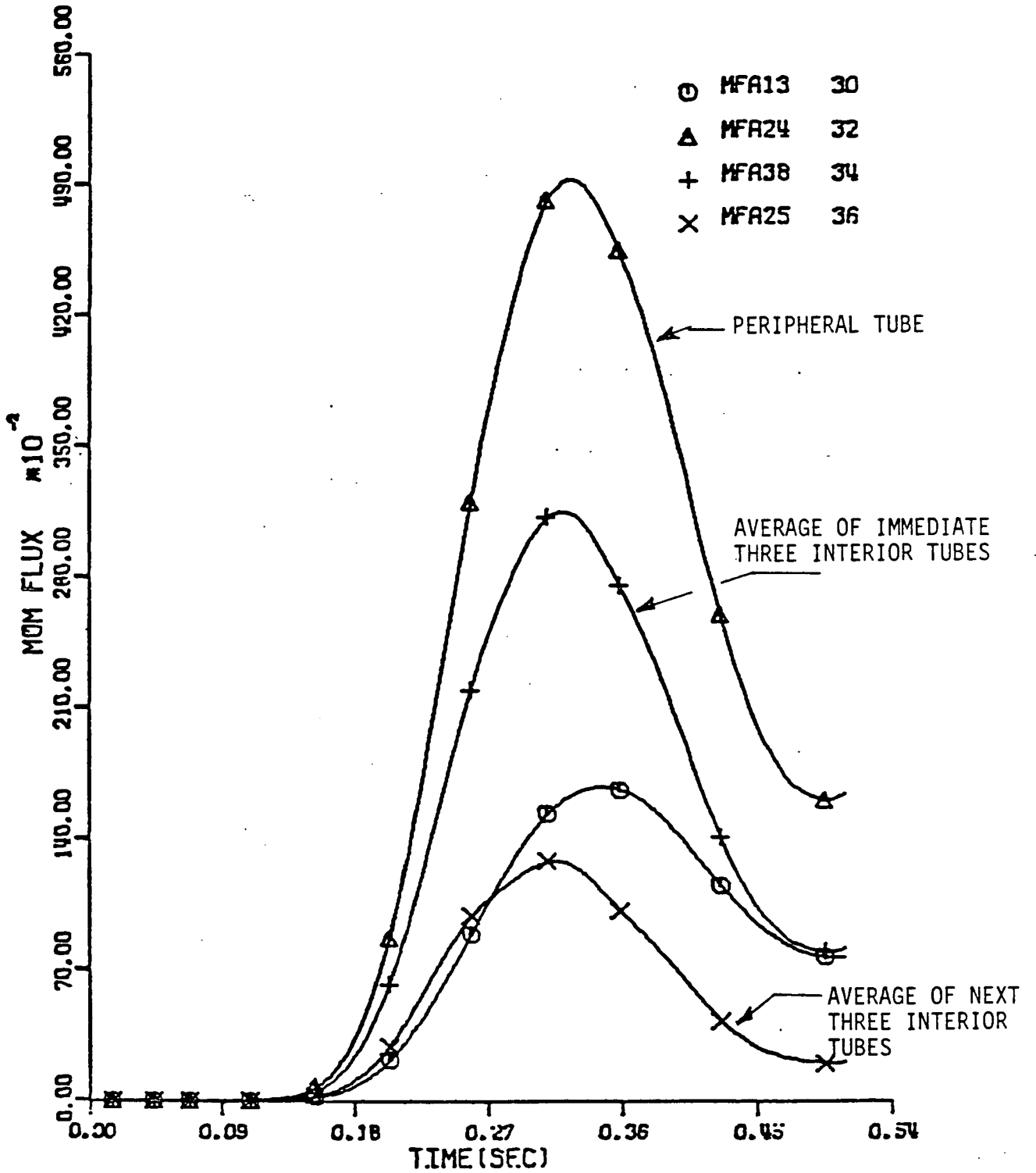


E STEAM LINE BREAK - WATER AT TOP SUPPORT PLATE - NO LOAD - 2.78 DRP area

Figure 2 Typical Momentum-Flux Variations During Postulated Main Steam Line Break

11.52.26.

08/24/82

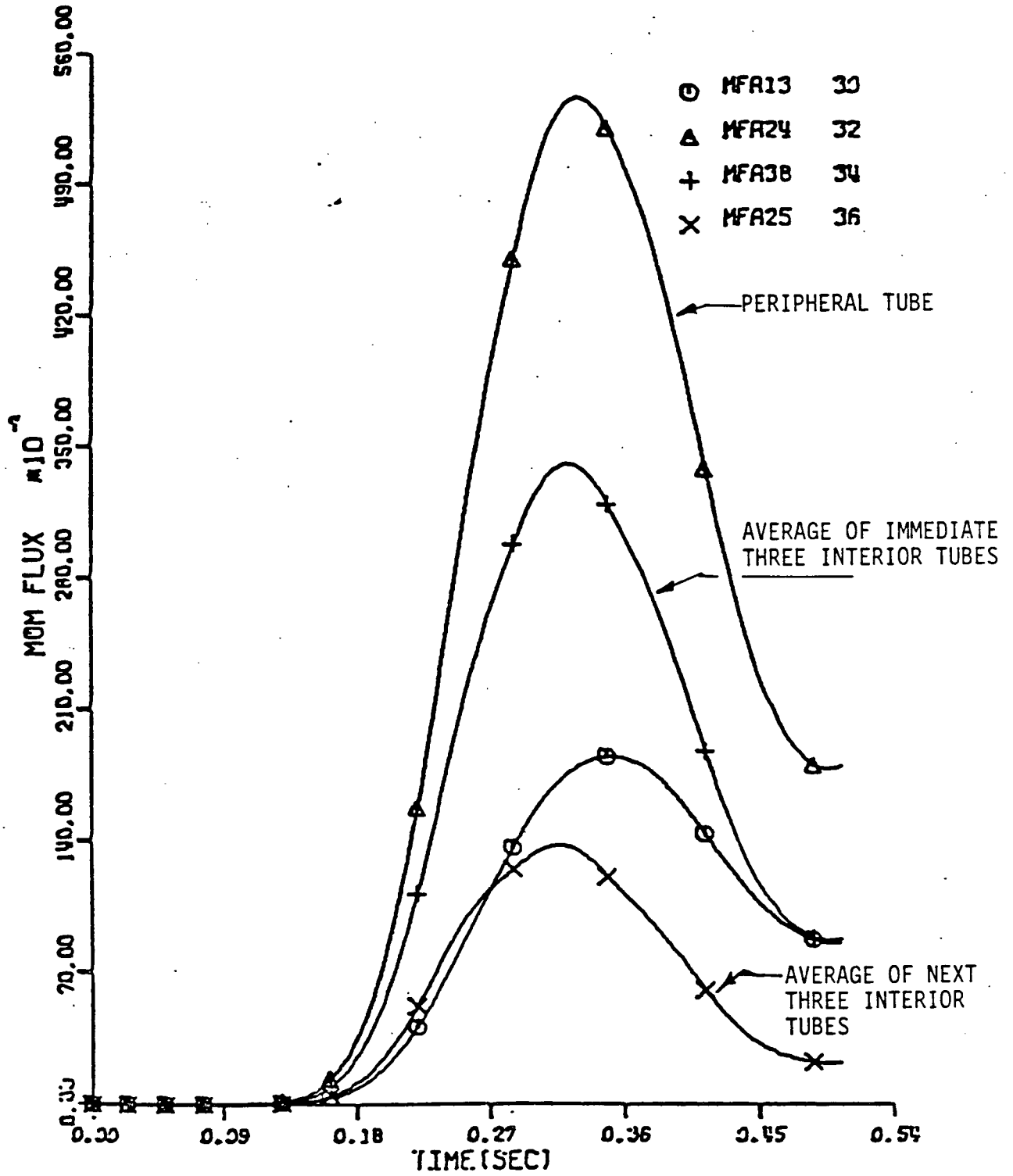


SCE STEAM LINE BREAK - WATER AT FEED RING - VARIABLE 3.20 DRP - DENT CORROSION

FIGURE 3 MOMENTUM FLUX VARIATIONS AT TUBESHEET SG A/C - CASE 18, REFERENCE (2)

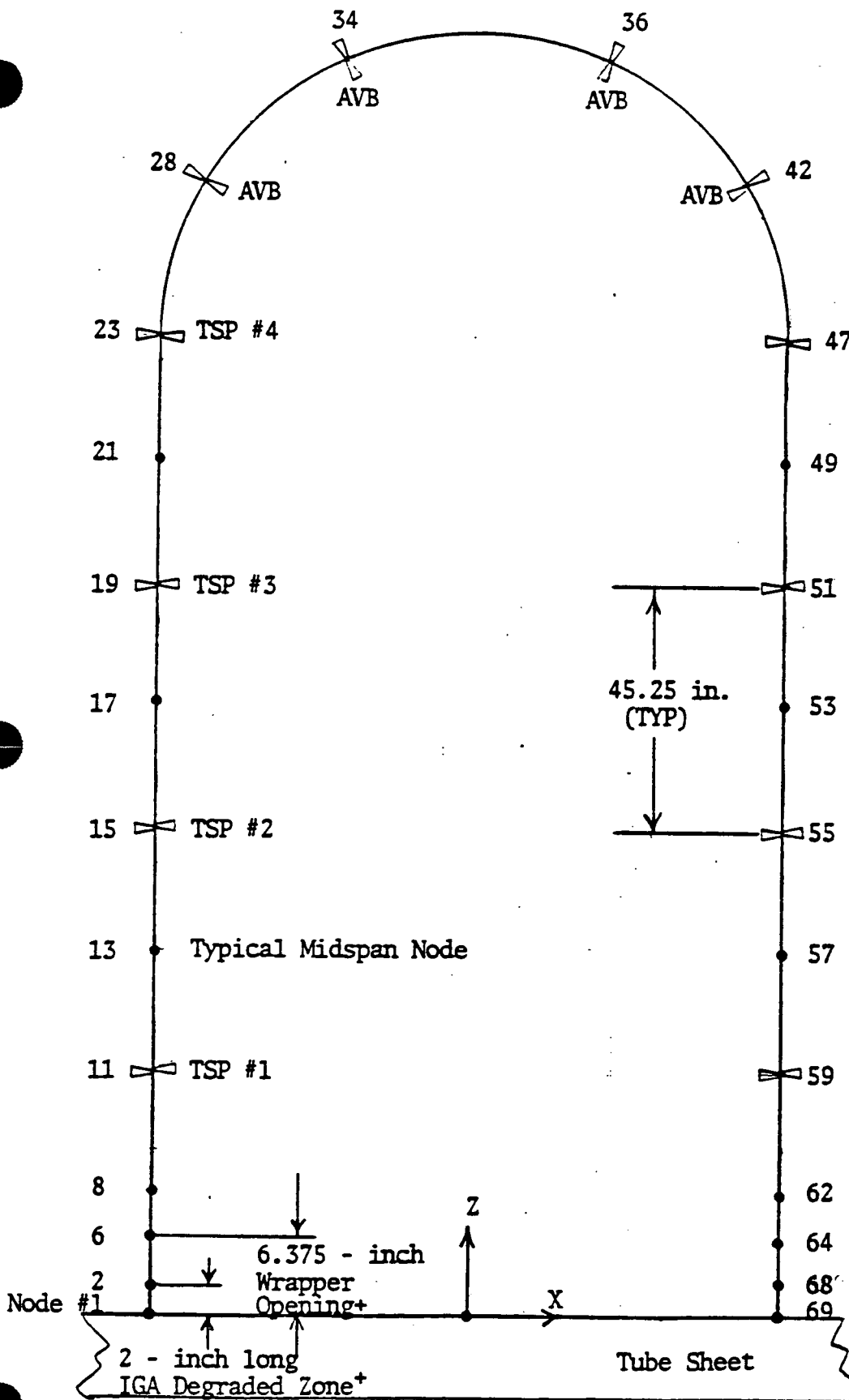
11.50.16.

08/24/82



SCE STEAM LINE BREAK - WATER AT FEED RING - VARIABLE 3.50 DRP - DENT, CORROSIC

FIGURE 4 MOMENTUM FLUX VARIATIONS AT TUBE SHEET SG B - CASE 19, REFERENCE (2)



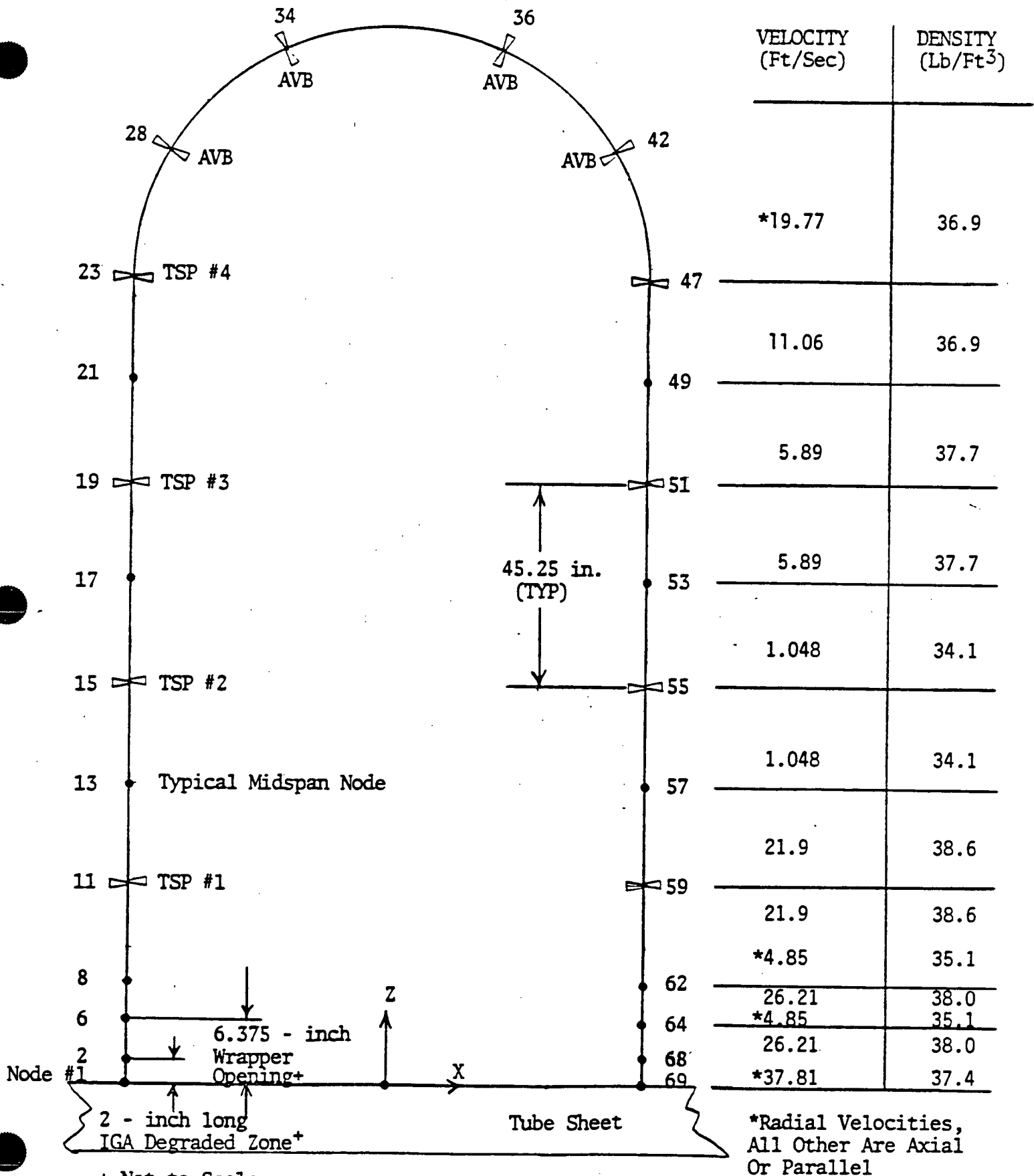
VELOCITY (Ft/Sec)	DENSITY (Lb/Ft <sup>3</sup> )
*19.93	37.0
11.15	37.0
6.02	37.9
6.02	37.9
1.25	35.3
1.25	35.3
21.36	38.8
21.36	38.8
* 4.61	35.4
24.89	38.2
* 4.61	35.4
24.89	38.2
*36.12	37.6

\*Radial Velocities,  
All Other Are Axial  
Or Parallel

+ Not to Scale

VELOCITY AND DENSITY DISTRIBUTION DURING A POSTULATED STEAM LINE BREAK BLOWDOWN  
MAXIMUM CROSSFLOW AT TUBESHEET (SG-A/C, CASE 18 IN REFERENCE 2)

FIGURE 5



VELOCITY AND DENSITY DISTRIBUTION DURING A POSTULATED STEAM LINE BREAK BLOWDOWN  
 MAXIMUM CROSSFLOW AT TUBESHEET (SG-B, CASE 19 IN REFERENCE 2)

FIGURE 6

HYDRAULIC ANALYSIS OF POSTULATED  
STEAM LINE BREAK FOR SCE (MODEL 27)  
STEAM GENERATOR

This section provides a summary  
of the results calculated in  
MPR Report 743 dated  
August 1982.



## I. INTRODUCTION

This report presents the results of several postulated steam line break transients for the SCE (Model 27) steam generator, as requested by Nuclear Technology Division, Westinghouse. In each case an instantaneous, complete break of the steam line immediately downstream of the steam nozzle is assumed. A total of 19 steam line break transients are calculated from hot standby (zero power) initial conditions. The following initial water levels are considered: the top tube support plate, downcomer resistance plate, lower deck plate, feedwater ring, swirl vane and mid-deck plate. In addition the effects of the following parameters are considered: downcomer resistance plate flow area, tube support plate flow area, sludge pile on tubesheet, variable downcomer resistance plate flow area and a venturi flow nozzle at the steam exit.

The results are summarized in Section II of this report and are discussed in more detail in Section III. The computer model of the SCE (Model 27) steam generator is also described in Section III. The plotted output results are presented in Appendix A.

These calculations are performed with the computer program TRANFLO which is documented in Appendix C. A preprocessor program, PRETRAN, is used to generate input to TRANFLO. The input data calculations are presented in Appendix B. Appendix D contains the computer output.

## II. SUMMARY

Thermal hydraulic transients following a postulated steam line break are analyzed for the SCE (Model 27) steam generator. Table II-1 summarizes the initial conditions of each case.

Table II-2 summarizes the maximum pressure drops and loads, calculated across steam generator internals. The maximum vertical wrapper load is 371,200 pounds. The maximum pressure drop across the top tube support plate is 10.31 psi and the combined maximum load on all tube support plate is 121,300 pounds.

Table II-3 summarizes the maximum calculated momentum fluxes across the tube bundle for steam generator B; Table II-4 summarizes the maximum momentum fluxes applicable to steam generators A and C. The maximum cross-flow momentum flux and corresponding velocity at the bottom of the tube bundle are 53,476 lbs/ft-sec<sup>2</sup> and -37.81 ft/sec respectively. The maximum cross-flow momentum flux and corresponding velocity at the middle of the tube span between the bottom tube support plate and tubesheet are 1630 lbs/ft-sec<sup>2</sup> and -7.30 ft/sec respectively. The maximum momentum flux and corresponding velocity across the U-bends are 35,372 lbs/ft-sec and 30.57 ft/sec, respectively.

Summaries of calculated loads, velocities and momentum fluxes are presented in Section III of this report. The plots for all monitored variables for the 19 transients analyzed are presented in Appendix A.

TABLE II-I

SUMMARY OF INITIAL CONDITIONS OF POSTULATED  
STEAM LINE BREAK TRANSIENTS

<u>CASE</u>	<u>WATER LEVEL</u>	<u>DRP (1) FLOW AREA (FT<sup>2</sup>)</u>	<u>DENTING AND CORROSION OF TUBE SUPPORT</u>	<u>SLUDGE EFFECT INCLUDED</u>	<u>VENTURI IN STEAM LINE</u>	<u>DETAILED CROSS FLOW REGION MODEL</u>
1	Top Tube Support	3.92	No	No	No	No
2	DRP (1)	3.92	No	No	No	No
3	Lower Deck Plate	3.92	No	No	No	No
4	Feedwater Ring	3.92	No	No	No	No
5	Swirl Vanes	3.92	No	No	No	No
6	Mid-Deck Plate	3.92	No	No	No	No
7	Feedwater Ring	3.92	Yes	No	No	No
8	Feedwater Ring	3.92	Yes	No	No	Yes
9	Feedwater Ring	3.92	Yes	Yes	No	Yes
10	Feedwater Ring	2.42	No	No	No	No
11	DRP (1)	2.42	No	No	No	No
12	Top Tube Support Plate	2.42	Yes	No	No	No
13	Feedwater Ring	3.92	No	No	Yes	No
14	Feedwater Ring	2.42	Yes	No	No	No
15	Feedwater Ring	Variable (2)	Yes	Yes	No	Yes
16	Feedwater Ring	Variable (3)	Yes	Yes	No	Yes
17	Top Tube Support	Variable (4)	No	No	No	Yes
18	Feedwater Ring	Variable (2)	Yes	No	No	Yes
19	Feedwater Ring	Variable (3)	Yes	No	No	Yes

(1) Downcomer Resistance Plate

(2) Initial flow area is 3.20 ft<sup>2</sup>, applicable to steam generators A or C.

(3) Initial flow area is 3.50 ft<sup>2</sup>, applicable to steam generator B.

(4) Initial flow area is 2.42 ft<sup>2</sup>, corresponding to minimum, fully lowered area.

TABLE II-2

SUMMARY OF WORST CASE LOADS  
ON STEAM GENERATOR INTERNALS (LB)

<u>STEAM GENERATOR COMPONENT</u>	<u>MAXIMUM VALUE (1)</u>	<u>CASE (2)</u>
Tube Bundle Wrapper	371,200	14
Tube Support Plates (Total)	121,300	12
Top Tube Support Plate	56,800 (10.31) (3)	12
Swirl Vanes	130,700	10
Lower Deck	161,400	10
Wrapper Cone	56,930	3
Sum of Swirl Vanes, Lower Deck and Wrapper Cone	323,600	10
Downcomer Resistance Plate	189,300	11
Feed Ring	50,700	16
Mid-deck Plate	200,400	6
Secondary Separator Plate	599,500	6
Secondary Separator	368,600	6
Perforated Dished Head	2,912,100	6

(1) Upward loads are positive; downward loads are negative.

(2) See Table II-1 for definition of cases.

(3) Pressure differential in psi.

TABLE II-3  
SUMMARY OF WORST CASE  
TUBE BUNDLE MOMENTUM FLUXES  
STEAM GENERATOR B

<u>LOCATION</u>	<u>VELOCITY</u> (Ft/sec)	<u>MOMENTUM FLUX</u> (lbs/ft-sec <sup>2</sup> )	<u>CASE</u>
U-bends	30.57 (1)	35,372	1
Bottom of Bundle at Tubesheet	-37.81 (2)	53,476	19
Mid-span Between Tubesheet and Bottom Support Plate	-7.30	1630	16

(1) Positive flow is upwards.

(2) Negative flow is radial outward.

TABLE II-4

SUMMARY OF WORST CASE  
TUBE BUNDLE MOMENTUM FLUXES  
STEAM GENERATORS A AND C

<u>LOCATION</u>	<u>VELOCITY</u> (Ft/sec)	<u>MOMENTUM FLUX</u> (lbs/ft-sec <sup>2</sup> )	<u>CASE</u>
U-bends	30.57 (1)	35,372	1
Bottom of Bundle at Tubesheet	-36.12 (2)	49,081	18
Mid-span Between Tubesheet and Bottom Support Plate	-6.42 (2)	1360	15

(1) Positive flow is upwards.

(2) Negative flow is radial outward.

### III. DISCUSSION AND RESULTS

#### A. Description of Computational Model and Discussion of Results

##### 1. SCE (Model 27) Steam Generator Computational Model

The steam line break transients presented in this report are calculated with the TRANFLO computer program documented in Appendix C. The TRANFLO calculational model used for transient Cases 1 through 7 and 10 through 14 (see Table II-1) includes the following elements:

- 20 nodes representing the secondary side steam and water volumes and boundary nodes;
- 23 fluid connectors between the secondary side nodes;
- 9 fluid nodes representing the primary coolant fluid inside the tubes;
- 10 fluid connectors between the primary side nodes;
- 9 heat nodes representing the tube bundle;
- 9 heat connectors between the primary side and the tubes and 18 heat connectors between the tubes and the secondary side.

Figures III-1 through III-3 identify these fluid nodes, fluid connectors, heat nodes and heat connectors.

This model is used to calculate loads on steam generator internals based on worst case combinations of initial water level and current steam generator conditions including tube support corrosion, downcomer resistance plate position and tubesheet sludge as discussed with Westinghouse and also specified in References 9, 12 and 13. The worst case transients with respect to cross-flow momentum flux are repeated with a second, more detailed model which allows more accurate calculation of velocities and momentum flux in the

vicinity of the tubesheet. This more detailed model is also used to calculate the transients with a variable downcomer resistance plate area, discussed in Section III.C.1, below.

The more detailed model divides the region between the tubesheet and lowest tube support plate into ten secondary side nodes interconnected by cross-flow and axial flow connectors, as depicted in Figures III-4 through III-6. This model is used for Cases 8, 9 and 15 through 19, as defined by Table II-1.

The preprocessor program, PRETRAN, is used to obtain input data for TRANFLO. All input calculations are presented in Appendix B.

The flow out of the steam break is calculated with the Moody two-phase critical flow model with a discharge coefficient of 1.0. Recent work reported in Reference 8 indicates that one-dimensional critical flow models such as Moody tend to overpredict actual flow rates because they neglect the two-dimensional nature of the flow at the entrance to the break. Based on the length to diameter ratio of the SCE (27 Series) steam nozzle, it appears that the Moody model used in this report may overpredict the flow rate out of the steam nozzle by 10 to 15 percent. Sensitivity analyses were performed which indicate the tube bundle wrapper loads and momentum flux loads across the tubes presented in this report would be reduced by approximately 20% if the break flow is reduced by 15%. To predict accurately the break flow for the SCE steam nozzle, a two-dimensional analysis would be required. In lieu of such an analysis no reduction in critical flow rate due to two-dimensional effects is assumed in this report.

## 2. Description of Calculated Transients

Steam line breaks are calculated from hot standby (zero power) with initial water levels at the top tube support plate, downcomer resistance plate, lower deck plate, feed ring, swirl vanes and mid-deck plate. Hot standby initial conditions result in maximum loads on steam generator internals because they provide a distinct water level inside the tube bundle wrapper. During a steam line break the steam volume above the water



level depressurizes more quickly than the water volume below the water level thereby maximizing the pressure differences and loads across the steam generator internals. Previous analyses of postulated steam line break transients (Reference 1) confirm that worst case tube bundle wrapper loads occur for hot standby initial conditions.

Sensitivity calculations are also performed to determine the effects of downcomer resistance plate flow area, tube support plate flow area, sludge pile on tubesheet, variable downcomer resistance plate flow area and a venturi flow nozzle at the steam exit. Each of these effects is discussed below in Section III-C. A summary table of cases analyzed is included in Section II, Table II-1.

### 3. Summary of Results

Cases 1 through 6 allow a determination of the effect of initial water on steam generator loads and momentum fluxes. Cases 7, 10 and 13 show the sensitivity of the calculated results to the effects of the downcomer resistance plate flow area, denting and corrosion in the tube support plates and a flow-limiting venturi in the steam outlet nozzle, respectively. Cases 11, 12 and 14 combine the worst initial conditions for calculating limiting loads on the downcomer resistance plate, top tube support plate and tube bundle wrapper, respectively.

Cases 8, 9 and 15 through 19 employ a more detailed nodalization model to calculate worst case momentum fluxes in the tube bundle and to evaluate the effect of the sludge pile on the tubesheet. Cases 15 through 19 include the effect of increasing the flow area around the downcomer resistance plate during the course of a steam line break. This increasing area results from the calculated deformation of the downcomer resistance plate due to pressure loads applied to the plate during the course of the transient, and is discussed in more detail below. Cases 15 and 16 include the effect of the sludge pile.

Computer input and sample computer output for each of these transients is included in Appendix D. Complete computer output for the monitored variables is provided separately on microfiche. The calculated loads are summarized in Table III-1. The cross-flow momentum fluxes across the tube bundle are summarized in Tables III-2 through III-6. The worst case loads are summarized in Table II-2.

Results plotted in Appendix A include pressure drops and loads across steam generator internals, tube bundle velocities and momentum flux values as functions of time during each transient. Appendix A includes the identification of the plotted variables and plots for each of the 19 transients.

## B. Discussion of Calculated Results for Steam Generator Internals

### 1. Tube Bundle Velocities and Momentum Fluxes

The velocities and momentum flux ( $\rho V^2$ ) are of greatest interest at the U-bends and in the cross-flow region at the bottom of the tube bundle. The fluid velocity and momentum flux across tubes in the bundle result in fluid forces on the tubing. The momentum flux is not necessarily maximum at the same time peak velocity is achieved since fluid densities vary considerably during the transient. Calculation of momentum flux and velocity is described in Appendix C.

Table III-3 lists the velocities and momentum fluxes throughout the tube bundle for steam generators A and C at the time the cross-flow momentum flux is maximum near the tubesheet. This maximum occurs for Case 19: water level at feed ring, variable downcomer resistance plate flow area with an initial area of 3.20 ft<sup>2</sup>, denting and corrosion at the tube support plates, detailed cross-flow region model. Table III-4 lists the same variables for steam generator B with an initial downcomer flow area of 3.50 ft<sup>2</sup>. Table III-5 lists the velocities and momentum fluxes throughout the tube bundle at the time when the cross-flow momentum flux is maximum at the middle of the tube span between the bottom tube support plate and tubesheet. This maximum occurs for Case 16: same

as Case 19, described above, but with the addition of the sludge pile (see Section III.C.2, below).

Table III-6 lists the velocities and momentum fluxes across the tube bundle at the time when the cross-flow momentum flux is maximum at the U-bend region. This maximum occurs for Case 1: water level at top tube support plate, maximum downcomer resistance plate flow area, using the simplified nodalization model for the cross-flow region.

## 2. Pressure Drops and Loads Across the Tube Support Plates

The load on each of the four tube support plates is calculated as the form loss pressure drop (based on pipe tap flow coefficients) multiplied by the flow area upstream of each plate. The total tube support plate load is the sum of the loads on the four tube support plates.

Table III-7 summarizes the loads and pressure drops across the tube support plates and the other wrapper load components at the time the total load on all four tube support plates is maximum and at the time the load is maximum across the top tube support plate. The maximum total tube support plate load is 121,300 pounds; the maximum top tube support plate load is 56,800 pounds. Both of these maxima occur for Case 12: water level at top tube support plate, minimum downcomer resistance plate flow area, denting and corrosion at the tube support plates.

Based on previous model calculations, the maximum pressure differentials and loads across the lower plates will not exceed the maximum pressure differentials and loads across the top tube support plate.

## 3. Tube Bundle Wrapper Load

The tube bundle wrapper load is the sum of the loads on the lower deck plate, vertical component of the load on the conical section of the tube bundle wrapper, swirl vanes and all tube support plates. The wrapper load due to skin friction drag along the surface of the tube bundle wrapper was determined to be less than one percent of the total wrapper load. Consequently, this drag load

is considered negligible and is not included in the total wrapper load calculations presented in this report. A more detailed description of the calculation of wrapper load is given in Appendix C.

Table III-8 lists the total wrapper load and its components at the time the wrapper load is a maximum and when the sum of the loads on the swirl vanes, lower deck plate and wrapper cone is maximum. The sum of the loads on the swirl vanes, lower deck plate, and wrapper cone is the load on the wedge support of the tube support plates.

The maximum vertical load on the tube bundle wrapper is 371,200 pounds acting in the upward direction. This occurs for Case 14: initial water level at the feedwater ring, minimum downcomer resistance plate flow area, denting and corrosion at the tube support plates.

The maximum sum of the loads on the swirl vanes, lower deck plate, and wrapper cone is 322,900 pounds and occurs for Case 10: water level at feedwater ring, minimum downcomer resistance flow area.

#### 4. Radial Pressure Differentials Across the Wrapper

The radial pressure drop is calculated as the difference in pressures of the two nodes on either side of the tube bundle wrapper corrected for static head due to differences in nodal elevations. Table III-9 presents maximum radial pressure drops across the tube bundle wrapper at several elevations along the wrapper. The maximum radial outward pressure differential is 33 psi with the water level at the feedwater ring (Case 19). The maximum radial inward pressure drop occurs with the initial water level at the top support plate and is 10 psi (Case 17)

#### 5. Mid-deck Plate Load

The mid-deck plate load is the sum of the loads on the portion of the mid-deck plate outside and above the swirl vane downcomer barrels and the upward load on the swirl vane orifices.

As indicated in Table II-2, the maximum total load on the mid-deck plate is 200,400 pounds acting in the upward direction and occurs for Case 6: initial water level at the mid-deck plate, maximum downcomer resistance plate flow area.

The mid-deck plate load is not calculated for every transient. Previous transient model analyses show the mid-deck plate load to be maximum with the initial water level at the mid-deck plate.

6. Horizontal Load on the Secondary Separators

Horizontal loads are calculated on the secondary separators and on the secondary separator perforated plates. As indicated in Table II-2, the maximum total horizontal load on the secondary separators is 368,600 pounds while the maximum load on the secondary separator perforated plates is 599,500 pounds. Both occur for Case 6: water level at mid-deck plate, maximum downcomer resistance plate flow area.

7. Downcomer Resistance Plate

The load on the downcomer resistance plate is the product of the pressure drop due to form loss across the plate and the upstream flow area of the plate. As indicated in Table II-2, the maximum load on the downcomer resistance plate is 189,300 pounds and occurs for Case 11: water level at downcomer resistance plate, minimum downcomer resistance plate flow area. Under this calculated load, the downcomer resistance plate is expected to lift and distort. This effect is discussed further in Section C.1, below.

8. Perforated Dished Head

The load on the perforated dished head is the product of the pressure drop due to form loss across the perforated head and the flow area upstream of the head. As indicated in Table II-2, the maximum load on the perforated dished head is 2,912,100 pounds and occurs for Case 6: water level at mid-deck plate, maximum downcomer resistance plate flow area.

Plots of the load on the perforated dished head presented in Appendix A include an anomalous spike at the peak of the curve for several cases indicating an even higher calculated load than reported in Table II-2. However, this spike reflects a calculational anomaly for a single time step that corresponds to an instantaneous change in connector density and should not be used for evaluating the adequacy of the internals.

C. Sensitivity of Results to Modeling Assumptions

1. Effect of Downcomer Resistance Plate Flow Area

A range of flow areas for the downcomer resistance plate are analyzed for the SCE steam generators. The minimum flow area is  $2.42 \text{ ft}^2$ , (Cases 10, 11, 12 and 14) corresponding to a completely lowered position. (Detailed calculations are included in Appendix B.) Cases 1 through 9 and 13 are analyzed with a flow area of  $3.92 \text{ ft}^2$  corresponding to an average "as shipped" condition. Based on information in Reference 13, the downcomer resistance plates for the SCE steam generators were lowered in the field such that steam generator B has an area of  $3.50 \text{ ft}^2$  and the flow areas for steam generators A and C are  $3.20 \text{ ft}^2$  or less.

Calculations performed by Westinghouse (Reference 12) indicate that during a steam line break some deformation of the downcomer resistance plate assembly will occur. This deformation will increase the flow area around the plate. To take this effect into account, Cases 15 through 19 are calculated with a downcomer resistance plate area which increases during the course of the transient. The increasing flow area is based on the varying calculated load on the downcomer resistance plate during the transient. For Case 17 the initial flow area is  $2.42 \text{ ft}^2$ . For Cases 15 and 18, the initial flow area is  $3.20 \text{ ft}^2$ , applicable to steam generators A and C. For Cases 16 and 19, the flow area is  $3.50 \text{ ft}^2$ , applicable to steam generator B.

The flow area through the downcomer resistance plate determines the flow resistance through the plate. This, in turn, determines how much of the fluid initially in the tube bundle flows into the downcomer and up through the downcomer resistance

plate and how much flows up through the tube bundle and through the swirl vanes.

Maximum flow into and up the downcomer results in maximum momentum fluxes across the bottom of the tube bundle. Thus, the controlling worst case transient for tube bundle momentum flux is with the maximum flow area of Case 19.

The momentum flux across the bottom of the tube bundle when the downcomer resistance plate area is  $2.42 \text{ ft}^2$  is approximately 43 percent of the momentum flux when the area is  $3.92 \text{ ft}^2$ .

On the other hand, maximum flow up through the tube bundle results in maximum tube bundle wrapper loads. Thus, the worst case transient for wrapper load is with the minimum flow area of  $2.42 \text{ ft}^2$ . The wrapper load for the  $3.92 \text{ ft}^2$  area is approximately 93 percent of that for the  $2.42 \text{ ft}^2$  area.

## 2. Effect of Sludge Pile on Tubesheet

A mound of hardened sludge is deposited on both the cold leg and hot leg sides of the tube bundle on top of the tubesheet, as reported in Reference 9. The detailed nodalization model used for calculating maximum tube bundle momentum flux (Case 8) is modified in Cases 9, 15 and 16 to determine the effect of the sludge. The sludge pile represented by these calculations is depicted in Figure III-7; a detailed description of the corresponding model change is included in Appendix B.

The effect of the sludge pile is to decrease the cross-flow momentum flux near the tubesheet by 14 percent and to increase the cross-flow momentum flux at the mid-span between the tubesheet and the bottom tube support plate by approximately 11 percent.

The addition of the sludge pile was found to have a negligible effect (less than one percent increase) on the tube bundle wrapper load, based on calculations with the simpler nodalization model. Consequently, the sludge pile was not included in worst case calculations for the maximum tube bundle wrapper loads.

3. Effect of Denting and Corrosion on Tube Support Plates

Significant amounts of corrosion and denting are reported for the tube support plates. To determine the effect on the steam line break, the flow area through the tube support plates is assumed to be reduced in two ways. First, it is assumed the gap between the tube outside diameter and the nominal hole diameter in the tube support plate is filled with corrosion. Second, it is assumed that the denting causes "hourglassing" of the flow slots in the tube support plates such that one-half the area of the flow slots is lost.

The total reduction in the tube support plate flow area due to denting and corrosion is 10 percent (1.72 ft<sup>2</sup>). This results in a 2 percent increase in the maximum calculated wrapper load and a thirty-two percent increase in the total tube support plate load.

4. Potential Effect of Steam Nozzle Flow Restrictor

Current design Westinghouse steam generators include a flow-limiting venturi in the steam outlet nozzle. A typical venturi nozzle would reduce the maximum break flow area to 35 percent of the steam nozzle area. As a result, the flow out the break would be reduced. Calculations performed with a venturi in the SCE steam line (Case 13) indicate that both the wrapper load and the cross-flow momentum flux are reduced to approximately 23 percent of the unrestricted steam line break configuration.



TABLE III-1

Summary of Maximum Values  
For Loads on Steam Generator Internals (lb)\*

Case	Tube Bundle Wrapper	Swirl Vanes	Lower Deck Plate	Tube Bundle Wrapper Cone	Total Tube Support Plate	Sum of Loads on Swirl Vane Lower Deck Plate and Wrapper Cone
1	187,500	61,300	69,000	23,800	94,700	154,050
2	264,300	91,600	98,800	35,300	79,200	223,800
3	318,900	117,400	130,500	56,900	59,100	285,320
4	332,700	123,900	155,200	55,500	33,900	299,830
5	310,900	113,800	142,200	50,900	24,900	287,650
6	233,900	93,200	113,700	40,600	20,000	220,590
7	339,000	121,700	155,000	55,400	44,600	294,600
10	358,400	130,700	161,400	56,700	35,500	323,600
11	288,500	96,800	108,100	37,400	84,500	N.A.**
12	236,300	71,200	81,100	27,800	121,300	180,060
13	77,400	22,400	46,300	17,200	10,800	74,744
14	371,200	130,200	159,000	56,600	48,700	322,930
15	324,800	118,600	154,100	54,900	40,100	N.A.
16	321,700	116,400	153,700	54,700	39,800	N.A.
17	142,600	50,100	56,400	20,000	85,400	N.A.
18	328,300	118,200	153,900	55,000	42,600	N.A.
19	324,700	117,800	153,500	54,700	42,300	N.A.

\*Positive value is vertical upward.

\*\*Not available; other calculated cases are controlling.

TABLE III-1 (Cont'd)

Summary of Maximum Values  
for Loads on Steam Generator Internals (lb)\*

Case	Mid-deck Plate	Downcomer Resistance Plate	Feedwater Ring	Secondary Separator Plate	Secondary Separator	Perforated Dished Head
1	N.A.**	115,300	800	68,400	71,200	313,200
2	N.A.	136,300	10,300	69,100	111,900	1,268,300
3	N.A.	129,000	9,300	143,900	219,300	2,387,100
4	N.A.	124,400	49,900	244,600	253,000	2,750,300
5	N.A.	98,000	38,100	388,900	313,700	2,785,900
6	200,400	71,900	23,500	599,500	368,600	2,912,100
7	-34,000	124,500	49,900	243,500	253,000	2,766,100
10	-33,800	170,200	49,200	236,400	251,600	2,760,500
11	16,000	189,300	1,900	68,400	104,400	310,700
12	16,000	171,500	-1,542	68,500	66,500	313,200
13	N.A.	27,100	7,700	11,200	21,300	44,700
14	-34,300	168,200	48,300	258,600	264,400	2,647,300
15	N.A.	120,200	50,700	N.A.	N.A.	N.A.
16	N.A.	118,900	50,700	N.A.	N.A.	N.A.
17	11,400	122,500	1,800	68,300	28,900	305,600
18	-33,300	121,200	50,300	N.A.	N.A.	N.A.
19	-33,300	120,800	50,300	N.A.	N.A.	N.A.

\*Positive value is vertical upward.

\*\*Not available; other calculated cases are controlling.

TABLE III-2

Effect of Initial Water Level  
and Modeling Assumptions on  
Cross-Flow Momentum Fluxes  
Across the Tube Bundle\*

CASE	NEAR TUBESHEET (Lb/Ft-Sec <sup>2</sup> )	AT U-BENDS (Lb/Ft-Sec <sup>2</sup> )
1	32,290	33,810
2	26,530	28,940
3	30,820	23,420
4	34,840	17,180
5	31,280	11,930
6	24,000	9,310
7	36,170	16,400
10	15,010	17,810
11	10,200	30,550
12	18,010	32,980
13	7,880	5,270
14	17,750	17,540

\*Momentum fluxes summarized in this table are the sum of the individual steam and water momentum fluxes, calculated with the simpler nodalization model. Worst case momentum fluxes reported in Tables III-3 through III-6 are conservatively based on average two-phase densities and velocities. Calculation of momentum flux is described in Appendix C.

TABLE III-3

Steam Generator B  
Velocities and Momentum Fluxes Across the Tube  
Bundle at the Time When the Cross-Flow Momentum Flux  
is Maximum Near Tubesheet<sup>(1)</sup>

LOCATION	VELOCITY (FT/SEC)	MOMENTUM FLUX LB/FT-SEC <sup>2</sup> )
U-bends (Cross-flow) (2)	19.77	14,435
Below Top Tube Support Plate (Axial flow) (3)	11.06	4518
Above and Below 2nd Tube Support Plate (Axial Flow)	5.89	1308
Above and Below 3rd Tube Support Plate (Axial Flow)	1.048	37.47
Above and Below Bottom Tube Support Plate (Axial Flow)	-21.90	18,531
At Mid-Span Between Bottom Tube Support Plate Tubesheet (Cross-Flow)	-6.17 (4) (-4.85) (5)	1310 (4) (826) (5)
Near Tubesheet (Axial Flow)	-26.21	26,101
Near Tubesheet (Cross-Flow)	-37.81	53,476

(1) Maximum occurs for Case 19: water level at feedwater ring, variable downcomer resistance flow area with an initial area of 3.50 ft<sup>2</sup>, denting and corrosion of tube support plates, detailed model of cross-flow region.  
Time = 0.3274 sec.

(2) Cross-flow is perpendicular to the tubes.

(3) Axial flow is in the vertical direction.

(4) Worst case at this elevation.

(5) At same tube as maximum at tubesheet.

TABLE III-4

Steam Generators A and C  
Velocities and Momentum Fluxes Across the Tube  
Bundle at the Time When the Cross-Flow Momentum Flux  
is Maximum Near Tubesheet<sup>(1)</sup>

LOCATION	VELOCITY (FT/SEC)	MOMENTUM FLUX LB/FT-SEC <sup>2</sup> )
U-bends (Cross-flow) (2)	19.93	14,713
Below Top Tube Support Plate (Axial flow) (3)	11.15	4605
Above and Below 2nd Tube Support Plate (Axial Flow)	6.02	1373
Above and Below 3rd Tube Support Plate (Axial Flow)	1.25	55.20
Above and Below Bottom Tube Support Plate (Axial Flow)	-21.36	17,681
At Mid-Span Between Bottom Tube Support Plate Tubesheet (Cross-Flow)	-5.75 <sup>(4)</sup> (-4.61) <sup>(5)</sup>	1143 <sup>(4)</sup> (753) <sup>(5)</sup>
Near Tubesheet (Axial Flow)	-24.89	23,680
Near Tubesheet (Cross-Flow)	-36.12	49,081

(1) Maximum occurs for Case 18: water level at feedwater ring, variable downcomer resistance flow area with an initial area of 3.20 ft<sup>2</sup>, denting and corrosion of tube support plates, detailed model of cross-flow region.  
Time = 0.3264 sec.

(2) Cross-flow is perpendicular to the tubes.

(3) Axial flow is in the vertical direction.

(4) Worst case at this elevation.

(5) At same tube as maximum at tubesheet.

TABLE III-5

Velocities and Momentum Fluxes Across the Tube Bundle at the Time When the Cross-Flow Momentum Flux is Maximum At Middle of Tube Span between Bottom Tube Support Plate and Tubesheet<sup>(1)</sup>

LOCATION	VELOCITY (FT/SEC)	MOMENTUM FLUX (LB/FT-SEC <sup>2</sup> )
U-Bends (Cross-flow) <sup>(2)</sup>	17.31	10,068
Below Top Tube Support Plate (Axial Flow) <sup>(3)</sup>	9.68	3,151
Above and Below 2nd Tube Support Plate (Axial Flow)	5.05	877
Above and Below 3rd Tube Support Plate (Axial Flow)	0.267	0.533
Above and Below Bottom Tube Support Plate (Axial Flow)	-22.39	17,901
At Mid-Span Between Bottom Tube Support Plate and Tubesheet (Cross-Flow)	-7.30	1,630
Near Tubesheet (Axial Flow)	-27.95	27,131
Near Tubesheet (Cross-Flow)	-34.48	42,010

(1) Maximum occurs for Case 16: water level at feedwater ring, variable downcomer resistance plate flow area, initial downcomer resistance plate flow area of 3.50 ft<sup>2</sup>, denting and corrosion of tube support plate, detailed model of cross-flow region, sludge pile on tubesheet. Time = 0.3810 sec.

(2) Cross-flow is perpendicular to the tubes.

(3) Axial flow is in the vertical direction.

TABLE III-6

Velocities and Momentum Fluxes  
Across the Tube Bundle at the Time  
When the Cross Flow Momentum Flux  
is Maximum at the U-Bend Region<sup>(1)</sup>

LOCATION	AVERAGE VELOCITY (FT/SEC)	MOMENTUM FLUX (LB/FT/SEC <sup>2</sup> )
U-Bends (Cross-Flow) (2)	30.57	35,372
Below Top Tube Support Plate (Axial Flow) (3)	17.10	11,070
Above and Below 2nd Tube Support Plate (Axial Flow)	13.59	7365
Above and Below 3rd Tube Support Plate (Axial Flow)	9.34	3505
Above and Below 4th Tube Support Plate (Axial Flow)	3.68	530
Mid-Span between Bottom Tube Support Plate and Tubesheet (Axial Flow)	-2.68	286
At Wrapper Opening (Cross-Flow)	-25.75	26,425

(1) Maximum occurs for Case 1: water level at top tube support plate, maximum downcomer resistance plate flow area. Time = 0.1981 seconds.

(2) Cross-flow is flow in the horizontal direction.

(3) Axial flow is flow in the vertical direction.

TABLE III-7

Summary of Loads and Pressure Drops for  
Worst Case Tube Support Plate Load<sup>(1)</sup>

COMPONENT	TIME OF MAXIMUM TOTAL TUBE SUPPORT PLATE LOAD (lb) (2)	TIME OF MAXIMUM TOP TUBE SUPPORT PLATE LOAD (lb) (3)
Top Tube Support Plate	55,400 (10.06) (4)	56,800 (10.31)
Second Tube Support Plate	36,700 (6.67)	35,900 (6.52)
Third Tube Support Plate	21,300 (3.88)	15,800 (2.87)
Fourth Tube Support Plate	7,820 (1.42)	2,450 (0.45)
Total Tube Support Plate	121,300 (22.03)	110,900 (20.15)
Swirl Vanes	19,900	28,300
Lower Deck Plate	2,850	18,900
Wrapper Cone	1,530	6,940

(1) Worst case tube support plate load is Case 12: water level at top tube support plate, minimum downcomer resistance plate flow area, denting and corrosion.

(2) Time = 0.1661 seconds.

(3) Time = 0.2039 seconds.

(4) Pressure differential in psi are given in parenthesis.



TABLE III-8

Summary of Loads on Steam Generator Internals  
For Worst Case Tube Bundle Wrapper Load

COMPONENT	LOAD (LB) (1)	LOADS (LB) (2)
Tube Bundle Wrapper	358,400	371,200
Swirl Vanes	128,900	128,400
Lower Deck	143,500	143,400
Wrapper Cone	51,200	51,000
Sum of Swirl Vanes, Lower Deck, and Wrapper Cone	323,600	322,850
Downcomer Resistance Plate	150,900	150,200
Feed Ring	1,560	1710
Mid-Deck Plate	7,350	7150
Secondary Separator Plate	66,300	59,700
Secondary Separator	80,600	73,200
Perforated Dished Head	293,900	293,300
Tube Support Plates (Total)	34,800	48,400
Top Tube Support Plate	21,600 (3.93) (3)	29,700 (5.40)
Second Tube Support Plate	10,200 (1.85)	14,600 (2.64)
Third Tube Support Plate	2,800 (0.51)	4,000 (0.73)
Fourth Tube Support Plate	200 (0.03)	100 (0.02)

(1) Worst case sum of loads on swirl vanes, lower deck plate, and wrapper cone is Case 10: water level at feed ring, minimum DRP flow area. Time = 0.2919 sec.

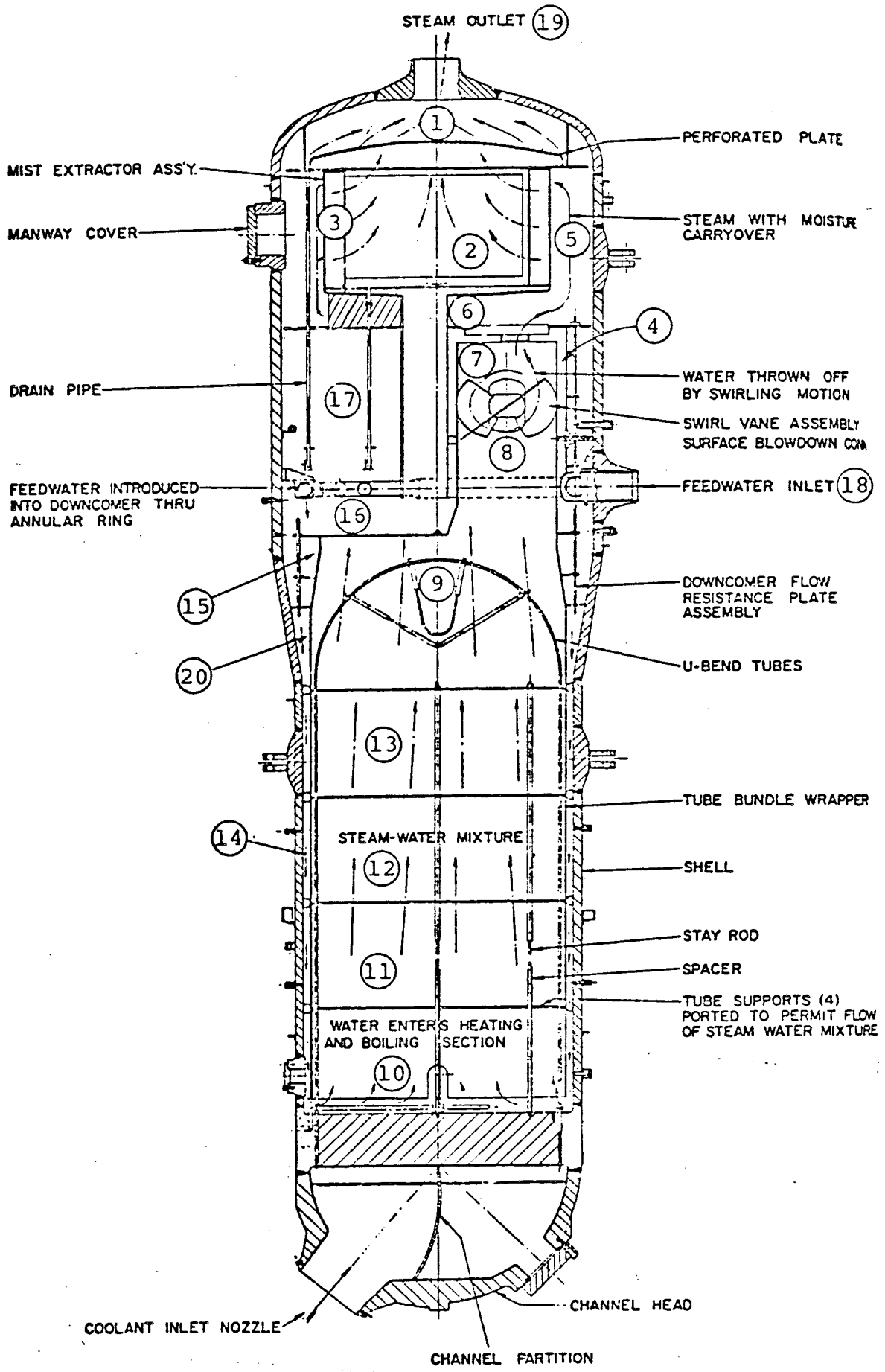
(2) Worst case tube bundle wrapper load is Case 14: water level at feed ring, minimum DRP flow area; denting and corrosion. Time = 0.2946

(3) Pressure differentials in psi are in parenthesis.

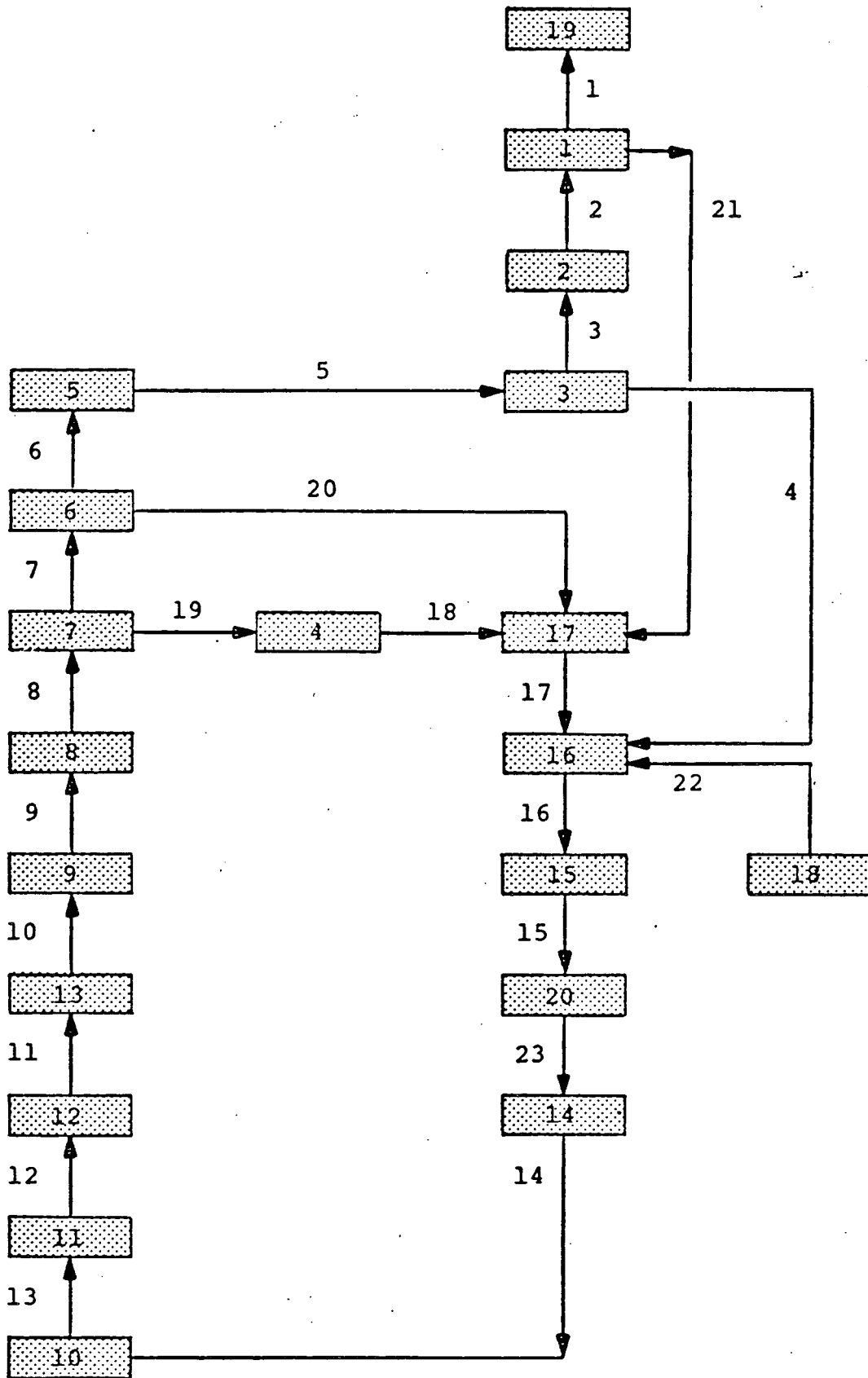
TABLE III-9

Summary of Maximum Radial  
Pressure Differentials for the Tube Bundle Wrapper

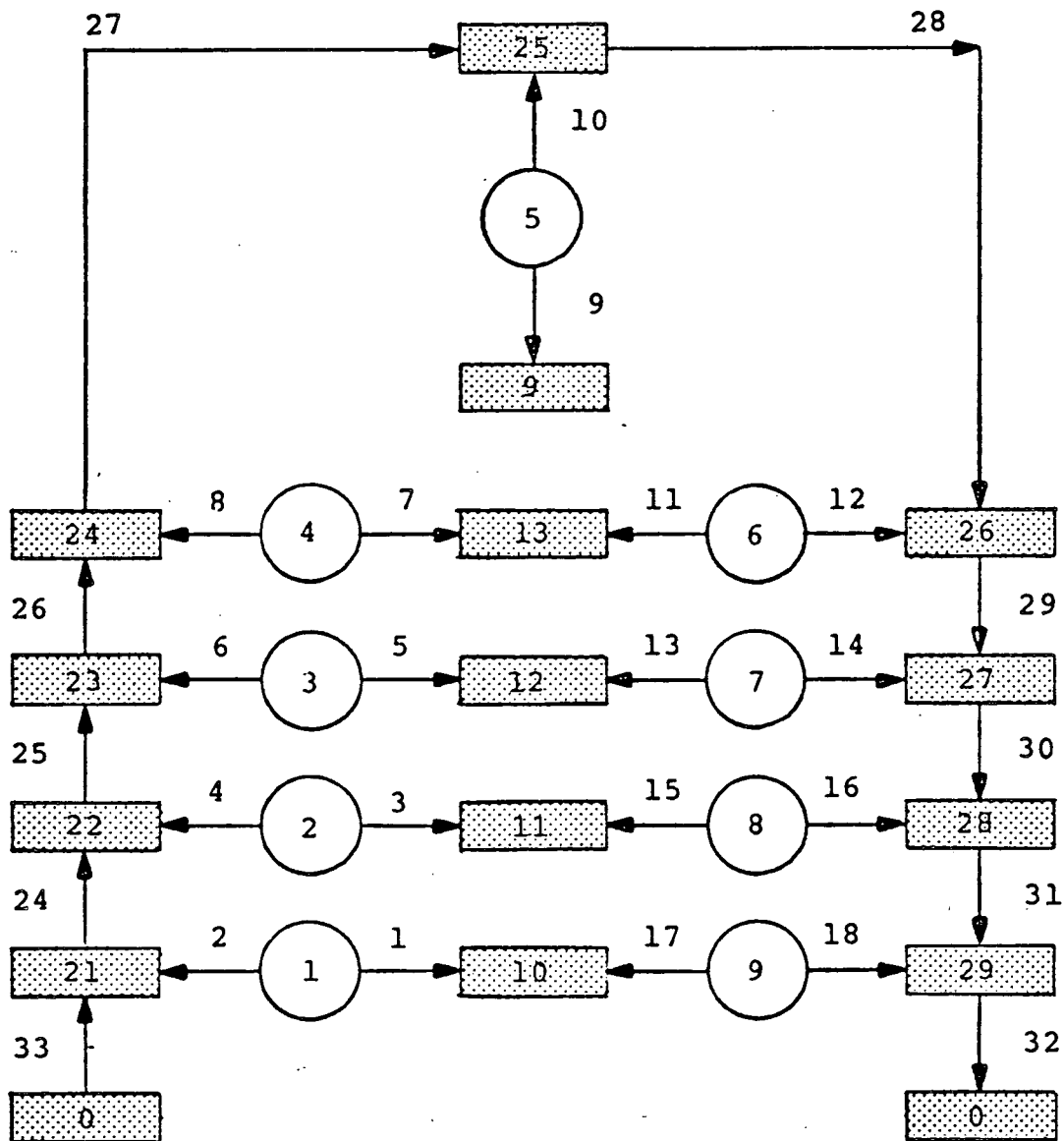
LOCATION	OUTWARD PRESSURE DROP (psi)	CASE	INWARD PRESSURE DROP (psi)	CASE
Between tubesheet and bottom tube support plate	30.340	7	5.69	17
Between bottom tube support plate and third tube support plate	32.64	19	6.68	17
Between third tube support plate and second tube support plate	32.32	1	8.49	17
Between second tube support plate and top tube support plate	28.75	16	10.34	17



FLOW SCHEMATIC  
 27 SERIES (SCE)  
 MODEL 1  
 FIGURE III-1

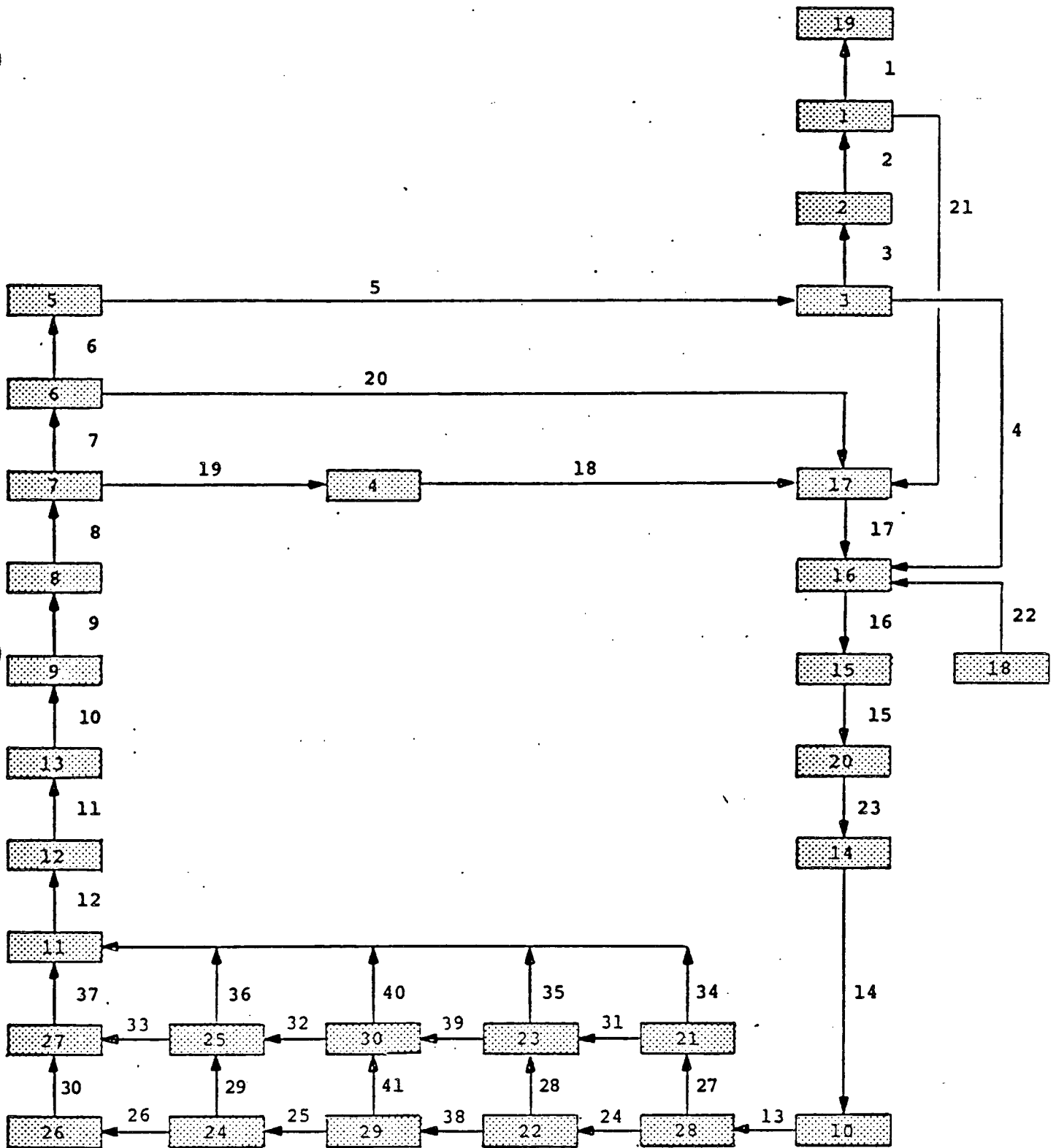


SECONDARY SIDE  
 FLUID NODES AND CONNECTORS  
 MODEL 1  
 FIGURE III-2



PRIMARY SIDE  
 FLUID NODES AND CONNECTORS  
 AND  
 HEAT NODES AND CONNECTORS  
 MODEL 1

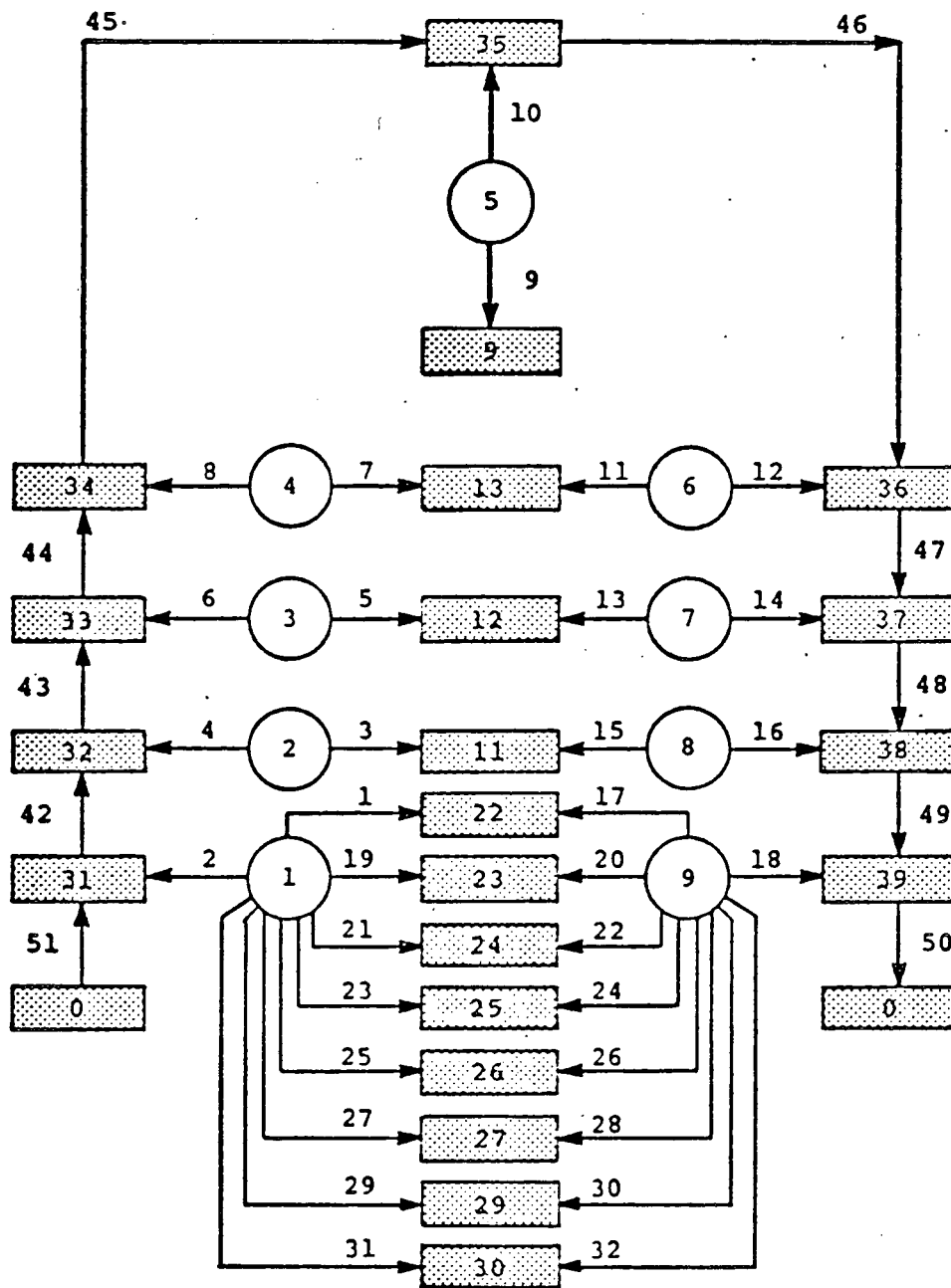
FIGURE III-3



SECONDARY SIDE  
FLUID NODES AND CONNECTORS

MODEL 2

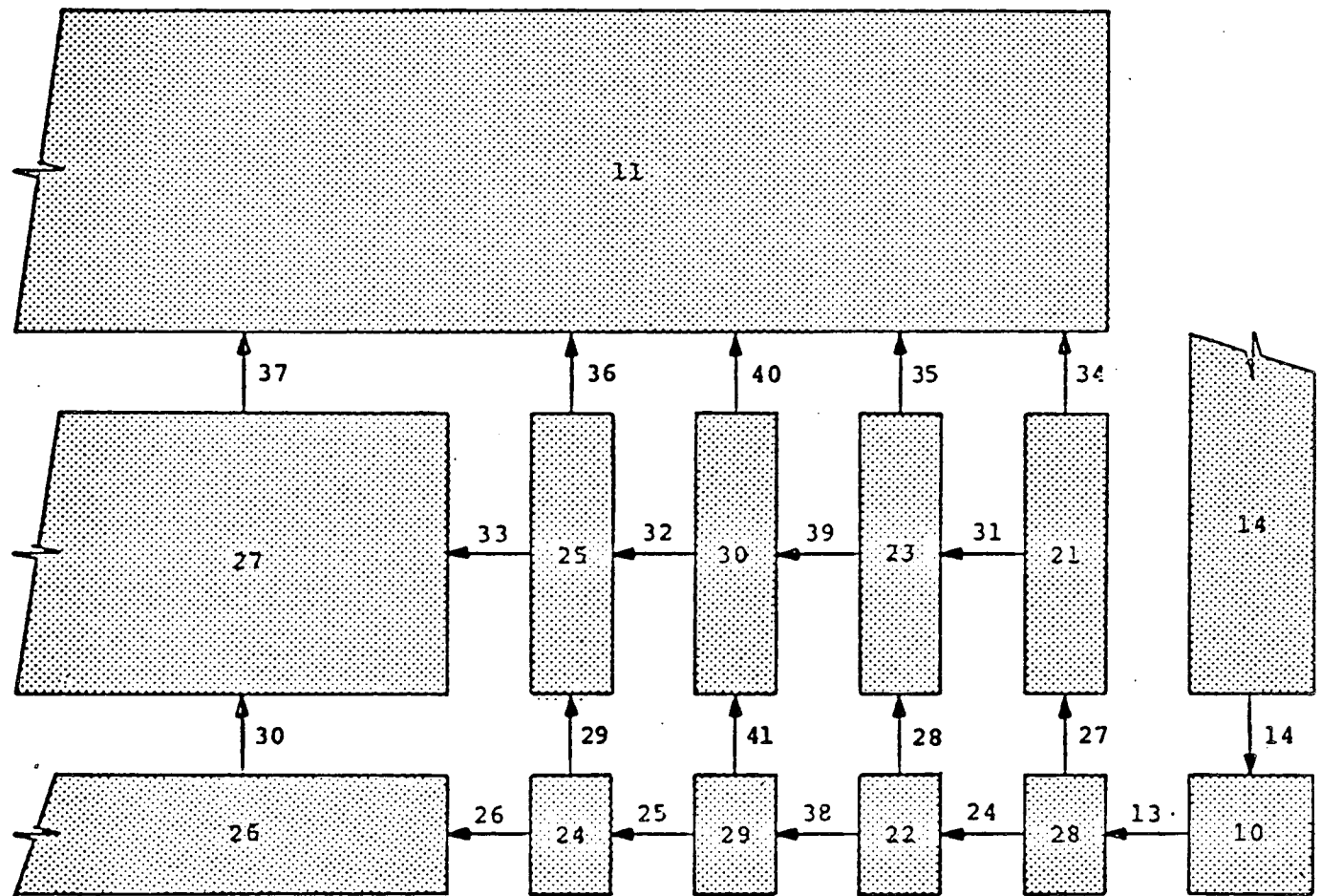
FIGURE III-4



PRIMARY SIDE  
 FLUID NODES AND CONNECTORS  
 AND  
 HEAT NODES AND CONNECTORS

MODEL 2

FIGURE III-5

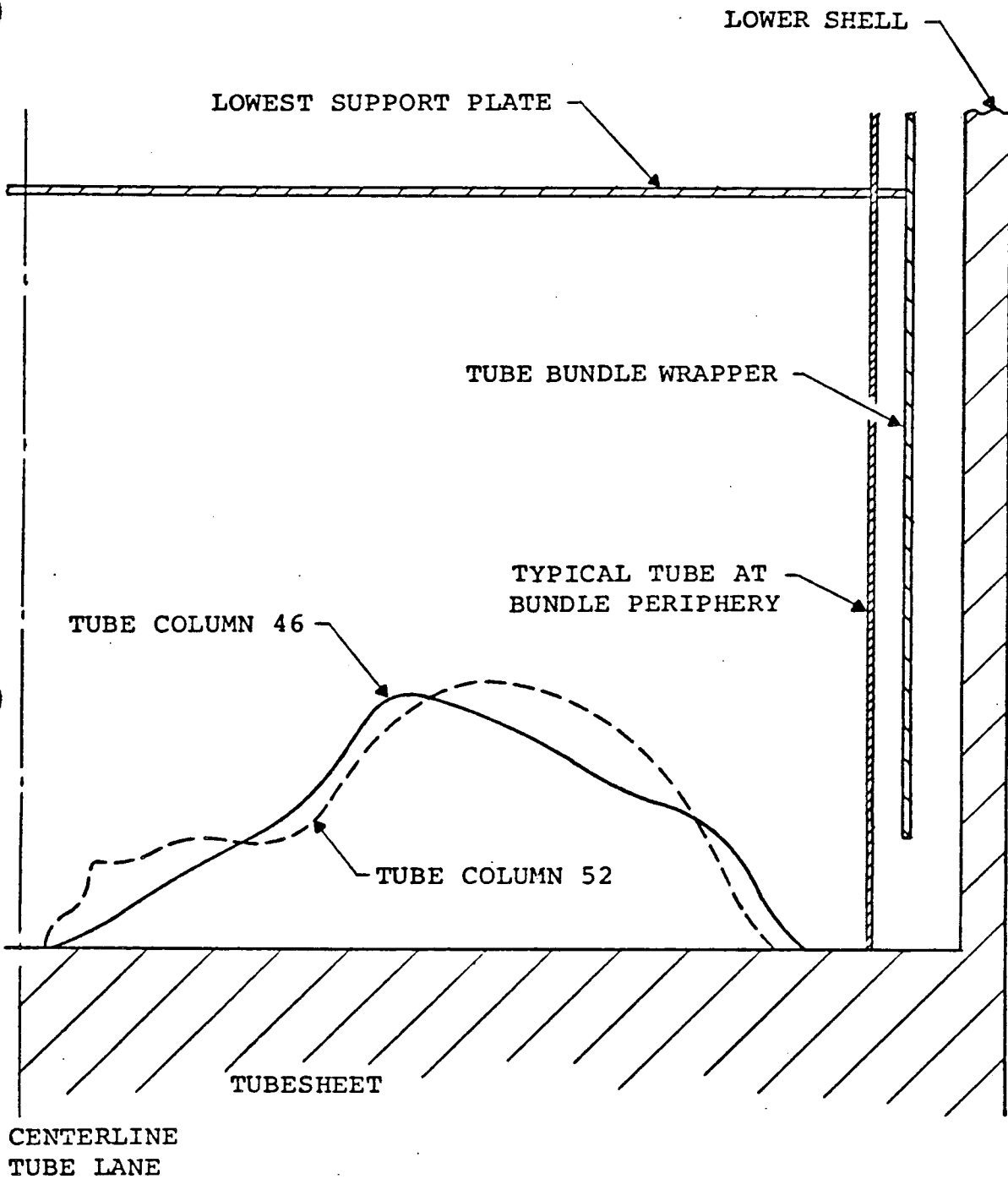


SECONDARY SIDE  
 FLUID NODES AND CONNECTORS  
 LOWER TUBE BUNDLE REGION

MODEL 2

FIGURE III-6





TYPICAL SLUDGE PROFILES  
STEAM GENERATOR A

FIGURE III-7

IV. REFERENCES

1. Hydraulic Analysis of Postulated Steam Line Break for Model 44A Steam Generator, MPR Report 680, June 1981.
2. TRANFLO; A Computer Program for Transient Thermal Hydraulic Analysis with Drift Flux, MPR Report 663, November 1980.
3. 27 Series (SCE) GENF Output Parameters, and 27 Series (SCE) Steam Pressure vs. Load forwarded by Westinghouse letter SGTI-053(82) dated April 21, 1982 from J. D. Roarty to A. Zarechnak (MPR).
4. Westinghouse drawings, 671J541, "27,700 Sq. Ft. Vertical Steam Generator - General Assembly and Final Machining" and 671J547, "27,700 Sq. Ft. Vertical Steam Generator - Tube Bundle Assembly and Details."
5. The following information was transmitted in a telephone conversation from J. D. Roarty (Westinghouse) to A. Zarechnak (MPR) on April 28, 1982:
  - a. There are 1290 holes with a diameter of 59/64 inches in the perforated dished head upstream of the steam nozzle.
  - b. There are 3 drains with a diameter of 1.0 inch from the demister separator (in addition to the large central drains) and also 3 - 1.0 inch drains from the steam dome.
  - c. The vertical opening at the top of the swirl vane riser below the mid-deck plate is approximately 6.5 inches.
  - d. The inner diameter of the swirl vane downcomer barrels is 48.25 inches.
  - e. There is an open annulus approximately 10 inches wide around the mid-deck plate as well as a 25"x5" hatch cover opening.
  - f. The flow area through the perforated plate in front of the demister separators is approximately 19% of the open area.

6. In a telephone conversation on 6-1-82, R. Welder of Westinghouse, Tampa, informed A. Zarechnak of MPR that: (1) the inside radius of the downcomer resistance plate was 4'5-3/8" and the plate thickness was 7-1/2", and (2) the inside diameter of the lower deck is 8'2-1/4" and its thickness is 5/16.
7. In a telephone conversation on 6-1-82, P. Bird of Westinghouse, Tampa informed A. Zarechnak of MPR that the total flow area through the downcomer resistance plate for the "as shipped" San Onofre steam generator was 3.92 feet<sup>2</sup> consisting of 1.44 feet<sup>2</sup> through 117 - 1.5-inch holes and 2.48 feet<sup>2</sup> around edge; total radial dimension between wrapper and shell at the elevation of the downcomer resistance plate is 8.5 inches corresponding to an approach area of 21.12 feet<sup>2</sup>.
8. "Multidimensional Effects in Critical Two-Phase Flow" by J. R. Travis, C. W. Hirt and W. C. Rivard, Nuclear Science and Engineering: 68, 338-348 (1978).
9. Westinghouse Letter SGTI-062(82) dated July 15, 1982 from J. D. Roarty to J. A. Swope.
10. In a telephone conversation on July 9, 1982, J. D. Roarty (Westinghouse) informed J. A. Swope (MPR) that there are 7588 tube holes with a diameter of 49/64 inches and 7524 flow circulations with a diameter of 35/64 inches in each tube support plate.
11. The following information was received from D. J. Green (Westinghouse) in a telephone conversation with J. A. Swope (MPR) on June 21, 1982:

Perforated dished head I.D.	=	8.75 feet
Total perforated dished head height	=	0.958 feet
Perforated head cylinder height	=	0.1979 feet
Perforated head thickness	=	0.04167 feet
Tube bundle wrapper cone height	=	2.25 feet

Tube bundle wrapper upper cylinder height = 0.500 feet  
 Tube bundle wrapper upper cylinder I.D. = 8.1875 feet  
 Secondary separator length = 4.583 feet  
 Secondary separator thickness = 0.667 feet

12. In telephone conversations on August 13 and August 16, 1982, O. Bertsch (W) informed A. Zarechnak (MPR) that under steam line break loadings the downcomer resistance plate (DRP) assembly would rise and deform such that the flow area around the plate increases with load as follows:

<u>Load on DRP (lb)</u>	<u>Added Flow Area(ft<sup>2</sup>)</u>
0	0.00
1,000	1.42
116,362	1.42
150,000	9.77
189,300	13.81

13. In a telephone conversation on August 19, 1982, L. Ermold (Westinghouse) informed A. Zarechnak (MPR) that the "as is" downcomer resistance plate flow area for steam generator B is 3.50 ft<sup>2</sup> and the flow area for steam generators A and C is 3.20 ft<sup>2</sup> or less.

The following discussion is intended to replace the final paragraph on page 6.205 of SE-SP-40(80) Rev. 1:

### Conclusions

During the normal operation, the maximum dynamic bending stress due to flow-induced vibrations of a sleeved tube is [

<sup>a,c</sup>] This level of stress is insignificant, referring to the design fatigue curve in Figure 6.2.4. The cumulative fatigue usage factor of a sleeved tube is thus practically unaffected by flow-induced vibrations.

During a SLB, although the third mode (for case 1) is unstable, it is noted that the ratio is only marginally above 1.0 and that the analysis is based on conservative assumptions of a rather low damping ratio of 1% and relatively high velocities (three times the normal condition velocities). Additionally, the fluid-elastic excitation is self-limiting, that is, with increased vibration amplitudes, the damping increases, resulting in stable motion although with somewhat larger amplitude. From the viewpoint of flow-induced loading, the blowdown duration is typically only [ <sup>a,b,c</sup> ] thereby imposing an insignificantly low number [ <sup>a,b,c</sup> ] of cycles of alternating stress. Therefore, consideration of tube instability during a short duration transient such as a SLB is irrelevant from the viewpoint of tube integrity due to fatigue from flow-induced vibrations. [

<sup>a,b,c</sup>

AGENDA ITEM 4.1 - NDE CAPABILITIES OF REFERENCE JOINT, EXPANSION TRANSITIONS AND SLEEVE ENDS

ECT qualification data have been obtained to demonstrate that an adequate inspection of the sleeve and tube walls can be performed at the expansion transition regions of the upper joint and of the tube wall at and near the sleeve ends using a conventional probe.

In order to constitute an adequate inspection, the tube inspection must be capable of detecting partial wall penetration such that there is [

] <sup>a,b,c</sup>

The present inspection of the sleeved assembly involves the use of a conventional bobbin eddy current probe operated with multiple frequency excitation. Prior to the base line inspection of Unit I (spring 1981), there was work performed to document the sensitivity of the bobbin probe inspection. A result of this work was to place limits on the sensitivity of the conventional coil inspection. At the transitions in the sleeved assembly, degradation equivalent to [ <sup>a,b,c</sup> ] the volume of the ASME calibration standard hole could be detected; this is demonstrated in Figure 4.1-1.

In addition, on any region of the sleeve that was undistorted, the sensitivity of the inspection was consistent with any normal tubing inspection. However, at both the braze joint and the end of the sleeve, no statement about the sensitivity could be made. For these locations, a program of comparison of the eddy current response was adopted. While in the region of the braze, no definitive statement about the condition of the tube could be made from a single measurement, due to the variations in braze signatures. Comparison of changes in the joint response are quite sensitive to the condition of the assembly in this vicinity. Figure 4.1-2 shows the results of inserting a [ <sup>a,b,c</sup> ] notch through the tube wall in a reference joint. The resultant signal is clearly discernable as a change in the [ <sup>a,b,c</sup> ] joint response. For the region of the tube near the sleeve end, Figure 4.1-3 shows the results of putting a [ <sup>a,b,c</sup> ] notch [ <sup>a,b,c</sup> ] through the tube with one end at

the end of the sleeve and extending into the free tube and [ <sup>a,b,c</sup> ] under the sleeve. Since the notch is discernable in both orientations, a crack [ <sup>a,b,c</sup> ] could be found in this location. Similarly, [ <sup>a,b,c</sup> ] uniform wall loss [ <sup>a,b,c</sup> ] centered at the end of the sleeve is detectable, Figure 4.1-4.

With this background of simulations, we believe that the conventional bobbin probe provides an adequate inspection of the sleeved assembly. The overall results are presented in tabular form in Tables 4.1-1 to 4.1-3.

TABLE 4.1-1

INSPECTABILITY OF SLEEVED TUBES  
IN THE BRAZE REGION

BRAZE REGION PRODUCES A COMPLEX SIGNAL  
COMPOSED OF [ <sup>a,b,c</sup> ] AND MAGNETIC OXIDE  
RESPONSES.

DETECTION OF [ <sup>a,b,c</sup> ] IN  
LENGTH IS ACCOMPLISHED BY SIGNATURE  
COMPARISON WITH BASELINE DATA.



TABLE 4.1-2

INSPECTABILITY OF SLEEVED TUBES  
AT EXPANSION TRANSITIONS

BASIS FOR ACCEPTABILITY

DETECT [ <sup>a,b,c</sup> ] DEGRADATION

CAPABILITY

DETECT DEGRADATION SUFFICIENT TO  
PRODUCE AN EC INDICATION [ <sup>a,b,c</sup> ]  
WITH STANDARD BOBBIN PROBE.

APPLIES WITHOUT RESPECT TO DEPTH  
OF PENETRATION BUT CRACKING BELOW  
[ <sup>a,b,c</sup> ] IS GENERALLY NOT  
DETECTABLE.

TABLE 4.1-3

INSPECTABILITY OF SLEEVED TUBES  
AT THE SLEEVE ENDS

SIGNAL PRODUCED AT SLEEVE END POSES LARGE  
AMPLITUDE INTERFERENCE RESULTING FROM ABRUPT  
DIAMETER CHANGE.

DETECTION DEMONSTRATED FOR [ ]<sup>a,b,c</sup>  
THE SLEEVE END.

[ ]<sup>a,b,c</sup>  
ON THE SLEEVE END PRODUCES CLEARLY OBSERVABLE  
RESPONSE.

EXPANSION TRANSITIONS

a,b,c

TOP - 50  
BOT - UP MIX

EXPANSION TRANSITION  
NO FLAW

TOP - 50  
BOT - UP MIX

EXPANSION TRANSITION a,b,c

TOP - 50  
BOT - UP MIX

EXPANSION TRANSITION a,b,c

FIGURE 4.1-2 EFFECT ON E.C. BRAZE RESPC OF [

]THRU THE TUBEWALL

a, b, c

IN MAGNETIC FIELD

IN MAGNETIC FIELD

FIGURE 4.1-3 EFFECT OF TUBING DISCONTINUITIES AT THE END OF THE SLEEVE

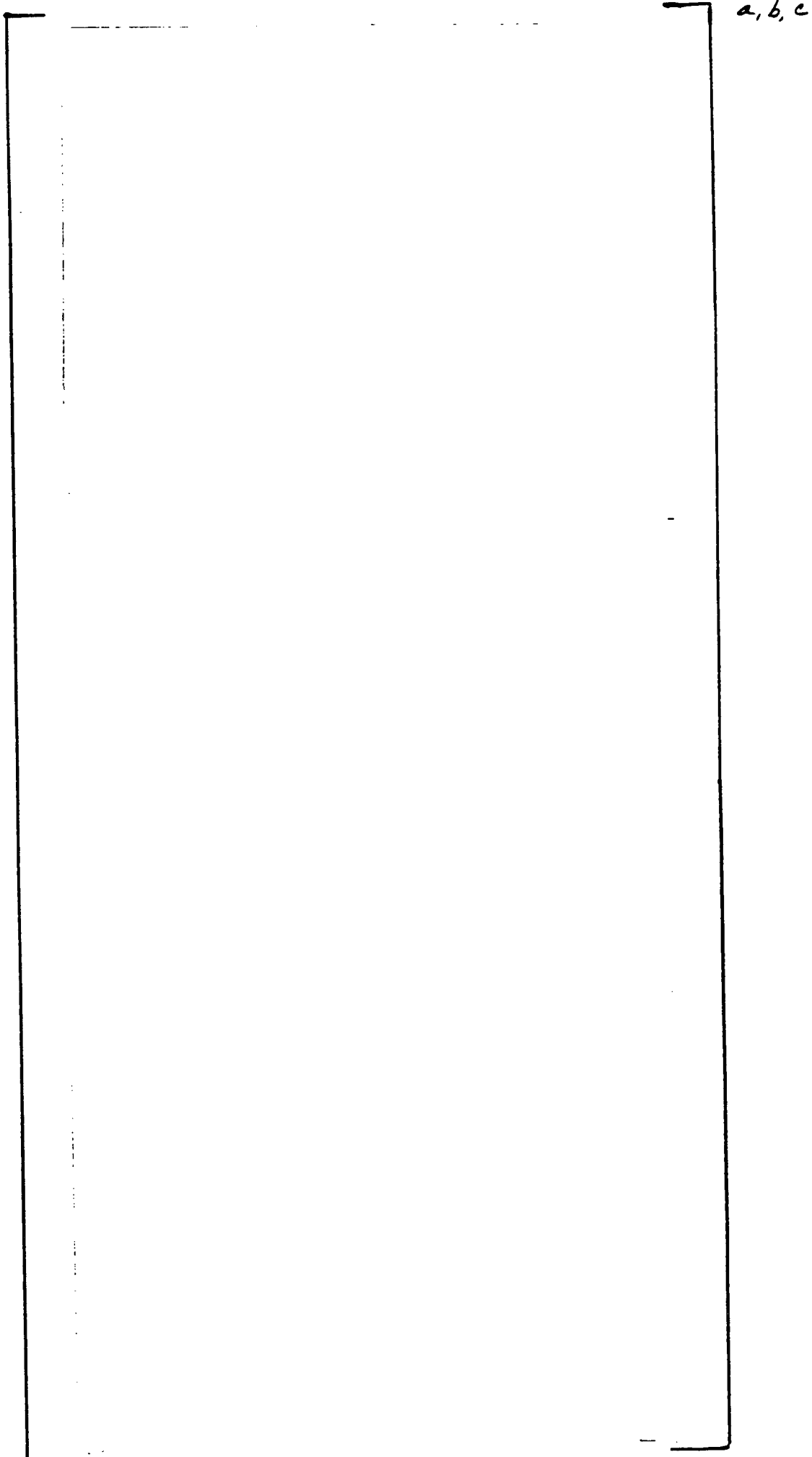
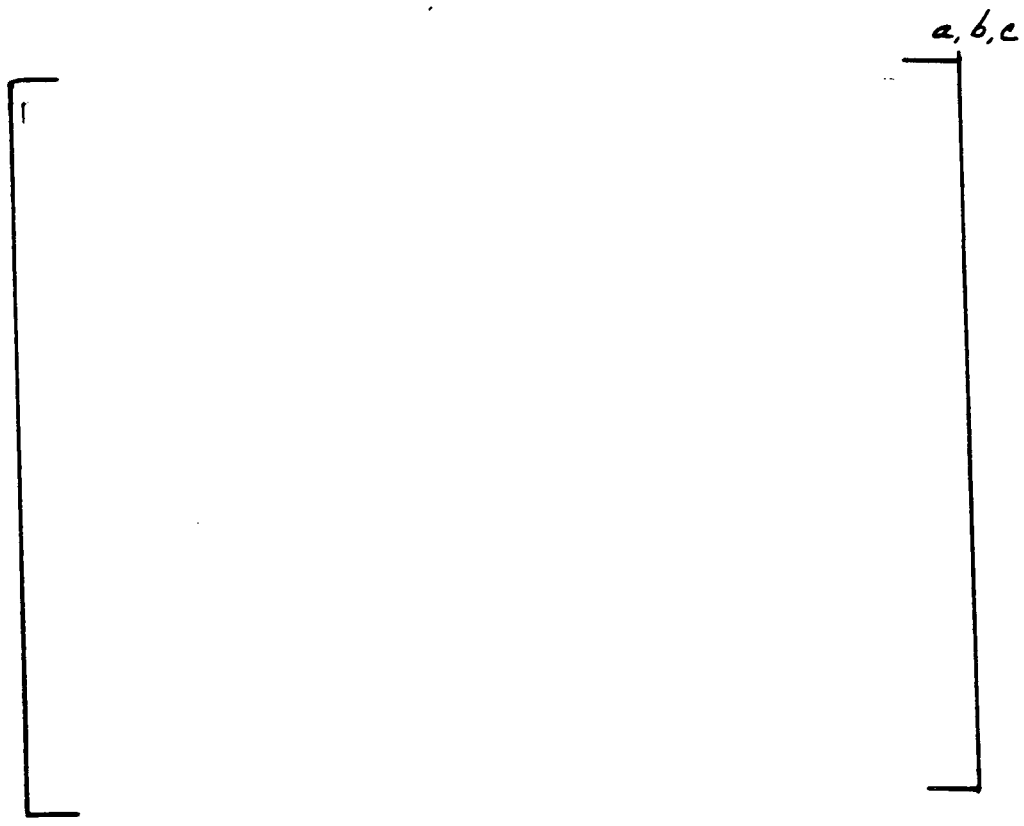


FIGURE 4.1-4 EFFECT OF  
CIRCUMFERENTIAL WALL LOSS CENTERED AT SLEEVE END



## AGENDA ITEM 4.2 - INFLUENCE OF MAGNETITE ON EDDY CURRENT SIGNALS

In order to account for a number of indications (Figure 4.2-1) found during the eddy current inspection of the sleeved portion of the steam generators at San Onofre Unit 1, a number of simulations were performed. The simulations involved the placement of magnetite in the annulus between the sleeve and the tube. Figures 4.2-2 and 4.2-3 show a number of these simulations. In Figure 4.2-2, both the eddy current response of a normal transition as well as a ring of magnetite are shown for reference. Also in Figure 4.2-2 are two simulations with magnetite in the transition region. Figure 4.2-3 shows further simulation with various amounts and location of the magnetite in the transition region.

From the simulations shown in Figures 4.2-2 and 4.2-3, it is concluded that the signals found in the transition region of the sleeves installed at Unit 1 are consistent in eddy current response with the presence of magnetite in the annulus between the sleeve and the tube at the transition.

A summary of the results of this investigation are presented as Table 4.2-1.

TABLE 4.2-1

SIMULATION OF EC RESPONSES  
FROM MAGNETITE IN SLEEVED TUBE JOINTS

PRESENCE OF NEW EC SIGNALS IN THE  
TRANSITION REGIONS WAS REPORTED IN THE  
MARCH 1982 INSPECTION.

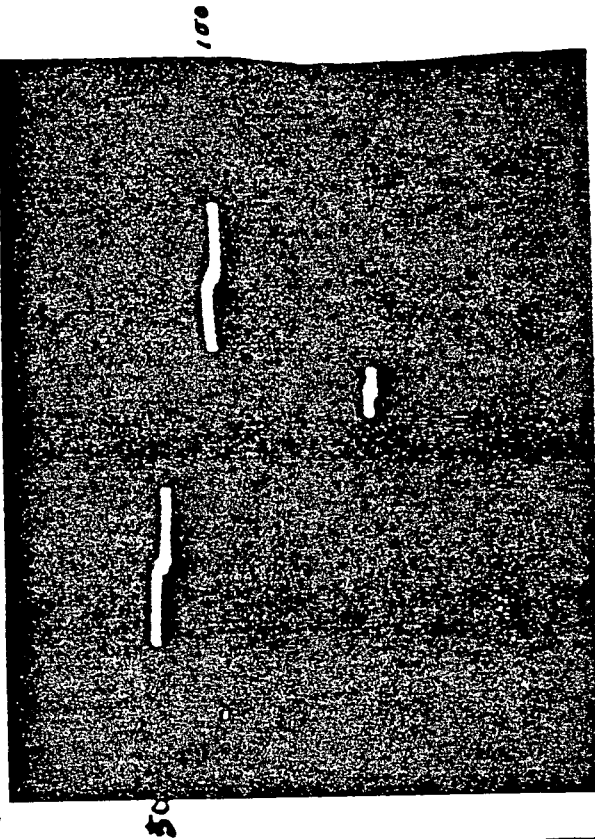
LABORATORY SIMULATIONS USING MAGNETITE  
PACKED JOINTS PRODUCED SIMILAR RESPONSES.

ELIMINATION OF MAGNETITE FROM FIELD DATA  
PRODUCED NORMAL TRANSITION SIGNALS AS THE  
RESIDUAL.



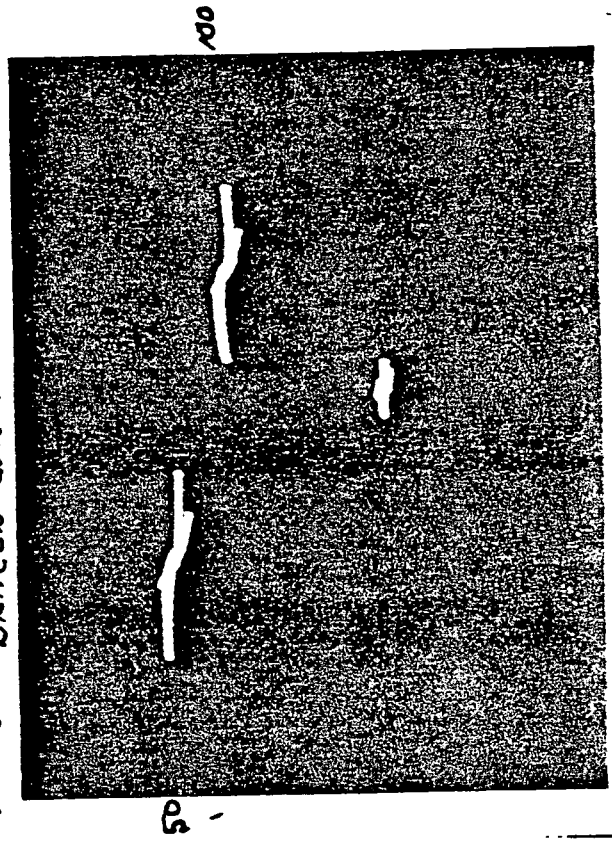
FIGURE 4.2-1 A COMPARISON OF THE EDDY CURRENT RESPONSE OF FOUR MECHANICAL JOINTS IN UNIT I S/G C FROM THE 2/81 AND 3/82 INSPECTIONS. DATA WAS OBTAINED AT [ a,b,c ]

R7C18 BRAZE CONVERTED SLEEVE 5/81



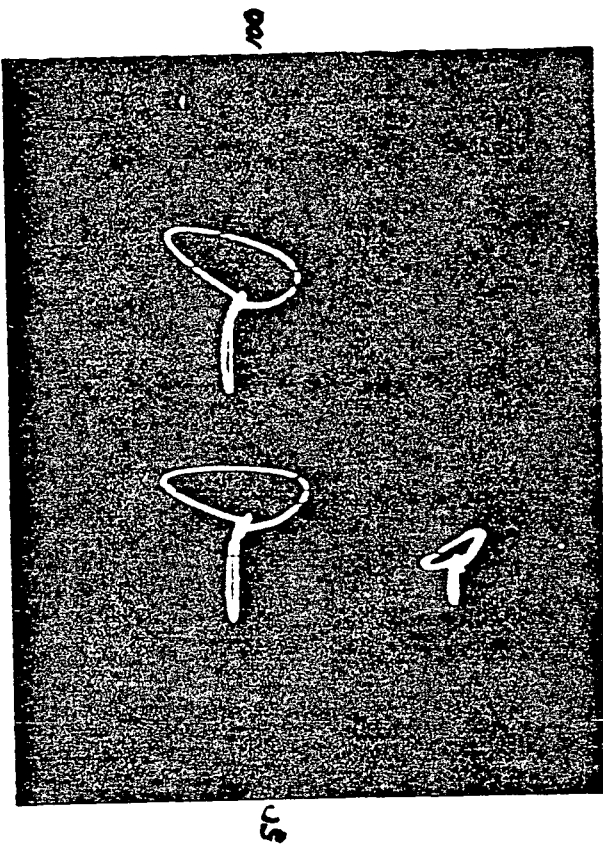
4V/D SIGNAL AT TOP OF 20 UPPER MECH. EXP.

R7C21 BRAZED CONV. SLEEVE 5/81



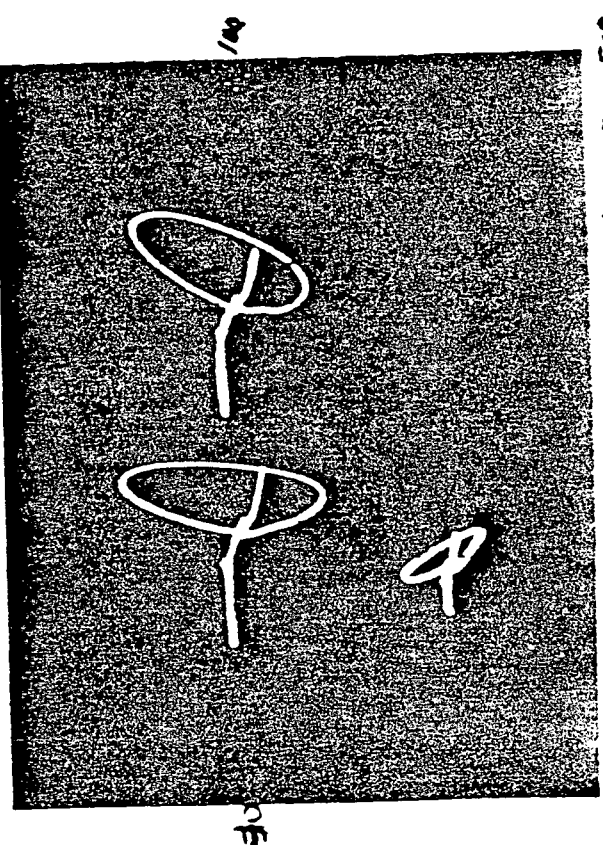
4V/D SIGNAL AT TOP OF 20 UPPER MECH EXP.

R7C18 BRAZED CONVERTED SLEEVE 1982



4V/D 25 SIGNAL AT TOP OF UPPER MECH. EXP.

R7C21 BRAZED CONVERTED SLEEVE 1982

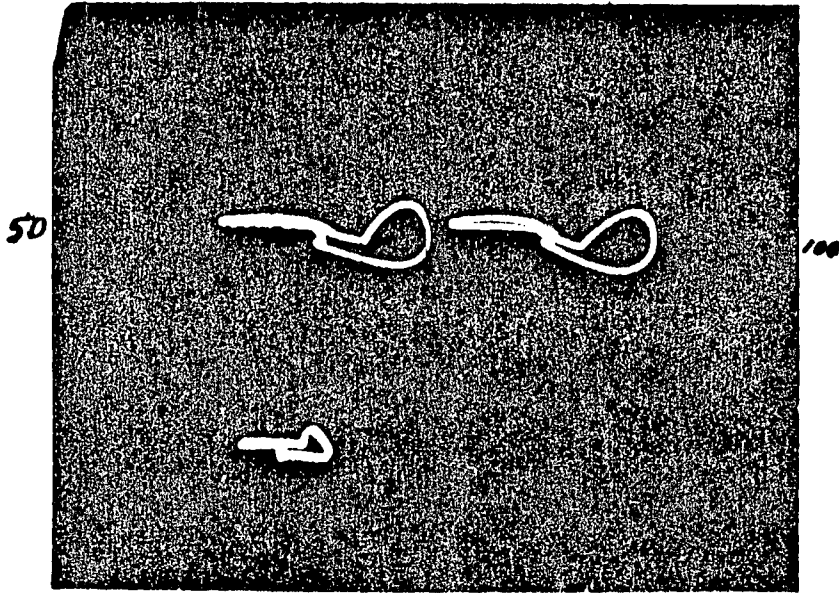


4V/D 25 SIGNAL AT TOP OF UPPER MECH EXP.

R19C75

NO BRAZED CONV.

1982



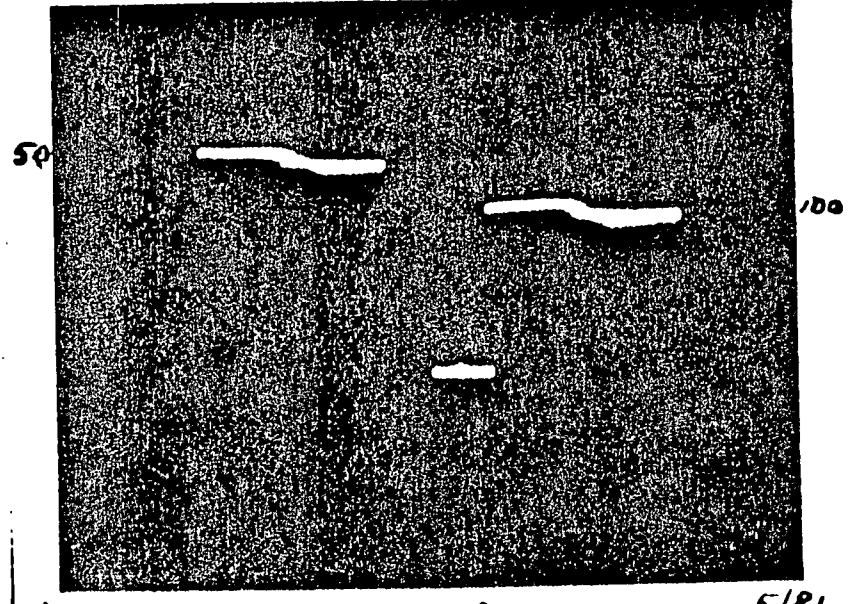
50

100

4V/D 25" SIGNAL AT TOP OF UPPER MECH. EXP.

R19C75

SIGNAL AT UPPER TRANS. UPPER EXP



50

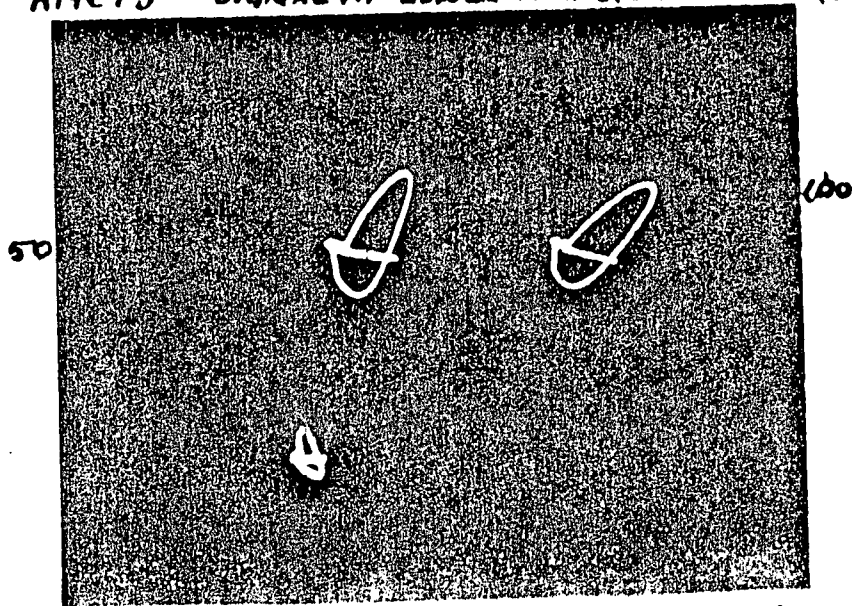
100

4V/D NO BRAZE CONN 20

5/81

R19C75

SIGNAL AT LOWER TRANS. OF LOWER EXP



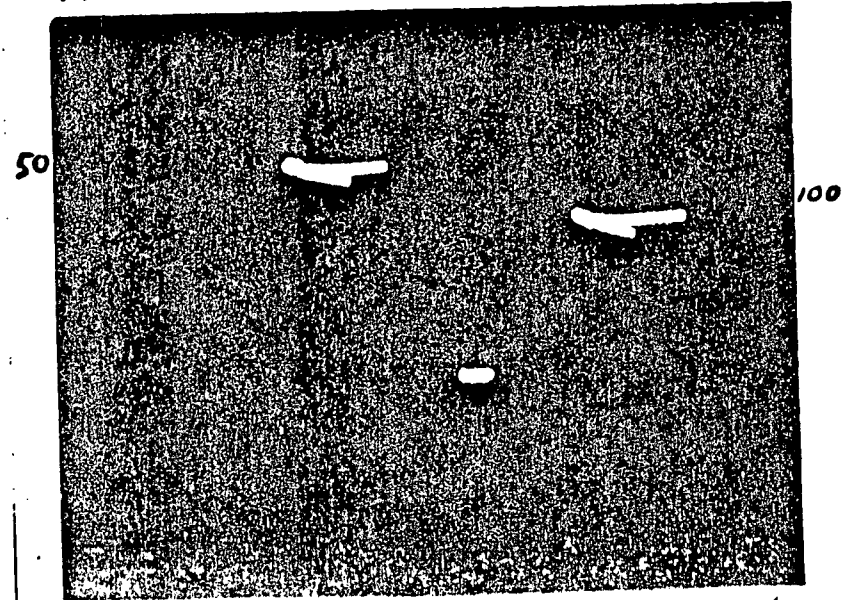
50

100

NO BRAZED CONV 1982

R19C75

SIGNAL AT LOWER TRANS. LOWER EXP.



50

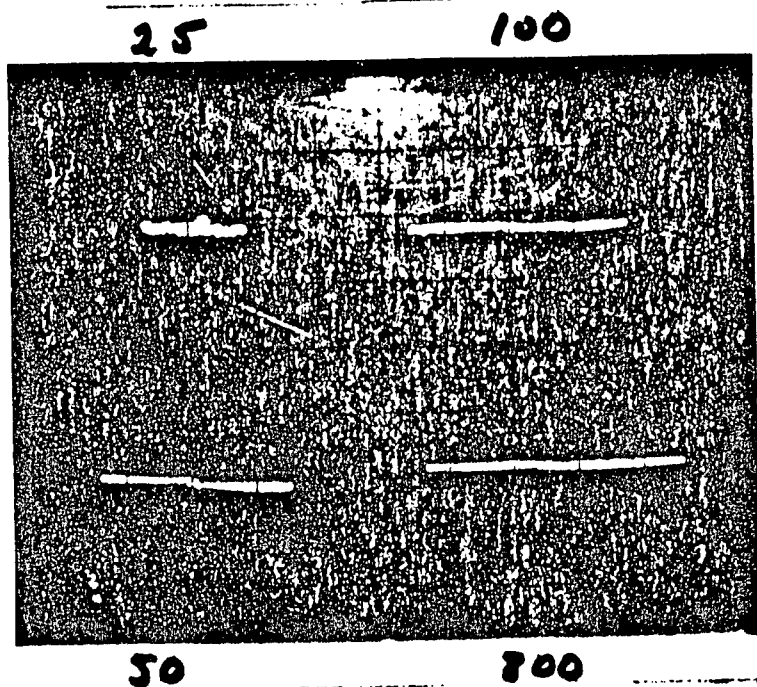
100

4V/D NO BRAZED CONV. 20

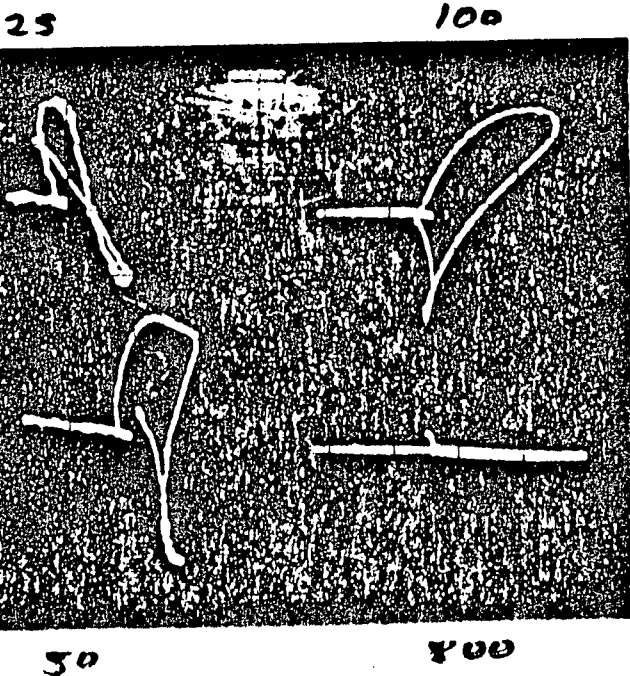
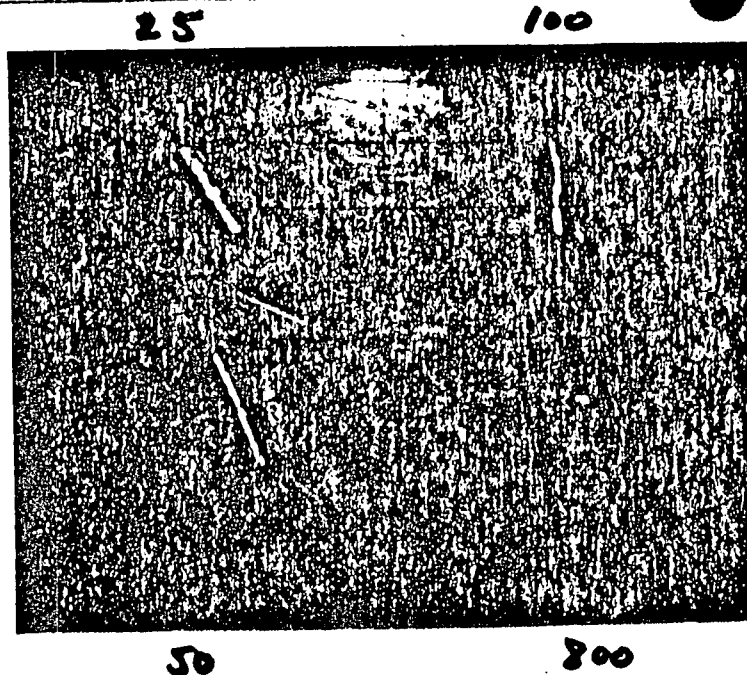
5/81

FIGURE 4.2-1 (CONTINUED)

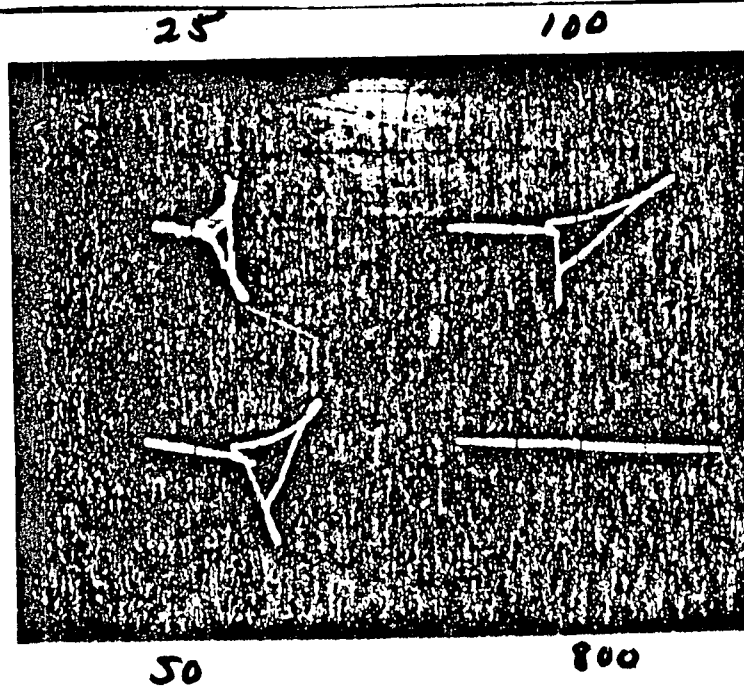
TRANSITION ALONE



MAGNETITE IN ANNULUS ALONE



TRANSITION & MAGNETITE



TRANSITION & MAGNETITE

FIGURE 4.2-2 THE EDDY CURRENT RESPONSE OF MAGNETITE & EXPANSION TRANSITIONS [ a, b, c ]

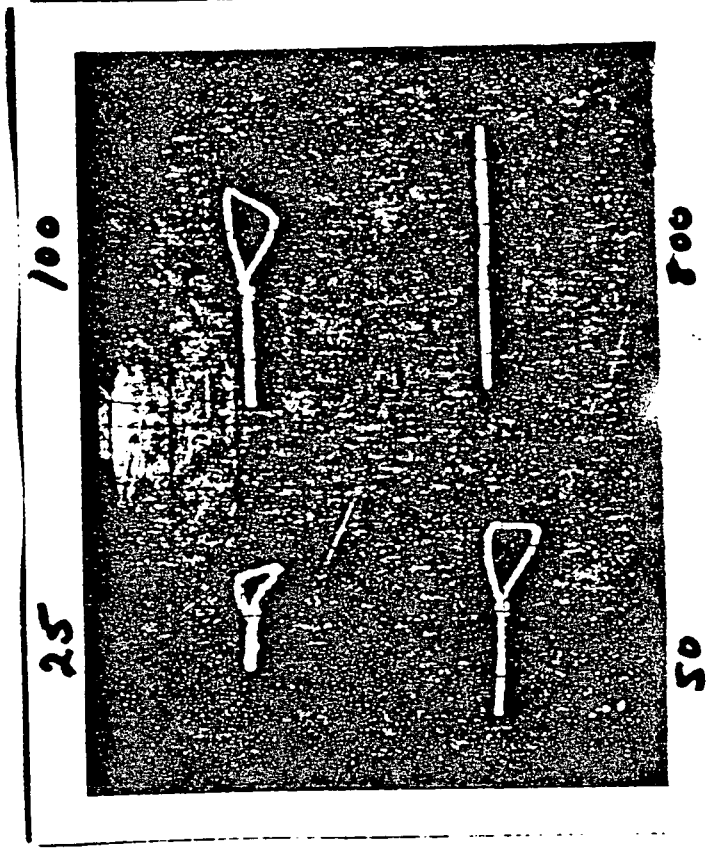
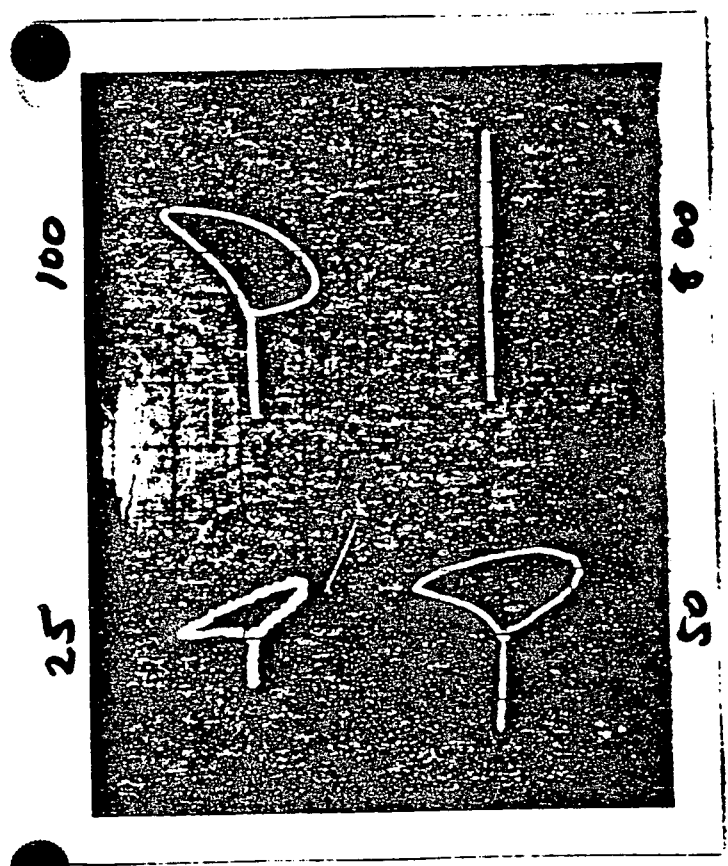
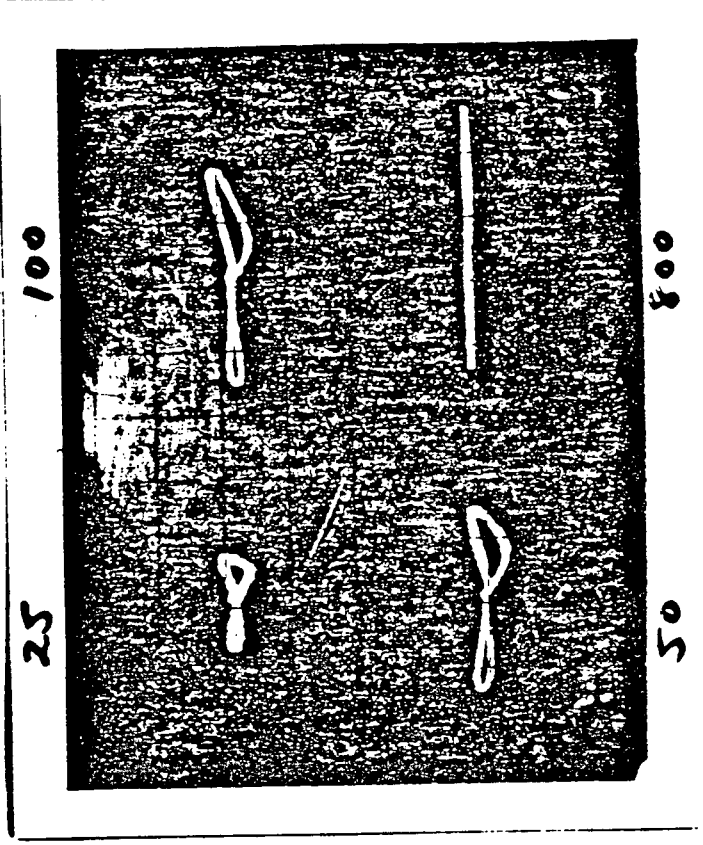
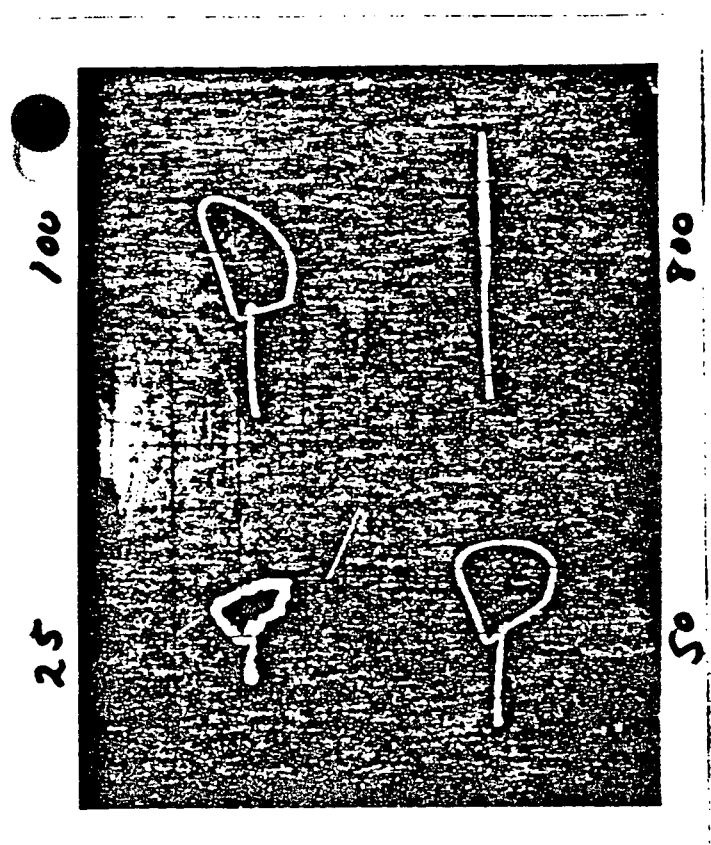


FIGURE 4.2-3 ADDITIONAL EDDY CURRENT RESPONSES OF  
 TRANSITION & MAGNETITE [ a, b, c ]

AGENDA ITEM 4.3 - MASKING SIGNALS FROM THROUGH-WALL IGA PENETRATION

The conclusions that can be drawn from the baseline inspection of the sleeves regarding the sensitivity of a conventional probe inspection to sleeve wall degradation in the presence of masking signals from through wall IGA penetrations of the outer tube wall and the technical basis for these conclusions are as follows:

The degradation that has occurred at the top of the tubesheet did not produce a significant response to the conventional bobbin probe in the parent tube alone. This was the reason that the RPC was employed during the 1980 inspections.

With a primary inspection frequency [ <sup>a,b,c</sup> ] for the sleeve, the tube response that is produced is reduced over [ <sup>a,b,c</sup> ] compared to the [ <sup>a,b,c</sup> ] inspection of the tube alone, this lessens the possibility of anomalous signals in the sleeve at this location. Second, assuming that the tube degradation response was large enough to cause ambiguities, multiple frequency processing of the inspection results may be employed to reduce the response from the degradation in much the same fashion as the removal of support plate indications.

Figure 4.3-1 shows the results of putting the 20% ASME sleeve standard under a large volume loss in the tube wall [ <sup>a,b,c</sup> ] and demonstrates that mixing does indeed reduce the effects of the tubing involvement, improving the visibility of the sleeve degradation.

A summary of these results is presented as Table 4.3-1.

TABLE 4.3-1

RESOLUTION OF TUBE DEGRADATION  
FROM SLEEVE INSPECTION DATA

EXISTENCE OF OUTER TUBE DEGRADATION, E.G., IGA,  
THINNING, POSES QUESTION CONCERNING SLEEVE  
DEGRADATION EVALUATION.

- o OUTER TUBE CONDITION IS ASSESSED FROM [ ]<sup>a,b,c</sup>  
DATA; SLEEVE CONDITION FROM [ ]<sub>a,b,c</sub>
- o TUBE RESPONSE AT [ ]<sup>a,b,c</sup> IS REDUCED GREATER  
THAN [ ]<sup>a,b,c</sup> COMPARED TO REFERENCE [ ]<sup>a,b,c</sup> DATA,  
FOR WHICH INSPECTION WAS NOT VERY SENSITIVE.

ASSUMING INTERFERENCE ANYWAY, MIXING OF TWO FREQUENCY  
CHANNELS AKIN TO SUPPORT PLATE ELIMINATION WOULD  
REDUCE OUTER TUBE SIGNAL SUBSTANTIALLY.

PRESENCE OF SEVERE TUBE DEGRADATION

a. b. c

--	--	--

AGENDA ITEM 4.4.1 - "D" COIL DEVELOPMENT STATUS

The repair report stated that a number of eddy current probes and techniques were being explored for improving the inspection of the sleeved assembly at the various geometric discontinuities. The main thrust of this effort has been to evaluate the [ ]<sup>a,b,c</sup> coil for improving the inspection in the vicinity of the transition locations. Figure 4.4.1-1 shows that by using the [ ]<sup>a,b,c</sup> probe, a penetration of the tube wall at the transition could be detected when its volume was equivalent to that of the ASME calibration standard. This represents a factor of [ ]<sup>a,b,c</sup> improvement in sensitivity over the test using the conventional bobbin coils. This sensitivity is expected to be further improved by multi-frequency data processing techniques. A [ ]<sup>a,b,c</sup> probe was evaluated in the 3/82 inspection, after laboratory testing indicated improved sensitivity. The data generated, however, did not show the type of improvement in inspection sensitivity that was anticipated. An analysis of the data has indicated that mechanical difficulties had interfered with the performance of the probes. The future efforts, Table 4.4.1-1, are aimed at achievement of the laboratory-indicated sensitivity for the [ ]<sup>a,b,c</sup> probe in the field. Further evaluations will be made as to the suitability of this probe design for improving the inspection of other regions of the joint. [ ]

] <sup>a,b,c</sup>



TABLE 4.4.1-1

DEVELOPMENT OF IMPROVED INSPECTION  
TECHNIQUES FOR SLEEVED TUBES

- [  
a,b,c ]
- o [ a,b,c ] -- PROBE PROVIDES [ a,b,c ] COVERAGE  
WITHOUT MULTIPLE ELECTRONICS REQUIREMENT.
  - ENABLES USE OF EXISTING EC EQUIPMENT, E.G.,  
4 FREQUENCY TESTER.
- o [ ] a,b,c ]
- o FIELD TESTING WITH [ ] a,b,c COILS WAS NOT CONSISTENT  
WITH EXPECTATIONS BASED ON LAB RESULTS.
  - MULTIPLE ATTEMPTS WERE MADE TO UNDERSTAND  
DIFFICULTIES.
  - UNBALANCED COILS AND INADEQUATE CENTERING  
WERE MAJOR DIFFICULTIES.
- o PRODUCTION PROBLEMS BEING ADDRESSED WITH EXPECTATION  
THAT A RELIABLE PROBE WILL RESULT.

FIGURE 4.4.1-1 SENSITIVITY [ ] TO 40% ASME  
FLAT BOTTOM HOLE IN TUBE OVER A SLEEVE TRANSITION

a.b.c

AGENDA ITEM 4.4.2 - UT DEVELOPMENT STATUS

The inspection of the reference joint by [

]<sup>a,b,c</sup> Certain aspects

of the UT inspection could also be applicable to a general inspection of the joint. First, it was considered that the UT inspection could identify sleeves, which underwent dissolution of the sleeve

[ ]<sup>a,b,c</sup> itself. However, the specialized EC test [

]<sup>a,b,c</sup> developed for this purpose, proved more

sensitive and rapid.

Second, it should be noted that as part of the calibration of the UT system, an EDM notch [ ]<sup>a,b,c</sup> through

the tube wall must be discernable for the calibration to be valid.

Since this type of discontinuity is often used to simulate a crack, it is possible that the UT system would be sensitive to degradation of the assembly. In the present system, this degradation would be registered as an unacceptable region of the joint. Thus, without a baseline with which to compare, there is no way of distinguishing service induced degradation from a pre-existing unacceptable joint.

Other types of UT inspection of the assembly could be postulated; however, it is not clear how these techniques would deal with the problem of intermittent joint integrity. For example, in the limit of a total lack of joining, there is no path for the sound to reach the tube and therefore no inspection of the tube could be performed (Figure 4.4.2-1). For the near term, UT is not considered a viable means of inspecting the joint, except in those regions where a baseline exists and the joint was initially acceptable.

TABLE 4.4.2-1

FEASIBILITY OF ULTRASONIC TESTING  
FOR REFERENCE JOINT INSPECTION

[ ..... ]<sup>a, b, c</sup> MIGHT BE  
ADAPTABLE FOR TUBE AND/OR SLEEVE EVALUATION.

COVERAGE OF THE JOINT BRAZE MUST BE KNOWN (I.E.,  
BASELINE INSPECTION); INTERMITTENT JOINT INTEGRITY  
WILL CREATE REFLECTORS PREVENTING TRANSMISSION.

DETECTION OF [ ..... ]<sup>a, b, c</sup> IS PART OF THE BRAZE  
UT CALIBRATION PROCEDURE.

NEAR-TERM USAGE IS VIABLE ONLY FOR REGIONS WITH  
ACCEPTABLE JOINT INTEGRITY.

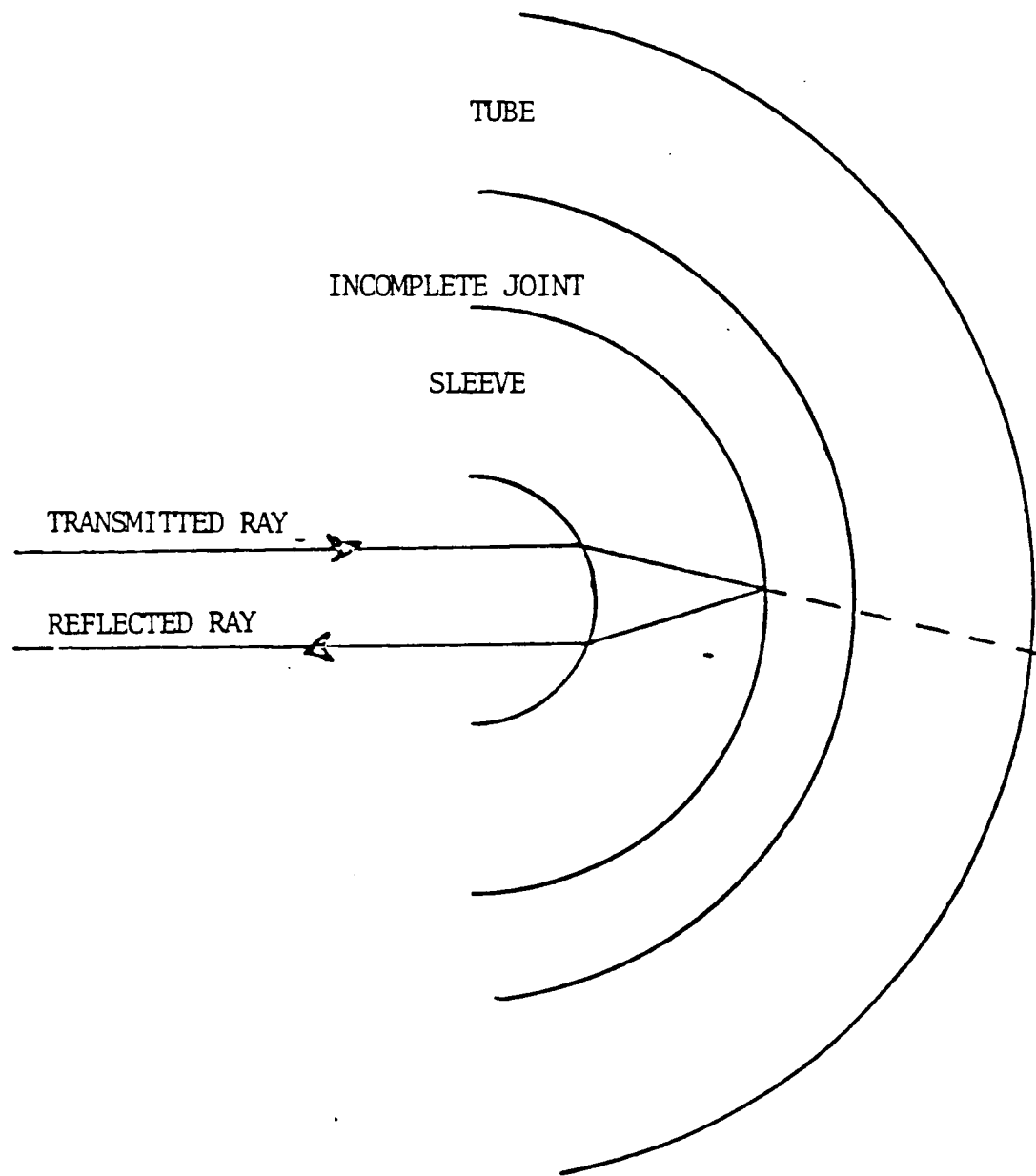


FIGURE 4.4.2-1

ULTRASONIC RAY DIAGRAM FOR CASE WHEN THE JOINT IS NOT FULLY FORMED. NO SOUND ENERGY REACHES THE TUBE TO PERFORM THE INSPECTION.

## AGENDA ITEM 5 - REVIEW OF SAFETY ASSESSMENT

In order to bring together all the information on NDE inspectability and tube integrity into a safety evaluation, two factors must be considered. Firstly, the level of degradation which eddy current can detect at the various tube locations and secondly, how these detection limits fit in with the minimum tube structural requirements for safe operation of the plant.

In the non-expanded region of the tube, or the length between the joints, the inspectability is consistent with a normal tubing inspection since there are no transitions or braze material which could distort the eddy current response.

In expansion transition areas, eddy current techniques can detect degradation equivalent to [

a,b,c] This is significant because the degradation can be detected before it reaches the critical crack length of [ a,b,c] for San Onofre size tubing. Furthermore, depending on the exact location of the degradation in the braze region, it may be detected by eddy current before a primary-to-secondary leak develops.

Another area to be considered with regard to tube inspectability is the region at the top end of the sleeve. Eddy current can detect [

a,b,c] The same consideration applies here as in the braze region, namely that degradation can be detected before it reaches the critical crack size. Also, the degradation can be detected before it goes through-wall and develops a primary-to-secondary leak.

Conclusions can be drawn about tube integrity, and therefore, safe operation of the plant, based on the foregoing levels of inspectability. First, eddy current can detect [

a,b,c] Second, a crack that is smaller than the critical crack length can be detected, in some cases even before it goes through wall. This greatly reduced the chances for a large leakage event. For a crack smaller in length than the critical crack length, but through wall, the leak before break criteria apply.

When the plugging limit of 40% at SCE is coupled with these conclusions, a large safety margin is maintained for safe operation of the plant with sleeves installed and the risk to the public health and safety is low.

A summary of the safety assessment is provided in Tables 5-1 to 5-3.

---

\*The field data observed from inspection of tubes removed from the field indicates that stress corrosion cracks are likely to emanate from an area of substantial IGA. The EC detectability of regions with IGA is considered to be dependent on the presence of these cracks.

TABLE 5-1

SAFETY EVALUATION OF SLEEVE JOINT

- o EDDY CURRENT INSPECTABILITY
- o TUBE INTEGRITY



TABLE 5-2

DETECTION OF TUBE WALL PENETRATION  
BY EDDY CURRENT

- o INSPECTION IN NON-EXPANDED REGIONS IS CONSISTENT WITH NORMAL TUBING INSPECTION.
  
- o EDDY CURRENT CAN DETECT DEGRADATION EQUIVALENT TO [ a,b,c ]
  
- o EDDY CURRENT CAN DETECT A [ a,b,c ]
  
- o EDDY CURRENT DETECTS [ a,b,c ] OR [ a,b,c ]

TABLE 5-3

TUBE INTEGRITY

- o THINNING
  - EDDY CURRENT CAN DETECT THINNING [a, b, c]
  
- o CRITICAL CRACK
  - EDDY CURRENT CAN DETECT A CRACK SMALLER THAN THE CRITICAL FLAW SIZE. LEAK BEFORE BREAK APPLIES.
  
- o MARGIN IS PRESENT FOR EDDY CURRENT UNCERTAINTY AND A GENERAL CORROSION ALLOWANCE.